Methods for the Synthesis of Tungsten Alkylidenes: Ring-Opening of Cyclopropenes and Alkylidene Transfer from Phosphoranes

Thesis by

Lynda K. Johnson

In Partial Fulfillment of the Requirements
for the Degree of Doctor of Philosophy

California Institute of Technology
Pasadena, California

1992

(Defended April 27, 1992)

to my family

Acknowledgements

I am grateful to my advisor Bob Grubbs for his enthusiasm, support, and most of all, for creating such a great environment for doing research. I wish that I could individually list all of the contributions of the Grubbs group members, past and present, to my education and to my life in general, but after five and a half years of graduate school, the list would be longer than this thesis. For all of your advice, help, and friendship, thanks! Also, thanks to all of the chemistry and math faculty members at Wartburg College and Bob Angelici at Iowa State University for their contributions to my undergraduate education and for their encouragement.

Many people directly contributed to the research reported in this thesis, and I'm very grateful to them. The studies involving the ring-opening of cyclopropenes reported in Chapter 2 wouldn't have been started if it weren't for the gifts of initial supplies of diphenyl-, dimethyl-, and ketalcyclopropenes received from Jeff Moore, Zhe Wu, and Eric Ginsburg. Also, thanks to Zhe for obtaining the two-dimensional spectra reported in the same chapter.

Scott Virgil started the studies involving alkylidene transfer from phosphoranes to tungsten that are discussed in the first half of Chapter 3. Tammy Ulibarri carried out the preparative-scale syntheses of $W(=CHC_6H_4\text{-}p\text{-}CF_3)Cl_2(NPh)(PMePh_2)_2$ and $W(=CHC_6H_4\text{-}p\text{-}Me)Cl_2(NPh)(PMePh_2)_2$ that are reported in the same chapter and grew the single crystals that were used to obtain the structure of the latter compound. Marcus Frey synthesized the bis(alkylidene) complex mentioned at the end of Chapter 3. Studies involving the compound $W[\eta^2\text{-(7-oxanorbornene)}]Cl_2(NPh)(PMePh_2)_2$ (Chapter 4) have been further pursued by Brent Flatt.

Dr. Joseph W. Ziller was very helpful in carrying out all of the X-ray diffraction studies. I'm thankful to the NMR GLA's—Eric Anslyn, Dave Wheeler, Dom McGrath, Nat Finney, Bryan Coughlin, Zhe, and Sonbinh Nguyen—for their help and for doing a difficult job so well. Thanks also to Dave for sharing his knowledge on many other

topics in chemistry and to Sonbinh for proofreading this thesis. The elemental analyses were performed at the Caltech Analytical Facility by Fenton Harvey or at Oneida Research Laboratories. Graduate research fellowships from the NSF, Sandia National Laboratories, and Amoco were greatly appreciated.

I'm grateful to my roommates—Kay, Sarah, Margat, Wen-Jean, Jen-Sue, Sonali, Pippa, and Vittu—for their friendship and many good times. Finally, and most importantly, thanks to my family for their love and support.

Abstract

In the research reported in this thesis, two methods for synthesizing alkylidene complexes were investigated: (1) ring-opening of cyclopropenes to give vinyl alkylidene complexes and (2) alkylidene transfer from phosphorus ylides to metal centers. Tungsten(IV) imido precursors of the form $WX_2(NAr)L_n$ (X = Cl or OR; Ar = Ph, 2,6-C_6H_3-Me_2, 2,6-C_6H_3-(*i*-Pr)$_2$; L_n = PR_3, $P(OR)_3$ or ether donor ligands) were used throughout the investigation.

A brief overview of the syntheses and uses of high-valent alkylidene complexes is given in Chapter 1. The reactions of $WCl_2(NAr)(PX_3)_3$ (X = R or OR) precursors with 3,3-diphenylcyclopropene and 4,8-dioxaspiro[2.5]oct-1-ene are reported in Chapter 2. η^2-Cyclopropene complexes [$W(\eta^2$-cyclopropene)$Cl_2(NAr)(PX_3)_2$] were synthesized from precursors containing the smaller imido ligands; increasing the steric bulk of the imido ligand favored the ring-opening of the cyclopropenes to yield the vinyl alkylidene compounds [$W(=CH-CH=CR'_2)Cl_2(NAr)(PX_3)_2$]. Conversion of thermally stable η^2-cyclopropene complexes to give the corresponding vinyl alkylidene compounds was observed upon photolysis or addition of catalytic amounts of $HgCl_2$.

The transfer of alkylidenes from $Ph_3P=CHAr'$ and $Ph_3P=CH-CH=CMe_2$ to $WCl_2(NPh)(PMePh_2)_3$ to give $W(=CHR')Cl_2(NPh)(PMePh_2)_2$ is reported in the first half of Chapter 3, and the effects of varying the solvent, the ylides, and the tungsten precursors are discussed. The remainder of Chapter 3 deals with the in situ reduction and trapping of $WCl_2(NAr)[OCMe(CF_3)_2]_2(THF)$ precursors by $Ph_3P=CHAr'$ to give $W(=CHAr')(NAr)[OCMe(CF_3)_2]_2(PPh_3)$. The use of the chelating *o*-methoxy-benzylidene was especially effective here, as coordination by the *o*-methoxy group greatly aided the transfer reaction and, in addition, stabilized the resulting product.

Chapter 4 documents initial studies involving the reactions of $WCl_2(NAr)(PX_3)_3$ precursors with *exo*-5,6-dimethoxymethyl-7-oxanorbornene. For reactions involving tungsten precursors with the smaller imido ligands, formation of η^2-olefin complexes

$W[\eta^2$-(7-oxanorbornene]$Cl_2(NAr)(PX_3)_2$ was observed. Oxygen abstraction to give 5,6-dimethoxymethylcyclohexadiene occurred upon reaction of this olefin with $WCl_2[N$-2,6-C_6H_3-(*i*-Pr)$_2$][P(OMe)$_3$]$_3$.

Table of Contents

Chapter 1 Introduction

Background p. 2
Thesis Research p. 6
References and Notes p. 8

Chapter 2 Synthesis and Reactivity of $WCl_2(NAr)(PX_3)_3$ (X = R, OR) Complexes: Formation of Tungsten Vinyl Alkylidene Complexes via the Rearrangement of Cyclopropenes

Introduction p. 12
Results and Discussion p. 14
Experimental Section p. 53
References and Notes p. 85

Chapter 3 Alkylidene Transfer from Phosphoranes to Tungsten(IV) Imido Complexes

Introduction p. 91
Results and Discussion p. 94
Conclusions p. 111
Experimental Section p. 114
References and Notes p. 137

Chapter 4 Reactions of $WCl_2(NAr)(PX_3)_3$ [$PX_3 = PR_3$, $P(OMe)_3$] Complexes with *exo*-5,6-Dimethoxymethyl-7-Oxanorbornene

Introduction p. 142
Results p. 142
Discussion p. 145
Experimental Section p. 148
References and Notes p. 151

Appendix Data for X-ray Diffraction Studies p. 154

List of Tables, Schemes, and Figures

Tables

Chapter 1

Table 1 Formation of Alkylidene Ligands by α-Hydrogen Abstraction p. 5

Chapter 2

Table 1 NMR Spectral Data for the $\mathrm{P(OMe)_3}$ Ligands of $\mathrm{WCl_2(N\text{-}2,6\text{-}C_6H_3\text{-}R_2)[P(OMe)_3]_3}$ Complexes p. 17

Table 2 Selected Bond Lengths and Angles for $\mathrm{WCl_2[N\text{-}2,6\text{-}C_6H_3\text{-}(\mathit{i}\text{-}Pr)_2][P(OMe)_3]_3}$ p. 19

Table 3 η^2-Cyclopropene Complex Stability p. 26

Table 4 Selected NMR Spectral Data for η^2-Cyclopropene Complexes p. 27

Table 5 Selected Bond Lengths and Angles for $\mathrm{W(H\overline{C{=}CH\text{-}C}Ph_2)Cl_2\text{-}(NPh)[P(OMe)_3]_2}$ p. 30

Table 6 Selected NMR Spectral Data for 2,6-Dimethyl- and 2,6-Di-*i*-Propylphenylimido Diphenylvinyl Alkylidene Complexes p. 34

Table 7 Selected Bond Lengths and Angles for $\mathrm{W({=}CH\text{-}CH{=}CPh_2)[N\text{-}2,6\text{-}C_6H_3\text{-}(\mathit{i}\text{-}Pr)_2][OCMe(CF_3)_2]_2[P(OMe)_3]}$ p. 38

Table 8 Selected NMR Spectral Data for 2,6-Dimethyl- and 2,6-Di-*i*-Propylphenylimido Ketalvinyl Alkylidene Complexes p. 41

Table 9 Selected Bond Lengths and Angles for **21-C** p. 47

Chapter 3

Table 1 Selected NMR Data for $\mathrm{W({=}CHR)Cl_2(NPh)(PMePh_2)_2}$ Complexes p. 95

Table 2 Selected Bond Lengths and Angles for $\mathrm{W({=}CHC_6H_4\text{-}\mathit{p}\text{-}Me)Cl_2(NPh)(PMePh_2)_2}$ p. 97

Table 3 Selected NMR Data for Alkylidene Complexes Prepared by the In Situ Trapping of Reduced Tungsten Complexes by Phosphoranes p. 102

Table 4 Selected Bond Lengths and Angles for $W(=CHC_6H_4$-*o*-OMe)(N-2,6-C_6H_3-Me_2)[$OCMe(CF_3)_2]_2$(THF) p. 106

Table 5 Selected Bond Lengths and Angles for $W(=CHC_6H_4$-*o*-OMe)[N-2,6-C_6H_3-(*i*-Pr)$_2$][$OCMe(CF_3)_2]_2$ p. 109

Table 6 Comparison of the Rates of Alkylidene Transfer from *ortho*-, *meta*-, and *para*-Substituted Aryl Ylides Ph_3P=CHAr' to $WCl_2(NPh)(PMePh_2)_3$ p. 115

Table 7 Survey of the Reactivity of Phosphoranes with $WCl_2(NPh)(PMePh_2)_3$ p. 116

Chapter 4

Table 1 Selected NMR Spectral Data for η^2-(*exo*-5,6-Dimethoxymethyl-7-Oxanorbornene) Complexes p. 144

Schemes

Chapter 1

Scheme 1 Synthesis of Arylimido Tungsten Alkylidenes p. 2

Chapter 2

Scheme 1 Proposed Mechanism for the Formation of **B** and **C** p. 50

Chapter 3

Scheme 1 Proposed Mechanism for Alkylidene Transfer from Ph_3P=CHR to $WCl_2(NPh)(PMePh_2)_3$ p. 99

Scheme 2 Reaction Sequence for the Synthesis of *o*-Methoxybenzylidene Complexes p. 104

Figures

Chapter 1

Figure 1 Reactions catalyzed by transition-metal alkylidene and metallacyclobutane catalysts. p. 3

Figure 2 Representative examples of metallacyclobutane and alkylidene olefin metathesis catalysts. p. 4

Figure 3 Partial molecular orbital diagram for an octahedral imido complex. p. 7

Chapter 2

Figure 1 ORTEP plot of $WCl_2[N\text{-}2,6\text{-}C_6H_3\text{-}(i\text{-}Pr)_2][P(OMe)_3]_3$. p. 18

Figure 2 ORTEP plot of $W(H\overline{C{=}CH\text{-}C}Ph_2)Cl_2(NPh)[P(OMe)_3]_2$ p. 29

Figure 3 A comparison of the structural data and strain energies of cyclopropane, 3,3-dimethylcyclopropene, and $W[\eta^2$-diphenylcyclopropene$]Cl_2(NPh)[P(OMe)_3]_2$. p. 31

Figure 4 ORTEP plot of $W(=CH\text{-}CH{=}CPh_2)[N\text{-}2,6\text{-}C_6H_3\text{-}(i\text{-}Pr)_2][OCMe(CF_3)_2]_2[P(OMe)_3]$ p. 37

Figure 5 ORTEP plot of **21-C**. p. 46

Figure 6 $^1H\text{-}^1H$ COSY spectrum of **20-B**. p. 83

Figure 7 $^1H\text{-}^{13}C$ COSY spectrum of **20-B**. p. 84

Chapter 3

Figure 1 Examples of reactions of phosphoranes with transition-metal complexes. p. 91

Figure 2 The three known examples of alkylidene transfer from phosphoranes to transition-metal centers. p. 92

Figure 3 ORTEP plot of $W(=CHC_6H_4\text{-}p\text{-}Me)Cl_2(NPh)(PMePh_2)_2$. p. 96

Figure 4 ORTEP plot of $W(=CHC_6H_4\text{-}o\text{-}OMe)(N\text{-}2,6\text{-}C_6H_3\text{-}Me_2)[OCMe(CF_3)_2]_2(THF)$. p. 105

Figure 5 ORTEP plot of $W(=CHC_6H_4\text{-}o\text{-}OMe)[N\text{-}2,6\text{-}C_6H_3\text{-}(i\text{-}Pr)_2][OCMe(CF_3)_2]_2$. p. 108

Chapter 4

Figure 1 Proposed activation of metathesis catalyst precursors by oxygen. p. 146

Chapter 1

Introduction

Background

Transition-metal alkylidene and metallacyclobutane complexes are important intermediates in acyclic olefin metathesis,[1] ring-opening metathesis polymerization (ROMP),[1] acyclic diene[2] and alkyne[3] polymerizations, and carbonyl olefinations[4] (Figure 1). Notable among the isolable complexes[5,6] that catalyze these transformations are the titana-[7] and tantalacyclobutane[8] derivatives and certain alkylidene complexes of tungsten,[9-12] molybdenum,[13] rhenium,[14] and ruthenium[15] (Figure 2). The arylimido tungsten and molybdenum alkylidene complexes are the most effective metathesis catalysts synthesized to date.[9,13] These tetracoordinate, monomeric complexes are stabilized by the substantial steric bulk of the imido, alkoxide, and alkylidene ligands, although addition of a strong Lewis base does enable less bulky derivatives to be isolated. The electrophilicity of the metal center and, hence, the reactivity of the catalyst, can be varied by the substitution of trifluoromethyl groups on the alkoxide ligands. The *t*-butoxide derivative of these complexes catalyzes the living polymerization of strained, cyclic olefins, while the more active hexafluoro-*t*-butoxide derivative rapidly metathesizes acyclic olefins and catalyzes the polymerization of relatively unstrained cyclic olefins such as cyclooctatetraene and its derivatives.[16] Several methods for synthesizing these catalysts have been reported, making them readily available. For example, the synthesis of $W(=CHR)(NAr)(OR')_2$, as shown in Scheme 1, is short and easily reproduced.[9c]

Scheme 1. Synthesis of Arylimido Tungsten Alkylidenes[9c]

$$WO_2Cl_2 \xrightarrow[\text{dme}]{2\ ArNH_2} W(NAr)_2Cl_2(dme) \xrightarrow{2\ RCH_2MgCl} W(NAr)_2(CH_2R)_2$$

$$\xrightarrow[-\ ArNH_3OTf,\ -\ RCH_3]{3\ TfOH,\ dme} W(CHR)(NAr)(OTf)_2(dme) \xrightarrow{2\ LiOR'} W(CHR)(NAr)(OR')_2$$

(R = t-Bu or CMe$_2$Ph

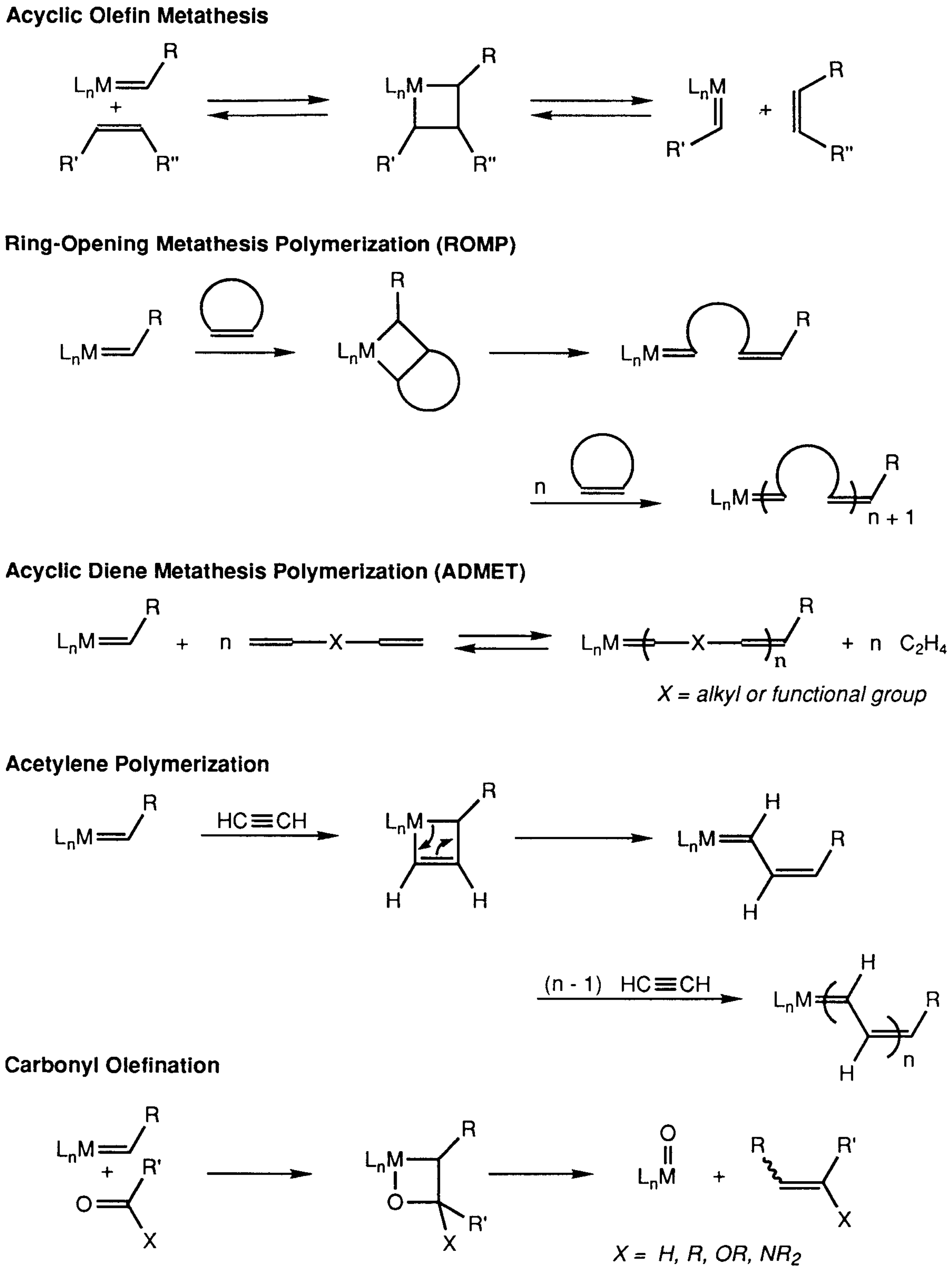

Figure 1. Reactions catalyzed by transition-metal alkylidene and metallacyclobutane catalysts.[1-4]

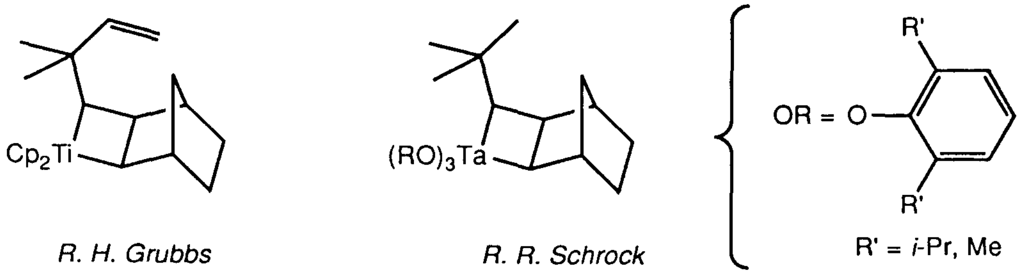

R. H. Grubbs *R. R. Schrock*

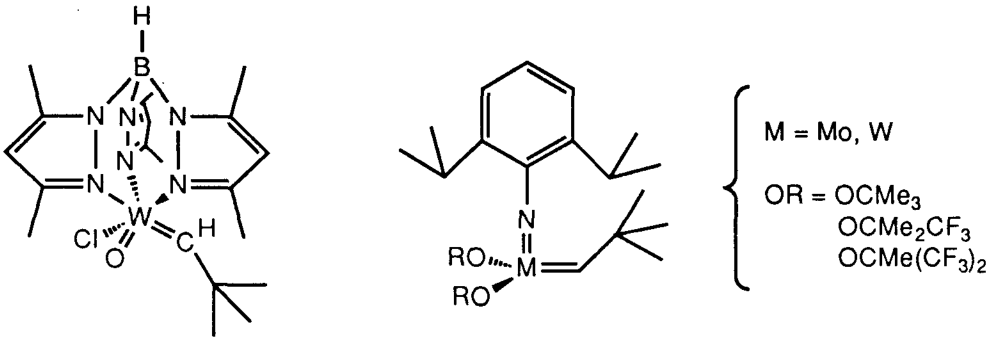

J. M. Boncella *R. R. Schrock*

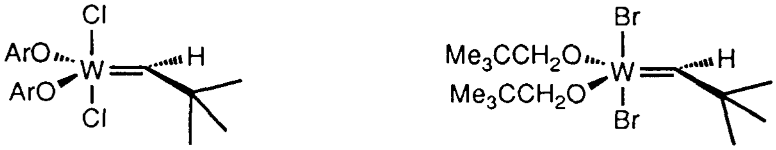

J. M. Basset *J. A. Osborn*

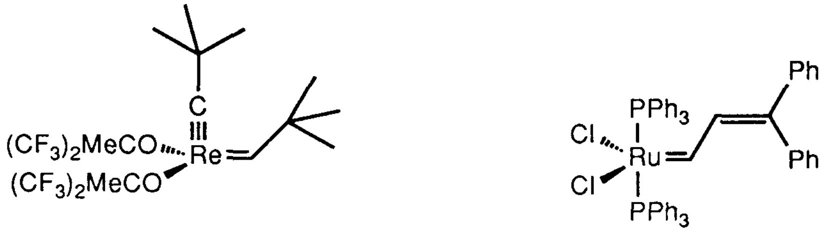

R. R. Schrock *R. H. Grubbs*

Figure 2. Representative examples of metallacyclobutane and alkylidene olefin metathesis catalysts.[7-15]

Table 1. Formation of Alkylidene Ligands by α-Hydrogen Abstraction[a,b]

Starting Complex	Additive	Product
$Ta(CH_2Ph)_3Cl_2$	CpTl	$Cp_2Ta(=CHPh)(CH_2Ph)$
$Ta(Np)Cl_4$	PMe_3, Na(Hg)	$Ta(=CH\text{-}t\text{-}Bu)H(PMe_3)Cl_2$
$Cp^*Ta(CH_2Ph)_2Cl_2$	$Ph_3P=CH_2$	$Cp^*Ta(=CHPh)(CH_2Ph)Cl$
$Ta[N(TMS)_2]_2Cl_3$	$LiCH_2TMS$	$Ta(=CHTMS)(CH_2TMS)[N(TMS)_2]_2$
$TaMe_3(OAr)_2$	*hv*	$Ta(=CH_2)Me(OAr)_2$
$Ta(Np)Cl_2(C_2H_4)(PMe_3)_2$	—	$Ta(=CH\text{-}t\text{-}Bu)EtCl_2(PMe_3)_2$
$Ta(=CH\text{-}t\text{-}Bu)(Np)_3$	PMe_3	$Ta(=CH\text{-}t\text{-}Bu)_2(Np)(PMe_3)_2$
$Mo(N\text{-}t\text{-}Bu)(Np)_3Cl$	LiNp	$Mo(N\text{-}t\text{-}Bu)(=CH\text{-}t\text{-}Bu)Np_2$
$MoCl_5$	$LiCH_2SiMe_3$	$Mo(=CHSiMe_3)(CH_2SiMe_3)_3$
$W(OAr)_2Cl_4$	$MgNp_2\cdot$dioxane	$W(=CH\text{-}t\text{-}Bu)(OAr)_2Cl_2$
$W(NPh)(Np)_3Cl$	$Ph_3P=CH_2$	$W(NPh)(=CH\text{-}t\text{-}Bu)Np_2$
$Re(NAr)_2(Np)Cl_2$	DBU	$Re(NAr)_2(=CH\text{-}t\text{-}Bu)Cl$
$Re(N\text{-}t\text{-}Bu)_2Cl_3$	NpMgCl	$Re(N\text{-}t\text{-}Bu)_2(=CH\text{-}t\text{-}Bu)Np$

[a] Reproduced from p. 53 of *Metal-Ligand Multiple Bonds* by W. A. Nugent and J. M. Mayer.[19]
[b] Abbreviations: Np = neopentyl; TMS = trimethylsilyl;
DBU = 1,8-diazabicyclo[5.4.0]undec-7-ene

The incorporation of different alkylidene ligands in metathesis catalysts is important, as it enables the tuning of catalyst reactivity,[17] the incorporation of different polymer end-groups in ROMP,[18] and the variation of the products synthesized in carbonyl olefinations.[4] Presently, the vast majority of all known alkylidene syntheses involve α-hydrogen abstraction routes, and Table 1, which is reproduced from a recent review that provides a comprehensive discussion of alkylidene syntheses,[19] contains representative examples. As is illustrated in this table, the cleavage of an α C-H bond can be achieved by a number of methods, and it is often promoted by an increase in steric congestion around the metal center. For example, the incorporation of strongly basic, bulky alkyl groups such as neopentyl ligands or the addition of a strongly coordinating base such as PMe_3 normally precedes alkylidene formation via α-hydrogen abstraction.[19] Thus, alkylidene ligands are usually limited to the sterically bulky neopentylidene and its analogues (e.g., the neophylidene ligand), although benzylidene and methylidene ligands have also been made by this method. Other alkylidene ligands must be incorporated on the metal center by the metathesis reaction.[20]

Thesis Research

The goal of the research reported in this dissertation was the further development of alternative routes to alkylidene complexes, as such routes might lead to the synthesis of new metathesis catalysts and/or enable greater flexibility in varying the structure of existing catalysts. Two promising, but currently underdeveloped, methods for synthesizing alkylidene complexes were investigated: (1) ring-opening of cyclopropenes to give vinyl alkylidene complexes (eq 1)[21] and (2) alkylidene transfer from phosphorus ylides to metal centers (eq 2).[22]

(1)

$$[M] \quad + \quad Ph_3P{=}CHR \longrightarrow [M]{=}CHR \qquad (2)$$

Tungsten(IV) imido precursors of the form $WX_2(NAr)L_n$ (X = Cl or OR; Ar = Ph, 2,6-C_6H_3-Me_2, 2,6-C_6H_3-(i-Pr)$_2$; L_n = PR_3, $P(OR)_3$ or ether donor ligands) were used throughout the investigation for the following reasons: (1) Tungsten commonly participates in metal-ligand multiple bonding, thus favoring the potential synthesis of alkylidene ligands by the above methods.[23] (2) The electronic structure of the tungsten(IV) d^2 center (Figure 3) is ideal for alkylidene formation. The two d electrons occupy the relatively high energy d_{xy} HOMO and are thus available for π-bonding to the alkylidene.[24] In the resulting complex, the alkylidene ligand will be coplanar with the

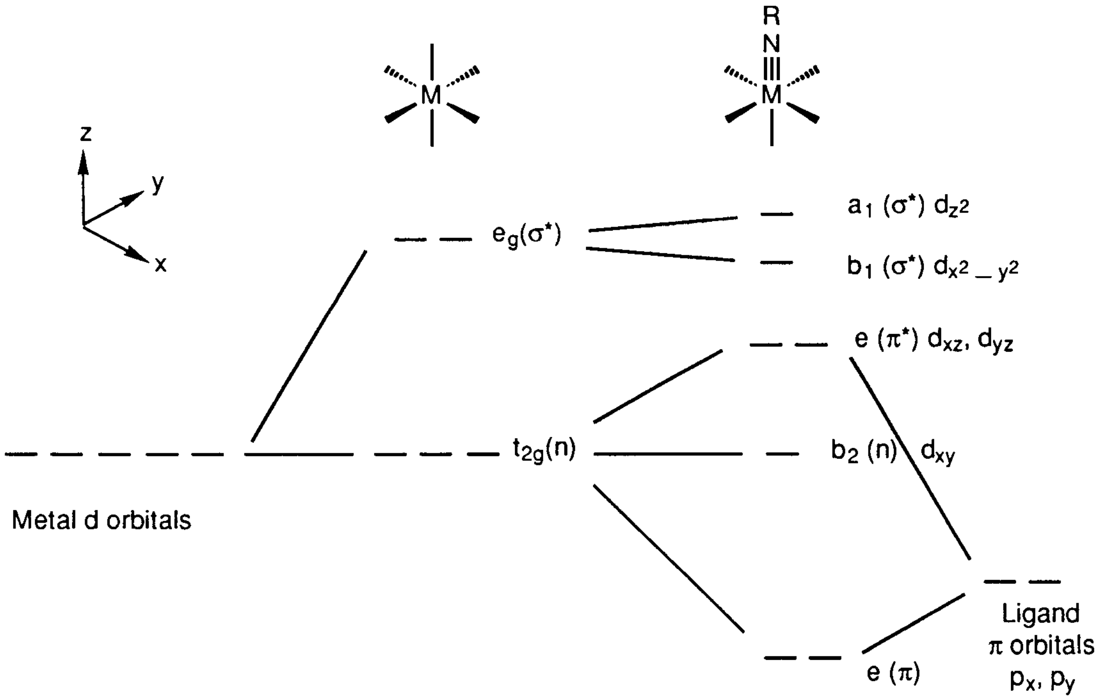

Figure 3. Partial molecular orbital diagram for an octahedral imido complex. (Reproduced from p. 33 of *Metal-Ligand Multiple Bonds* by W. A. Nugent and J. M. Mayer.)

imido ligand, with the alkylidene alkyl substituent lying either syn or anti to the imido ligand.[25] (3) Numerous variations in the imido, anionic, and donor ancillary ligands of the starting complex are possible, enabling the steric and electronic tuning of the precursor. (4) Finally, the resulting complexes are potential precursors to the arylimido tungsten alkylidene metathesis catalysts.[9]

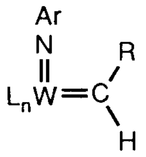

syn

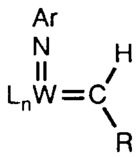

anti

References and Notes

(1) For general references on the metathesis reaction, see: (a) Grubbs, R. H.; Tumas, W. *Science* **1989**, *243*, 907-915. (b) Ivin, K. J. *Olefin Metathesis*; Academic Press: London, 1983. (c) Grubbs, R. H. In *Comprehensive Organometallic Chemistry*; Wilkinson, G., Ed.; Pergamon Press, Ltd.: New York, 1982; Vol. 8, pp 499-551. (d) Leconte, M.; Basset, J. M.; Quignard, F.; Larroche, C. In *Reactions of Coordinated Ligands*; Braterman, P. S., Ed.; Plenum: New York, 1986; Vol. 1, pp 371-420.

(2) Wagener, K. B.; Boncella, J. M.; Nel, J. G. *Macromolecules* **1991**, *24*, 2649-2657.

(3) (a) Schlund, R.; Schrock, R. R.; Crowe, W. E. *J. Am. Chem. Soc.* **1989**, *111*, 8004-8006. (b) Park, L. Y.; Schrock, R. R.; Stieglitz, S. G.; Crowe, W. E. *Macromolecules* **1991**, *24*, 3489-3495. (c) Wallace, K. C.; Liu, A. H.; Davis, W. M.; Schrock, R. R. *Organometallics* **1989**, *8*, 644-654.

(4) (a) Brown-Wensley, K. A.; Buchwald, S. L.; Cannizzo, L.; Clawson, L.; Ho, S.; Meinhardt, D.; Stille, J. R.; Straus, D.; Grubbs, R. H. *Pure & Appl. Chem.* **1983**, *55*, 1733-1744. (b) Pine, S. H.; Zahler, R.; Evans, D. A.; Grubbs, R. H. *J. Am. Chem. Soc.* **1980**, *102*, 3270-3272. (c) Aguero, A.; Kress, J.; Osborn, J. A. *J. Chem. Soc., Chem. Commun.* **1986**, 531-533. (d) Heppert, J. A.; Dietz, S. D.; Morton, M. D. *Abstracts of Papers*, 199th National Meeting of the American Chemical Society, Boston, MA; American Chemical Society: Washington, DC, 1990; INOR 262. (e) Bazan, G. C.; Schrock, R. R.; O'Regan, M. B. *Organometallics* **1991**, *10*, 1062-1067.

(5) For general references on transition-metal alkylidene complexes, see: (a) Feldman, J.; Schrock, R. R. In *Progress in Inorganic Chemistry*; Lippard, S. J., Ed.; John Wiley & Sons: New York, 1991; pp 1-74. (b) Nugent, W. A.; Mayer, J. M. *Metal-Ligand Multiple Bonds*; John Wiley & Sons: New York, 1988. (c) Schrock, R. R. In *Reactions of Coordinated Ligands*; Braterman, P. S., Ed.; Plenum: New York, 1986; Vol. 1, pp 221-283. (c) Collman, J. P.; Hegedus, L. S.; Norton, J. R.; Finke, R. G. *Principles and Applications of Organotransition Metal Chemistry*; University Science Books: Mill Valley, CA, 1987; 119-137. (d) Crabtree, R. H. *The Organometallic Chemistry of the Transition Metals*; John Wiley & Sons: New York, 1988; Chapter 11.

(6) For general references on metallacycle complexes, see: (a) Ingrosso, G. In *Reactions of Coordinated Ligands*; Braterman, P. S., Ed.; Plenum: New York, 1986; Vol. 1, pp 639-677. (b) Collman, J. P.; Hegedus, L. S.; Norton, J. R.; Finke, R. G. *Principles and Applications of Organotransition Metal Chemistry*; University Science Books: Mill Valley, CA, 1987; Chapter 9.

(7) Gilliom, L. R.; Grubbs, R. H. *J. Am. Chem. Soc.* **1986**, *108*, 733-742.

(8) (a) Wallace, K. C.; Liu, A. H.; Dewan, J. C.; Schrock, R. R. *J. Am. Chem. Soc.* **1988**, *110*, 4964-4975. (b) Wallace, K. C.; Schrock, R. R. *Macromolecules* **1987**, *20*, 448-450. (c) Wallace, K. C.; Dewan, J. C.; Schrock, R. R. *Organometallics* **1986**, *5*, 2162-2164.

(9) (a) Schrock, R. R.; DePue, R. T.; Feldman, J.; Schaverien, C. J.; Dewan, J. C.; Liu, A. H. *J. Am. Chem. Soc.* **1988**, *110*, 1423-1435. (b) Schrock, R. R.; Feldman, J.; Cannizzo, L. F.; Grubbs, R. H. *Macromolecules* **1987**, *20*, 1169-1172. (c) Schrock, R. R.; DePue, R. T.; Feldman, J.; Yap, K. B.; Yang, D. C.; Park, L.; DiMare, M.; Schofield, M.; Anhaus, J.; Walborsky, E.; Evitt, E.; Kruger, C.; Betz, P. *Organometallics* **1990**, *9*, 2262-2275.

(10) (a) Kress, J.; Aguero, A.; Osborn, J. A. *J. Mol. Catal.* **1986**, *36*, 1-12. (b) Kress, J.; Osborn, J. A.; Greene, R. M. E.; Ivin, K. J.; Rooney, J. J. *J. Am. Chem. Soc.* **1987**, *109*, 899-901.

(11) (a) Quignard, F.; Leconte, M.; Basset, J. M. *J. Mol. Catal.* **1986**, *36*, 13-29. (b) Quignard, F.; Leconte, M.; Basset, J.-M. *J. Chem. Soc., Chem. Commun.* **1985**, 1816-1817.

(12) Blosch, L. L.; Abboud, K.; Boncella, J. M. *J. Am. Chem. Soc.* **1991**, *113*, 7066-7068.

(13) (a) Murdzek, J. S.; Schrock, R. R. *Organometallics* **1987**, *6*, 1373-1374. (b) Murdzek, J. S.; Schrock, R. R. *Macromolecules* **1987**, *20*, 2640-2642. (c) Schrock, R. R.; Murdzek, J. S.; Bazan, G. C.; Robbins, J.; DiMare, M.; O'Regan, M. *J. Am. Chem. Soc.* **1990**, *112*, 3875-3886. (d) Bazan, G. C.; Oskam, J. H.; Cho, H.-N.; Park, L. Y.; Schrock, R. R. *J. Am. Chem. Soc.* **1991**, *113*, 6899-6907.

(14) (a) Toreki, R.; Schrock, R. R. *J. Am. Chem. Soc.* **1990**, *112*, 2448-2449. (b) Schofield, M. H.; Schrock, R. R.; Park, L. Y. *Organometallics* **1991**, *10*, 1844-1855.

(15) Nguyen, S. T.; Johnson, L. K.; Grubbs, R. H.; Ziller, J. W. *J. Am. Chem. Soc.* **1992**, *114*, 3974-3975.

(16) Schrock, R. R. *Acc. Chem. Res.* **1990**, *23*, 158-165, and references therein.

(17) For example, see: Wu, Z.; Wheeler, D. R.; Grubbs, R. H. *J. Am. Chem. Soc.* **1992**, *114*, 146-151.

(18) (a) Cannizzo, L. F.; Grubbs, R. H. *Macromolecules* **1987**, *20*, 1488-1490. (b) Risse, W.; Grubbs, R. H. *Macromolecules* **1989**, *22*, 1558-1562. (c) Mitchell, J. P.; Gibson, V. C.; Schrock, R. R. *Macromolecules* **1991**, *24*, 1220-1221.

(19) Nugent, W. A.; Mayer, J. M. *Metal-Ligand Multiple Bonds*; John Wiley & Sons: New York, 1988; Chapter 3.

(20) (a) Crowe, W. E.; Mitchell, J. P.; Gibson, V. C.; Schrock, R. R. *Macromolecules* **1990**, *23*, 3536-3538. (b) Schrock, R. R.; Yap, K. B.; Yang, D. C.; Sitzmann, H.; Sita, L. R.; Bazan, G. C. *Macromolecules* **1989**, *22*, 3191-3200. (c) Kress, J.; Osborn, J. A. *J. Am. Chem. Soc.* **1987**, *109*, 3953-3960.

(21) Binger, P.; Muller, P.; Benn, R.; Mynott, R. *Angew. Chem., Int. Ed. Engl.* **1989**, *28*, 610-611.

(22) (a) Sharp, P. R.; Schrock, R. R. *J. Organomet. Chem.* **1979**, *171*, 43-51. (b) Schwartz, J.; Gell, K. I. *J. Organomet. Chem.* **1980**, *184*, C1-C2. (c) van Asselt, A.; Burger, B. J.; Gibson, V. C.; Bercaw, J. E. *J. Am. Chem. Soc.* **1986**, *108*, 5347-5349.

(23) Nugent, W. A.; Mayer, J. M. *Metal-Ligand Multiple Bonds*; John Wiley & Sons: New York, 1988; pp 29-32 and 145-147.

(24) (a) Nugent, W. A.; Mayer, J. M. *Metal-Ligand Multiple Bonds*; John Wiley & Sons: New York, 1988; pp 33-36. (b) Su, F.-M.; Bryan, J. C.; Jang, S.; Mayer, J. M. *Polyhedron* **1989**, *8*, 1261-1277.

(25) Schrock, R. R.; Crowe, W. E.; Bazan, G. C.; DiMare, M.; O'Regan, M. B.; Schofield, M. H. *Organometallics* **1991**, *10*, 1832-1843.

Chapter 2

Synthesis and Reactivity of $WCl_2(NAr)(PX_3)_3$ (X = R, OR) Complexes: Formation of Tungsten Vinyl Alkylidenes via the Rearrangement of Cyclopropenes

Introduction

Recently, it was reported that 3,3-disubstituted cyclopropenes react with bis(cyclopentadienyl)titanium(II) and -zirconium(II) precursors containing labile phosphine and olefin ligands, respectively, to give vinyl alkylidene, η^2-cyclopropene, and metallacyclopentane complexes (eq 1).[1] Clean vinyl alkylidene formation was observed in the reaction of 3,3-diphenyl- and 3-methyl-3-phenylcyclopropene with $Cp_2Ti(PMe_3)_2$, while the reaction of 3,3-dimethylcyclopropene with $Cp_2Ti(PMe_3)_2$ yielded a mixture of all three products. The zirconium olefin complex $Cp_2Zr(PMe_3)(H_2C{=}CHCH_2CH_3)$ formed the metallacyclopentane product exclusively upon reaction with 3,3-dimethylcyclopropene, and the reaction of the same precursor with 3,3-diphenylcyclopropene produced a 1:1 mixture of the vinyl alkylidene and η^2-cyclopropene complexes. The failure of these latter two complexes to equilibrate or interconvert upon heating (eq 2) led to the conclusion that vinyl alkylidene formation occurred by direct opening of the 3-membered ring, not via an η^2-cyclopropene intermediate.

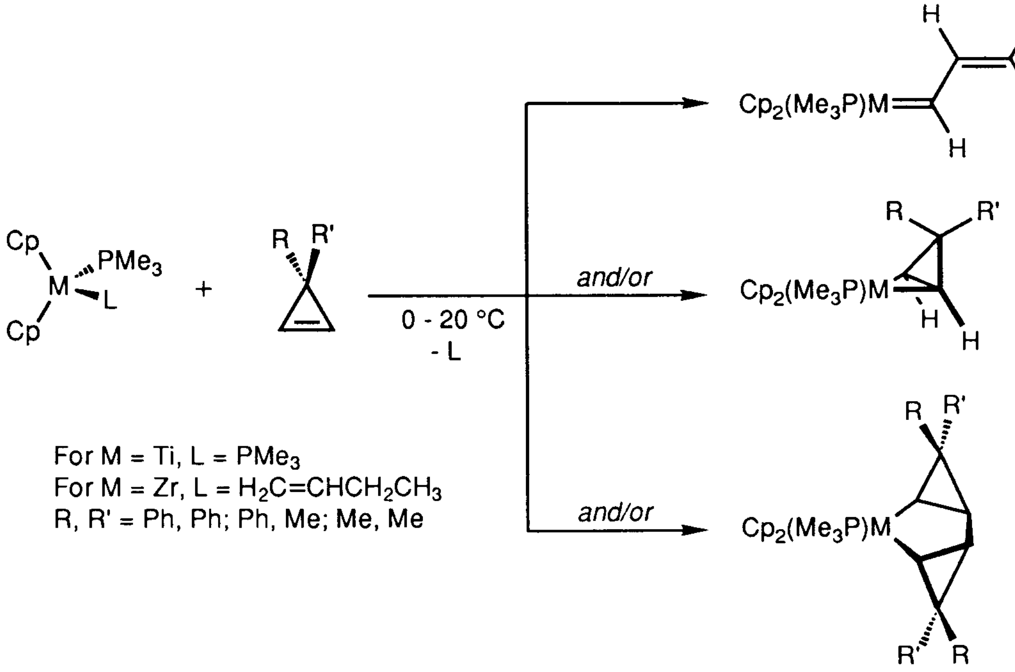

(1)

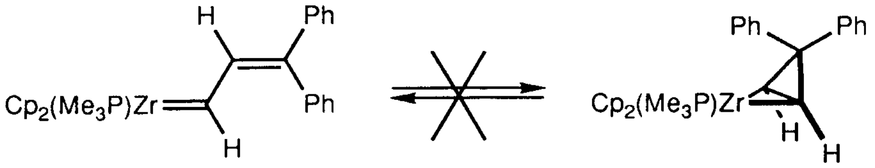

(2)

The ring-opening of cyclopropenes to give vinyl alkylidenes constitutes a new entry to transition-metal alkylidene complexes,[2,3] and the generality of this reaction is thus of interest, especially given the importance of transition metal alkylidenes/carbenes in catalyzing a number of synthetically useful transformations, including olefin metathesis[4] and carbonyl olefinations.[5] Therefore, the reactivity of 3,3-disubstituted cyclopropenes with $WCl_2(NAr)(PX_3)_3$ [Ar = Ph; 2,6-C_6H_3-Me_2; 2,6-C_6H_3-(*i*-Pr)$_2$ and X = R, OR] complexes was investigated. The synthesis of $WCl_2(NPh)(PR_3)_3$ complexes was first reported in 1983,[6] and their selection as precursors for this study was based upon their ability to form a variety of π-acceptor (L) complexes of the form $WCl_2(NPh)(L)(PR_3)_2$ via the substitution of one phosphine ligand (eq 3).[7] The formation

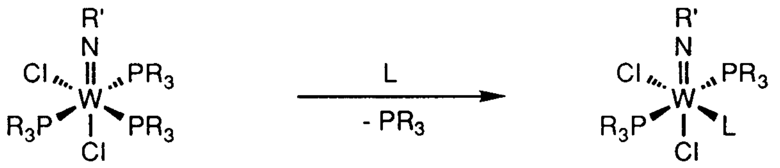

(3)

R' = Ph, *i*-Pr; PR_3 = PMe_3, $PMePh_2$

L = CO, CN-*t*-Bu, MeC(O)H, olefins, and acetylenes

of the π-complex is sensitive to the steric bulk and donating ability of the phosphine ligand, with the displacement of $PMePh_2$ being particularly facile, presumably due to steric crowding in the equatorial plane. The smaller cone angle and greater donating ability of PMe_3 versus $PMePh_2$ make the formation of π-acceptor complexes from $WCl_2(NPh)(PMe_3)_3$ more difficult; high temperatures are often required. This difficulty in displacing PMe_3 led to the development of the in situ trapping of the tungsten(IV) intermediate [$WCl_2(NPh)(PMe_3)_2$] by π-acceptors upon reduction of the corresponding tungsten(V) precursor $WCl_3(NPh)(PMe_3)_2$ (eq 4).[8] In addition, similar imido complexes

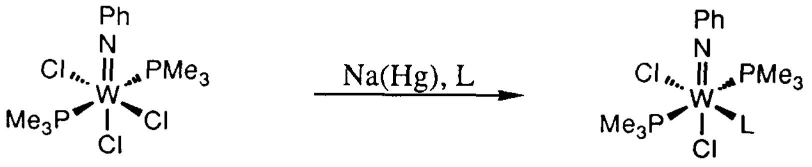

(4)

L = CO, olefins

containing π-acceptor ligands have been synthesized by the oxidative addition of unsaturated molecules to $WCl_2(PMePh_2)_4$ (eq 5).[9]

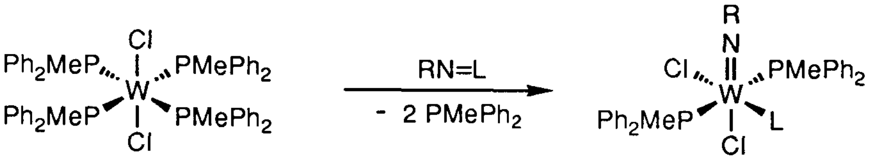

(5)

RN=L: t-BuN=CO, t-BuN=CN-t-Bu, p-Me-C_6H_4N=CO,
Me_3SiN=CO, Me_3SiN=N_2, p-Me-C_6H_4N=CR'_2

Results and Discussion

Synthesis, Characterization, and Reactivity of $WCl_2(NAr)(PX_3)_3$ Complexes

Synthesis. The thermal ring-opening of 3,3-disubstituted cyclopropenes to give tungsten vinyl alkylidene complexes required the synthesis of several new $WCl_2(NAr)(PX_3)_3$ derivatives containing both substituted arylimido ligands and labile PX_3 ligands (*vide infra*). Substituted arylimido precursors $WCl_4(NAr)$ [Ar = 2,6-C_6H_3-Me_2, 2,6-C_6H_3-(i-Pr)$_2$] were synthesized via the established method of reacting $WCl_4(O)$ with the corresponding isocyanate (eq 6).[6] However, in comparison to the generation of $WCl_4(NPh)$ by this route, longer reaction times and higher temperatures were required for complete formation of the substituted arylimido derivatives. For example, the synthesis of $WCl_4(NPh)$ was reported in refluxing benzene, while the syntheses of $WCl_4(N\text{-}2,6\text{-}C_6H_3\text{-}Me_2)$ and $WCl_4[N\text{-}2,6\text{-}C_6H_3\text{-}(i\text{-}Pr)_2]$ were accomplished in refluxing toluene and *p*-xylene, respectively.[10] The lowering of the reaction rates when employing sterically demanding isocyanates is consistent with the postulated [2+2] cycloaddition of the tungsten oxo bond and the isocyanate (eq 6),[11] and it also corresponds with the report that $WCl_4(NCMe_3)$ cannot be made by this method.[12]

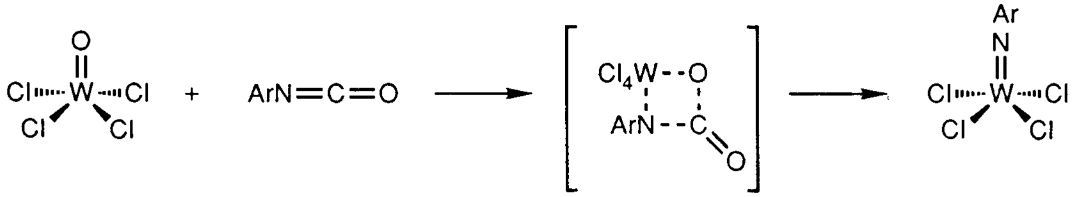

(6)

Since one $PMePh_2$ ligand of $WCl_2(NPh)(PMePh_2)_3$ is readily displaced at room temperature,[7] initial efforts focused on the synthesis of the 2,6-dimethyl- and 2,6-di-*i*-propylphenylimido analogues $WCl_2(NAr)(PMePh_2)_3$. Although resonances consistent with the formation of $WCl_2(N\text{-}2,6\text{-}C_6H_3\text{-}Me_2)(PMePh_2)_3$ were observable by ^1H NMR spectroscopy,[13] initial attempts to cleanly isolate this complex in reasonable yields were unsuccessful. For reactions involving the 2,6-di-*i*-propylphenylimido precursor, NMR signals characteristic of $WCl_2(NAr)(PMePh_2)_3$ were not observed. Presumably, unfavorable steric interactions between the arylimido alkyl substituents and the bulky $PMePh_2$ ligands, which are known to favor coordination in a meridional arrangement cis to the imido group,[6,14] were responsible for the poor yields in these reactions. When PEt_2Ph, a more donating and slightly smaller phosphine than $PMePh_2$,[15] was used, the synthesis and clean isolation of $WCl_2(N\text{-}2,6\text{-}C_6H_3\text{-}Me_2)(PEt_2Ph)_3$ (**1**) was achieved.

Due to the sensitivity of the stability of $WCl_2(NAr)(PR_3)_3$ complexes to the size of the phosphine ligand, the synthesis of phosphite analogues was pursued. It was hoped that the small size of $P(OMe)_3$ in combination with its weak donating ability, relative to that of phosphines,[16] would enable the synthesis of isolable complexes containing both bulky arylimido substituents and labile donor ligands. This proved to be the case: $WCl_2(NAr)[(P(OMe)_3]_3$ [Ar = Ph (**2**), 2,6-C_6H_3-Me_2 (**3**), and 2,6-C_6H_3-(*i*-Pr)$_2$ (**4**)] complexes were synthesized via the sodium amalgam reduction of their respective $WCl_4(NAr)$ precursors in the presence of $P(OMe)_3$ and isolated in good yields (eq 7). The formation of a light purple-gray solution, typically after about one hour of rapid stirring, provided a clear indicator of the complete formation of $WCl_2(NAr)[(POMe)_3]_3$.[17] The reaction was stopped at this point, as additional stirring led to poor yields and difficulties in clean isolation of the product. The syntheses of the phosphine analogues do not exhibit the same sensitivity to reaction times,[6] and therefore, it is likely that the π-accepting capability of the phosphite ligand enables reduction beyond the tungsten(IV) oxidation state.[16]

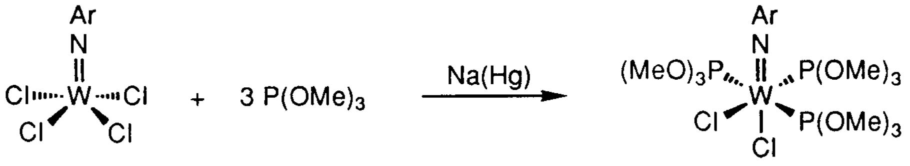

(7)

Ar = Ph (**2**); 2,6-C_6H_3-Me_2 (**3**); 2,6-C_6H_3-(*i*-Pr)$_2$ (**4**)

Characterization. Spectroscopic data for the $WCl_2(NAr)[(P(OMe)_3]_3$ complexes (Table 1) is consistent with the expected meridional arrangement of the $P(OMe)_3$ ligands.[6] For example, a virtual triplet and a doublet appear in the ^1H and ^{13}C NMR spectra of these species and correspond, respectively, to the two mutually trans phosphite ligands and the phosphite ligand trans to a chloride ligand. In the ^{31}P NMR spectra, coupling between the inequivalent phosphite ligands gives rise to doublet and triplet resonances in a 2:1 ratio. The structure of these complexes was further confirmed by an X-ray crystallographic study of $WCl_2[N$-2,6-C_6H_3-(*i*-Pr)$_2][(POMe)_3]_3$ (**4**).[18] An ORTEP diagram of this complex is shown in Figure 1 and selected bond distances and angles are

Table 1. NMR Spectral Data for the P(OMe)$_3$ Ligands of WCl$_2$(N-2,6-C$_6$H$_3$-R$_2$)[P(OMe)$_3$]$_3$ Complexes

R	Mutually Trans P(OMe)$_3$ Ligands										P(OMe)$_3$ Ligand Trans To Cl									
	^{1}H [P(OCH_3)$_3$]^a			^{13}C [P(OCH$_3$)$_3$]^a			^{31}P [P(OCH$_3$)$_3$]^b				^{1}H [P(OCH_3)$_3$]^a			^{13}C [P(OCH$_3$)$_3$]^a			^{31}P [P(OCH$_3$)$_3$]^b			
	δ	m	J_{HP}	δ	m	J_{CP}	δ	m	J_{PP}	J_{PW}	δ	m	J_{HP}	δ	m	J_{CP}	δ	m	J_{PP}	J_{PW}
H	3.65	t	5.4	52.9	t	2.6	129.3	d	22	454	3.63	d	10.5	53.3	d	6.6	141.4	t	22	564
Me	3.71	t	5.2	52.8	t	2.6	127.8	d	20	456	3.68	d	10.5	53.2	d	7.3	144.8	t	20	568
i-Pr	3.71	t	5.4	52.9	t	2.2	128.0	d	20	456	3.72	d	10.3	53.5	d	7.3	143.4	t	20	566

^{a}In CD$_2$Cl$_2$. ^{b}In C$_6$D$_6$.

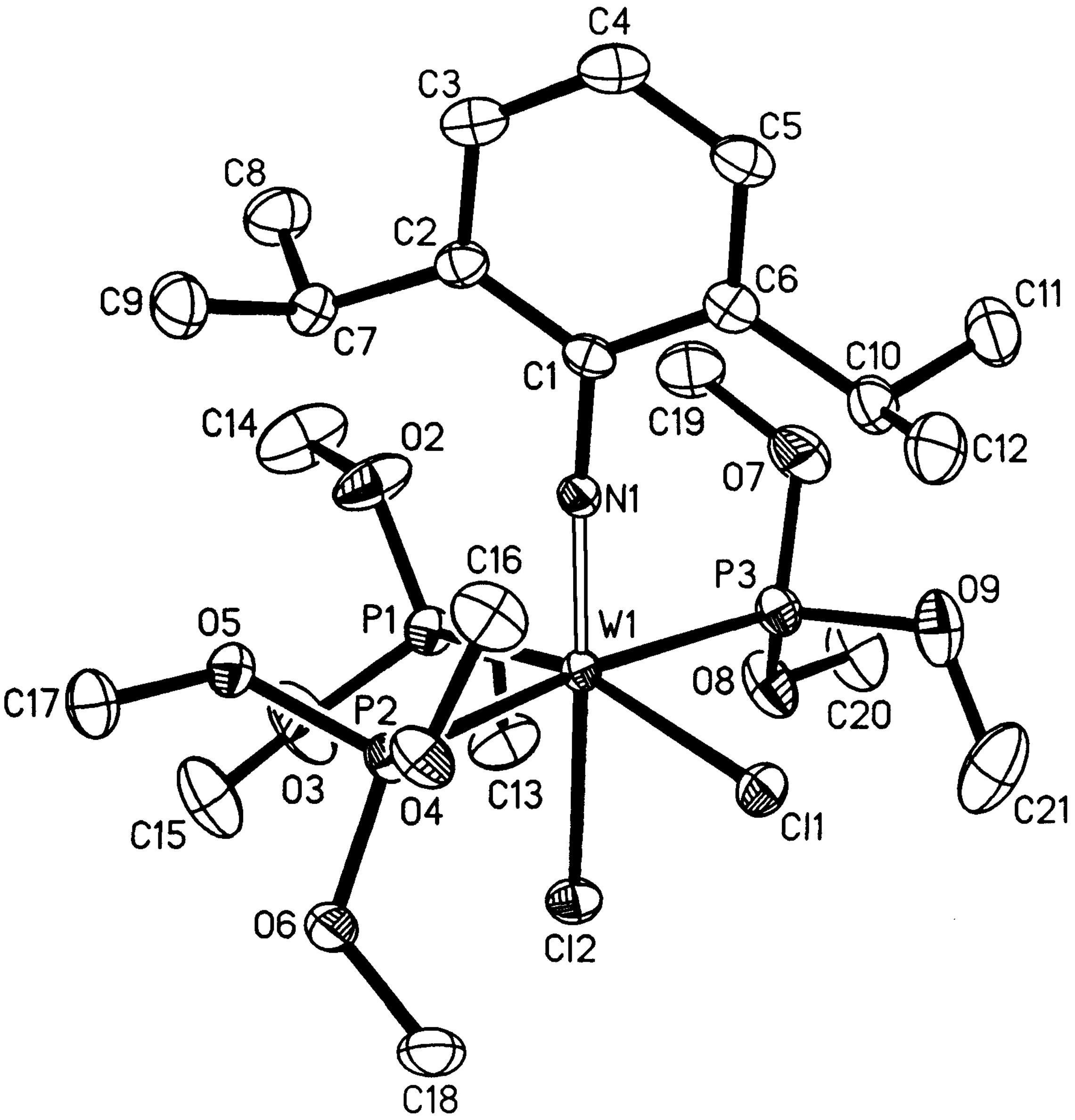

Figure 1. ORTEP plot of $WCl_2[N\text{-}2,6\text{-}C_6H_3\text{-}(i\text{-}Pr)_2][P(OMe)_3]_3$ (**4**). Thermal ellipsoids are drawn at the 50% probability level.

Table 2. Selected Bond Lengths and Angles for $WCl_2[N\text{-}2,6\text{-}C_6H_3\text{-}(i\text{-}Pr)_2][P(OMe)_3]_3$ (**4**)

Bond Lengths (Å)

W(1) - Cl(1)	2.495(1)	W(1) - Cl(2)	2.475(1)
W(1) - P(1)	2.451(1)	W(1) - P(2)	2.486(1)
W(1) - P(3)	2.497(1)	W(1) - N(1)	1.767(3)

Bond Angles (°)

Cl(1) - W(1) - Cl(2)	85.0(1)	Cl(1) - W(1) - P(1)	163.0(1)
Cl(2) - W(1) - P(1)	78.1(1)	Cl(1) - W(1) - P(2)	83.4(1)
Cl(2) - W(1) - P(2)	89.1(1)	P(1) - W(1) - P(2)	97.7(1)
Cl(1) - W(1) - P(3)	89.5(1)	Cl(2) - W(1) - P(3)	88.6(1)
P(1) - W(1) - P(3)	88.6(1)	P(2) - W(1) - P(3)	172.7(1)
Cl(1) - W(1) - N(1)	98.0(1)	Cl(2) - W(1) - N(1)	177.0(1)
P(1) - W(1) - N(1)	98.9(1)	P(2) - W(1) - N(1)	90.9(1)
P(3) - W(1) - N(1)	91.8(1)	W(1) - N(1) - C(1)	173.5(2)

given in Table 2. The arrangement of the ligands about the metal center exhibits several distortions from a perfect octahedral geometry: The equatorial chloride ligand and the phosphite ligand trans to it [Cl(1) and P(1)] both lie on the opposite side of equatorial plane from the imido group, a wide angle [97.7(1)°] exists between two of the cis phosphite moieties [P(1) and P(2)], and the imido group is bent away from these same two phosphite ligands. These distortions appear to relieve steric crowding between the arylimido substituents and the equatorial ligands, an observation that is consistent with the proposal that $WCl_2[N\text{-}2,6\text{-}C_6H_3\text{-}(i\text{-}Pr)_2](PMePh_2)_3$ could not be synthesized due to unfavorable steric interactions between the imido substituents and the $PMePh_2$ ligands (*vide supra*). The W(1) - P(1) bond length of the phosphite lying trans to a chloride ligand (2.451(1) Å) is shorter than the W(1) - P(2) and W(1) - P(3) bond lengths of the two mutually trans phosphite ligands (2.486(1) and 2.497(1), and this difference is reflected in the ^{31}P NMR chemical shifts and coupling constants. That is, the triplet resonance for P(1) is shifted downfield and exhibits a larger tungsten-phosphorus coupling constant than the doublet resonance for P(2) and P(3).

π-Complex Formation. The lability of the phosphine/phosphite ligands of complexes **1** - **4** was determined by the reactions of these complexes with ethylene and with phenyl- and diphenylacetylene.[19] Diphenylacetylene reacted at room temperature with $WCl_2(N\text{-}2,6\text{-}C_6H_3\text{-}Me_2)(PEt_2Ph)_3$ (**1**) to give $W(PhC{\equiv}CPh)Cl_2(N\text{-}2,6\text{-}C_6H_3\text{-}Me_2)(PEt_2Ph)_2$ (**5**). The high lability of a PEt_2Ph ligand of **1** is apparent when this reaction is contrasted with the synthesis of the analoguous PMe_3 complex $W(PhC{\equiv}CPh)Cl_2(NPh)(PMe_3)_2$, which required 20 h of refluxing in benzene.[7a]

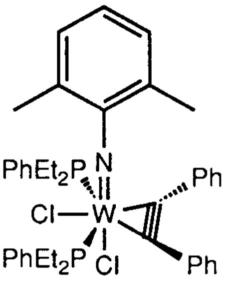

(**5**)

The phosphite complexes **2** - **4** readily underwent substitution reactions, generally at room temperature, with even relatively weak π-acceptors such as ethylene. In the ^1H NMR spectrum of the ethylene complex $W(H_2C{=}CH_2)Cl_2[N\text{-}2,6\text{-}C_6H_3\text{-}(i\text{-}Pr)_2][P(OMe)_3]_2$ (**6**), two multiplets were observed for the ethylene protons (syn and anti to the imido ligand) at 3.25 and 2.85 ppm. According to difference NOE measurements, the upfield ethylene multiplet (2.85 ppm) is syn to the imido ligand. For example, an 8.1% enhancement was observed at 2.85 ppm upon irradiation of the *i*-propyl methine proton, and conversely, an 8.0% enhancement was observed for the *i*-propyl methine proton upon irradiation of the 2.85 ppm ethylene multiplet. In the ^{13}C NMR spectrum, an upfield shift to 42.3 ppm (Δ = 80.9 ppm) was observed for the ethylene carbon resonance upon complexation. This value lies inbetween the chemical shifts reported for $W(H_2C{=}CH_2)Cl_2(NPh)(PMe_3)_2$ (39.4 ppm)[7e] and $W(H_2C{=}CH_2)Cl_2(NPh)(PMePh_2)_2$ (48.0 ppm)[7e] and thus indicates that in $W(L)Cl_2(NAr)[P(OMe)_3]_2$ complexes, there is strong back-donation to the π-acceptor ligand (L), despite the poor donating/competing π-accepting ability of the ancillary phosphite ligands.

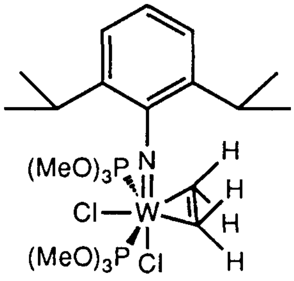

(6)

The room temperature reaction of $WCl_2(N\text{-}2,6\text{-}C_6H_3\text{-}Me_2)[P(OMe)_3]_3$ (3) and $PhC{\equiv}CH$ in toluene resulted in the formation of the corresponding acetylene complex $W(PhC{\equiv}CH)Cl_2(N\text{-}2,6\text{-}C_6H_3\text{-}Me_2)[P(OMe)_3]_2$ (7) in good yield. According to the NMR spectral data of **7**, the two phosphite groups are inequivalent, but not coupled. That is, these ligands appeared as two separate doublets in the ^1H and ^{13}C NMR spectra and as two singlets [118.8 ppm (J_{PW} = 354 Hz) and 117.6 ppm (J_{PW} = 366 Hz)] in the ^{31}P NMR spectrum. Coupling of the acetylenic proton to the two inequivalent phosphites gave rise to a doublet of doublets at 10.43 ppm (J_{HP} = 16.85, 5.62 Hz). NOE enhancements were observed in both directions between the acetylenic proton and the imido methyl groups and also between the acetylenic proton and the phosphite ligand at 3.58 ppm. In addition, irradiation of the imido methyl groups resulted in small NOE enhancements of both phosphite ligands. Slow rotation about the imido group in **7** was evidenced by the observation of a broad singlet for the imido methyl protons.

The above data is consistent with a crowded equatorial plane containing two phosphites, one of which lies cis to the acetylenic proton. Although the lack of coupling between the two inequivalent phosphites initially appears indicative of a cis arrangement of these ligands, a comparison with the analogous phosphine complex of phenylacetylene $W(PhC{\equiv}CH)Cl_2(NPh)(PMe_3)_2$ suggests otherwise.[7a] The only indication of a trans geometry for the inequivalent phosphine ligands in this complex is a large J_{PP} coupling constant; coupling between these two phosphines was not observed in the ^1H or ^{13}C NMR spectra. The doublet of doublets observed for the acetylenic protons (J_{HP} = 17.26, 5.90 Hz) closely resembles the same resonance of the phosphite complex 7. In addition, for initial investigations involving $W(PhC{\equiv}CPh)Cl_2[N\text{-}2,6\text{-}C_6H_3\text{-}(i\text{-}Pr)_2][P(OMe)_3]_2$, a mutually trans arrangement of the phosphites could be unambiguously assigned on the basis of ^1H, ^{13}C, and ^{31}P NMR spectral data.[20] Therefore, the geometry of the phosphite moieties in **7** is most likely trans, with the extremely close chemical shifts of the two phosphite ligands responsible for their lack of coupling.

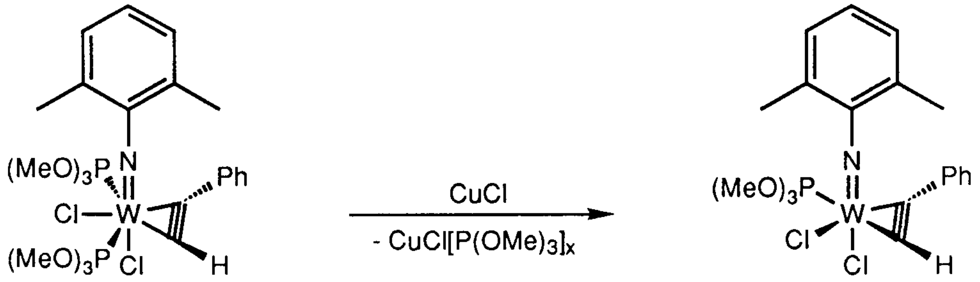

(7) (8) (8)

In contrast to the analogous phosphine complexes of $PhC{\equiv}CH$,[7] an equilibrium between 7 and the monophosphite adduct $W(PhC{\equiv}CH)Cl_2(N\text{-}2,6\text{-}C_6H_3\text{-}Me_2)[P(OMe)_3]$ (**8**) was observed in solution.[21] The addition of CuCl, a phosphine/phosphite "sponge",[22] resulted in the clean and selective formation of **8** (eq 8), which was characterized by its ^1H, ^{13}C, and ^{31}P NMR spectra. Loss of one phosphite resulted in a downfield shift of the remaining tungsten-bound phosphite ligand in the ^{31}P NMR spectrum and an increase in the phosphorus-tungsten coupling constant, and it also caused a downfield shift of the acetylenic carbons in the ^{13}C NMR spectrum, all consistent with stronger donation by the phosphite and acetylene ligands to the 16-electron complex **8**.[23] The decrease in steric crowding upon loss of a phosphite ligand enabled free rotation about the imido ligand, as was indicated by the appearance of a sharp singlet for the imido methyl protons. According to ^1H and ^{13}C NMR data, the phosphite ligand lies trans to the acetylenic proton (J_{HP} = 20.03 Hz for PhC≡C*H*) and cis to the acetylenic phenyl group (J_{CP} = 7.55 Hz for Ph*C*≡CH).

In general, these reactions with simple π-acceptor ligands demonstrated several points: (1) One donor ligand in complexes **1** - **4** is readily displaced at room temperature. (2) The phosphite complexes are capable of strong back-donation to π-acceptor ligands. (3) The major difference between the reactivity of the phosphine and phosphite tungsten(IV) complexes is the higher lability of a second phosphite ligand upon π-complex formation. This latter observation is consistent with the relative donating/π-accepting abilities of phosphine and phosphite ligands. More specifically, the electron density of the metal center of the tris(phosphine) precursors $WCl_2(NPh)(PR_3)_3$ should be greater than that of the resulting π-acceptor (L) complexes $WCl_2(L)(NAr)(PR_3)_2$, thus electronically favoring more rapid loss of phosphine from the tris(phosphine) precursor. In contrast, the combined donating/π-accepting ability of a phosphite ligand and the π-acceptor ligand (L) may be fairly comparable, making the rate of loss of a phosphite ligand from the tris(phosphite) and π-acceptor complexes competitive and perhaps determined by the relative sizes of the two ligands.

η^2-Cyclopropene Complexes

Synthesis and Stability. The reactions of the $WCl_2(NAr)(PX_3)_3$ precursors with 3,3-diphenylcyclopropene[24] and 4,8-dioxaspiro[2.5]oct-1-ene[25,26] (referred to throughout the remainder of this chapter as diphenylcyclopropene and ketalcyclopropene, respectively) were investigated, and two modes of reactivity were identified: η^2-cyclopropene coordination and vinyl alkylidene formation.[27] Many of the η^2-cyclopropene complexes were not stable at room temperature in standard NMR solvents (e.g., C_6D_6, tol-d_8, THF-d_8, and CD_2Cl_2), thus limiting the conditions under which they could be synthesized (eq 9). The preparation of η^2-cyclopropene complexes from phosphite precursors **2** - **4** was most readily accomplished in Et_2O, as the starting tris(phosphite) complexes were moderately soluble in Et_2O and the resulting η^2-cyclopropene complexes were only sparingly soluble. Thus, when the cyclopropene was added to a concentrated, heterogeneous purple mixture of the tris(phosphite) complex in Et_2O, the yellow η^2-cyclopropene complex began to precipitate almost immediately. The low solubility and high concentrations of the η^2-cyclopropene complex generally prevented any measurable conversion to the vinyl alkylidene on the time-scale of the reaction. After the reaction was complete, the resulting yellow or tan powders were purified by filtration and washing with Et_2O or pentane. Although recrystallization was not feasible for the less stable derivatives, it was possible to obtain X-ray quality crystals of W(η^2-diphenylcyclopropene)$Cl_2(NPh)[P(OMe)_3]_2$ (**10**) upon cooling a saturated toluene/benzene solution of this complex to 0 °C (*vide infra*).

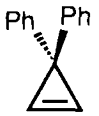

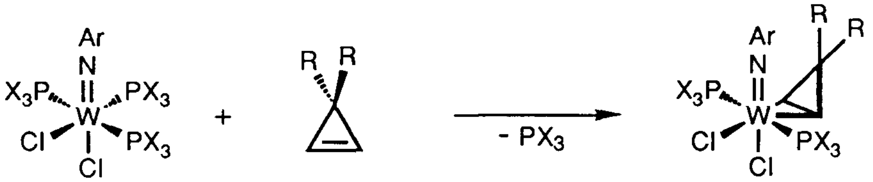

(9)

The preparations of η^2-cyclopropene complexes from the phenylimido precursor $WCl_2(NPh)[P(OMe)_3]_3$ **2** were especially sensitive to concentration effects. In dilute C_6D_6 solutions, the cyclopropenes were rapidly transformed to unidentified products without any measurable loss of **2**. A reasonable explanation, based on the reactivity of **2** - **4** with simple π-acceptor substrates and on the extensive documentation of oxidative addition reactions by cyclopropenes to form metallacycles, is that the small size of the phenylimido group, the lability of a second phosphite ligand, and the dilute conditions favor the competitive reaction of the η^2-cyclopropene complex with a second equivalent of cyclopropene. Careful identification of the organic products would provide further insight.

Several η^2-cyclopropene complexes were synthesized and are listed in Table 3 along with observations regarding their thermal stability. Two general trends emerged from the observations reported in this table: (1) The stability of the η^2-cyclopropene complexes decreased as the steric bulk of the imido substituents increased. (2) For the same imido and phosphite ancillary ligands, the η^2-diphenylcyclopropene complexes were more stable than the corresponding η^2-ketalcyclopropene complexes.

Spectroscopic Data. Characteristic of η^2-olefin complex formation, upfield shifts were observed for the olefinic proton and carbon resonances of the cyclopropenes upon complexation, along with corresponding 24 - 36 Hz decreases in the value of J_{CH}. (Table 4). These resonances appeared as triplets due to coupling with the two trans phosphine/phosphite ligands. The trends in stability documented in Table 3 were supported by the NMR spectroscopic data: For the phosphite complexes, the upfield shift

Table 3. η^2-Cyclopropene Complex Stability

Complex	Stability	
	Solid State	CD_2Cl_2 Soln (~12 h at r.t.)
$W(HC{=}CH\text{-}CPh_2)Cl_2(NPh)(PMePh_2)_2$ (**9**)	stable for months at r.t.	stable
$W(HC{=}CH\text{-}CPh_2)Cl_2(NPh)[P(OMe)_3]_2$ (**10**)	stable for months at r.t.	partial decomposition and conversion to vinyl alkylidene
$W(HC{=}CH\text{-}CPh_2)Cl_2(N\text{-}2,6\text{-}C_6H_3\text{-}Me_2)[P(OMe)_3]_2$ (**11**)	stored at -30 °C	conversion to vinyl alkylidene
$W(HC{=}CH\text{-}COCH_2CH_2CH_2O)Cl_2(NPh)(PMePh_2)_2$ (**12**)	stable for months at r.t.	stable
$W(HC{=}CH\text{-}COCH_2CH_2CH_2O)Cl_2(NPh)[P(OMe)_3]_2$ (**13**)	stored at -30 °C—after several months at r.t., yellow powder converted to a red/black oil—vinyl alkylidene observed	partial decomposition and conversion to vinyl alkylidene
$W(HC{=}CH\text{-}COCH_2CH_2CH_2O)Cl_2(N\text{-}2,6\text{-}C_6H_3\text{-}Me_2)[P(OMe)_3]_2$ (**14**)	stored at -30 °C	conversion to vinyl alkylidene

Table 4. Selected NMR Spectral Data for η^2-Cyclopropene Complexes^a

η^2-Cyclopropene Complex	^{1}H (t, *H*C=C*H*)^b		^{1}H (t, *H*C=C*H*)		^{13}C (t, H*C*=*C*H)				^{31}P (*P*X$_3$)	
	δ	J_{HP}	δ	J_{HP}	δ	J_{CH}	J_{CP}	J_{CW}	δ	J_{PW}
W(HC=CH-CPh$_2$)Cl$_2$(NPh)(PMePh$_2$)$_2$ (**9**)	4.19	5.68	3.75	5.63	72.4	195	9	45	5	208
W(HC=CH-CPh$_2$)Cl$_2$(NPh)[P(OMe)$_3$]$_2$ (**10**)	5.08	5.82	4.50	6.01	64.8	193	16	37	118	364
W(HC=CH-CPh$_2$)Cl$_2$(N-2,6-C$_6$H$_3$-Me$_2$)[P(OMe)$_3$]$_2$ (**11**)	5.29	5.98	4.74	5.79	66.2	194	15	40	110	379
W(HC=CH-COCH$_2$CH$_2$CH$_2$O)Cl$_2$(NPh)(PMePh$_2$)$_2$ (**12**)	3.66	5.86	3.30	5.71	67.5	188	9	42	5	212
W(HC=CH-COCH$_2$CH$_2$CH$_2$O)Cl$_2$(NPh)[P(OMe)$_3$]$_2$ (**13**)	4.82	5.62	4.14	5.98	59.9	210	15	37	120	361
W(HC=CH-COCH$_2$CH$_2$CH$_2$O)Cl$_2$(N-2,6-C$_6$H$_3$-Me$_2$)[P(OMe)$_3$]$_2$ (**14**)	4.96	5.71	4.27	5.91	61.5	194	15	31	114	376

[a] All spectra were acquired in CD$_2$Cl$_2$ unless noted otherwise. [b] In C$_6$D$_6$.

[c] Uncomplexed HC=CH-CPh$_2$: ^{1}H (CD$_2$Cl$_2$) δ 7.54 (*H*C=C*H*); ^{13}C (CD$_2$Cl$_2$) δ 113.8 (J_{CH} = 230, H*C*=*C*H).

[d] Uncomplexed HC=CH-COCH$_2$CH$_2$CH$_2$O: ^{1}H (CD$_2$Cl$_2$) δ 7.85 (*H*C=C*H*); ^{13}C (CD$_2$Cl$_2$) δ 126.0 (J_{CH} = 224, H*C*=*C*H).

of the η^2-cyclopropene olefinic proton and carbon resonances decreased as the steric bulk of the imido ligand increased, corresponding to weaker binding of the cyclopropene. Although the chemical shifts of the olefinic proton resonances differed substantially in CD_2Cl_2 and C_6D_6, the trend remained the same in both solvents. Clear trends in the coupling constants (e.g., J_{CW} and J_{CH}) were not discernable, although for the three η^2-ketalcyclopropene complexes, J_{CW} did decrease as the stability of the complexes decreased.

For the η^2-diphenylcyclopropene complexes **9** and **10**, substantial upfield shifts to 5.51 and 6.31 ppm, respectively, were observed for the *ortho* protons of the imido ring. These upfield shifts are best explained by the shielding of these resonances by one of the phenyl rings of the η^2-cyclopropene, requiring that the cyclopropene substituents lie syn to the imido ligand. Consistent with this explanation, similar upfield shifts of the phenylimido *ortho* protons were not observed in the corresponding η^2-ketalcyclopropene complexes **12** and **13**. However, a syn arrangement of the imido ligand and the ketal substituent of the cyclopropene was indicated by difference NOE spectroscopy of W(η^2-ketalcyclopropene)Cl_2(NPh)$[P(OMe)_3]_2$ (**13**). Specifically, irradiation of the phenylimido *ortho* protons resulted in a 2% enhancement of the 3.72 ppm resonance corresponding to one set of ether methylene protons and conversely, irradiation of the

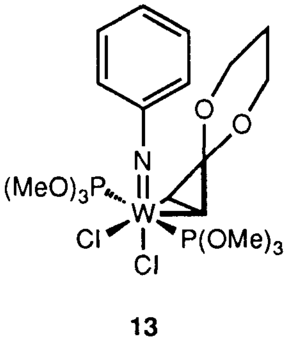

13

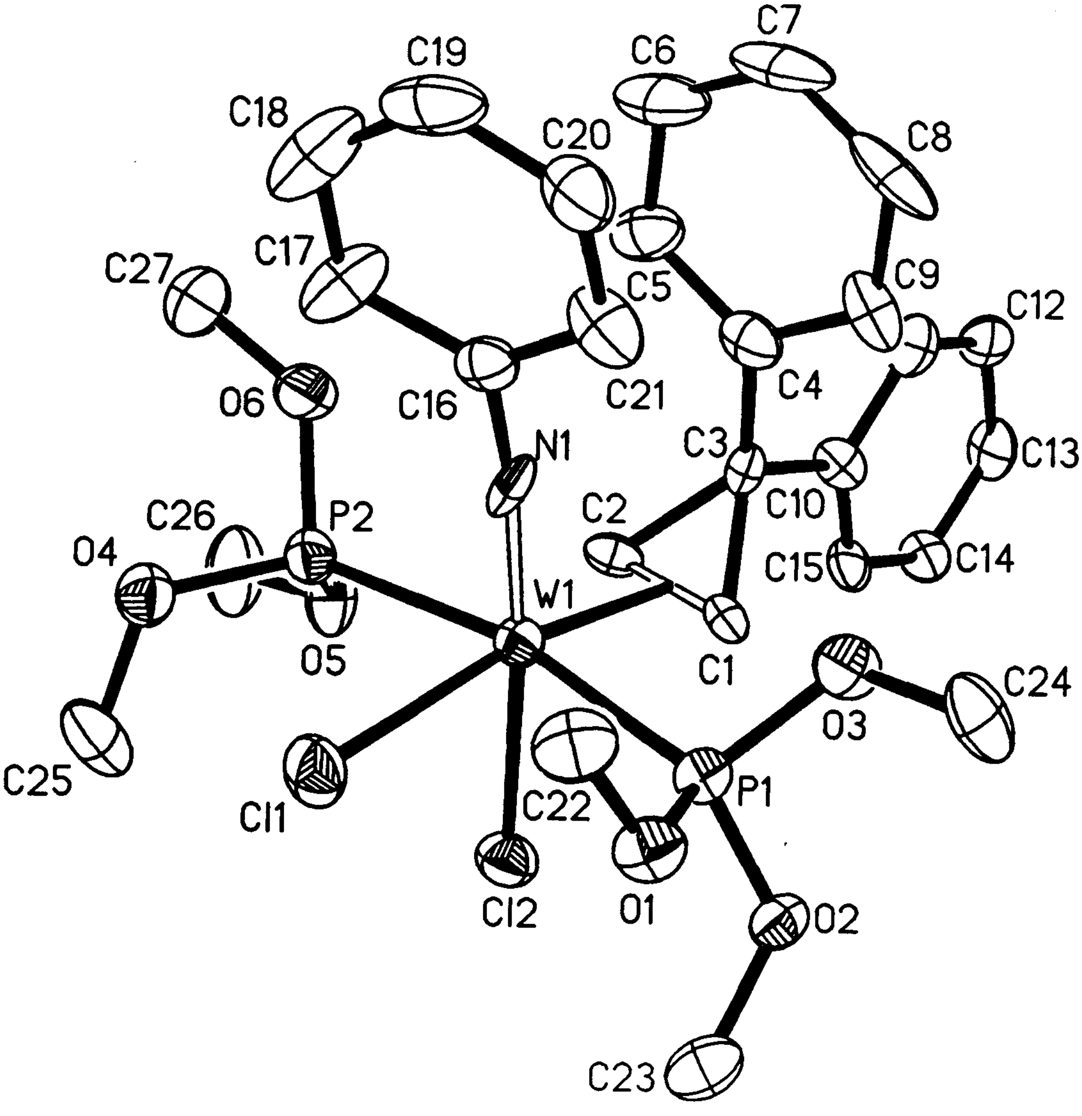

Figure 2. ORTEP plot of W(HC=CH-CPh$_2$)Cl$_2$(NPh)[P(OMe)$_3$]$_2$ (**10**). Thermal ellipsoids are drawn at the 50% probability level.

Table 5. Selected Bond Lengths and Angles for $\mathrm{W(H\overline{C{=}CH{-}C}Ph_2)Cl_2(NPh)[P(OMe)_3]_2}$ (**10**)

Bond Lengths (Å)

W(1) - Cl(1)	2.486(3)	W(1) - Cl(2)	2.482(3)
W(1) - P(1)	2.517(2)	W(1) - P(2)	2.530(3)
W(1) - N(1)	1.747(8)	W(1) - C(1)	2.171(9)
W(1) - C(2)	2.160(9)	W(1) - Cnt[a]	2.040
N(1) - C(16)	1.404(13)	C(1) - C(2)	1.452(12)
C(1) - C(3)	1.526(12)	C(2) - C(3)	1.518(13)
C(3) - C(4)	1.484(14)	C(3) - C(10)	1.531(13)

Bond Angles (°)

Cl(1) - W(1) - Cl(2)	83.9(1)	Cl(1) - W(1) - P(1)	84.3(1)
Cl(2) - W(1) - P(1)	89.3(1)	Cl(1) - W(1) - P(2)	84.2(1)
Cl(2) - W(1) - P(2)	86.1(1)	P(1) - W(1) - P(2)	168.0(1)
Cl(1) - W(1) - N(1)	90.8(2)	Cl(2) -W(1) - N(1)	174.6(2)
P(1) - W(1) - N(1)	91.5(2)	P(2) - W(1) - N(1)	92.1(2)
Cl(1) - W(1) - C(1)	156.3(2)	Cl(2) - W(1) - N(1)	82.9(2)
P(1) - W(1) - C(1)	76.0(2)	P(2) - W(1) - C(1)	114.3(2)
N(1) - W(1) - C(1)	102.5(3)	Cl(1) - W(1) - C(2)	156.7(3)
Cl(2) - W(1) - C(2)	83.6(2)	P(1) - W(1) - C(2)	115.1(3)
P(2) - W(1) - C(2)	75.3(3)	N(1) - W(1) - C(2)	101.0(3)
C(1) - W(1) - C(2)	39.2(3)	Cnt - W(1) - N(1)[a]	102.5
Cnt - W(1) - P(1)[a]	95.5	Cnt - W(1) - P(2)[a]	94.9
Cnt - W(1) - Cl(1)[a]	166.7	Cnt - W(1) - Cl(2)[a]	82.8
W(1) - N(1) - C(16)	170.8(6)	C(2) - C(1) - C(3)	61.3(6)
C(1) - C(2) - C(3)	61.8(6)	C(1) - C(3) - C(2)	57.0(6)
C(1) - C(3) - C(4)	123.7(8)	C(2) - C(3) - C(4)	124.3(8)
C(1) - C(3) - C(10)	112.4(7)	C(2) - C(3) - C(10)	113.2(8)
C(4) - C(3) - C(10)	114.3(8)		

---

[a] Cnt is the centroid of the C(1) - C(2) bond.

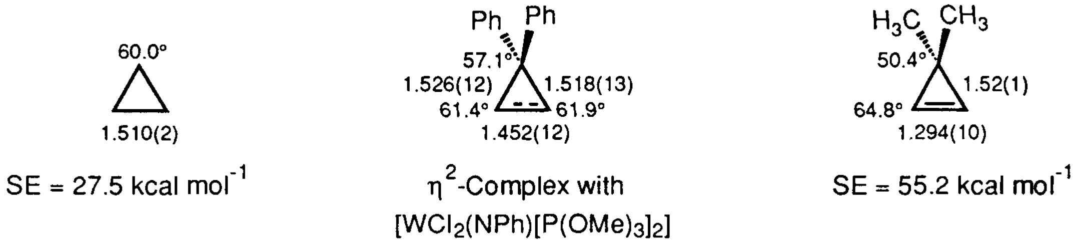

SE = 27.5 kcal mol^{-1}

η^2-Complex with $[WCl_2(NPh)[P(OMe)_3]_2]$

SE = 55.2 kcal mol^{-1}

Figure 3. A comparison of the structural data and strain energies of cyclopropane, 3,3-dimethylcyclopropene, and $W[\eta^2$-diphenylcyclopropene$]Cl_2[(NPh)[P(OMe)_3]_2$.[3a, 28]

3.72 ppm resonance resulted in a 4.5% enhancement of the phenylimido *ortho* protons. Irradiation of the olefinic protons did not enhance the *ortho* proton resonance of the arylimido ligand and vice versa.

Crystal Structure. A syn arrangement of the imido ligand and the cyclopropene substituents was further supported by an X-ray diffraction study of $W(\eta^2$-diphenylcyclopropene$)Cl_2(NPh)[P(OMe)_3]_2$ (**10**). An ORTEP diagram of this complex is shown in Figure 2 and selected bond lengths and angles are given in Table 5. This molecule is best described as a distorted octahedron with the olefinic carbons occupying one position in the equatorial plane. In addition to relieving steric crowding between the equatorial ligands, the displacement of the olefinic carbons ~12.5° beneath the equatorial plane also reduces unfavorable steric interactions between the imido phenyl ring and the cyclopropene phenyl ring that lies syn to tungsten. Adjustments that further accommodate the steric bulk of this cyclopropene phenyl ring include its stacking arrangement with the imido phenyl ring, the bending of the imido ligand away from the cyclopropene substituents, resulting in a W(1) - N(1) - C(16) angle of 170.8(6)°, and the bending of the cyclopropene phenyl rings away from the imido ligand (e.g., the C(2) - C(3) - C(4) angle is 11.1° larger than the C(2) - C(3) - C(10) angle).

A similar syn arrangement of a substituted arylimido ligand and the cyclopropene would yield unfavorable steric interactions between the imido substituents and the phosphite ligands and/or the cyclopropene substituents, thus accounting for the lesser stability of the substituted arylimido derivatives. The arylimido methyl substituents of W(η^2-diphenylcyclopropene)Cl_2(N-2,6-C_6H_3-Me_2)[P(OMe)$_3$]$_2$ (**11**) are equivalent at room temperature and at -80 °C, according to ^1H NMR spectroscopy. Given the crowded nature of this molecule, restricted rotation about the imido ligand is likely, especially at -80 °C, and this would place the arylimido ring in the P - W(N) - P plane, similar to the solid-state structure of **10**.

Strong π-back-donation by tungsten to the cyclopropene is evidenced in the structure of **10** by a substantial lengthening of the double bond and an accompanying large increase of the apical angle of the cyclopropene ring as compared to that of uncomplexed cyclopropene (Figure 3). The structure of the complexed cyclopropene more closely resembles that of a cyclopropane ring than a cyclopropene ring, and thus, a large decrease in ring strain accompanies complexation. Given this substantial amount of π-back-donation, the η^2-cyclopropene complexes are most accurately described as metallabicyclobutanes.

Diphenylvinyl Alkylidene Complexes

General Observations and Trends. In general, diphenylvinyl alkylidene formation was slower than η^2-diphenylcyclopropene coordination and an increase in the steric bulk of the imido ligand of the tungsten(IV) precursor favored the generation of the diphenylvinyl alkylidene complex over the η^2-diphenylcyclopropene complex. The W(=CH-CH=CPh_2)Cl_2(NAr)(PX_3)$_2$ compounds were observed as bright orange solutions and isolated as orange or yellow-orange powders. Coordination of the diphenylvinyl alkylidene moiety to tungsten was indicated spectroscopically by the downfield shifts of H_α and C_α,[29] the splitting of these resonances by the phosphite ligands, and the coupling of C_α to tungsten (Table 6). In addition, a downfield shift of H_β of the alkylidene moiety was also observed, and the large coupling between H$_\alpha$ and H$_\beta$ was indicative of a trans arrangement of the double bonds of the diphenylvinyl alkylidene ligand.

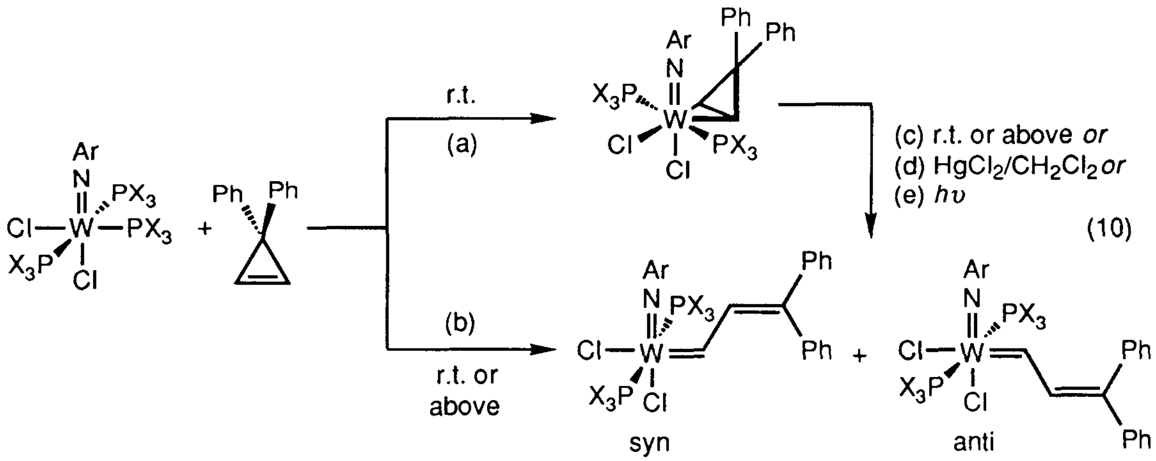

(10)

2,6-Di-*i*-Propylphenylimido Precursor. The clean synthesis of W(=CH-CH=CPh$_2$)Cl$_2$[N-2,6-C$_6$H$_3$-(*i*-Pr)$_2$][P(OMe)$_3$]$_2$ (**15**) and complete consumption of both starting materials was achieved when a slight excess of diphenylcyclopropene and WCl$_2$[N-2,6-C$_6$H$_3$-(*i*-Pr)$_2$][P(OMe)$_3$]$_3$ (**4**) were stirred together for 2 hours at 80 °C (eq 10b). Small amounts of **4** that remained unreacted could be separated from **15** by recrystallization from Et$_2$O or by washing the product mixture with a solution of THF in pentane. The observation of characteristic H$_\alpha$ and H$_\beta$ resonances coupled to the two mutually trans phosphite ligands provide confirmation of the preparation of **15**, and difference NOE and low-temperature spectra lent further insight into its structure. For example, the observation of a 19.2% NOE enhancement of the alkylidene H$_\alpha$ resonance of **15** upon irradiation of the *i*-propyl methine resonance and a 12.4% NOE enhancement in the other direction was indicative of an anti arrangement of the alkylidene ligand relative to the imido group. In the 90 MHz ^{1}H NMR spectrum of **15** at room temperature, the *i*-propyl methyl and methine protons gave rise to one doublet and one septet, respectively, indicative of free rotation about the arylimido ligand. Upon cooling

Table 6. Selected NMR Spectral Data for 2,6-Dimethyl- and 2,6-Di-*i*-Propylphenylimido Diphenylvinyl Alkylidene Complexes[a]

Diphenylvinyl Alkylidene Complex	H_α			H_β	C_α			
	δ	J_{HH}	J_{HP}	δ	δ	J_{CH}	J_{CP}	J_{CW}
anti-W[*trans*(=CH-CH=CPh$_2$)]Cl$_2$-[N-2,6-C$_6$H$_3$-(*i*-Pr)$_2$][P(OMe)$_3$]$_2$ (**15**)	12.9[b]	12.8	6.37	10.2	277	130	18.2	123
anti-W[*trans*(=CH-CH=CPh$_2$)][N-2,6-C$_6$H$_3$-(*i*-Pr)$_2$][OCMe(CF$_3$)$_2$]$_2$[P(OMe)$_3$] (**16**)	12.3	14.4	8.06	8.72	264	151	20.8	153
syn-W[*trans*(=CH-CH=CPh$_2$)][N-2,6-C$_6$H$_3$-(*i*-Pr)$_2$][OCMe(CF$_3$)$_2$]$_2$[P(OMe)$_3$] (**16**)	11.6	11.0	5.13	8.72	256	—	21.7	—
anti-W[*trans*(=CH-CH=CPh$_2$)][N-2,6-C$_6$H$_3$-(*i*-Pr)$_2$][O-2,6-C$_6$H$_3$-(*i*-Pr)$_2$]$_2$[P(OMe)$_3$] (**17**)	12.4	14.3	7.89	9.32	259	152	20.8	156
syn-W[*trans*(=CH-CH=CPh$_2$)][N-2,6-C$_6$H$_3$-(*i*-Pr)$_2$][O-2,6-C$_6$H$_3$-(*i*-Pr)$_2$]$_2$[P(OMe)$_3$] (**17**)	12.2	11.4	6.31	8.89	253	125	22.2	164
anti-W[*trans*(=CH-CH=CPh$_2$)]Cl$_2$-(N-2,6-C$_6$H$_3$-Me$_2$)(PEt$_2$Ph)$_2$ (**18**)	12.2	13.1	4.4	9.55	272	128	12.6	—
syn-W[*trans*(=CH-CH=CPh$_2$)]Cl$_2$-(N-2,6-C$_6$H$_3$-Me$_2$)(PEt$_2$Ph)$_2$ (**18**)	11.9	13.1	4.4	8.72	278	130	12.6	—
anti-W[*trans*(=CH-CH=CPh$_2$)]Cl$_2$-(N-2,6-C$_6$H$_3$-Me$_2$)[P(OMe)$_3$]$_2$ (**19**)	12.9	13.0	6.24	9.62	277	130	17.6	117
syn-W[*trans*(=CH-CH=CPh$_2$)]Cl$_2$-(N-2,6-C$_6$H$_3$-Me$_2$)[P(OMe)$_3$]$_2$ (**19**)	12.4	13.3	6.69	8.80	284	133	17.5	—

[a] All spectra were acquired in CD$_2$Cl$_2$ unless indicated otherwise. [b] Tol-d_8.

to -80 °C, restricted rotation resulted in two doublet resonances for the *i*-propyl methyl protons and two septet resonances for the methine protons, thus requiring that the arylimido ring lie in the Cl - W(N) - C$_\alpha$ plane, an arrangement that would minimize steric interactions between the *i*-propyl groups and the phosphite ligands.

High temperatures were necessary for the complete conversion of **4** and diphenylcyclopropene to the diphenylvinyl alkylidene **15**. For example, stirring a 1:1 mixture of diphenylcyclopropene and **4** in a concentrated Et$_2$O or Et$_2$O/CH$_2$Cl$_2$ solution for as long as 48 h at room temperature did not lead to complete vinyl alkylidene formation. Instead an orange mixture composed of **4**, **15**, and what are tentatively assigned as two η^2-cyclopropene species was isolated. An approximately 2:1 ratio of triplets at 5.31 (J_{HP} = 5.91 Hz) and 5.36 (J_{HP} = 5.36 Hz) ppm in the ^{1}H NMR spectrum in C_6D_6 were indicative of η^2-cyclopropene complex formation. These chemical shifts are slightly downfield of that observed for the analogous dimethylphenylimido compound **11**, again consistent with weaker binding of the cyclopropene to the sterically more bulky imido precursor. For all other combinations of imido and phosphine/phosphite ancillary ligands that were studied, only one form of the η^2-cyclopropene complex was observed. Perhaps for the di-*i*-propylphenylimido complex, the stabilities of the syn and anti η^2-cyclopropene isomers are comparable, due to a large destabilization of the syn adduct by the steric bulk of the imido substituents.

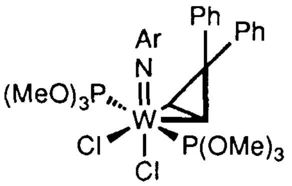

syn

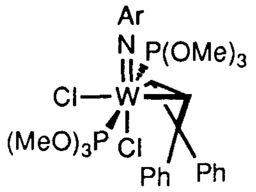

anti

Reactions of **15** with two equivalents of $LiOCMe(CF_3)_2$ or LiO-2,6-C_6H_3-(*i*-Pr)$_2$ yielded the mono(phosphite) adducts of the corresponding tungsten alkoxide complexes W(=CH-CH=CPh_2](N-2,6-C_6H_3-(*i*-Pr)$_2$][$OCMe(CF_3)_2$]$_2$[$P(OMe)_3$] (**16**) and W(=CH-CH=CPh_2)[N-2,6-C_6H_3-(*i*-Pr)$_2$][O-2,6-C_6H_3-(*i*-Pr)$_2$]$_2$[$P(OMe)_3$] (**17**) (eq 11). Both complexes were isolated as a mixture of syn and anti rotamers. Difference NOE measurements for **16** were consistent with the synthesis of mainly the anti rotamer, and syn and anti designations for **17** are based on comparisons with analogous vinyl alkylidene complexes.[30]

An X-ray diffraction study of **16** provided further confirmation of the ring-opening of diphenylcyclopropene to give the corresponding vinyl alkylidene ligand. An ORTEP diagram of the structure is shown in Figure 4 and selected bond lengths and

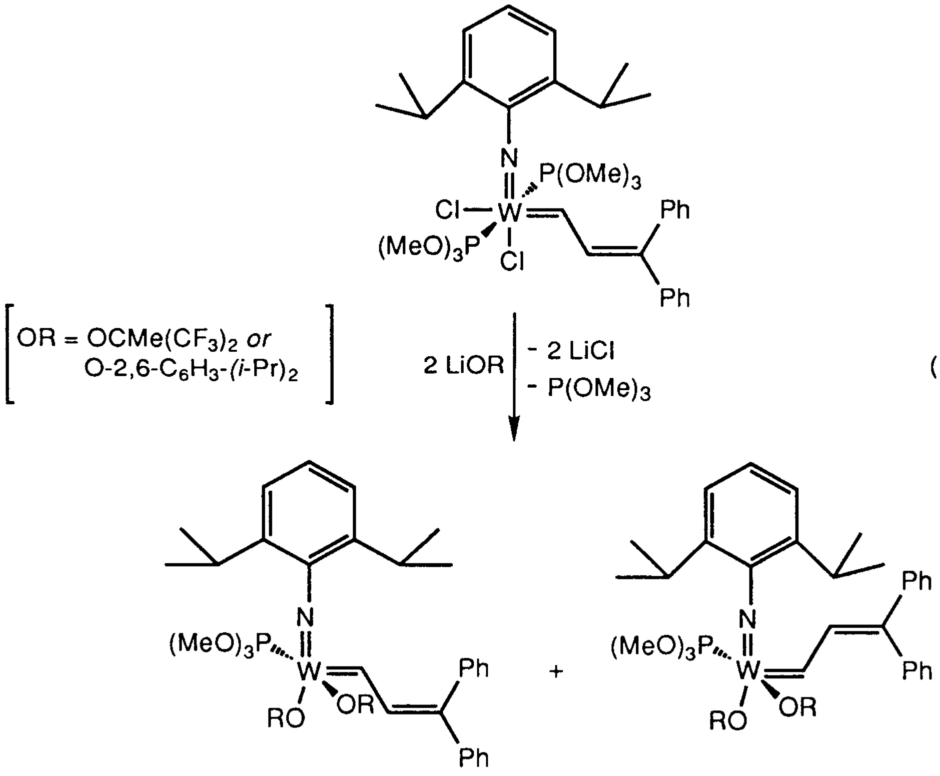

(11)

angles are given in Table 7. The geometry of **16** is a distorted trigonal bipyramid with the phosphite ligand and one alkoxide ligand [P(1) and O(2)] occupying the apical positions. This structure closely resembles that of *anti*-W[*trans*(=CH-CH=CHMe)][N-2,6-C_6H_3-(*i*-Pr)$_2$][OCMe(CF_3)$_2$]$_2$(quinuclidene),[30] and therefore, the similar geometries and ligand environments of the two complexes should enable a fairly accurate comparison of the two different vinyl alkylidene ligands. These alkylidenes are bound to tungsten(VI) and are therefore nucleophilic, or Schrock-type alkylidenes, that are polarized in the M^+—C^- direction.[31] Both vinyl alkylidene ligands are resonance-stabilized, however, the potential for greater delocalization of the negative charge on the

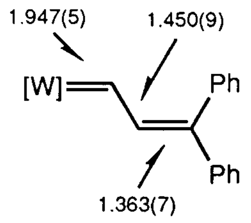

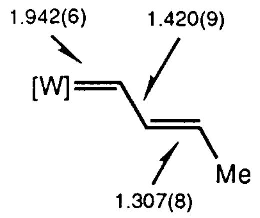

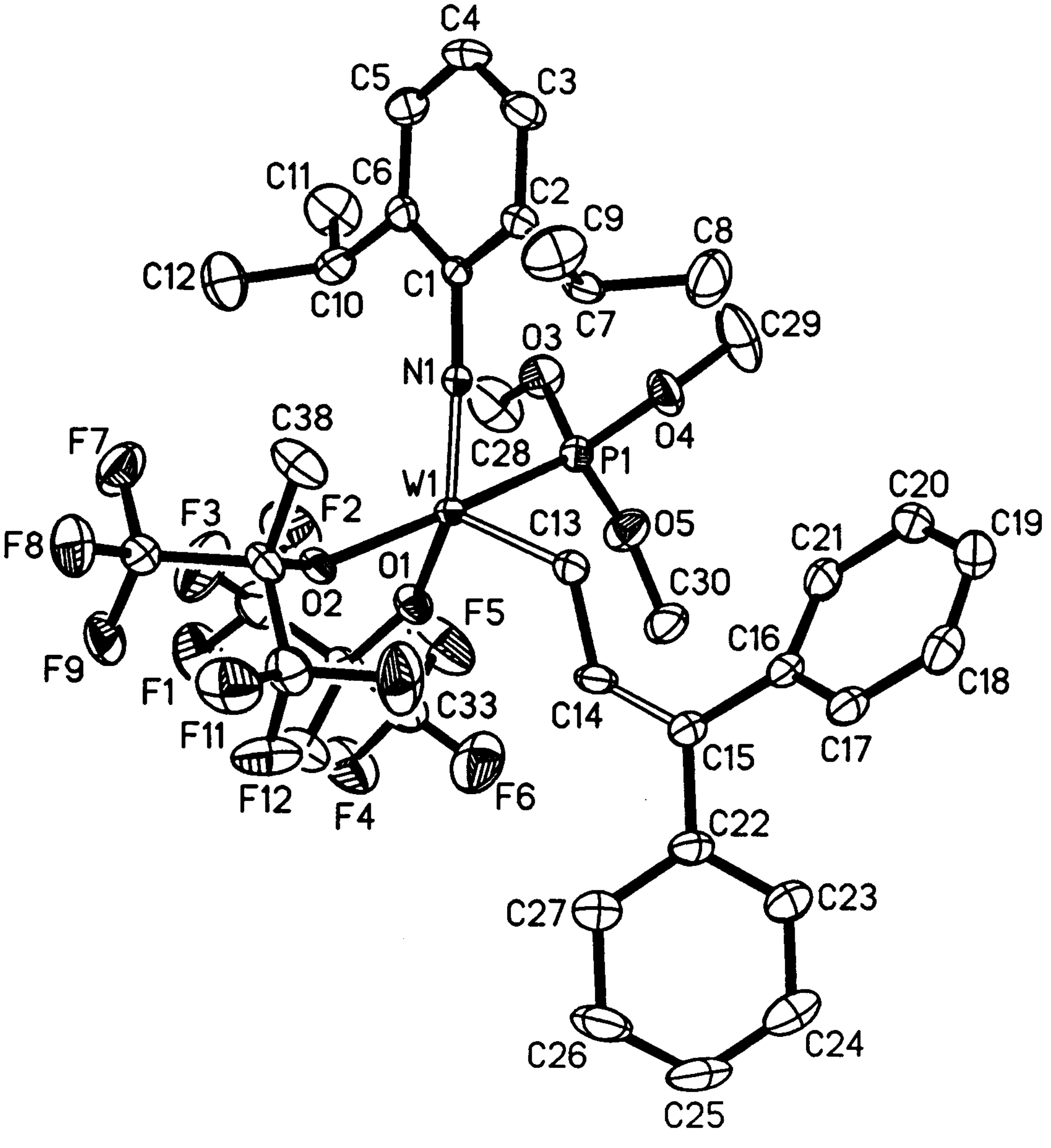

Figure 4. ORTEP plot of W(=CH-CH=CPh$_2$)[N-2,6-C$_6$H$_3$-(*i*-Pr)$_2$][OCMe(CF$_3$)$_2$]$_2$-[P(OMe)$_3$] (**16**). Thermal ellipsoids are drawn at the 50% probability level.

Table 7. Selected Bond Lengths and Angles for W(=CH-CH=CPh_2)[N-2,6-C_6H_3-(*i*-Pr$)_2$][OCMe($CF_3)_2]_2$[P(OMe$)_3$] (**16**)

Bond Lengths (Å)

W(1) - P(1)	2.505(1)	W(1) - O(1)	1.975(4)
W(1) - O(2)	1.996(3)	W(1) - N(1)	1.753(4)
W(1) - C(13)	1.947(5)	C(13) - C(14)	1.450(9)
C(14) - C(15)	1.363(7)	C(15) - C(16)	1.479(7)
C(15) - C(22)	1.483(9)		

Bond Angles (°)

P(1) - W(1) - O(1)	81.8(1)	P(1) - W(1) - O(2)	163.7(1)
O(1) - W(1) - O(2)	84.6(1)	P(1) - W(1) - N(1)	83.6(1)
O(1) - W(1) - N(1)	146.9(2)	O(2) - W(1) - N(1)	103.3(2)
P(1) - W(1) - C(13)	86.7(1)	O(1) - W(1) - C(13)	109.8(2)
O(2) - W(1) - C(13)	106.4(2)	N(1) - W(1) - C(13)	98.8(2)
W(1) - O(1) - C(31)	150.4(3)	W(1) - O(2) - C(35)	137.5(3)
W(1) - N(1) - C(1)	168.0(3)	W(1) - C(13) - C(14)	122.2(4)
C(13) - C(14) - C(15)	127.5(5)	C(14) - C(15) - C(16)	123.1(5)
C(14) - C(15) - C(22)	118.7(5)		

diphenylvinyl alkylidene ligand is illustrated by the lengthening of the bonds of this alkylidene as compared to those of the methylvinyl alkylidene moiety and is consistent with the observation that in the crystal structure of **16**, the phenyl rings lie in conjugation with the vinyl alkylidene group.

2,6-Dimethylphenylimido Precursors. The room-temperature reaction of diphenylcyclopropene with the phosphine precursor WCl_2(N-2,6-C_6H_3-Me_2)($PEt_2Ph)_3$ (**1**) in a mixture of Et_2O and pentane produced the yellow-orange vinyl alkylidene complex W(=CH-CH=CPh_2)Cl_2(N-2,6-C_6H_3-Me_2)($PEt_2Ph)_2$ (**18**) in good yield as an approximately two to one mixture of rotamers (eq 10b). Irradiation of the imido methyl groups of the major rotamer resulted in a 20% NOE enhancement of the alkylidene H_α

resonance, indicative of an anti arrangement of the two ligands, and correspondingly, irradiation of the imido methyl groups of the minor rotamer caused a 14% enhancement of the alkylidene H_β resonance, indicative of a syn arrangement of the two ligands.

In contrast, stirring a mixture of diphenylcyclopropene with the analogous phosphite precursor $WCl_2(N\text{-}2,6\text{-}C_6H_3\text{-}Me_2)[P(OMe)_3]_3$ (**3**) in Et_2O gave the yellow η^2-cyclopropene complex $W(\eta^2\text{-diphenylcyclopropene})Cl_2(N\text{-}2,6\text{-}C_6H_3\text{-}Me_2)[P(OMe)_3]_2$ (**11**) (eq 10a). A room-temperature, concentrated CD_2Cl_2 solution of this compound was monitored over a 24 h period by ^1H, ^{13}C, and ^{31}P NMR spectroscopy, enabling the observation of the clean and complete conversion of the η^2-diphenylcyclopropene species to the diphenylvinyl alkylidene complex $W(=CH\text{-}CH=CPh_2)Cl_2(N\text{-}2,6\text{-}C_6H_3\text{-}Me_2)[P(OMe)_3]_2$ (**19**) (eq 10c). Addition of excess diphenylcyclopropene to a CD_2Cl_2 solution of **11** slowed the rate of conversion to vinyl alkylidene and also resulted in the production of what is tentatively assigned as the alkylidene complex resulting from ring-opening metathesis of diphenylcyclopropene by **19** (Table 10, Experimental Section).

Phenylimido Precursors. The phenylimido precursors $WCl_2(NPh)(PMePh_2)_3$ and $WCl_2(NPh)[P(OMe)_3]_3$ formed relatively stable η^2-cyclopropene complexes, and the results of initial attempts to thermally convert these complexes to vinyl alkylidenes were not promising. However, there are literature precedents for the ring-opening of cyclopropenes upon photolysis[32] or upon catalysis by $HgCl_2$,[33] and therefore, both of these methods were investigated. Catalytic amounts of $HgCl_2$ converted CH_2Cl_2 solutions of the metallabicyclobutanes **9** and **10** to the corresponding tungsten vinyl alkylidenes within several hours (eq 10d and Table 11, Experimental Section). Conversion was complete within minutes upon the addition of 1 equiv of $HgCl_2$; however, such large amounts of $HgCl_2$ also slowly catalyzed the decomposition of the vinyl alkylidene complex. Photolyzing dilute solutions of the η^2-cyclopropene complexes **9** and **10** at 0 °C also resulted in the rearrangement to the corresponding vinyl alkylidene compounds (eq 10e and Table 12, Experimental Section).

Ketalvinyl Alkylidene Complexes

Similar to vinyl alkylidene syntheses from diphenylcyclopropene, an increase in the steric bulk of the imido ligand favored formation of the ketalvinyl alkylidene complex over the corresponding η^2-ketalcyclopropene complex. Moreover, ring-opening of ketalcyclopropene occurred more readily than for 3,3-diphenylcyclopropene. However, the chemistry was also more complex, as several forms of the ketalvinyl alkylidene were noted. As shown in eq 12, in addition to syn and anti rotamers of the *trans*-vinyl alkylidene ligand **A**, the chelating *cis*-vinyl alkylidene ligand **B** and the ring-opened chelating chloro-alkylidene **C** were also observed and were the thermodynamic products of the reaction. In the remainder of this chapter, the formulas for these ketalvinyl alkylidene compounds will be written as $W(CHR_Y)Cl_m(NAr)(PX_3)_n$, where Y = A, B, or C and denotes the structure of the alkylidene.

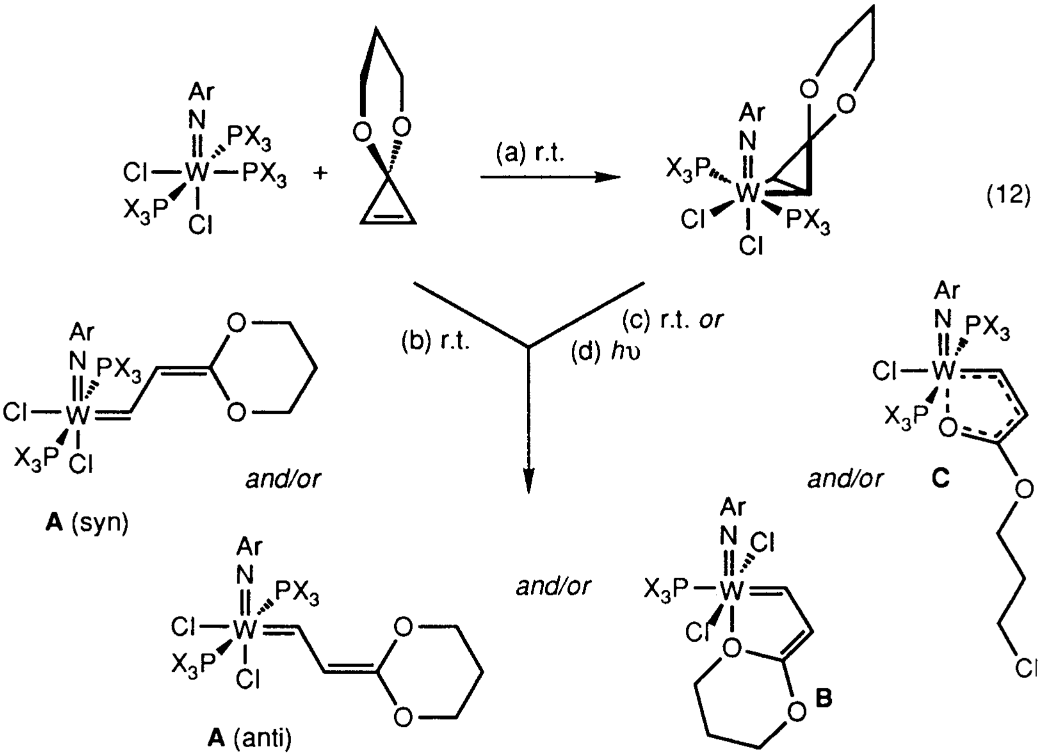

Table 8. Selected NMR Spectral Data for 2,6-Dimethyl- and 2,6-Di-*i*-Propylphenylimido Ketalvinyl Alkylidene Complexes[a]

Diphenylvinyl Alkylidene Complex	H$_\alpha$			C$_\alpha$				C$_\gamma$	OCH$_2$	XCH$_2$
	δ	J$_{HH}$	J$_{HP}$	δ	J$_{CH}$	J$_{CP}$	J$_{CW}$	δ	δ	δ
W(CHR$_B$)Cl$_2$[N-2,6-C$_6$H$_3$-(*i*-Pr)$_2$][P(OMe)$_3$] (**20-B**)	11.7	9.81	6.82	260	144	20.7	124	165	68.8	67.6[b]
W(CHR$_C$)Cl[N-2,6-C$_6$H$_3$-(*i*-Pr)$_2$][P(OMe)$_3$]$_2$ (**20-C**)	12.6	8.26	2.30	257	—	10.2	—	177	62.3	41.1[c]
W(CHR$_A$)Cl$_2$(N-2,6-C$_6$H$_3$-Me$_2$)(PEt$_2$Ph)$_2$ (**21-A**)[d]	12.7	14.2	3.98	264	—	11.0	—	—	—	—
W(CHR$_A$)Cl$_2$(N-2,6-C$_6$H$_3$-Me$_2$)(PEt$_2$Ph)$_2$ (**21-A**)[d]	12.6	13.6	3.79	270	—	10.8	—	—	—	—
W(CHR$_B$)Cl$_2$(N-2,6-C$_6$H$_3$-Me$_2$)(PEt$_2$Ph) (**21-B**)	11.5	9.93	5.51	—	—	—	—	—	—	—
W(CHR$_C$)Cl(N-2,6-C$_6$H$_3$-Me$_2$)(PEt$_2$Ph)$_2$ (**21-C**)	12.3	8.07	2.13	262	134	7.2	119	174	61.9	41.6[c]
W(CHR$_B$)Cl$_2$(N-2,6-C$_6$H$_3$-Me$_2$)Cl$_2$[P(OMe)$_3$] (**22-B**)	11.9	9.79	6.80	260	145	20.5	122	165	68.7	67.5[b]
W(CHR$_C$)Cl(N-2,6-C$_6$H$_3$-Me$_2$)[P(OMe)$_3$]$_2$ (**22-C**)	12.7	—	—	258	135	10.0	114	177	62.2	41.0[c]

[a]All spectra were acquired in CD$_2$Cl$_2$ unless indicated otherwise. [b]X = O. [c]X = Cl. [d]Syn or anti rotamer.

The ketalvinyl alkylidenes **A**, **B**, and **C** could be distinguished by color and by spectroscopic data. Solutions of **A** and/or **B** were red, whereas solutions of **C** were green. The distinguishing feature of **A** was the large coupling between H$_\alpha$ and H$_\beta$ of the *trans*-ketalvinyl alkylidene ligand, which was similar to that of the diphenylvinyl alkylidene ligand. The coupling between H$_\alpha$ and H$_\beta$ was smaller in both **B** and **C**, due to the cis arrangement of the double bonds. However, a marked upfield shift (~20 ppm) of the ^{13}C NMR resonance of one of the ether methylene carbons occurred upon substitution of oxygen by chlorine and provided a clear indication of the formation of **C**. In addition, another very characteristic indication of conversion to **C** was an approximately 10 ppm downfield shift of C$_\gamma$, resulting from the contribution of the enone resonance form to the structure of **C** (Table 8).

2,6-Di-*i*-Propylphenylimido Precursor. Ketalcyclopropene reacted with $WCl_2[N\text{-}2,6\text{-}C_6H_3\text{-}(i\text{-}Pr)_2][P(OMe)_3]_3$ (**4**) at room temperature to give the corresponding *cis*-vinyl alkylidene **20-B**. When the reaction was followed by ^1H NMR spectroscopy, the η^2-cyclopropene complex was not observed. The reaction yields were highest when a highly concentrated, heterogeneous mixture of the tris(phosphite) precursor **4** in Et_2O was mixed with a slight excess of ketalcyclopropene, although even under these conditions, some of the tris(phosphite) precursor always remained after all of the ketalcyclopropene had reacted. The nature of the side reaction was not identified. The tris(phosphite) compound was separated from **20-B** by washing the reaction mixture with an Et_2O solution containing ~5-6 equiv of $P(OMe)_3$, and the product was then isolated as a golden bis(phosphite) adduct, which exhibited poor solubility in C_6D_6 and tol-d_8 but dissolved readily in THF-d_8 and CD_2Cl_2. In CD_2Cl_2, only the red mono(phosphite) adduct of the *cis*-vinyl alkylidene **B** was observed along with one equivalent of free $P(OMe)_3$.

The proposed structure of the chelating *cis*-ketalvinyl alkylidene **B** is based upon substantial spectroscopic data and comparisons with known compounds of similar geometry. For complex **20-B**, the proton and carbon assignments are based upon ^1H, ^{13}C, DEPT (coupled and decoupled), and ^1H-^1H and ^1H-^{13}C COSY spectra. In the NOESY spectrum of **20-B**, enhancements were observed between H_α and the *i*-propyl methine resonance and also between H_α and H_β, consistent, respectively, with an anti orientation of the alkylidene ligand relative to the imido group and a cis arrangement of the double bonds of the alkylidene moiety. The coupling constant between H_α and H_β is 9.55 Hz, which is smaller than that of *trans*-vinyl alkylidene ligands and again indicative of cis double bonds.

In previous studies of vinylalkylidene ligands, a trans geometry of the vinyl alkylidene double bonds was observed, and therefore, chelation by the ketalvinyl alkylidene group, which would necessarily require a cis geometry of the double bonds, is implied. The coordination of only one phosphite/phosphine ligand in complexes **B** further supports displacement of the other donor ligand by the chelating alkylidene ligand. In order to maximize π-bonding, the alkylidene substituents must lie in the N - W - C_α plane, which would place the chelating ketal functionality trans to the imido ligand.[34] Given these restrictions, the phosphite and chloride ligands must lie in the equatorial plane, with the phosphite ligand either cis or trans to the alkylidene ligand. A comparison of all the ketalvinyl alkylidene complexes **A**, **B**, and **C** indicates that the coupling of the alkylidene H_α and C_α resonances with phosphorus is larger in **B** than in **A** or **C**, and therefore, the structure in which the phosphite ligand lies trans to the alkylidene ligand is tentatively assigned. Given this geometry, the observation of one *i*-propyl methine resonance and two *i*-propyl methyl resonances at both room temperature and -80 °C implies that there is restricted rotation about the imido ligand with the aryl ring lying in the Cl - W(N) - Cl plane. Further support for the proposed structure of **B** is evidenced by its resemblance to the structure of the analogous chelating *o*-methoxybenzylidene complex, which was determined by X-ray crystallography.

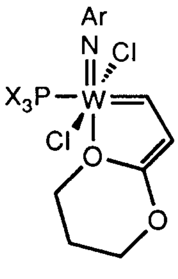

B

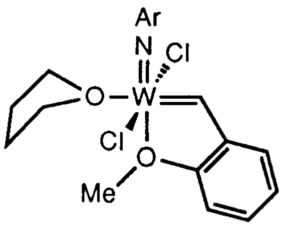

The poor solubility of complex **20-B** in C_6D_6 and tol-d_8 and its isolation as a bis(phosphite) adduct were puzzling. The most reasonable explanation at the present time is that the form of **20-B** that precipitates from the Et_2O solution is a cationic species in which a phosphite ligand has displaced a chloride. This would account for the difficulties encountered in redissolving **20-B** in benzene or toluene and is consistent with the observed rearrangement of complexes **B** to form **C**. Upon dissolution in CH_2Cl_2, the cationic species must rapidly rearrange to the neutral complex **20-B**, the form that is observed in solution (eq 13).

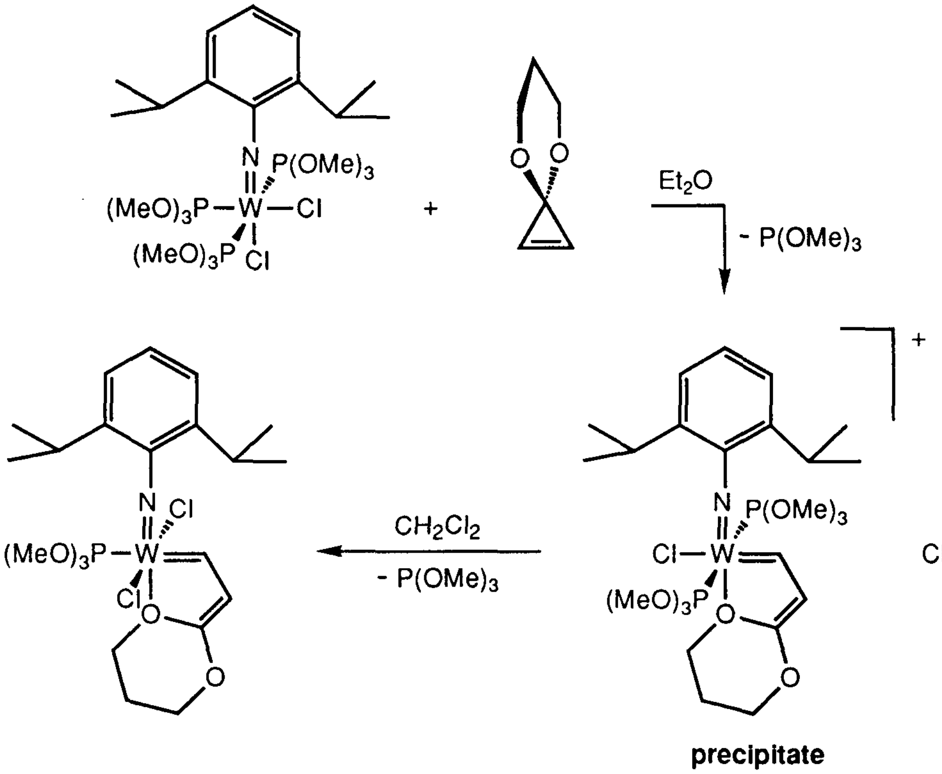

(13)

In CD_2Cl_2 solution and in the solid state, slow conversion of **20-B** to **20-C** was observed. Specifically, less than 50% of **20-B** converted to **20-C** during 12 hours in a concentrated CD_2Cl_2 solution, and conversion of **20-B** to **20-C** occurred over a period of months in the solid state at room temperature. These observations are consistent with the proposed ability of **20-B** to form a cationic species and the isolation of **20-B** in this form. Upon removal of one equivalent of phosphite from the complex, the rearrangement of **20-B** to **20-C** was not observed after a few days in CD_2Cl_2 solution, and this observation implies that in the absence of a second equivalent of phosphite, the cationic intermediate is quickly trapped by the chloride anion to generate the neutral complex. Slower nucleophilic attack of the chloride anion on the ether methylene carbon, which would result in opening of the 6-membered ring and production of **20-C**, is thus not observed.

2,6-Dimethylphenylimido Precursors. The room-temperature reaction of ketalcyclopropene with $WCl_2(N\text{-}2,6\text{-}C_6H_3\text{-}Me_2)(PEt_2Ph)_3$ in a mixture of Et_2O and pentane resulted in the isolation of a mixture of **21-A, 21-B,** and **21-C** as a red powder in good yield. NMR spectra (^1H, ^{13}C, and ^{31}P) of solutions of this powder were clean but complex, and only the H_α and C_α resonances were assigned. Large H_α - H_β coupling constants of two of the isomers, which composed 71% of the isomeric mixture, were indicative of syn and anti rotamers of **21-A**. The H_α resonances of these rotomers appeared at 12.70 (J_{HH} = 14.17 Hz, J_{HP} = 3.98 Hz) and 12.66 (J_{HH} = 13.60 Hz, J_{HP} = 3.79 Hz) ppm and the C_α chemical shifts appeared at 270.4 and 263.9 ppm. Five percent of the product mixture was the mono(phosphite) adduct **21-B**. Consistent with its assigned structure, the H_α resonance of **21-B** was shifted one ppm upfield of that of **21-A** to 11.54 ppm, and the H_α - H_β coupling constant and H_α - P coupling constant of this resonance (J_{HH} = 9.93 Hz, J_{HP} = 5.51 Hz) were smaller and larger, respectively, than the analogous couplings observed for H_α of **21-A**.

The red isomeric mixture turned green upon dissolution in CD_2Cl_2 for less than a day at room temperature, and only the fourth isomer, **21-C**, was then observed. Single crystals of **21-C** were grown from a saturated pentane solution that was slowly cooled to -20 °C, and the structure of this complex was then determined by an X-ray diffraction study. An ORTEP diagram of **21-C** is shown in Figure 5 and Table 9 contains selected bond angles and lengths. The geometry of **21-C** is basically a distorted octahedron with all of the equatorial ligands lying on the opposite side of the plane from the apical imido ligand. The arylimido ring lies in the N(1) - W(1) - C(1) plane, thus further minimizing unfavorable steric interactions between the imido methyl groups and the equatorial phosphine ligands. The W(1) - C(1) bond length is longer than that of a normal tungsten alkylidene, and a substantial amount of π-delocalization of the chelating 5-membered ring

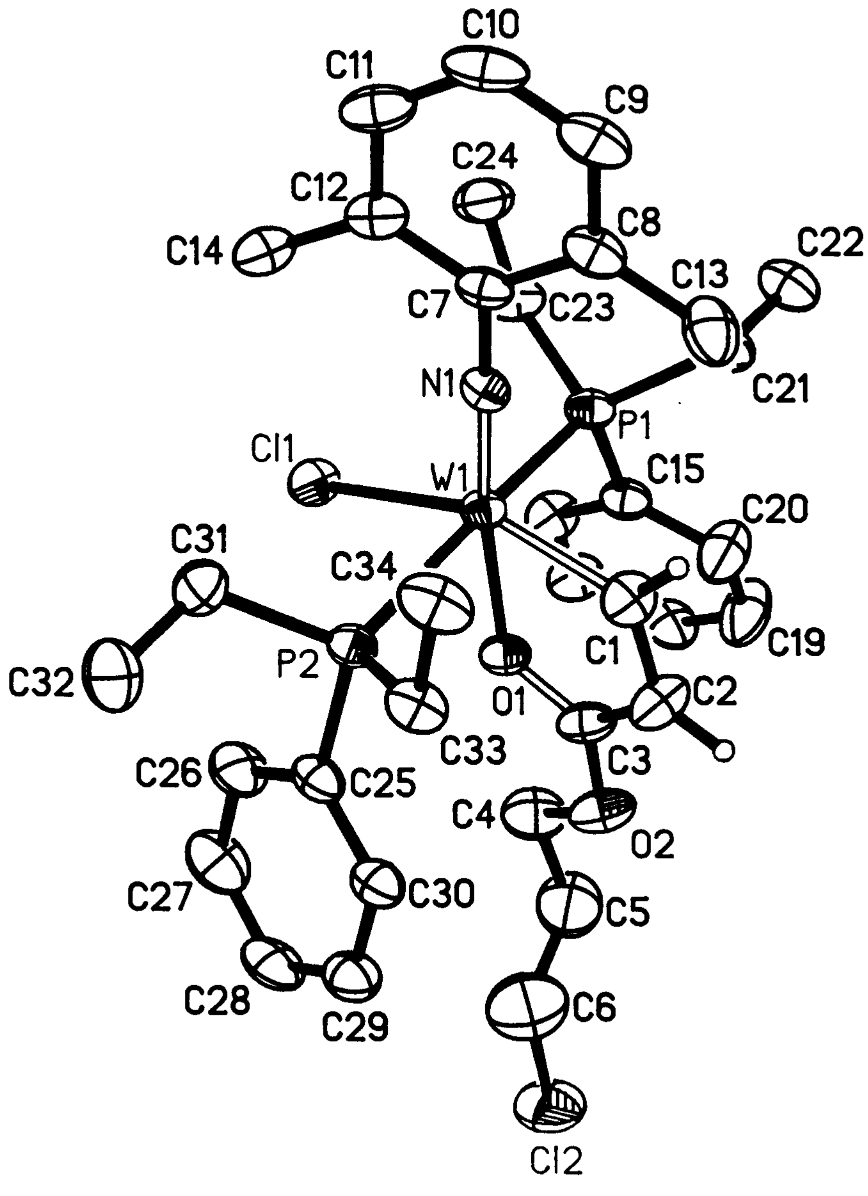

Figure 5. ORTEP plot of **21-C**. Thermal ellipsoids are drawn at the 50% probability level.

Table 9. Selected Bond Lengths and Angles for **21-C**

Bond Lengths (Å)

W(1) - Cl(1)	2.495(1)	W(1) - P(1)	2.509(1)
W(1) - P(2)	2.512(1)	W(1) - O(1)	2.191(3)
W(1) - N(1)	1.766(3)	W(1) - C(1)	2.032(5)
Cl(2) - C(6)	1.819(8)	O(1) - C(3)	1.275(6)
O(2) - C(3)	1.350(5)	O(2) - C(4)	1.430(7)
N(1) - C(7)	1.393(5)	C(1) - C(2)	1.398(6)
C(2) - C(3)	1.388(7)	C(4) - C(5)	1.519(8)
C(5) - C(6)	1.430(10)		

Bond Angles (°)

Cl(1) - W(1) - P(1)	85.5(1)	Cl(1) - W(1) - P(2)	85.7(1)
P(1) - W(1) - P(2)	166.1(1)	Cl(1) - W(1) - O(1)	81.0(1)
P(1) - W(1) - O(1)	83.9(1)	P(2) - W(1) - O(1)	84.2(1)
Cl(1) - W(1) - N(1)	106.6(1)	P(1) - W(1) - N(1)	95.7(1)
P(2) - W(1) - N(1)	97.1(1)	O(1) - W(1) - N(1)	172.4(1)
Cl(1) - W(1) - C(1)	154.5(1)	P(1) - W(1) - C(1)	94.7(1)
P(2) - W(1) - C(1)	88.7(1)	O(1) - W(1) - C(1)	73.8(1)
N(1) - W(1) - C(1)	98.8(2)	C(3) - O(2) - C(4)	115.7(4)
W(1) - O(1) - C(3)	114.9(3)	W(1) - C(1) - C(2)	120.0(4)
W(1) - N(1) - C(7)	177.6(3)	O(1) - C(3) - O(2)	119.4(4)
C(1) - C(2) - C(3)	111.5(5)	O(2) - C(3) - C(2)	121.0(4)
O(1) - C(3) - C(2)	119.6(4)	C(4) - C(5) - C(6)	111.8(6)
O(2) - C(4) - C(5)	109.5(5)	Cl(2) - C(6) - C(5)	113.0(6)

is indicated by its structure, which lies intermediate between the tungsten enolate and chelating enone resonance forms, although the bond lengths are slightly closer to those of the latter resonance structure. The two phenyl rings of the phosphine ligands stack with the 5-membered, tungsten-containing ring.

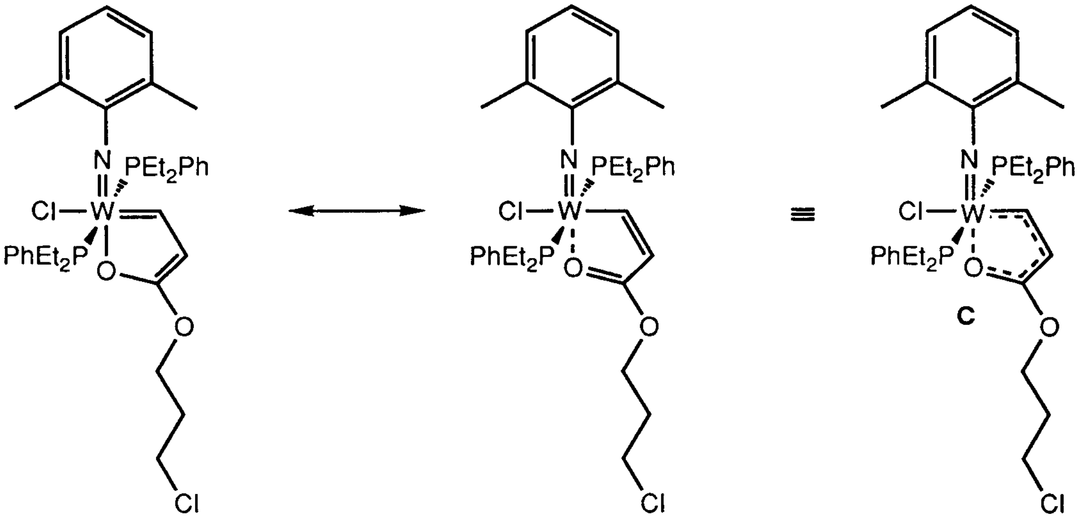

The NMR spectra of **21-C** are consistent with its structural determination. For example, the H_α and C_α resonances are coupled to the two mutually trans phosphine ligands and are shifted slightly upfield of the same resonances of **21-A**. The coupling of these resonances to phosphorus and to tungsten is smaller than the analogous coupling observed in **21-A**, indicative of a lengthening of the W - C_α bond, and the coupling between H_α and H_β is relatively small (7.96 Hz) due to the cis arrangement of the alkylidene double bonds. In the ^{13}C NMR spectrum, only one methylene carbon adjacent to oxygen was observed at 61.9 ppm, the methylene carbon adjacent to chlorine appeared 20 ppm upfield at 41.6 ppm, and C_γ was shifted downfield to 174 ppm.

Stirring an extremely concentrated Et_2O mixture of $WCl_2(N\text{-}2,6\text{-}C_6H_3\text{-}Me_2)[P(OMe)_3]_3$ (**3**) and ketalcyclopropene for several hours yielded the tan η^2-cyclopropene complex **14**. Clean and complete conversion of $W(\eta^2\text{-ketalcyclopropene})\text{-}Cl_2(N\text{-}2,6\text{-}C_6H_3\text{-}Me_2)[P(OMe)_3]_2$ (**14**) to **22-B** (25%) and **22-C** (75%) was observed after it was dissolved in a concentrated CD_2Cl_2 solution at room temperature for one day.

When the same starting materials, **3** and ketalcyclopropene, were stirred together in a more dilute Et_2O solution, the red vinyl alkylidene **22-B** was isolated as a mono(phosphite) adduct, which did not undergo a rearrangement when dissolved in CD_2Cl_2 for 12 h or when stored in the solid state for months at room temperature, again indicating that a second equivalent of phosphite is needed to promote the conversion of **B** to **C**. An anti arrangement of the alkylidene and imido ligands of **22-B** was determined by difference NOE measurements, and the methyl groups of the imido ligand were equivalent at both room temperature and -80 °C.

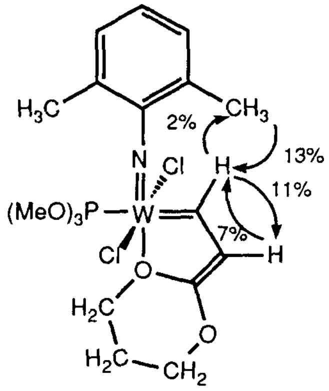

Phenylimido Precursors. As with the η^2-diphenylcyclopropene complexes, clean thermal conversion of the η^2-ketalcyclopropene phenylimido complexes to the corresponding vinyl alkylidene species was not observed. In fact, the cleanest thermal conversion observed thus far for the phenylimido compounds was the decomposition of $W(\eta^2\text{-ketalcyclopropene})Cl_2(NPh)[P(OMe)_3]_2$ (**12**) in the solid state over a period of several months, which resulted in the formation of the ketalvinyl alkylidene ligand along with $WCl_2(NPh)[P(OMe)_3]_3$ and other products. Although $W(\eta^2\text{-ketalcyclopropene})$-$Cl_2(NPh)(PX_3)_2$ decomposed upon addition of $HgCl_2$, photochemical conversion to the ketalvinyl alkylidene was observed (Table 12, Experimental Section).

Possible Mechanism for the Formation of B and C. A mechanism for the formation of isomers **B** and **C** is tentatively proposed in Scheme 1 and is based upon the following observations: (1) The *trans*-vinyl alkylidene **A** was only observed in the case

Scheme 1. Proposed Mechanism for the Formation of **B** and **C**

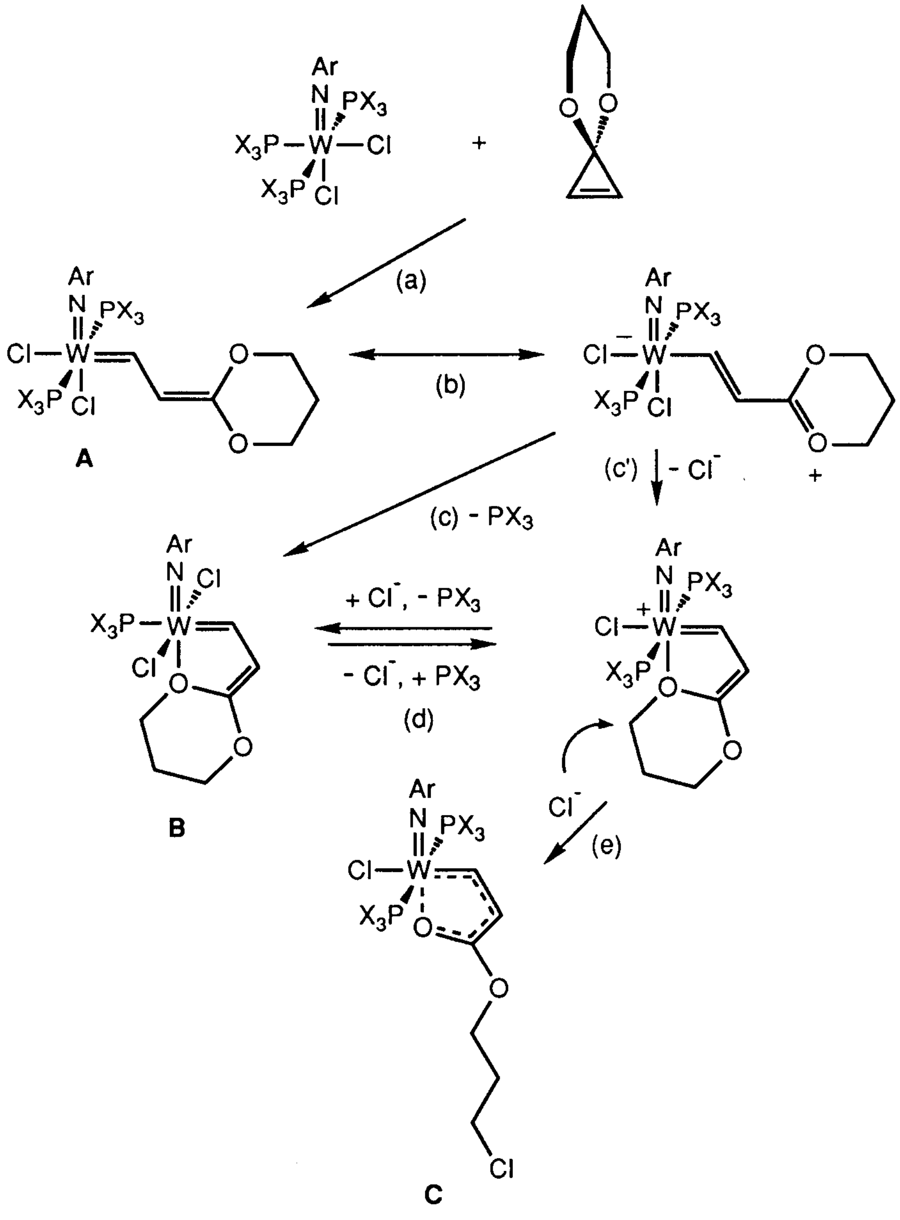

of the phosphine precursor $WCl_2(N\text{-}2,6\text{-}C_6H_3\text{-}Me_2)(PEt_2Ph)_3$, and (2) for the same precursor, only a small percentage of **B** was observed and conversion to **C** was more rapid than for the phosphite precursors. (3) For the phosphite precursors, isomer **B** was formed more rapidly than for the phosphine complex and slower conversion to **C** was then observed in CH_2Cl_2. (4) All of the experimental data pointed toward the isolation of **20-B** as a cationic complex, in which a phosphite ligand had displaced one of the chloride ligands.

These observations are consistent with the initial formation of the *trans*-vinyl alkylidene complex **A** upon ring-opening of ketalcyclopropene. Strong donation by the ketalvinyl alkylidene to the metal center via the M^-—C^+ resonance form would aid loss of a chloride ligand or loss of a phosphite/phosphine ligand. Loss of a chloride ligand and rotation of the alkylidene ligand would enable trapping of a cationic intermediate, such as was proposed in the isolation of **20-B**, by the ketal functionality of the alkylidene ligand. Alternatively, loss of a phosphite/phosphine ligand and rotation to a cis alkylidene ligand would result in formation of **B**. One or both pathways (c and c') may be operating, perhaps depending on the nature of the donating ligand. For example, poorer binding by the phosphite ligand may favor path c and thus account for the rapid production of **B** by phosphite precursors. Stronger donation by the phosphine versus the phosphite ligands would stabilize the cationic intermediate and thus promote rapid rearrangement to **C** via nucleophilic attack by the chloride counter ion on the ether methylene carbon.

Regarding the Mechanism of the Rearrangement of Cyclopropenes to Tungsten Vinyl Alkylidenes. Observations that may be relevant to the mechanism of the rearrangement of cyclopropenes to tungsten vinyl alkylidenes are as follows: (1) Vinyl alkylidene formation was generally slower than η^2-cyclopropene complex formation and was observed thermally for those precursors that formed the least stable η^2-cyclopropene complexes or that were unable to form η^2-cyclopropene complexes. (2) Conversion of η^2-cyclopropene complexes to vinyl alkylidene compounds was slowed by the addition of excess cyclopropene. (3) An equimolar mixture of $W(\eta^2$-diphenylcyclopropene$)Cl_2(N\text{-}2,6\text{-}C_6H_3\text{-}Me_2)[P(OMe)_3]_2$ (**11**) and ketalcyclopropene and an equimolar mixture of $W(\eta^2$-ketalcyclopropene$)Cl_2(N\text{-}2,6\text{-}C_6H_3\text{-}Me_2)[P(OMe)_3]_2$ (**14**) and diphenylcyclopropene did not yield the same ratio of products after 5.6 h in CD_2Cl_2

solution (Table 13, Experimental Section). The product mixtures were complex, and more careful reactions and more detailed product analyses need to be done. However, a bias was noted toward the formation of the vinyl alkylidene corresponding to the cyclopropene that was originally coordinated to tungsten. (4) The formation of both diphenyl- and ketalvinyl alkylidenes was observed at room temperature.

Although additional studies are needed in order to determine the mechanism of conversion, the above observations point toward a metal-catalyzed rearrangement, as uncatalyzed thermal ring-openings of cyclopropenes normally require higher temperatures.[35] One potential mechanism is the interaction of tungsten with one of the sigma bonds of the cyclopropene ring to give a metallacyclobutene intermediate. This mechanism is consistent with the present evidence and is supported by (1) extensive documentation of the ring-opening of cycloproprane rings by transition metals,[36] (2) the proposed rearrangement of metallacyclobutene intermediates to vinyl alkylidenes in the metathesis of acetylenes by alkylidene complexes (Figure 1, Chapter 1), and (3) the isolation of a stable platinum metallacyclobutene complex upon reaction of $[(Ph_3P)_2Pt]$ with cyclopropenone.[3c] Future studies by others should shed further light on the mechanism of rearrangement and enable the further development of this promising method for the synthesis of transition-metal alkylidene complexes.

Experimental Section

General Considerations

All manipulations of air- and/or water-sensitive compounds were performed using standard high-vacuum or Schlenk techniques. Argon was purified by passage through columns of BASF R3-11 catalyst (Chemalog) and 4 Å molecular sieves (Linde). Solid organometallic compounds were transferred and stored in a nitrogen-filled Vacuum Atmospheres drybox. All photolyses were pyrex-filtered and conducted with a 450 watt high-pressure mercury Hanovia lamp. Temperatures were maintained with a clear pyrex dewar filled with ice water. NMR spectra were recorded with either a JEOL FX-90Q (89.60 MHz ^{1}H; 22.53 MHz ^{13}C; 36.20 MHz ^{31}P), a JEOL GX-400 (399.65 MHz ^{1}H; 100.40 MHz ^{13}C), or a QE-300 Plus (300.10 MHz ^{1}H; 75.49 MHz ^{13}C) spectrometer. All coupling constants are reported in Hz.

Materials

Toluene, benzene, diethyl ether and tetrahydrofuran were distilled or vacuum-transferred from sodium-benzophenone ketyl. *p*-Xylene was dried over CaH_2 and distilled under argon. Pentane was stirred over concentrated H_2SO_4, dried over $MgSO_4$ and CaH_2, and then transferred onto sodium-benzophenone ketyl solubilized with tetraglyme. Benzene-d_6, toluene-d_8, and THF-d_8 were dried over sodium-benzophenone ketyl. Chloroform-*d* and methylene chloride-d_2 were dried over P_2O_5, vacuum-transferred, and then degassed by repeated freeze-pump-thaw cycles. Isocyanates were purified by fractional distillation under argon. $WCl_4(O)$ was purchased from Aldrich or synthesized according to published methods.[37] $WCl_4(NPh)$ was synthesized according to the procedure of Nielson.[6] $(CF_3)_2CH_3COH$ was purchased from PCR, dissolved in Et_2O, and deprotonated with one equivalent of BuLi. White crystals of $(CF_3)_2CH_3COLi$ were obtained by recrystallization at low temperature from a filtered Et_2O/pentane solution. The high lability of the PEt_2Ph ligands prevented satisfactory analyses of complexes **1** and **5** from being obtained.

$WCl_4(N\text{-}2,6\text{-}C_6H_3\text{-}Me_2)(Et_2O)$

2,6-Dimethylphenyl isocyanate (11.2 mL, 80.4 mmol) was added via syringe to a suspension of $WCl_4(O)$ (25.02 g, 73.24 mmol) in 115 mL of toluene. After refluxing for 48 h, the toluene was removed in vacuo, and the resulting brick-red powder was dissolved in 400 mL of Et_2O. The solution was filtered and then slowly cooled to -50 °C to give 37.2 g of brown crystals in three crops (97.8%): ^1H (C_6D_6) δ 6.75 (d, 2, J = 7.6, H_m), 5.89 (t, 1, J = 7.6, H_p), 4.34 (q, 4, J = 6.9, Et_2O), 3.29 (s, 6, Me), 1.07 (t, 6, J = 6.9, Et_2O); ^{13}C (C_6D_6) δ 148.3 (C_{ipso}), 145.4 (C_o), 133.9 and 126.1 (C_m and C_p), 65.9 (Et_2O), 17.6 (Me) and 13.0 (Et_2O). After removing the Et_2O in vacuo (several days under vacuum), an elemental analysis was obtained for orange-brown $WCl_4(N\text{-}2,6\text{-}C_6H_3\text{-}Me_2)$: Anal. Calcd for ($C_8H_9Cl_4NW$): C, 21.60; H, 2.04; N, 3.15. Found: C, 21.96; H, 2.15; N, 3.08.

$WCl_4[N\text{-}2,6\text{-}C_6H_3\text{-}(i\text{-}Pr)_2]$[10]

2,6-Diisopropylphenyl isocyanate (11.59 g, 57.00 mmol) was added via cannula to a suspension of $WCl_4(O)$ (19.47 g, 57.00 mmol) in 100 mL of *p*-xylene. After refluxing for 12 h, the hot solution was added via cannula to 400 mL of pentane, inducing the precipitation of a red-brown powder. After cooling the solution to -50 °C, brick-red crystals (25.9 g, 90.5%) were isolated: ^1H (THF-d_8) δ 7.63 (d, 2, J = 8.06, H_m), 6.74 (t, 1, J = 7.69, H_p), 4.62 (septet, 2, J = 6.59, $CHMe_2$), 1.37 (d, 12, J = 6.59, $CHMe_2$); ^{13}C (THF-d_8) δ 156.3 (C_{ipso}), 146.1 (C_o), 135.0 and 122.7 (C_m and C_p), 28.2 ($CH(CH_3)_2$), 26.4 ($CH(CH_3)_2$).

$WCl_4[N-2,6-C_6H_3-(i-Pr)_2](THF)$

Brick-red $W[N-2,6-C_6H_3-(i-Pr)_2]Cl_4$ (3.02 g, 6.03 mmol) was dissolved in 10 mL of THF and 90 mL of Et_2O. After the solution was filtered, recrystallization at -50 °C gave feathery green crystals (2.58 g, 74.7%): ^1H (CD_2Cl_2) δ 7.59 (d, 2, J = 7.81, H_m), 6.71 (t, 1, J = 7.81, H_p), 4.74 (m, 4, THF), 4.58 (septet, 2, J = 6.59, $CHMe_2$), 2.17 (m, 4, THF), 1.40 (d, 12, J = 6.59, $CHMe_2$); ^{13}C (CD_2Cl_2) δ 156.3 (C_{ipso}), 145.7 (C_o), 134.7 and 122.1 (C_m and C_p), 74.1 (THF), 27.8 ($CH(CH_3)_2$), 26.3 ($CH(CH_3)_2$), 26.1 (THF). Anal. Calcd for ($C_{16}H_{25}Cl_4NOW$): C, 33.54; H, 4.40; N, 2.44. Found: C, 33.72; H, 4.35; N, 2.57.

$WCl_3[N-2,6-C_6H_3-(i-Pr)_2](PMe_3)_2$

Trimethylphosphine (12.0 mL, 116 mmol, 3.87 equiv) was vacuum-distilled into a flask equipped with a teflon Kontes valve and then transferred via cannula into a 150 mL THF suspension of $WCl_4[N-2,6-C_6H_3-(i-Pr)_2]$. The suspension was refluxed for 13.5 h and allowed to cool. An additional 120 mL of THF was then added in order to dissolve all of the product, and the solution was filtered off of the white precipitate. Brown crystals formed as the solution was slowly cooled to -50 °C. Isolation of 4 crops yielded 16.7 g (90.1%) of product. Anal. Calcd for ($C_{18}H_{35}Cl_3NP_2W$): C, 35.00; H, 5.71; N, 2.27. Found: C, 34.72; H, 5.70; N, 2.14.

$WCl_2(N-2,6-C_6H_3-Me_2)(PEt_2Ph)_3$ (1)

Diethylphenylphosphine (14.4 mL, ~3.5 equiv) was added via syringe to a green solution of $WCl_4(N-2,6-C_6H_3-Me_2)\cdot Et_2O$ (12.25 g, 24.0 mmol) in 140 mL of benzene. The resulting brown solution was transferred via cannula onto a 1% sodium amalgam (1.99 g Na, 86.6 mmol) and stirred for 11.5 h. The spent amalgam was allowed to settle and the solution was transferred via cannula into a septum-covered centrifuge tube that had been previously evacuated and back-filled with argon. After being centrifuged, the solution was transferred via cannula into another flask. The spent amalgam was washed twice with a total of 165 mL of benzene and the resulting solution was also centrifuged. The combined solvent was then removed in vacuo and the product was washed 3 times with a total of 240 mL of pentane. A tan powder (11.31 g, 53%) was obtained: ^{1}H NMR (C_6D_6) δ 7.4-6.5 (m, 18, H_{aryl}), 3.21 (m, 2, $P(CH_2CH_3)_2Ph$), 2.59 (m, 2, $P(CH_2CH_3)_2Ph$), 2.22 (br s, 6, Ar: Me), 2.17-1.84 (m, 8, $P(CH_2CH_3)_2Ph$), 1.39 (m, 6, $P(CH_2CH_3)_2Ph$), 0.74 (m, 12, $P(CH_2CH_3)_2Ph$); ^{13}C NMR (C_6D_6) δ 156.5 (Ar: C_{ipso}), 141.5 (t, J_{CP} = 15.4, C_{ipso} of mutually trans PEt_2Ph's), 138.0 (d, J_{CP} = 29.4, C_{ipso} of PEt_2Ph trans to Cl), 135.2 (br s, Ar: C_o), 133.3 (d, J_{CP} = 7.0, C_o of PEt_2Ph trans to Cl), 131.6 (t, J_{CP} = 3.8, C_o of mutually trans PEt_2Ph's), 129.1 and 128.4 (Ar: C_m, and C_p of mutually trans PEt_2Ph's), 128.6 (C_p of PEt_2Ph trans to Cl), 128.0 (t, J_{CP} = 3.5, C_m of mutually trans PEt_2Ph's), 127.8 (d, J_{CP} = 7.5, C_m of PEt_2Ph trans to Cl), 123.8 (Ar: C_p), 27.5 (d, J_{CP} = 25.6, $P(CH_2CH_3)_2Ph$ trans to Cl), 21.4 (Ar: Me), 18.1 (t, J_{CP} = 11.0, mutually trans $P(CH_2CH_3)_2Ph$'s), 15.8 (t, J_{CP} = 11.9, mutually trans $P(CH_2CH_3)_2Ph$'s), 11.4 (d, J_{CP} = 7.7, $P(CH_2CH_3)_2Ph$ trans to Cl), 8.3 and 8.0 (mutually trans $P(CH_2CH_3)_2Ph$'s); ^{31}P NMR (C_6D_6) δ -6.9 (s, J_{PW} = 356, PEt_2Ph trans to Cl), -9.2 (s, J_{PW} = 295, mutually trans PEt_2Ph's).

$WCl_2(NPh)[P(OMe)_3]_3$ (2)

Benzene (210 mL) was added to olive-green $WCl_4(NPh)$ (20.85 g, 50.02 mmol). Subsequent addition of 24 mL of $P(OMe)_3$ to the $WCl_4(NPh)$ suspension resulted in the formation of a green solution, which was then transferred via cannula onto a 1% sodium amalgam (4.15 g Na). After stirring for 27 minutes, the solution turned purple, and the mixture was then allowed to settle. The purple solution was transferred via cannula into another Schlenk flask. After the spent amalgam was washed with 90 mL of benzene, benzene and excess $P(OMe)_3$ were removed in vacuo. The resulting residue was dissolved in 200 mL of THF, the solution was filtered, and THF was then removed in vacuo. The remaining purple powder was washed with 100 mL of pentane and dried in vacuo (28.60 g, 79.6%): ^{1}H NMR (CD_2Cl_2) δ 7.25-7.17 (m, 5, H_{aryl}), 3.65 (t, 18, J_{HP} = 5.4, mutually trans P(OMe)$_3$'s), 3.63 (d, 9, J_{HP} = 10.5, P(OMe)$_3$ trans to Cl); ^{13}C NMR (CD_2Cl_2) δ 156.6 (C_{ipso}), 128.6 (Ar: C_m), 126.1(Ar: C_o), 125.7 (Ar: C_p), 53.3 (d, J_{CP} = 6.6, P(OMe)$_3$ trans to Cl), 52.9 (t, J_{CP} = 2.6, mutually trans P(OMe)$_3$'s); ^{31}P NMR (C_6D_6) δ 141.1 (t, J_{PP} = 22, J_{PW} = 564, P(OMe)$_3$ trans to Cl), 129.3 (d, J_{PP} = 22, J_{PW} = 454, mutually trans P(OMe)$_3$'s). Anal. Calcd for ($C_{15}H_{32}Cl_2NO_9P_3W$): C, 25.09; H, 4.49; N, 1.95. Found: C, 24.82; H, 4.37; N, 1.99.

$WCl_2(N\text{-}2,6\text{-}C_6H_3\text{-}Me_2)[P(OMe)_3]_3$ (3)

Trimethylphosphite (25.5 mL) was added to a benzene (210 mL) solution of $WCl_4(N\text{-}2,6\text{-}C_6H_3\text{-}Me_2)$(THF) (25.86 g, 50.0 mmol). The resulting green solution was transferred via cannula onto a 1% sodium amalgam (4.20 g Na), and the mixture was stirred until it turned purple (1 h). After the mixture settled, the solution was transferred via cannula into another Schlenk flask, and then the spent amalgam was washed with a total of 120 mL of benzene. After benzene and excess P(OMe)$_3$ were removed in vacuo, the remaining solid was dissolved in 180 mL of THF, and the solution was filtered. Next, THF was removed in vacuo, and the product was washed with 100 mL of pentane and dried in vacuo to give 29.86 g (80.0%) of gray powder: ^{1}H NMR (CD_2Cl_2) δ 6.99 (t, 1, J = 7.6, Ar: H_p), 6.87 (d, 2, J = 7.6, Ar: H_m), 3.71 (t, 18, J_{HP} = 5.2, mutually trans P(OMe)$_3$'s), 3.68 (d, 9, J_{HP} = 10.5, P(OMe)$_3$ trans to Cl), 2.46 (s, 6, Ar: Me); ^{13}C NMR (CD_2Cl_2) δ 154.0 (Ar: C_{ipso}), 137.9 (Ar: C_o), 127.9 (Ar: C_m), 125.8 (Ar: C_p), 53.2 (d, J_{CP} = 7.3, P(OMe)$_3$ trans to Cl), 52.8 (t, J_{CP} = 2.6, mutually trans P(OMe)$_3$'s), 19.2 (Ar: CH_3); ^{31}P NMR (C_6D_6) δ 144.8 (t, J_{PP} = 19.5, J_{PW} = 568, P(OMe)$_3$ trans to Cl), 127.8 (d, J_{PP} = 19.5, J_{PW} = 456, mutually trans P(OMe)$_3$'s). Anal. Calcd for ($C_{17}H_{36}Cl_2NO_9P_3W$): C, 27.37; H, 4.86; N, 1.88. Found: C, 27.48; H, 4.68; N, 1.87.

$WCl_2[N\text{-}2,6\text{-}C_6H_3\text{-}(i\text{-}Pr)_2][P(OMe)_3]_3$ (4)

Brick-red $WCl_4[N\text{-}2,6\text{-}C_6H_3\text{-}(i\text{-}Pr)_2]$ (25.04 g, 49.99 mmol) was suspended in 210 mL of benzene. Upon addition of 24.8 mL of $P(OMe)_3$ to the suspension, a green solution was formed. The solution was transferred via cannula onto a 1% sodium amalgam (4.15 g Na), and the mixture was stirred until it turned purple (45 min). After allowing the mixture to settle, the solution was transferred via cannula into another Schlenk flask, and the spent amalgam was washed with 70 mL of THF. The combined solvents and excess $P(OMe)_3$ were removed in vacuo, and the solid residue was dissolved in 250 mL of THF and filtered twice. After removing THF in vacuo, the purple-gray powder was washed with 100 mL of pentane and dried in vacuo to give 31.17 g (77.7%) of product: ^1H NMR (C_6D_6) δ 7.06 (2, Ar: H_m), 7.01 (t, 1, J = 5.7, Ar: H_p), 4.51 (septet, 2, J = 6.6, $C\mathit{H}Me_2$), 3.67 (t, 18, J_{HP} = 5.2, mutually trans $P(OMe)_3$'s), 3.58 (d, 9, J_{HP} = 10.5 Hz, $P(OMe)_3$ trans to Cl), 1.32 (d, 12, J = 6.6, $CH\mathit{Me}_2$); ^{13}C NMR (CD_2Cl_2) δ 150.9 (Ar: C_{ipso}), 147.9 (Ar: C_o), 126.5 (Ar: C_p), 123.5 (Ar: C_m), 53.5 (d, J_{CP} = 7.3, $P(OMe)_3$ trans to Cl), 52.9 (t, J_{CP} = 2.2, mutually trans $P(OMe)_3$'s), 27.3 ($\mathit{C}H(CH_3)_2$), 25.1 ($CH(\mathit{C}H_3)_2$); ^{31}P NMR (C_6D_6) δ 143.4 (t, J_{PP} = 20, J_{PW} = 566, $P(OMe)_3$ trans to Cl), 128.0 (d, J_{PP} = 20, J_{PW} = 456, mutually trans $P(OMe)_3$'s). Anal. Calcd for ($C_{21}H_{44}Cl_2NO_9P_3W$): C, 31.44; H, 5.53; N, 1.75. Found: C, 31.54; H, 5.52; N, 1.68.

$W(PhC{\equiv}CPh)Cl_2(N\text{-}2,6\text{-}C_6H_3\text{-}Me_2)(PEt_2Ph)_2$ (5)

A 7 mL Et_2O solution of $PhC{\equiv}CPh$ (314 mg, 1.76 mmol) was added to 1.54 g (1.76 mmol) of $WCl_2(N\text{-}2,6\text{-}C_6H_3\text{-}Me_2)(PEt_2Ph)_3$ (**1**). After the solution was stirred for 11.5 h, 30 mL of pentane was added in order to precipitate the product. The suspension was filtered, the light tan powder was washed with an additional 15 mL of pentane and then dried in vacuo to yield 674 mg (43.2%) of **5**: ^1H NMR (C_6D_6) δ 7.74-6.64 (m, 23, H_{aryl}), 3.44 (m, 2, $P(C\mathit{H}_2CH_3)_2Ph$), 2.99 (s, 3, NAr: *Me*), 2.62 (m, 2, $P(C\mathit{H}_2CH_3)_2Ph$), 2.22 (m, 2, $P(C\mathit{H}_2CH_3)_2Ph$), 2.08 (s, 3, NAr: *Me*), 1.99 (m, 2, $P(C\mathit{H}_2CH_3)_2Ph$), 1.38

(quintet, 6, J = 7.52, P(CH$_2$C*H*$_3$)(CH$_2$CH$_3$)'Ph), 0.52 (quintet, J = 7.18, P(CH$_2$CH$_3$)-(CH$_2$C*H*$_3$)'Ph); ^{13}C NMR (CD$_2$Cl$_2$) δ 157.3 (t, J_{CP} = 11.57, Ph*C*≡*C*Ph), 153.6 (t, J_{CP} = 2.33, NAr: C$_{ipso}$), 144.2 (*Ph*C≡C*Ph*: C$_{ipso}$), 143.0 and 139.7 (NAr: C$_o$, C$_o$'), 133.3 (t, J_{CP} = 20.11, PEt$_2$*Ph*: C$_{ipso}$), 130.6 (t, J_{CP} = 3.81, PEt$_2$*Ph*: C$_o$), 128.5 (PEt$_2$*Ph*: C$_p$), 129.1, 128.1, and 127.9 (NAr: C$_m$, C$_m$', C$_p$), 127.5 (*Ph*C≡C*Ph*: C$_m$), 127.4 (t, J_{CP} = 4.28, PEt$_2$Ph: C$_m$), 126.0 (*Ph*C≡C*Ph*: C$_o$), 125.2 (*Ph*C≡C*Ph*: C$_p$), 21.5 (NAr: Me), 19.9 (NAr: Me'), 16.6 (t, J_{CP} = 12.69, P(*C*H$_2$CH$_3$)(CH$_2$CH$_3$)'Ph), 14.9 (t, J_{CP} = 12.10, P(CH$_2$CH$_3$)(*C*H$_2$CH$_3$)'Ph), 8.0 (P(CH$_2$*C*H$_3$)(CH$_2$CH$_3$)'Ph), 7.3 (t, J_{CP} = 3.10, P(CH$_2$CH$_3$)(CH$_2$*C*H$_3$)'Ph); ^{31}P NMR (C$_6$D$_6$) δ 6.80 (J_{PW} = 203).

W(H$_2$C=CH$_2$)Cl$_2$[N-2,6-C$_6$H$_3$-(*i*-Pr)$_2$][P(OMe)$_3$]$_2$ (6)

Purple WCl$_2$[N-2,6-C$_6$H$_3$-(*i*-Pr)$_2$][P(OMe)$_3$]$_3$ (4) (1.56 g, 1.79 mmol) was dissolved in 20 mL of toluene, and the resulting solution was stirred under 1 atm of ethylene for 0.5 h at room temperature. Orange crystals precipitated from the toluene solution at -50 °C, and subsequent addition of the supernant to 60 mL of rapidly stirring pentane yielded a golden yellow powder. A total of 0.80 g (64%) was isolated: ^{1}H NMR (C$_6$D$_6$) δ 6.87-6.89 (s, 3, H$_{aryl}$), 3.95 (br m, 2, C*H*(CH$_3$)$_2$), 3.55 (t, 18, J = 5.19, P(OMe)$_3$), 3.25 (m, 2, *H*H'C=C*H*H', protons anti to the imido ligand), 2.85 (m, 2, H*H'*C=CH*H'*, protons syn to the imido ligand), 1.23 (d, 12, J = 6.75, CH(C*H*$_3$)$_2$); ^{13}C NMR (CD$_2$Cl$_2$) δ 150.0 (t, J_{CP} = 2.9, J_{CW} = 33, Ar: C$_{ipso}$), 149.8 (Ar: C$_o$), 127.5 (Ar: C$_p$), 123.5 (Ar: C$_m$), 53.7 (J_{CP} = 3.1, P(OMe)$_3$), 53.6 (J_{CP} = 2.9, P(OMe)$_3$), 42.3 (t, J_{CH} = 160.6, J_{CW} = 29, H$_2$*C*=*C*H$_2$), 26.9 (*C*H(CH$_3$)$_2$), 24.4 (CH(*C*H$_3$)$_2$); ^{31}P NMR (CD$_2$Cl$_2$) δ 120.48 (J_{PW} = 385.7, P(OMe)$_3$); NOEDS (C$_6$D$_6$) irradiation at 3.95 ppm, δ 3.55 (4.5% NOE), 2.85 (8.1% NOE), 1.23 (2.3% NOE); irradiation at 3.25 ppm, δ 2.85 (20.2% NOE); irradiation at 2.85 ppm, δ 3.95 (8.0% NOE), 3.55 (0.3% NOE), 3.25 (20.6% NOE), 1.23 (0.2% NOE); irradiation at 1.23 ppm, δ 3.95 (23.9% NOE), 3.55

(1.3% NOE), 2.85 (1.2% NOE). Anal. Calcd for ($C_{18}H_{35}Cl_2NO_6P_2W$): C, 31.88; H, 5.20; N, 2.07. Found: C, 32.11; H, 5.37; N, 2.05.

W(PhC≡CH)Cl_2(N-2,6-C_6H_3-Me_2)[P(OMe)$_3$]$_2$ (7)

A 15 mL benzene solution of phenylacetylene (1.09 g, 10.7 mmol) was transferred via cannula onto a 40 mL purple solution of WCl_2(N-2,6-C_6H_3-Me_2)(P(OMe)$_3$)$_3$. The solution turned golden brown after stirring for 1 h at 25 °C and then for 1 h at 44 °C. The solvent and free P(OMe)$_3$ were removed in vacuo to yield a yellow powder, which was moderately soluble in Et_2O and toluene. Recrystallization from these solvents yielded 6.45 g (85.8%) of yellow product: ^{1}H NMR (C_6D_6) δ 10.43 (dd, 1, J_{HP} = 16.85, 5.62, PhC≡C*H*), 7.74 (d, 2, J = 7.57, *Ph*C≡CH: C_o), 7.26 (t, 2, J = 7.81, *Ph*C≡CH: C_m), 7.05 (t, 1, J = 7.57, *Ph*C≡CH: C_p), 6.68 (d, 2, J = 7.81, NAr: C_m), 6.63 (t, 1, J = 7.57, NAr: C_p), 3.58 (dd, 9, J = 9.3, 0.98, P(OMe)$_3$), 3.42 (dd, 9, J = 9.8, 0.98, P(OMe)$_3$), 2.6 (br s, 6, NAr: Me_2); ^{13}C NMR (CD_2Cl_2) δ 153.1 (t, J = 2.9, NAr: C_{ipso}), 148.6 (dd, J_{CP} = 21.3, 6.6, Ph*C*≡CH), 142.6 (t, *Ph*C≡CH: C_{ipso}), 140.8 (br s, NAr: C_o), 135.6 (m, J_{CH} = 217.6, J_{CP} = 28.2, 7.7, PhC≡*C*H), 128.5, 127.9, 127.8, 127.5, and 126.7 (NAr: C_m, C_p and *Ph*C≡CH: C_o, C_m, C_p), 54.4 (d, J_{CP} = 6, P(OMe)$_3$), 52.9 (d, J_{CP} = 6, P(OMe)$_3$), 20.0 (NAr: Me_2); ^{31}P NMR (CD_2Cl_2) δ 118.8 (J_{PW} = 354), 117.6 (J_{PW} = 366); NOEDS (C_6D_6) irradiation at 10.43, δ 3.58 (1.2% NOE), 2.6 (2.2% NOE); irradiation at 3.58, δ 10.43 (7.3% NOE); irradiation at 3.42, no NOE's; irradiation at 2.6, δ 10.43 (6.9% NOE), 7.74 (5.8% NOE), 6.68 (12.2% NOE), 3.58 (0.5% NOE), 3.42 (0.6% NOE). Anal. Calcd for ($C_{22}H_{33}Cl_2NO_6P_2W$): C, 36.49; H, 4.59; N, 1.93. Found: C, 36.78; H, 4.51; N, 1.95.

Observation of W(PhC≡CH)Cl_2(N-2,6-C_6H_3-Me_2)[P(OMe)$_3$] (8)

Even in concentrated solutions (tol-d_8, C_6D_6, THF-d_8, and CD_2Cl_2), **7** was observed to be in equilibrium with the monophosphite adduct **8**. After equimolar amounts of CuCl and **7** were dissolved in CD_2Cl_2 for 24 h, only **8** was observed: ^1H NMR (CD_2Cl_2) δ 10.72 (d, 1, J_{HP} = 20.03, J_{HW} = 9.71, PhC≡C*H*), 7.81 - 6.75 (m, 8, H_{aryl}), 3.85 (d, 9, J_{HP} = 10.71, W(P(OMe)$_3$)), 3.67 (d, 9, J_{HP} = 12.59, Cu(P(OMe)$_3$)), 2.32 (s, 6, NAr: Me_2); ^{13}C NMR (CD_2Cl_2, selected C_{aryl} only) δ 161.3 (d, J_{CP} = 7.55, Ph*C*≡CH), 153.1 (d, J_{CP} = 3.49, NAr: C_{ipso}), 139.9 (d, J_{CP} = 2.14, NAr: C_o), 138.4 (m, PhC≡*C*H), 136.6 (J_{CP} = 3.78, *Ph*C≡CH: C_{ipso}), 54.0 (d, J_{CP} = 6.58, W(P(OMe)$_3$)), 51.2 (Cu(P(OMe)$_3$)), 19.14 (NAr: Me_2); ^{31}P NMR (CD_2Cl_2) δ 130.44 (J_{PW} = 405).

$W(HC{=}CH\text{-}CPh_2)Cl_2(NPh)(PMePh_2)_2$ (9)

3,3-Diphenylcyclopropene (420 mg, 2.19 mmol) was dissolved in 15 mL of toluene and then added via cannula to a 90 mL toluene solution of $WCl_2(NPh)(PMePh_2)_3$ (2.01 g, 2.13 mmol). After the reaction mixture was stirred for 9 h, all but ~10 mL of the toluene was removed in vacuo. Addition of 30 mL of pentane and filtration yielded 1.45 g (76.5%) of yellow powder, which was dried under vacuum: ^1H NMR (CD_2Cl_2) δ 7.68-6.59 (m, 33, H_{aryl}), 5.51 (d, 2, NPh: H_m), 3.75 (t, 2, J = 5.63, HC=CH), 2.47 (t, J_{HP} = 4.59, $PMePh_2$); ^{13}C NMR (CD_2Cl_2; only select C_{aryl} chemical shifts are listed) δ 153.2 and 153.1 (NAr: C_{ipso} and CPhPh': C_{ipso}), 144.6 (CPhPh': C'_{ipso}), 134.1 ($PMePh_2$: C_{ipso}), 130.5 ($PMePh_2$: C_{ipso}), 72.4 (t, J_{CH} = 195, J_{CP} = 9, J_{CW} = 45, HC=CH), 69.7 (*C*Ph_2), 12.1 (t, J_{CP} = 16, $PMePh_2$); ^{31}P NMR (CD_2Cl_2) δ 4.7 (J_{PW} = 208, $PMePh_2$).

$W(HC{=}CH\text{-}CPh_2)Cl_2(NPh)[P(OMe)_3]_2$ (10)

A 6 mL Et_2O solution of 3,3-diphenylcyclopropene (154 mg, 0.803 mmol) was added to a purple suspension of $WCl_2(NPh)[P(OMe)_3]_3$ (538 mg, 0.749 mmol) in 6 mL of Et_2O. A yellow precipitate formed as the reaction mixture was stirred for 23 h. Pentane (10 mL) was added to the suspension, the reaction mixture was filtered, and the pale yellow powder (477 mg, 80.9%) was dried in vacuo: ^1H NMR (CD_2Cl_2) δ 7.22-6.67 (m, 13, H_{aryl}), 6.31 (d, 2, J = 6.74, NPh: H_m), 4.50 (t, 2, J = 6.01, HC=CH), 3.92 (t, 18,

J_{HP} = 5.24, P(OMe)$_3$); ^{13}C NMR (CD_2Cl_2) δ 152.9 (C*Ph*Ph': C_{ipso}), 152.8 (t, J_{CP} = 3.3, NPh: C_{ipso}), 143.1 (CPh*Ph'*: C'_{ipso}), 131.7, 128.1, 127.5, 127.2 and 127.0 (NPh: C_m and CPhPh': C_o, C'_o, C_m, C'_m), 126.1, 125.9 and 125.4 (NPh: C_p and CPhPh': C_p, C'_p), 125.8 (t, J_{CP} = 3.3, NPh: C_o), 64.8 (t, J_{CH} = 193, J_{CP} = 16, J_{CW} = 37, HC=CH), 64.3 (*C*Ph$_2$), 54.4 (t, J_{CP} = 3.3, P(OMe)$_3$); ^{31}P NMR (CD_2Cl_2) δ 118.1 (J_{PW} = 364); ^{31}P (tol-d_8) δ 117.6 (J_{PW} = 361).

W(HC=CH-CPh$_2$)Cl$_2$(N-2,6-C$_6$H$_3$-Me$_2$)[P(OMe)$_3$]$_2$ (11)

A 30 mL Et_2O solution of 3,3-diphenylcyclopropene (392 mg, 2.04 mmol) was added via cannula to a 1.52 g (2.04 mmol) suspension of WCl_2(N-2,6-C_6H_3-Me$_2$)[P(OMe)$_3$]$_3$ in 120 mL of Et_2O. After being stirred for several h, the reaction mixture was filtered, and the yellow powder (668 mg, 40.2%) was dried in vacuo and stored at -30 °C: ^{1}H NMR (CD_2Cl_2) δ 7.35 - 6.49 (m, 13, H_{aryl}), 4.74 (t, 2, J = 5.79, HC=CH), 3.99 (t, 18, J = 4.64, P(OMe)$_3$), 2.22 (s, 6, NAr: Me); ^{13}C NMR (CD_2Cl_2) δ 153.2 (J_{CW} = 5.4, C*Ph*Ph': C_{ipso}), 151.2 (t, J_{CP} = 5.4, NAr: C_{ipso}), 142.1 (CPh*Ph'*: C'_{ipso}), 136.1 (NAr: C_o), 132.3, 127.7, 127.5, 127.0, and 126.6 (NAr: C_m and CPhPh': C_o, C'_o, C_m, C'_m), 125.6, 125.5 and 125.4 (NAr: C_p and CPhPh': C_p, C'_p), 66.7 (J_{CW} = 2.9, *C*Ph$_2$), 66.2 (t, J_{CH} = 194, J_{CP} = 15, J_{CW} = 40, HC=CH), 55.3 (t, J_{CP} = 4, P(OMe)$_3$), 19.7 (NAr: Me$_2$); ^{31}P NMR (CD_2Cl_2) δ 109.8 (J_{PW} = 379, P(OMe)$_3$). Anal. Calcd for ($C_{29}H_{39}Cl_2NO_6P_2W$): C, 42.77; H, 4.83; N, 1.72. Found: C, 42.63; H, 4.73; N, 1.48.

W(HC=CH-COCH$_2$CH$_2$CH$_2$O)Cl$_2$(NPh)(PMePh$_2$)$_2$ (12)

A 20 mL Et_2O solution of ketalcyclopropene (247 mg, 2.20 mmol) was added via cannula to a suspension of WCl_2(NPh)(PMePh$_2$)$_3$ (2.01 g, 2.13 mmol) in a mixture of 130 mL of Et_2O and 50 mL of toluene. After being stirred for 12 h, the reaction mixture was filtered to yield 643 mg (35.2%) of yellow powder, which was dried under vacuum: ^{1}H NMR (CD_2Cl_2) δ 7.67-6.86 (m, 25, H_{aryl}), 3.74 (t, 2, J = 5.07, OCH$_2$), 3.66 (t, 2, J =

5.15, OCH_2), 3.30 (t, 2, J = 5.71, HC=CH), 1.69 (quintet, 2, J = 5.22, $CH_2CH_2CH_2$); ^{13}C NMR (CD_2Cl_2) 154.1 (NPh: C_{ipso}), 134.2 (t, J_{CP} = 23.1, PMe*Ph*Ph': C_{ipso}), 133.8 (t, J_{CP} = 4.4, PMe*Ph*Ph': C_o), 132.9 (t, J_{CP} = 4.4, PMePh*Ph'*: C'_o), 131.4 (t, J_{CP} = 21.6, PMePh*Ph'*: C_{ipso}), 130.1 (2, PMe*PhPh'*: C_p, C'_p), 128.1 (t, J_{CP} = 4.8, PMe*Ph*Ph': C_m) 128.0 (t, J_{CP} = 4.4, PMePh*Ph'*: C'_m), 127.8 and 127.5 (NPh: C_o, C_m), 127.2 (NPh: C_p), 106.4 (HC=CH*C*O_2), 67.5 (t, J_{CH} = 188, J_{CP} = 9.2, J_{CW} = 41.6, HC=CH), 67.0 (OCH_2), 66.4 (OCH_2), 26.3 ($CH_2CH_2CH_2$), 12.0 (t, J_{CP} = 15.8, $PMePh_2$); ^{31}P NMR (CD_2Cl_2) δ 5.1 (J_{PW} = 212, $PMePh_2$). Anal. Calcd for ($C_{38}H_{39}Cl_2NO_2P_2W$): C, 53.17; H, 4.58; N, 1.63. Found: C, 52.78; H, 4.38; N, 1.22.

$W(HC{=}CH\text{-}COCH_2CH_2CH_2O)Cl_2(NPh)[P(OMe)_3]_2$ (13)

An 8 mL Et_2O solution of ketalcyclopropene (220 mg, 1.96 mmol) was added to 1.10 g (1.53 mmol) of purple $WCl_2(NPh)[P(OMe)_3]_3$. The suspension was stirred for 23 h, washed with 75 mL of pentane, and then filtered. The pale yellow powder (985 mg, 91.5%) was dried in vacuo and stored at -30 °C in the drybox freezer. (This compound decomposed to a black, sticky oil when stored at room temperature under nitrogen for 5 months.): ^1H NMR (CD_2Cl_2) δ 7.25 - 7.09 (m, 5, H_{aryl}), 4.14 (t, 2, J = 5.98, HC=CH), 4.03 (t, 2, J = 5.39, OCH_2), 3.86 (t, 18, J = 5.32, $P(OMe)_3$), 3.65 (t, 2, J = 5.22, OCH_2), 1.70 (quintet, 2, J = 5.23, $CH_2CH_2CH_2$); ^{13}C NMR (CD_2Cl_2) δ 153.0 (t, J_{CP} = 3.1, NPh: C_{ipso}), 127.5 (NPh: C_m), 126.7 (NPh: C_p), 126.4 (t, J_{CP} = 2.8, NPh: C_o), 103.5 (HC=CH-*C*O_2), 66.5 (OCH_2), 65.2 (OCH_2), 59.9 (t, J_{CH} = 209.9, J_{CP} = 15.3, J_{CW} = 36.6, HC=CH), 52.3 (t, J_{CP} = 2.0, $P(OMe)_3$), 25.7 ($CH_2CH_2CH_2$); ^{31}P NMR (CD_2Cl_2) δ 120 (J_{PW} = 361, $P(OMe)_3$); ^1H NMR (C_6D_6) δ 7.47 (d, 2, J = 7.58, NPh: H_o), 6.98 (t, 2, J = 7.83, NPh: H_m), 6.81 (t, 1, J = 7.51, NPh: H_p), 4.81 (t, 2, J_{HP} = 5.77, J_{HW} = 1.74), HC=CH), 3.96 (t, 2, J = 5.42, OCH_2 anti to tungsten), 3.72 (t, 2, J = 5.52, OCH_2 syn to tungsten), 3.60 (t, 18, J = 5.31, $P(OMe)_3$), 1.46 (quintet, 2, J = 5.39, $CH_2CH_2CH_2$); NOEDS (C_6D_6) irradiation at 7.47, δ 6.98 (9.2% NOE), 4.81 (0.8%

NOE), 3.96 (1.5% NOE), 3.72 (2.0% NOE), 3.60 (1.2% NOE), 1.46 (0.9% NOE); irradiation at 4.81, no NOEs; irradiation at 3.96, δ 4.81 (5.2% NOE), 3.60 (0.4% NOE), 1.46 (3.7% NOE); irradiation at 3.72, δ 7.47 (4.5% NOE), 3.96 (1.5% NOE), 1.46 (3.3% NOE); irradiation at 1.46, δ 3.96 (3.3% NOE), 3.72 (1.1% NOE). Anal. Calcd for ($C_{18}H_{31}Cl_2NO_8P_2W$): C, 30.62; H, 4.42; N, 1.98. Found: C, 29.86; H, 4.26; N, 1.91.

W(HC=CH-COCH$_2$CH$_2$CH$_2$O)Cl$_2$(N-2,6-C$_6$H$_3$-Me$_2$)[P(OMe)$_3$]$_2$ (14)

A 10 mL Et_2O solution of ketalcyclopropene (458 mg, 4.08 mmol) was added to 3.00 g (4.02 mmol) of $WCl_2(N\text{-}2,6\text{-}C_6H_3\text{-}Me_2)[P(OMe)_3]_3$, and the resulting suspension was stirred for 13 h. Removal of the solvent and free $P(OMe)_3$ in vacuo yielded a pale yellow powder, which was washed with one 30 mL portion and one 150 mL portion of pentane. The tan product (2.58 g, 87.4%) was dried under vacuum and stored at -30 °C in the drybox freezer: ^1H NMR (CD_2Cl_2) δ 7.02 - 6.78 (m, 3, H_{aryl}), 4.27 (t, 2, J = 5.91, HC=CH), 3.98 (t, 2, J = 5.32, OCH_2), 3.89 (t, 2, J = 5.15, $P(OMe)_3$), 2.50 (s, 6, NAr: Me_2), 1.60 (quintet, 2, J = 5.31, $CH_2CH_2CH_2$); ^{13}C NMR (CD_2Cl_2) δ 150.9 (t, J_{CP} = 2, J_{CW} = 16, NAr: C_{ipso}), 138.3 (NAr: C_o), 126.9 (NAr: C_m), 126.1 (NAr: C_p), 104.0 (HC=CH-CO_2), 66.7 (OCH_2), 64.9 (OCH_2), 61.5 (t, J_{CH} = 193.7, J_{CP} = 14.9, J_{CW} = 31.2, HC=CH), 54.5 (t, J_{CP} = 3.45, $P(OMe)_3$), 25.8 ($CH_2CH_2CH_2$), 18.8 (NAr: Me_2); ^{31}P NMR (CD_2Cl_2) δ 113 (J_{PW} = 376, $P(OMe)_3$). Anal. Calcd for ($C_{20}H_{35}Cl_2NP_2O_8W$): C, 32.72; H, 4.81; N, 1.91. Found: C, 33.01; H, 4.71; N, 1.59.

W(=CH-CH=CPh$_2$)Cl$_2$[N-2,6-C$_6$H$_3$-(*i*-Pr)$_2$][P(OMe)$_3$]$_2$ (15)

A 30 mL benzene solution of 3,3-diphenylcyclopropene (1.84 g, 9.55 mmol) was added via cannula to a 60 mL benzene solution of $WCl_2[N\text{-}2,6\text{-}C_6H_3\text{-}(i\text{-}Pr)_2][P(OMe)_3]_3$ (7.12 g, 8.88 mmol), and the reaction mixture was then stirred for 2 h at 80 °C. The solvent was removed in vacuo, and the resulting orange oil was left under dynamic vacuum for an additional 12 h. The product was then dissolved in 95 mL of THF and the resulting orange solution was filtered. After all but 10 mL of THF was removed in vacuo, addition of 150 mL of pentane yielded 5.50 g (72.1%) of orange powder: ^{1}H NMR [tol-d_8, r.t., 90 MHz (broad multiplets were observed for the CH*Me*$_2$ protons at higher fields due to slow rotation about the arylimido ligand)] δ 12.85 (d of t, 1, J_{HH} = 12.75, J_{HP} = 6.37, H_α), 10.23 (d of t, 1, J_{HH} = 12.65, J_{HP} = 2.45, H_β), 7.6 - 7.0 (m, Haryl), 4.56 (br m, 2, CHMe$_2$), 3.58 (t, 18, J_{HP} = 5.40, P(OMe)$_3$), 1.15 (d, 12, J = 6.37, CHMe$_2$); ^{1}H NMR (CD$_2$Cl$_2$, 300 Mz, -80 °C) δ 12.6 (d of t, 1, H_α), 9.36 (d, 1, J_{HH} = 12.02, H_β), 7.44-7.00 (m, 13, H_{aryl}), 4.30 (m, 1, C*H*Me$_2$), 3.91 (m, 1, C*H'*Me$_2$), 3.65 (t, 18, P(OMe)$_3$), 1.09 (d, 6, J = 5.82, CH*Me*$_2$), 0.65 (d, 6, J = 5.35, CH*Me'*$_2$); ^{13}C NMR (CD$_2$Cl$_2$) δ 276.8 (t, J_{CH} = 129.9, J_{CP} = 18.2, J_{CW} = 122.9, C_α), 150.5 (br s, NAr: C_o), 149.0 (t, J_{CP} = 3.0, NAr: C_{ipso}), 142.8 (t, J_{CP} = 5.9, C_γ), 141.1 (t, J_{CP} = 2.3, C*Ph*Ph': C_{ipso}), 139.5 (CPh*Ph'*: C_{ipso}), 139.0 (t, J_{CH} = 158.7, J_{CP} = 5.8, C_β), 131.6 (C*Ph*Ph': C_o), 129.7 (CPh*Ph'*: C_o), 128.5 (C*Ph*Ph': C_p), 128.3 (C*Ph*Ph': C_m), 128.2 (NAr: C_m), 128.1 (CPh*Ph'*: C_p), 128.0 (CPh*Ph'*: C_m), 123.1 (NAr: C_p), 53.3 (t, J_{CP} = 2.3, P(OMe)$_3$), 27.4 (C*H*Me$_2$), 24.5 (CH*Me*$_2$); ^{31}P NMR (tol-d_8) δ 130.5 (J_{PW} = 439, P(OMe)$_3$); NOEDS (C$_6$D$_6$) irradiation at 12.85 ppm, δ 10.23 (5.9% NOE), 4.56 (12.4% NOE), 1.15 (2.8% NOE); irradiation at 10.23, δ 12.85 (3.3% NOE), 1.15 (1.9% NOE); irradiation at 4.56 ppm, δ 12.85 (19.2% NOE), 1.15 (3.3% NOE); irradiation at 1.15, δ 12.85 (6.6% NOE), 4.56 (21.6% NOE). Anal. Calcd for ($C_{33}H_{47}Cl_2NO_6P_2W$): C, 45.54; H, 5.44; N, 1.61. Found: C, 44.96; H, 5.34; N, 1.58.

W(=CH-CH=CPh$_2$][N-2,6-C$_6$H$_3$-(*i*-Pr)$_2$][OCMe(CF$_3$)$_2$]$_2$[P(OMe)$_3$] (16)

A 30 mL THF solution of (CF$_3$)$_2$MeCOLi (878 mg, 4.67 mmol) was cooled to -78 °C and added via cannula over a period of 15 min to a 30 mL THF solution of W[=CH-CH=CPh$_2$]Cl$_2$[N-2,6-C$_6$H$_3$-(*i*-Pr)$_2$][P(OMe)$_3$] (2.02 g, 2.35 mmol). After the addition was complete, the orange solution was allowed to warm to room temperature as it was stirred for a total of 7.5 h. After the solvent and free P(OMe)$_3$ were removed in vacuo, the yellow powder was dissolved in Et_2O, filtered, and recrystallized from Et_2O at -50 °C (1.56 g, 64.0%): ^1H NMR (CD_2Cl_2) Anti Rotamer: δ 12.25 (dd, J_{HH} = 14.41, J_{HP} = 8.06, H_α), 8.72 (d, J = 14.16, H_β), 7.51 - 7.02 (m, 13, H_{aryl}), 3.74 (septet, 1, J = 6.59, *CH*Me_2), 3.60 (d, 9, J_{HP} = 10.25, $P(OMe)_3$), 3.53 (m, 1, C'*H*Me_2, overlaps with Syn: $P(OMe)_3$), 1.88 (s, 3, OC*Me*$(CF_3)_2$), 1.35 (s, 3, OC'*Me*$(CF_3)_2$), 1.27 (d, 3, J = 6.84, CH*Me*Me'), 1.23 (d, 3, J = 6.34, CHMe*Me'*), 1.09 (d, 3, J = 6.83, C'H*Me*Me'), 1.00 (d, 3, J = 6.83, C'HMe*Me'*); Syn Rotamer: δ 11.62 (dd, 1, J_{HH} = 11.00, J_{HP} = 5.13, H_α), 8.72 (d, 1, H_β, overlaps with Anti: H_β), 3.53 (d, 9, J_{HP} = 10.25, $P(OMe)_3$), 1.73 (s, 3, OC*Me*$(CF_3)_2$), 1.48 (s, 3, OC'*Me*$(CF_3)_2$), 1.3 - 1.2 (m, 12, CH*Me*$_2$, overlaps with Anti: $CHMe_2$); ^{13}C NMR (CD_2Cl_2) Anti Rotamer: δ 264.3 (d, J_{CH} = 150.6, J_{CP} = 20.8, J_{CW} = 153.4, C_α), 151.0 (d, J_{CP} = 3.0, NAr: C_{ipso}), 147.6 (d, J_{CP} = 2.5, NAr: C_o), 146.0 (d, J_{CP} = 2.5, NAr: C'_o), 140.3 (d, J_{CP} = 3.0, C*Ph*Ph': C_{ipso}), 138.9 (d, J_{CP} = 2.0, CPh*Ph'*: C_{ipso}), 136.0 (d, J_{CP} = 7.1, C_γ), 131.3 (C*Ph*Ph': C_o), 129.2 (CPh*Ph'*: C_o), 128.7 (C*Ph*Ph': C_m), 128.6 (d, NAr: C_m), 128.6 (C*Ph*Ph': C_p), 128.5 (CPh*Ph'*: C_m), 128.4 (d, J = 2.5, NAr: C'_m), 128.1 (CPh*Ph'*: C_p), 127.1 (NAr: C_p), 125.2 (q, J_{CF} = 287, $OCMe(CF_3)(CF_3)'$), 124.94 (q, J_{CF} = 290, OCMe(CF_3)(*C*F_3)'), 124.87 (q, J_{CF} = 290, OC'Me(*C*F_3)$(CF_3)'$), 124.8 (q, J_{CF} = 188, OC'Me(CF_3)(*C*F_3)'), 122.9 (d, J = 6.6, C_β), 82.1 (septet, J_{CF} = 29.0, O*C*Me$(CF_3)_2$), 80.8 (septet, J_{CF} = 28.3, O*C'*Me$(CF_3)_2$), 53.4 (d, J_{CP} = 7.1, $P(OMe)_3$), 29.9 (*C*HMe_2), 28.3 (*C'*HMe_2), 24.0 (CH*Me*$_2$), 23.54 (C'H*Me*Me'), 23.50 (C'HMe*Me'*), 19.4 ($OCMe(CF_3)_2$), 17.8 ($OCMe(CF_3)_2$); Syn Rotamer: 256.3 (d, J_{CP} = 21.7, C_α); ^{31}P NMR (CD_2Cl_2) Anti Rotamer: δ 147.6 (J_{CW} = 476); Syn Rotamer: δ 147.9 (J_{CW} = 481). Anal. Calcd for ($C_{38}H_{44}F_{12}NO_5PW$): C, 43.99; H, 4.27; N, 1.35. Found: C, 44.22; H, 4.14; N, 1.32.

W(=CH-CH=CPh_2)[N-2,6-C_6H_3-(*i*-Pr)$_2$]-[O-2,6-C_6H_3-(*i*-Pr)$_2$]$_2$[$P(OMe)_3$]$_2$ (17)

A mixture of W(=CH-CH=CPh_2)Cl_2[N-2,6-C_6H_3-(*i*-Pr)$_2$][$P(OMe)_3$]$_2$ (3.53 g, 4.11 mmol) and LiO-2,6-C_6H_3-(*i*-Pr_2)$_2$ (1.51 g, 8.17 mmol) was suspended in 40 mL of cold (-78 °C) Et_2O. The solution was allowed to warm to room temperature as it was stirred for a total of 1.5 h. The solvent and free $P(OMe)_3$ were removed in vacuo, and then the product was dissolved in 120 mL of hexane. The solution was filtered, concentrated to ~90 mL, and then cooled to yield 2.96 g (70.0%) of a deep yellow powder. Two isomers were observed in a 61:39 ratio, and the diagnostic NMR signals are as follows: ^1H NMR (CD_2Cl_2) Major Isomer: δ 12.24 (dd, 1, J_{HH} = 11.37, J_{HP} = 6.31, H_α), 8.89 (d, 1, J = 11.30, H_β); 3.68 (d, 9, J_{HP} = 10.39, $P(OMe)_3$); Minor Isomer: δ 12.38 (dd, 1, J_{HH} = 14.28, J_{HP} = 7.89, H_α), 9.32 (d, 1, J_{HH} = 14.55, H_β); 3.70 (d, 9, J_{HP} = 10.33, $P(OMe)_3$); ^{13}C NMR (CD_2Cl_2) Major Isomer δ 252.9 (d, J_{CH} = 125.4, J_{CP} = 22.2, J_{CW} = 163.8, C_α), 150.8 (J_{CW} = 31.1, NAr: C_{ipso}), 53.3 (J_{CP} = 7.0, $P(OMe)_3$); Minor Isomer: δ 258.9 (d, J_{CH} = 152.2, J_{CP} = 20.8, J_{CW} = 156.1, C_α), 151.6 (J_{CW} = 35.3, NAr: C_{ipso}), 53.2 (J_{CP} = 6.5, $P(OMe)_3$); ^{31}P NMR (CD_2Cl_2) Major Isomer: δ 145.3 (J_{PW} = 459); Minor Isomer δ 146.6 (J_{PW} = 435). Anal. Calcd for ($C_{54}H_{72}NO_5PW$): C, 62.97; H, 7.09; N, 1.36. Found: C, 61.95; H, 7.17; N, 1.37.

$W(=CH\text{-}CH=CPh_2)Cl_2(N\text{-}2,6\text{-}C_6H_3\text{-}Me_2)(PEt_2Ph)_2$ (18)

A 6 mL Et_2O solution of 3,3-diphenylcyclopropene (469 mg, 2.44 mmol) was added to a Schlenk flask containing 2.02 g (2.31 mmol) of tan $WCl_2(N\text{-}2,6\text{-}C_6H_3\text{-}Me_2)(PEt_2Ph)_3$. The solution was stirred for 0.5 h before 10 mL of pentane was added. After the yellow-orange suspension was stirred for an additional 16.5 h, the solvent was removed in vacuo. Next, the product was washed with one 25 mL portion and one 50 mL portion of pentane in order to remove free PEt_2Ph, and then the remaining orange-yellow powder (1.66 g, 79.9%) was dried in vacuo: ^1H NMR (CD_2Cl_2) Anti Rotamer: δ 12.15 (d of t, 1, J_{HH} = 13.1, J_{HP} = 4.4, H_α), 9.55 (d, 1, J = 13.1, H_β), 7.6-6.6 (m, H_{aryl}), 2.5-2.3 (m, $P(C\mathit{H}_2CH_3)_2Ph$), 2.42 (s, 3, NAr: *Me*Me'), 1.63 (s, 3, NAr: Me*Me'*), 1.2-1.0 (m, $P(CH_2C\mathit{H}_3)_2Ph$); Syn Rotamer: δ 11.89 (d of t, 1, J_{HH} = 13.1, J_{HP} = 4.4, H_α), 8.72 (d, 1, J_{HH} = 13.3, H_β), 2.33 (br s, NAr: Me_2); ^{13}C NMR (CD_2Cl_2) Anti Rotamer: δ 271.7

(t, J_{CH} = 128, J_{CP} = 12.6, C_α), 151.6 (NAr: C_{ipso}), 140.5 (t, J_{CP} = 4.7, C_γ), 138.2 (t, J_{CH} = 155.6, J_{CP} = 4.4, C_β), 21.0, 20.5 and 19.4 (NAr*Me*Me' and Syn: NAr*MeMe'*), 17.0 (t, J_{CP} = 13.4, $P(\mathit{C}H_2CH_3)(CH_2CH_3)'Ph$), 15.6 (t, J_{CP} = 13.0, $P(CH_2CH_3)(\mathit{C}H_2CH_3)'Ph$), 7.9 (NAr: Me*Me'*), 7.5 ($P(CH_2\mathit{C}H_3)_2Ph$ and Syn: $P(CH_2\mathit{C}H_3)_2Ph$); Syn Rotamer: δ 277.9 (t, J_{CH} = 130, J_{CP} = 12.6, C_α), 150.6 (NAr: C_{ipso}), 141.2 (br m, J_{CH} = 157.0, C_β), 139.3 (t, J_{CP} = 4.2, C_γ), 18.1 (t, J_{CP} = 13.6, $P(\mathit{C}H_2CH_3)(CH_2CH_3)'Ph$), 16.9 (t, J_{CP} = 15.5, $P(CH_2CH_3)(\mathit{C}H_2CH_3)'Ph$); ^{31}P NMR (CD_2Cl_2) Anti Rotamer: δ 15.3 (J_{PW} = 266); Syn Rotamer: δ 16.2 (J_{PW} = 263); NOEDS (CD_2Cl_2) Anti Rotamer: irradiation at 12.15 ppm, δ 9.55 (3.6% NOE), 2.58-2.19 (1.8% NOE), 1.63 (5.1% NOE), 1.2-1.0 (1.8% NOE); irradiation at 9.55 ppm, δ 12.15 (1.0% NOE); irradiation at 1.63 ppm, δ 12.15 (19.7% NOE); Syn Rotamer: irradiation at 8.72 ppm, δ 2.33 (0.3% NOE); irradiation at 2.33 ppm, δ 8.72 (13.9% NOE). Anal. Calcd for ($C_{34}H_{47}NO_2P_2W$): C, 57.48; H, 5.72; N, 1.56. Found: C, 56.36; H, 5.71; N, 1.57.

Observation of $W(=CH\text{-}CH=CPh_2)Cl_2(N\text{-}2,6\text{-}C_6H_3\text{-}Me_2)[P(OMe)_3]_2$ (19)

The cyclopropene complex $W(CH=CHCPh_2)Cl_2(N\text{-}2,6\text{-}C_6H_3\text{-}Me_2)[P(OMe)_3]_2$ (205.3 mg) was dissolved in 450 μL of CD_2Cl_2. In less than 24 h, complete conversion to the corresponding vinylcarbene complex (an 87:13 mixture of rotomers) was observed by NMR spectroscopy. No other products were observed: ^1H NMR (CD_2Cl_2) Major Rotomer: δ 12.88 (dt, 1, J_{HH} = 12.99, J_{HP} = 6.24, H_α), 9.62 (d, 1, J = 12.93, H_β), 7.5 - 6.8 (m, 13, H_{aryl}), 3.73 (t, 18, J_{HP} = 5.48, $P(OMe)_3$), 2.55 (s, 6, NAr: Me_2); Minor Rotomer: δ 12.41 (dt, 1, J_{HH} = 13.28, J_{HP} = 6.69, H_α), 8.80 (d, 1, J = 14.54, H_β), 2.75 (s, 6, NAr: Me_2); ^{13}C NMR (CD_2Cl_2) Major Rotamer: δ 276.6 (t, J_{CH} = 129.6, J_{CP} = 17.6, J_{CW} = 116.8, C_α), 151.9 (t, J_{CP} = 3.0, J_{CW} = 35.6, NAr: C_{ipso}), 142.8 (t, J_{CP} = 5.6, C_γ), 140.3 (br s, NAr: C_o), 140.1 (C*Ph*Ph': C_{ipso}), 139.3 (CPh*Ph'*: C'_{ipso}), 138.2 (t, J_{CP} = 5.7, C_β), 131.0 (C*Ph*Ph': C_o), 129.5 (CPh*Ph'*: C'_o), 128.5, 128.1, 127.9, 127.7, 127.6, 127.2 (NAr: C_m, C_p and C*PhPh'*: C_m, C'_m, C_p, C'_p), 53.1 (t, J_{CP} = 2.2,

$P(OMe)_3$), 19.5 (NAr: Me_2); Minor Rotamer: δ 283.7 (t, J_{CH} = 132.7, J_{CP} = 17.5, C_α); ^{31}P NMR (CD_2Cl_2) Major Rotamer δ 132.4 (J_{PW} = 442).

$W(=CHR_B)Cl_2[N\text{-}2,6\text{-}C_6H_3\text{-}(i\text{-}Pr)_2][P(OMe)_3]$ (20-B)·$P(OMe)_3$ and Observation of $W(=CHR_C)Cl[N\text{-}2,6\text{-}C_6H_3\text{-}(i\text{-}Pr)_2][P(OMe)_3]_2$ (20-C)

A 10 mL Et_2O solution of ketalcyclopropene (0.99 g, 8.85 mmol) was added via cannula to a purple suspension of $WCl_2[N\text{-}2,6\text{-}C_6H_3\text{-}(i\text{-}Pr)_2][P(OMe)_3]_3\cdot THF^*$ (6.12 g, 7.00 mmol) in 20 mL of Et_2O. After a few minutes of stirring, the solution turned deep red. As the stirring was continued for a total of 19.5 h, a large amount of tan precipitate formed. Pentane (120 mL) was added to the reaction mixture, which was then filtered to yield 4.48 g of tan powder and a pale green-yellow filtrate, which was discarded. At this point, a ^1H NMR spectrum of the tan powder in CD_2Cl_2 indicated a 86:14 mixture of **20-B·P(OMe)$_3$** and the tris(phosphite) precursor. The tan powder was then washed first with 30 mL of Et_2O containing 5 equiv of $P(OMe)_3$ and next with 30 mL of pentane to yield 2.84 g (51.3%) of pure **20-B·P(OMe)$_3$** as a tan powder. Anal. Calcd for ($C_{24}H_{43}Cl_2NO_8P_2W$): C, 36.47; H, 5.48; N, 1.77. Found: C, 36.82; H, 5.34, N 1.42.

A ^1H NMR spectrum of the tan powder indicated the presence of **21-B** and one equiv of free $P(OMe)_3$. This powder was sparingly soluble in most standard NMR solvents other than CD_2Cl_2. Characterization of **21-B·P(OMe)$_3$** by ^{13}C NMR spectroscopy was thus difficult, as a mixture of **21-B** and **21-C** was always observed due to the relatively fast rate of isomerization in CD_2Cl_2. Removal of the second equivalent of phosphite from **21-B·P(OMe)$_3$** was difficult and was only achieved after washing the compound several times with ~100 mL portions of pentane and leaving the compound under dynamic vacuum for at least a day after each washing. In the absence of the second equivalent of phosphite, isomerization of **21-B** to **21-C** was not observed and unambiguous characterization by ^{13}C NMR spectroscopy was possible: ^1H NMR

(CD_2Cl_2) δ 11.73 (dd, 1, J_{HH} = 9.81, J_{HP} = 6.82, H_α), 7.15 (s, 3, H_{aryl}), 6.00 (dd, 1, J_{HH} = 9.81, J_{HP} = 1.84, H_β), 5.08 (m, 1, OC*H*H'), 4.82 (m, 1, OCH*H'*), 4.32 (m, 2, OCH_2), 4.16 (septet, 2, J = 6.83, $CHMe_2$), 3.65 (d, 9, J = 10.89, $P(OMe)_3$), 2.55 (m, 1, $CH_2CHH'CH_2$), 2.09 (m, 1, $CH_2CHH'CH_2$), 1.28 (d, 6, J = 6.89, CH*Me*Me'), 1.25 (d, 6, J = 6.82, CHMe*Me'*); ^{13}C NMR (CD_2Cl_2) δ 259.5 (d, J_{CH} = 143.8, J_{CP} = 20.7, J_{CW} = 124.2, C_α), 165.4 (d, J_{CP} = 5.1, C_γ), 151.7 (d, J_{CP} = 3.0, J_{CW} = 38.9, NAr: C_{ipso}), 165.5 (d, J_{CP} = 2.4, NAr: C_o), 127.7 (NAr: C_p), 123.2 (NAr: C_m), 93.0 (d, J_{CP} = 6.1, C_β), 68.8 (OCH_2), 67.6 (OCH_2'), 53.4 (d, J_{CP} = 5.8, $P(OMe)_3$), 28.0 ($CHMe_2$), 24.5 ($CH_2CH_2CH_2$), 24.2 (CH*Me*Me'), 23.9 (CHMe*Me'*); ^{31}P NMR (CD_2Cl_2) δ 147.1 (J_{PW} = 520).

As mentioned previously, resonances assignable to **21-C** were observed in the ^{13}C NMR spectrum of **21-B·P(OMe)₃** in CD_2Cl_2 solution. Also, **21-B·P(OMe)₃** was observed to convert slowly to **21-C** in the solid state at room temperature (~15% conversion after 2 months). Spectral Data for **21-C**: ^1H NMR (CD_2Cl_2) δ 12.64 (d of t, J_{HH} = 8.26, J_{HP} = 2.30, H_α); ^{13}C NMR (CD_2Cl_2) δ 257.0 (t, J_{CP} = 10.2, C_α), 176.7 (C_γ), 98.8 (C_β), 62.3 (OCH_2), 41.1 (CH_2Cl); ^{31}P NMR (CD_2Cl_2) δ 144.1 (J_{PW} = 459).

A very concentrated CD_2Cl_2 solution was used for the ^{13}C spectrum of **21-B·P(OMe)₃** and under these conditions, a third alkylidene resonance was observed. This same resonance was also observed when 6 equiv of $P(OMe)_3$ was added to a more dilute sample of **21-B·P(OMe)₃**. [Spectral Data for third alkylidene resonance: ^1H NMR (CD_2Cl_2) δ 12.89 (d of t, J_{HH} = 13.97, J_{HP} = 5.04, H_α); ^{13}C NMR (CD_2Cl_2) δ 264.0 (t, J_{CP} = 14.4, C_α), 101.4 (C_β)].

[*Note: The THF adduct of the tris(phosphite) complex **3** was synthesized according to the procedure of this chapter, and the complex was then recrystallized from THF. The complex is easier to handle and very pure without recrystallization, and thus, recrystallization is not recommended.]

$W(CHR_A)Cl_2(N\text{-}2,6\text{-}C_6H_3\text{-}Me_2)(PEt_2Ph)_2$ (syn and anti) (21-A), $W(CHR_B)Cl_2(N\text{-}2,6\text{-}C_6H_3\text{-}Me_2)(PEt_2Ph)$ (21-B), and $W(CHR_C)Cl(N\text{-}2,6\text{-}C_6H_3\text{-}Me_2)(PEt_2Ph)_2$ (21-C)

A 6 mL solution of ketalcyclopropene (274 mg, 2.45 mmol) was added to a Schlenk flask containing 2.01 g (2.30 mmol) of tan $WCl_2(N\text{-}2,6\text{-}C_6H_3\text{-}Me_2)(PEt_2Ph)_3$. The solution was stirred for 0.5 h before adding 10 mL of pentane. After the red suspension was stirred for an additional 16.5 h, the solvent was removed in vacuo. Next, free PEt_2Ph was removed by washing the product with one 25 mL portion and one 50 mL portion of pentane, and the brick-red powder (1.39 g, 73.6%) was then dried in vacuo. ^1H, ^{13}C, and ^{31}P NMR spectra acquired immediately after the complex was dissolved in C_6D_6, tol-d_8, or CD_2Cl_2 indicated the presence of 4 alkylidene species: 3 bis(phosphine) adducts [**21-A** (syn and anti rotamers) and **21-C**] and one monophosphine adduct (**21-B**). An equivalent amount of free PEt_2Ph relative to the mono(phosphine) adduct **21-B** was observed by ^{31}P NMR spectroscopy: ^1H NMR (C_6D_6) **21-A** (syn and anti): δ 12.70 (d of t, J_{HH} = 14.17, J_{HP} = 3.98, H_α, 11%), 12.66 (d of t, J_{HH} = 13.60, J_{HP} = 3.79, H_α, 60%); **21-C**: δ 12.42 (d of t, J_{HH} = 7.96, J_{HP} = 2.03, H_α, 24%); **21-B**: δ 11.54 (d of d, J_{HH} = 9.93, J_{HP} = 5.51, H_α, 5%); ^{13}C NMR (CD_2Cl_2) **21-A** (syn and anti) δ 270.4 (t, J_{CP} = 10.8, C_α), 263.9 (t, J_{CP} = 11.0, C_α), **21-C**: δ 262.1 (t, J_{CP} = 7.14, C_α); ^{31}P NMR (tol-d_8) 33.0, 17.8 (J_{PW} = 283), 15.3 (J_{PW} = 278), 13.4 (J_{PW} = 276).

$W(=CHR_C)Cl(N\text{-}2,6\text{-}C_6H_3\text{-}Me_2)(PEt_2Ph)_2$ (21-C)

The red isomeric mixture of **21-A**, **21-B**, and **21-C** (812 mg, 1.00 mmol) was dissolved in 25 mL of CH_2Cl_2 and stirred for 19.5 h before removing the solvent in vacuo. The green residue (512 mg, 63.1%) was washed with 50 mL of pentane and dried in vacuo: ^1H NMR (CD_2Cl_2) δ 12.23 (d of t, 1, J_{HH} = 8.07, J_{HP} = 2.13, H_α), 7.7-6.8 (m, 13, H_{aryl}), 5.18 (d, 1, J = 8.04, H_β), 3.53 (t, 2, J = 6.58, CH_2Cl), 3.52 (t, 2, J = 5.99, OCH_2), 2.3 - 2.0 (m, 8, $P(CH_2CH_3)_2Ph$), 2.15 (s, 6, NAr: Me_2), 1.84 (quintet, 2, J = 6.27, $CH_2CH_2CH_2$), 1.08-0.87 (m, 12, $P(CH_2CH_3)_2Ph$); ^{13}C NMR (CD_2Cl_2) δ 261.6

(t, J_{CH} = 134.2, J_{CP} = 7.2, J_{CW} = 118.6, C_α), 174.3 (J_{CW} = 4.8, C_γ), 155.4 (J_{CW} = 19.0, NAr: C_{ipso}), 136 (br s, NAr: C_o), 132.6 (t, J_{CP} = 19.5, PEt_2Ph: C_{ipso}), 130.3 (t, J_{CP} = 3.8, $PEt_2\mathit{Ph}$: C_o), 128.3 and 128.0 (NAr: C_m and $PEt_2\mathit{Ph}$: C_p), 127.2 (t, J_{CP} = 3.8, PEt_2Ph: C_m), 123.0 (NAr: C_p), 94.8 (J_{CH} = 164.6, C_β), 61.9 (OCH_2), 41.6 (CH_2Cl), 32.0 ($CH_2\mathit{C}H_2CH_2$), 19.7 (br s, NAr: Me_2), 16.2 (t, J_{CP} = 12.1, $P(\mathit{C}H_2CH_3)(CH_2CH_3)'Ph$), 14.4 (t, J = 12.0, $P(CH_2CH_3)(\mathit{C}H_2CH_3)'Ph$), 6.9 ($(PCH_2\mathit{C}H_3)_2Ph$); ^{31}P NMR (CD_2Cl_2) δ 18.6 (J_{PW} = 283, PEt_2Ph); NOEDS (CD_2Cl_2) irradiation at 12.23 ppm, δ 5.18 (11.6% NOE), 2.15 (2.2% NOE); irradiation at 5.18 ppm, δ 12.23 (3.2% NOE); irradiation at 3.53 ppm, δ 1.84 (5.4% NOE), irradiation at 3.52 ppm, δ 1.84 (7.0% NOE), irradiation at 2.15 ppm, δ 12.23 (18.5% NOE); irradiation at 1.84 ppm, δ 3.52 (2.6% NOE). Anal. Calcd for ($C_{34}H_{47}NO_2P_2W$): C, 49.90; H, 5.79; N, 1.71. Found: C, 50.23; H, 5.78; N, 1.70.

$W(=CHR_B)Cl_2(N\text{-}2,6\text{-}C_6H_3\text{-}Me_2)[P(OMe)_3]$ (22-B)

A 30 mL Et_2O solution of ketalcyclopropene (319 mg, 2.84 mmol) was transferred via cannula onto a 30 mL Et_2O suspension of purple $WCl_2(N\text{-}2,6\text{-}C_6H_3\text{-}Me_2)[P(OMe)_3]_3$ (2.06 g, 2.76 mmol), and the reaction mixture was stirred for 14.25 h. Almost immediately, a yellow precipitate formed; later in the reaction, a red precipitate was observed. Pentane (60 mL) was added to the reaction mixture, which was then filtered, and the resulting red powder (758 mg, 45.0%) was dried in vacuo: ^1H NMR (CD_2Cl_2) δ 11.88 (dd, 1, J_{HH} = 9.79, J_{HP} = 6.80, H_α), 7.05 - 6.95 (m, 3, H_{aryl}), 6.00 (dd, 1, J_{HH} = 9.78, J_{HP} = 1.83, H_β), 5.08 (m, 1, $OC\mathit{H}H'$), 4.82 (m, 1, $OCH\mathit{H}'$), 4.32 (m, 2, OCH_2), 3.65 (d, 9, J = 10.95, $P(OMe)_3$), 2.64 (s, 6, NAr: Me_2), 2.35 (m, 1, $CH_2C\mathit{H}H'CH_2$), 2.20 (m, 1, $CH_2CH\mathit{H}'CH_2$); ^{13}C NMR (CD_2Cl_2) 259.7 (δ, J_{CH} = 144.7, J_{CP} = 20.5, J_{CW} = 122, C_α), 165.3 (C_γ), 154.2 (J_{CW} = 19.6, NAr: C_{ipso}), 137.5 (NAr: C_o), 127.7 (NAr: C_p), 126.8 (NAr: C_m), 92.7 (J_{CH} = 168.0, C_β), 68.7 (OCH_2), 67.5 (OCH_2), 53.1 (d, J_{CP} = 5.7, $P(OMe)_3$), 24.3 ($CH_2\mathit{C}H_2CH_2$), 19.1 (NAr: Me_2); ^{31}P NMR (CD_2Cl_2) δ

147.5 (J_{PW} = 522); NOEDS (CD_2Cl_2) irradiation at 11.88 ppm, δ 6.00 (10.7% NOE), 4.32 (1.3% NOE), 2.64 (2.0% NOE); irradiation at 6.00 ppm, δ 11.88 (6.6% NOE), 4.32 (1.6% NOE); irradiation at 4.32 ppm, δ 7.0 (1.2% NOE), 5.08 (4.3% NOE), 4.82 (9.7% NOE), 2.64 (1.6% NOE), 2.35 (5.6% NOE), 2.20 (6.0% NOE); irradiation at 2.64 ppm, δ 11.88 (12.9% NOE), 3.65 (0.4% NOE). Anal. Calcd for ($C_{17}H_{26}Cl_2NO_5PW$): C, 33.47; H, 4.30; N, 2.30. Found: C, 33.35; H, 4.32; N, 2.57.

Observation of $W(=CHR_B)Cl_2(N\text{-}2,6\text{-}C_6H_3\text{-}Me_2)[P(OMe)_3]$ (22-B) and $W(=CHR_C)Cl(N\text{-}2,6\text{-}C_6H_3\text{-}Me_2)[P(OMe)_3]_2$ (22-C)

The cyclopropene complex **14** (289 mg) was dissolved in 300 μL of CD_2Cl_2. In less than 24 h, complete conversion to a mono(phosphite) (**22-B**, 25%) and a bis(phosphite) (**22-C**, 75%) vinyl alkylidene complex was observed by NMR spectroscopy. The ^1H, ^{13}C, and ^{31}P NMR spectra of the mono(phosphite) vinyl alkylidene complex are identical with those of isolated **22-B** and the spectral assignments for **22-C** follow: ^1H NMR (CD_2Cl_2) δ 12.74 (m, 1, H_α); ^{13}C NMR (CD_2Cl_2) 257.5 (t, J_{CH} = 135.0, J_{CP} = 10.0, J_{CW} = 113.6, C_α), 176.5 (C_γ), 155.2 (J_{CW} = 38.8, NAr: C_{ipso}), 135.7 (NAr: C_o), 127.6 (NAr: C_m), 124.1 (NAr: C_p), 98.9 (J_{CH} = 166.7, C_β), 62.2 (OCH_2), 51.6 ($P(OMe)_3$), 41.0 (CH_2Cl), 31.6 ($CH_2CH_2CH_2$), 18.9 (NAr: Me_2); ^{31}P NMR (CD_2Cl_2) δ 147.1 (J_{PW} = 520).

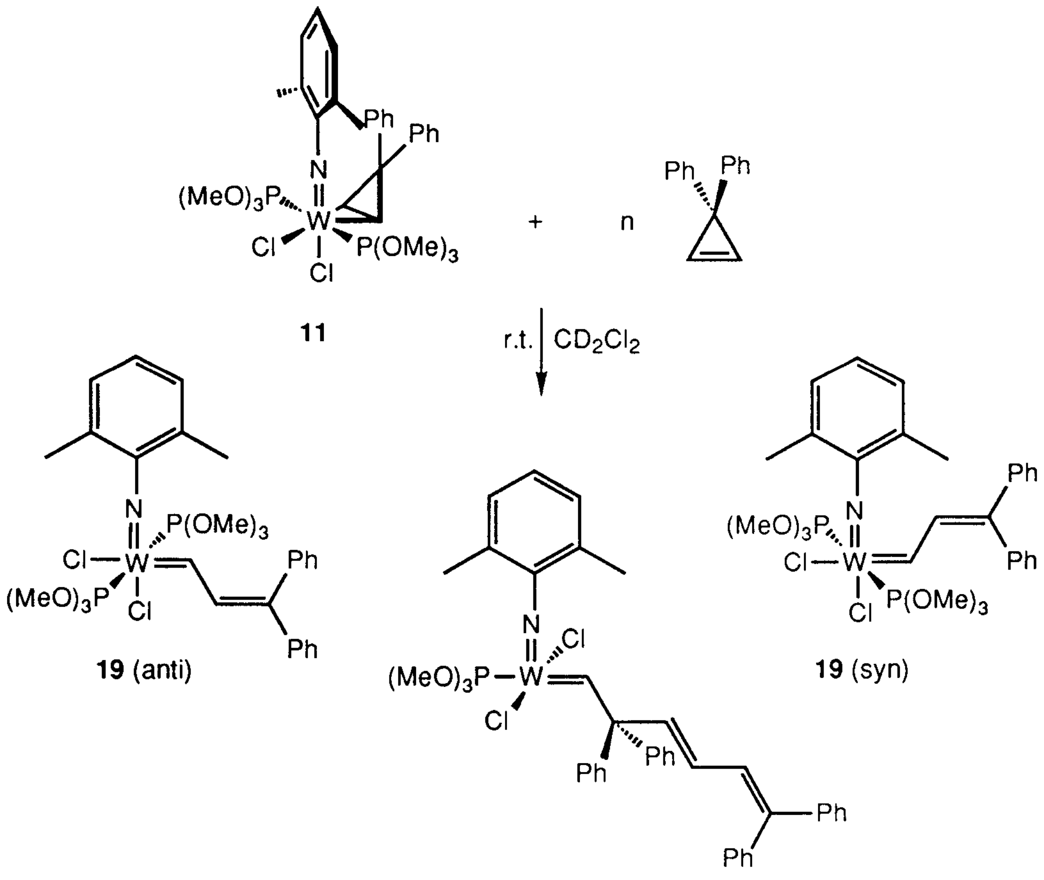

Table 10. Conversion of **11** to **19** in the Presence of Excess Diphenylcyclopropene[a]

n	time	**11**	diphenyl-cyclopropene	**19** anti	**19** syn	**19** + diphenyl-cyclopropene
0	3 h	38%	0%	28%	14%	0%
2.2	3 h	52%	141%	8%	5%	8%
0	22 h	0%	0%	65%	17%	0%
2.2	22 h	26%	131%	10%	10%	40%

[a] General Procedure: Complex **11** (34.2 mg, 0.0420 mmol) was dissolved in 600 μL of CD_2Cl_2 (0.0036 M in mesitylene internal standard) together with n equivalents (n = 0 or 2.2) of diphenylcyclopropene. The solution was transferred to an NMR tube, the NMR tube was capped with a rubber septum, and the septum was wrapped with Parafilm. The tube was mechanically rotated for 3 h before a ^1H NMR spectrum was acquired; after rotating the tube for an additional 19 h, another ^1H NMR spectrum was acquired. The percentages of compounds were determined by integration relative to the mesitylene internal standard. The insertion product derived from the reaction of diphenylcyclopropene with **19** is tentatively proposed on the basis of the following chemical shifts: δ 11.39 (d, J_{HP} = 4.79, H_α), 6.49 (d, J = 15.59, =C(*H*)-CPh_2 or C(*H*)=CPh_2), 6.08 (d, J = 11.17, =C(*H*)-CPh_2 or C(*H*)=CPh_2), 5.73 (dd, J = 15.69, 11.13, C(*H*)-C(H)=CPh_2).

Table 11. ^{1}H NMR Spectral Data for the $HgCl_2$-Catalyzed Conversions of the Phenylimido η^2-Cyclopropene Complexes **9** and **10** to Vinyl Alkylidene Complexes[a]

Cmpd	Reaction Conditions	Observations and ^{1}H NMR Spectral Data
9	0.8 equiv $HgCl_2$ rotated 2.7 h[b]	Complete Conversion to Vinyl Alkylidene Major Rotamer (85%): δ 12.39 (dt, J_{HH} = 13.09, J_{HP} = 5.71, H_α), 9.00 (dt, J_{HH} = 13.13, J_{HP} = 1.87, H_β). Minor Rotamer (15%): δ 12.55 (dt, J_{HP} = 6.24, H_α), 9.44 (dt, J_{HH} = 12.70, H_β).
9	1 equiv $HgCl_2$ shook briefly[b]	Complete Conversion to Vinyl Alkylidene Solution Immediately Turned from Yellow to Orange >95% Rotamer with 12.39 ppm H_α Resonance
	rotated overnight	Only 28% of the Vinyl Alkylidene Remained
10	0.9 equiv $HgCl_2$ rotated 2.7 h[b]	1.3:1 Ratio of η^2-Cyclopropene to Vinyl Alkylidene[c] ^{1}H (CD_2Cl_2) δ 11.96 (dt, J_{HH} = 13.28, J_{HP} = 4.23, H_α), 8.82 (dt, J_{HH} = 13.16, J_{HP} = 1.29, H_β).
10	$HgCl_2$ shook briefly[d]	Complete Conversion to Vinyl Alkylidene ^{1}H (C_6D_6/THF-d_8) δ 12.39 (dt, J_{HH} = 13.24, J_{HP} = 4.17, H_α), 9.16 (dt, J_{HH} = 13.24, H_β), 2.38 (t, J_{HP} = 4.41, $PMePh_2$).

---

[a] Attempted conversions of the η^2-ketalcyclopropene complexes **12** and **13** resulted only in decomposition.

[b] The η^2-cyclopropene complex (46 mg) was dissolved in 600 μL of CD_2Cl_2 and a ^{1}H NMR spectrum was acquired. Solid $HgCl_2$ was then added to the solution, and the mixture was shaken or mechanically rotated before acquiring a second ^{1}H NMR spectrum.

[c] A 6.3:1 ratio of η^2-cyclopropene to vinyl alkylidene was observed before the addition of $HgCl_2$.

[d] The η^2-cyclopropene complex (21 mg, 0.023 mmol) and $HgCl_2$ (6 mg, 0.02 mmol) were combined in a mixture of C_6D_6 and THF-d_8 and the reaction mixture was shaken briefly before acquiring a ^{1}H NMR spectrum.

Table 12. ^{1}H NMR Spectral Data for the Photolyses of the Phenylimido η^2-Cyclopropene Complexes **9**, **10**, **12**, and **13**.[a]

Cmpd	After Photolysis
	Complete Conversion to Vinyl Alkylidene[b]
9	75% Major Rotamer: δ 12.32 (dt, 1, J_{HH} = 13.35, J_{HP} = 4.27, H_α), 9.13 (dt, 1, J_{HH} = 13.41, J_{HP} = 13.41, H_β), 2.36 (t, 6, J_{HP} = 4.49, $PMePh_2$). 25% Minor Rotamer: δ 13.35 (H_α), 9.35 (H_β, J_{HH} = 13), 2.38 (t, J_{HP} = 4.23, $PMePh_2$).
	1:3.4 ratio of η^2-Cyclopropene to Vinyl Alkylidene
10	δ 12.84 (dt, 1, J_{HH} = 13.22, J_{HP} = 6.57, H_α), 9.36 (dt, 1, J_{HH} = 13.06, J_{HP} = 2.05, H_β), 3.61 (t, 18, J_{HP} = 5.41, $P(OMe)_3$).
	Complete Conversion to Vinyl Alkylidene
12	Major Rotamer (Isomer **A**): δ 12.48 (dt, 1, J_{HH} = 13.58, J_{HP} = 3.74, H_α), 3.49 (t, 2, J = 6.13, OCH_2), 3.44 (t, 2, J = 6.19, OCH_2), 2.47 (t, 6, J = 4.37, $PMePh_2$).
	1:3.3 ratio of η^2-Cyclopropene to Vinyl Alkylidene
13	53% Major Isomer: δ 13.14 (dt, J_{HH} = 13.98, J_{HP} = 4.69, H_α). 47% Minor Isomer (Form **B**): δ 11.72 (dd, J_{HH} = 9.54, J_{HP} = 7.02, H_α), 6.10 (dd, J_{HH} = 9.33, J_{HP} = 1.58, H_β).

---

[a] General Procedure: The η^2-cyclopropene complex (10.5 mg) was dissolved in 600 μL of toluene-d_8 (0.0035 M in mesitylene internal standard), the solution was immediately cooled to 0 °C, and a ^{1}H NMR spectrum was acquired. (Note: Complexes **10** and **13** were not completely soluble in tol-d_8 at these concentrations, possibly explaining their incomplete conversion.) The complex was photolyzed for 7 h at 0 °C before acquiring another ^{1}H NMR spectrum.

[b] Before photolysis a 10.4:1 mixture of **9**:vinyl alkylidene was observed.

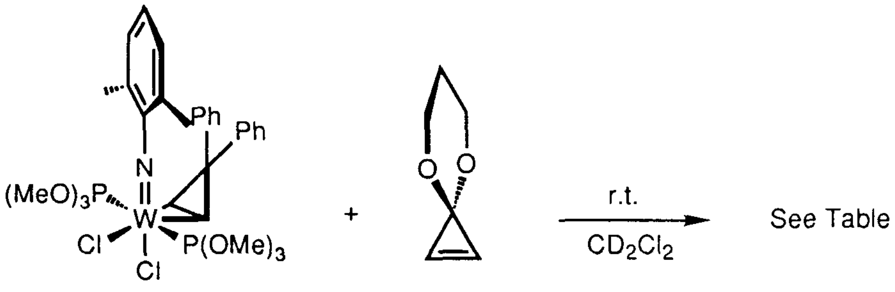

11

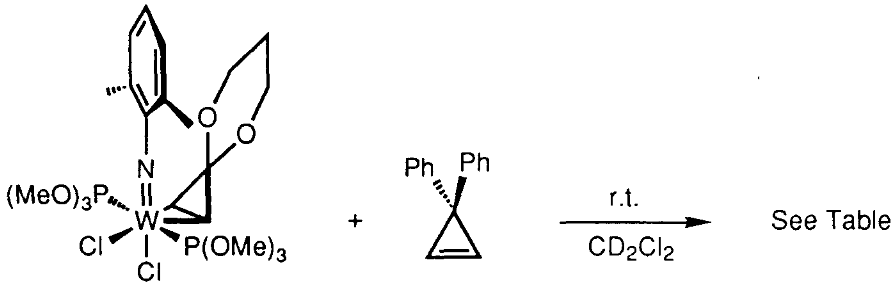

14

Table 13. Reaction of **11** with Ketalcyclopropene and of **14** with Diphenylcyclopropene—Species Observed after 5.6 Hours at Room Temperature[a,b]

Reaction	**11**	**14**	**19**	**22-B**	Ketal-cyclopropene	Diphenyl-cyclopropene
11 + Ketalcyclopropene	55%	0%	7%	4%	39%	12%
14 + Diphenylcyclopropene	0%	?[c]	<5%	25%	0%	63%

---

[a] General Procedure: The η^2-cyclopropene complex (0.086 mmol) and 1 equiv of 3,3-disubstituted cyclopropene were dissolved together in 600 μL of CD_2Cl_2 (0.0036 M in mesitylene internal standard). The NMR tube was capped with a rubber septum, the septum was wrapped with Parafilm, and the solution was then left at room temperature for 5.6 h without any external mixing. A ^1H NMR spectrum was then acquired, and the percentages of species present were determined by integration versus the mesitylene internal standard.

[b] Note: The reactions were quite complex, and only the readily identifiable species are reported here.

[c] Two overlapping triplets (84% together) were observed at 4.3 ppm. It is uncertain whether they can both be assigned as η^2-ketalcyclopropene complexes.

X-ray Data Collection, Structure Determination and Refinement for $WCl_2[N\text{-}2,6\text{-}C_6H_3\text{-}(i\text{-}Pr)_2][P(OMe)_3]_3$ (4)

A purple crystal of approximate dimensions 0.28 x 0.40 x 0.43 mm was oil-mounted on a glass fiber and transferred to the Siemens P3 diffractometer which is equipped with a modified LT-2 low temperature system. Determination of Laue symmetry, crystal class, unit cell parameters and the crystal's orientation matrix were carried out by previously described techniques similar to those of Churchill.[38] Low temperature (158 K) intensity data were collected via a θ-2θ scan technique with Mo$K\alpha$ radiation under the conditions given in Table 1.

All 7579 data were corrected for absorption and for Lorentz and polarization effects and placed on an approximately absolute scale. Any reflection with I(net) < 0 was assigned the value $|F_o| = 0$. The systematic extinctions observed were $0k0$ for $k = 2n + 1$ and $h0l$ for $l = 2n + 1$; the diffraction symmetry was 2/m. The centrosymmetric monoclinic space group $P2_1/c$ [C_{2h}^5; No. 14] is thus uniquely defined.

All crystallographic calculations were carried out using either the UCI modified version of the UCLA Crystallographic Computing Package[40] or the SHELXTL PLUS program set.[41] The analytical scattering factors for neutral atoms were used throughout the analysis;[42a] both the real ($\Delta f'$) and imaginary ($i\Delta f''$) components of anomalous dispersion[42b] were included. The quantity minimized during least-squares analysis was $\Sigma w(|F_o| - |F_c|)^2$ where $w^{-1} = \sigma^2(|F_o| + 0.0005(|F_o|)^2$.

The structure was solved via an automatic Patterson routine (SHELXTL PLUS); and refined by full-matrix least-squares techniques. Hydrogen atoms were included using a riding model with d(C-H) = 0.96 Å and U(iso) = 0.06 Å^2. Refinement of positional and anisotropic thermal parameters led to convergence with $R_F = 2.8\%$, $R_{wF} = 3.2\%$ and GOF = 1.26 for 334 variables refined against those 6690 data with $|F_o| > 3.0\sigma(|F_o|)$). A final difference-Fourier map yielded $\rho(\max) = 0.94$ eÅ^{-3}.

X-ray Data Collection, Structure Determination and Refinement for $W(HC{=}CH\text{-}CPh_2)Cl_2(NPh)[P(OMe)_3]_2$ (10)

A yellow/gold crystal of approximate dimensions 0.20 x 0.30 x 0.30 mm was oil-mounted on a glass fiber and transferred to the Syntex $P2_1$ diffractometer which is equipped with a modified LT-1 low temperature system. Determination of Laue symmetry, crystal class, unit cell parameters and the crystal's orientation matrix were carried out by previously described techniques similar to those of Churchill.[38] Low temperature (183 K) intensity data were collected via a θ-2θ scan technique with MoKα radiation under the conditions given in Table 1.

All 4899 data were corrected for absorption and for Lorentz and polarization effects and placed on an approximately absolute scale. Any reflection with I(net) < 0 was assigned the value $|F_o| = 0$. The systematic extinctions observed were $0k0$ for $k = 2n + 1$ and $h0l$ for $l = 2n + 1$; the diffraction symmetry was 2/m. The centrosymmetric monoclinic space group $P2_1/c$ [C_{2h}^5; No. 14] is thus uniquely defined.

All crystallographic calculations were carried out using either the UCI modified version of the UCLA Crystallographic Computing Package[40] or the SHELXTL PLUS program set.[41] The analytical scattering factors for neutral atoms were used throughout the analysis;[42a] both the real ($\Delta f'$) and imaginary ($i\Delta f''$) components of anomalous dispersion[42b] were included. The quantity minimized during least-squares analysis was $\Sigma w(|F_o| - |F_c|)^2$ where $w^{-1} = \sigma^2(|F_o| + 0.0005(|F_o|)^2$.

The structure was solved via an automatic Patterson routine (SHELXTL PLUS); and refined by full-matrix least-squares techniques. Hydrogen atoms were included using a riding model with d(C-H) = 0.96 Å and U(iso) = 0.08 Å^2. There is a benzene molecule located about an inversion center (1/2, 1/2, 1/2). Refinement of positional and anisotropic thermal parameters (isotropic for the three unique benzene carbon atoms) led to convergence with $R_F = 4.5\%$, $R_{wF} = 6.0\%$ and GOF = 1.45 for 364 variables refined against those 3721 data with $|F_o| > 3.0\sigma(|F_o|)$). A final difference-Fourier map yielded $\rho(\max) = 1.38$ eÅ^{-3}.

X-ray Data Collection, Structure Determination and Refinement for $W(=CHR_C)Cl_2(N\text{-}2,6\text{-}C_6H_3\text{-}Me_2)(PEt_2Ph)_2$ (21-C)

A green crystal of approximate dimensions 0.23 x 0.33 x 0.37 mm was oil-mounted on a glass fiber and transferred to the Siemens P3 diffractometer which is equipped with a modified LT-2 low temperature system. Determination of Laue symmetry, crystal class, unit cell parameters and the crystal's orientation matrix were carried out by previously described techniques similar to those of Churchill.[38] Low temperature (158 K) intensity data were collected via a θ-2θ scan technique with MoKα radiation under the conditions given in Table 1.

All 6596 data were corrected for absorption and for Lorentz and polarization effects and placed on an approximately absolute scale. Any reflection with I(net) < 0 was assigned the value $|F_o| = 0$. There were no systematic extinctions nor any diffraction symmetry other than the Friedel condition. The two possible triclinic space groups are the noncentrosymmetric P1 [C_1^1; No.1] or the centrosymmetric $P\bar{1}$ [C_1^1; No.2]. With Z = 2 and no expectation of a resolved chiral molecule, the latter centrosymmetric space group is far more probable,[39] and was later shown to be the correct choice.

All crystallographic calculations were carried out using either the UCI modified version of the UCLA Crystallographic Computing Package[40] or the SHELXTL PLUS program set.[41] The analytical scattering factors for neutral atoms were used throughout the analysis;[42a] both the real ($\Delta f'$) and imaginary ($i\Delta f''$) components of anomalous dispersion[42b] were included. The quantity minimized during least-squares analysis was $\Sigma w(|F_o| - |F_c|)^2$ where $w^{-1} = \sigma^2(|F_o| + 0.0004(|F_o|)^2$.

The structure was solved by direct methods (SHELXTL PLUS); and refined by full-matrix least-squares techniques. Hydrogen atoms were included using a riding model with d(C-H) = 0.96 Å and U(iso) = 0.08 Å^2. At convergence, $R_F = 3.0\%$, $R_{wF} = 3.7\%$ and GOF = 1.37 for 379 variables refined against those 6920 data with $|F_o| > 2.0\sigma(|F_o|))$.

A final difference-Fourier map yielded ρ(max) = 0.94 eÅ^{-3} at a distance of 1.36 Å from Cl(2).

X-ray Data Collection, Structure Determination and Refinement for $W(=CH\text{-}CH\text{-}CPh_2)[N\text{-}2,6\text{-}C_6H_3\text{-}(i\text{-}Pr)_2][OCMe(CF_3)_2]_2[P(OMe)_3]$ (16)

A yellow crystal of approximate dimensions 0.20 x 0.30 x 0.37 mm was oil-mounted on a glass fiber and transferred to the Siemens P3 diffractometer which is equipped with a modified LT-2 low temperature system. Determination of Laue symmetry, crystal class, unit cell parameters and the crystal's orientation matrix were carried out by previously described techniques similar to those of Churchill.[38] Low temperature (158 K) intensity data were collected via a θ-2θ scan technique with MoKα radiation under the conditions given in Table 1.

All 6801 data were corrected for absorption and for Lorentz and polarization effects and placed on an approximately absolute scale. Any reflection with I(net) < 0 was assigned the value $|F_o| = 0$. There were no systematic extinctions nor any diffraction symmetry other than the Friedel condition. The two possible triclinic space groups are the noncentrosymmetric P1 [C_1^1; No.1] or the centrosymmetric $P\bar{1}$ [C_i^1; No.2]. With Z = 2 and no expectation of a resolved chiral molecule, the latter centrosymmetric space group is far more probable, and was later shown to be the correct choice.

All crystallographic calculations were carried out using either the UCI modified version of the UCLA Crystallographic Computing Package[40] or the SHELXTL PLUS program set.[41] The analytical scattering factors for neutral atoms were used throughout the analysis;[42a] both the real ($\Delta f'$) and imaginary ($i\Delta f''$) components of anomalous dispersion[42b] were included. The quantity minimized during least-squares analysis was $\Sigma w(|F_o| - |F_c|)^2$ where $w^{-1} = \sigma^2(|F_o|) + 0.0005(|F_o|)^2$.

The structure was solved via an automatic Patterson routine (SHELXTL PLUS); and refined by full-matrix least-squares techniques. Hydrogen atoms were included using a riding model with d(C-H) = 0.96 Å and U(iso) = 0.06 Å^2. Refinement of positional and anisotropic thermal parameters led to convergence with $R_F = 2.8\%$, $R_{wF} = 3.2\%$ and GOF = 1.26 for 334 variables refined against those 6690 data with $|F_o| > 3.0\sigma(|F_o|)$). A final difference-Fourier map yielded $\rho(\max) = 0.94$ eÅ^{-3}.

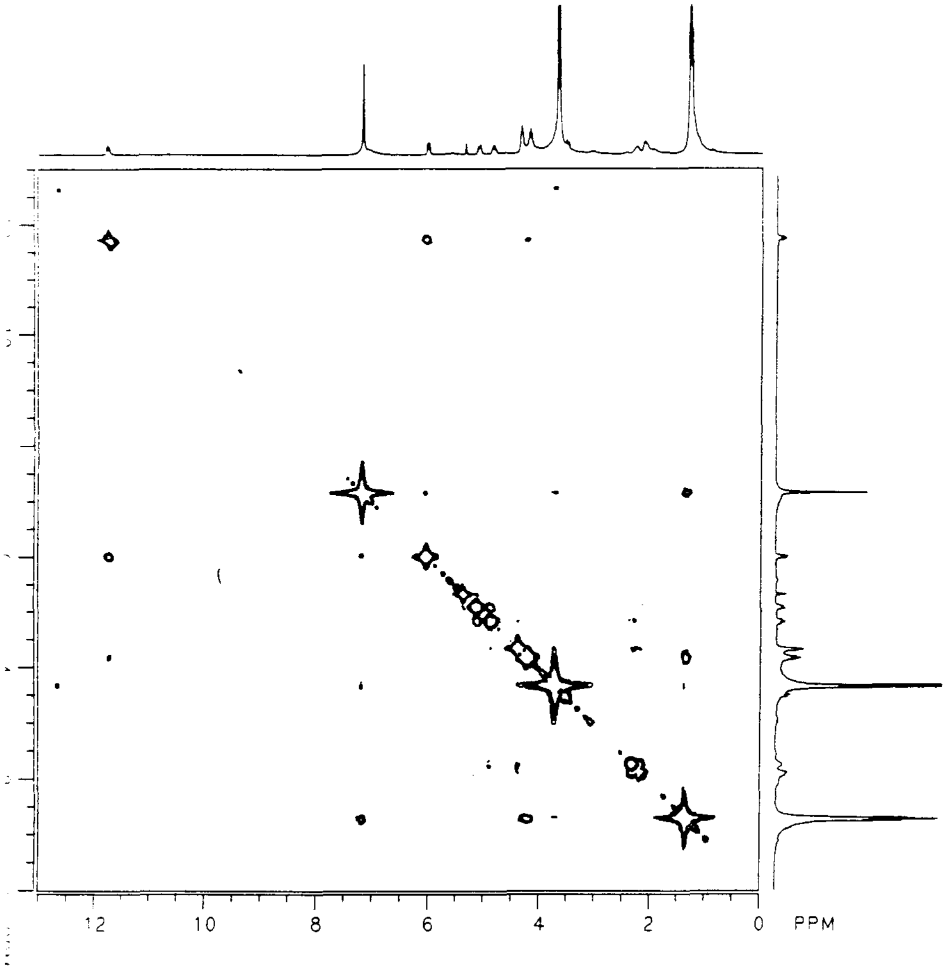

Figure 6. ^{1}H-^{1}H COSY spectrum of **20-B**.

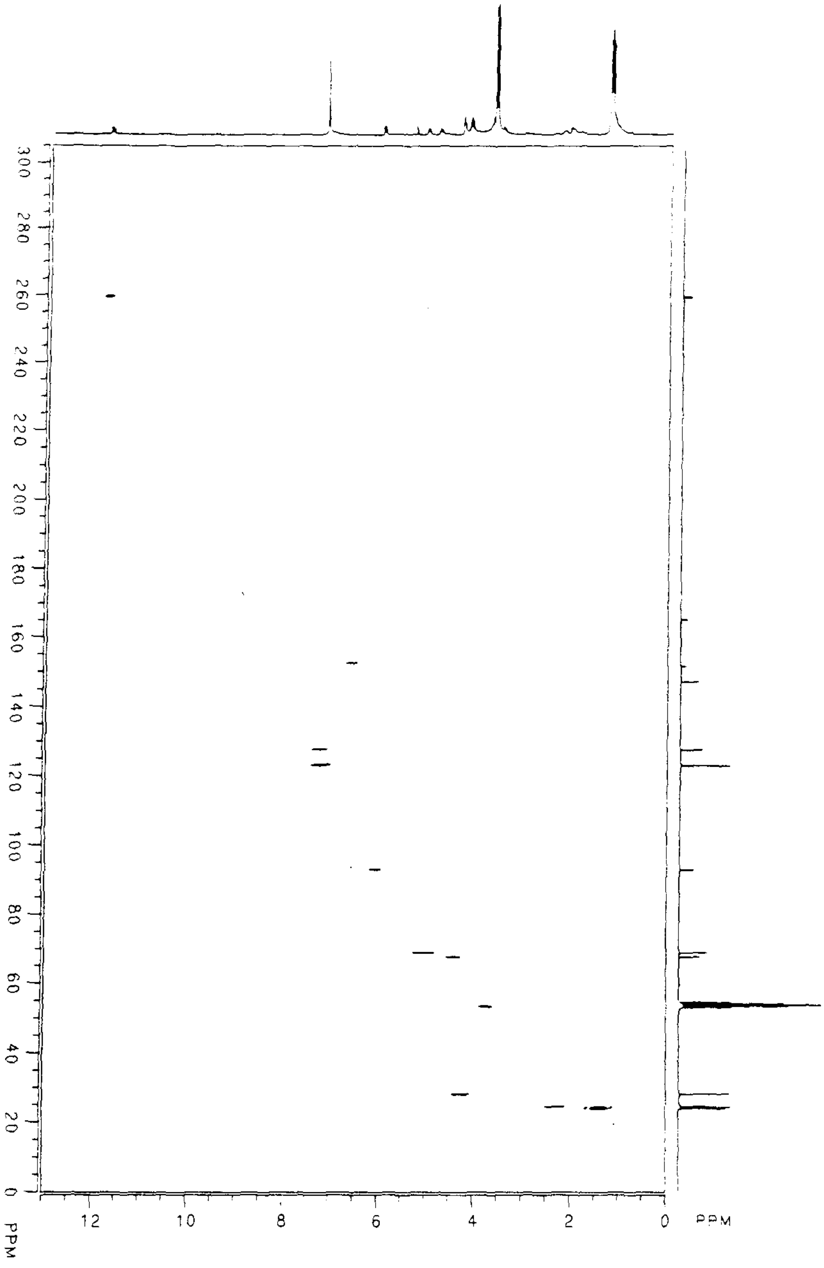

Figure 7. ^1H-^{13}C COSY spectrum of **20-B**.

References and Notes

(1) Binger, P.; Muller, P.; Benn, R.; Mynott, R. *Angew. Chem., Int. Ed. Engl.* **1989**, *28*, 610-611.

(2) For other examples of systems in which cyclopropenes are proposed as precursors to vinyl alkylidene intermediates, please see: (a) Fischer, H.; Hofmann, J.; Mauz, E. *Angew. Chem., Int. Ed. Engl.* **1991**, *30*, 998-999. (b) Padwa, A.; Kassir, J. M.; Xu, S. L. *J. Org. Chem.* **1991**, *56*, 6971-6972. (c) Hoye, T. R.; Dinsmore, C. J. *Tetrahedron Lett.* **1991**, *32*, 3755-3758. (d) Muller, P.; Pautex, N.; Doyle, M. P.; Bagheri, V. *Helv. Chim. Acta* **1990**, *73*, 1233-1241.

(3) For general discussions regarding the physical properties, synthetic utility, and multifunctional reactivity of cyclopropenes, see: (a) Binger, P.; Buch, H. M. *Top. Curr. Chem.* **1987**, *135*, 77-151. (b) Baird, M. S. *Top. Curr. Chem.* **1988**, *144*, 137-209. (c) Halton, B.; Banwell, M. G. In *The Chemistry of the Cyclopropyl Group*; Rappoport, A., Ed.; John Wiley & Sons: New York, 1987; Part 2, Chapter 21.

(4) For general references on the metathesis reaction, see: (a) Grubbs, R. H.; Tumas, W. *Science* **1989**, *243*, 907-915. (b) Ivin, K. J. *Olefin Metathesis*; Academic Press: London, 1983. (c) Grubbs, R. H. In *Comprehensive Organometallic Chemistry*; Wilkinson, G., Ed.; Pergamon Press, Ltd.: New York, 1982; Vol. 8, pp 499-551. (d) Leconte, M.; Basset, J. M.; Quignard, F.; Larroche, C. In *Reactions of Coordinated Ligands*; Braterman, P. S., Ed.; Plenum: New York, 1986; Vol. 1, pp 371-420.

(5) (a) Brown-Wensley, K. A.; Buchwald, S. L.; Cannizzo, L.; Clawson, L.; Ho, S.; Meinhardt, D.; Stille, J. R.; Straus, D.; Grubbs, R. H. *Pure & Appl. Chem.* **1983**, *55*, 1733-1744. (b) Pine, S. H.; Zahler, R.; Evans, D. A.; Grubbs, R. H. *J. Am. Chem. Soc.* **1980**, *102*, 3270-3272. (c) Aguero, A.; Kress, J.; Osborn, J. A. *J. Chem. Soc., Chem. Commun.* **1986**, 531-533. (d) Heppert, J. A.; Dietz, S. D.; Morton, M. D. *Abstracts of Papers*, 199th National Meeting of the American Chemical Society, Boston, MA; American Chemical Society: Washington, DC, 1990; INOR 262. (e) Bazan, G. C.; Schrock, R. R.; O'Regan, M. B. *Organometallics* **1991**, *10*, 1062-1067.

(6) (a) Bradley, D. C.; Hursthouse, M. B.; Malik, K. M. A.; Nielson, A. J.; Short, R. L. *J. Chem. Soc., Dalton Trans.* **1983**, 2651-2656. (b) Nielson, A. J.; McCarley, R. E.; Laughlin, S. L.; Carlson, C. D. In *Inorg. Syn.*; Schreeve, J. M., Ed.; John Wiley & Sons: New York, 1986; Vol. 24, pp 194-200.

(7) (a) Nielson, A. J.; Ware, D. C. *Polyhedron* **1990**, *9*, 603-610. (b) Clark, G. R.; Nielson, A. J.; Rickard, C. E. F.; Ware, D. C. *J. Chem. Soc., Chem. Commun.* **1989**, 343-345. (c) Clark, G. R.; Nielson, A. J.; Rickard, C. E. F. *J. Chem. Soc., Chem. Commun.* **1989**, 1157-1159. (d) Su, F.-M.; Cooper, C.; Geib, S. J.; Rheingold, A. L.; Mayer, J. M. *J. Am. Chem. Soc.* **1986**, *108*, 3545-3547. (e) Su, F.-M.; Bryan, J. C.; Jang, S.; Mayer, J. M. *Polyhedron* **1989**, *8*, 1261-1277.

(8) Clark, G. R.; Nielson, A. J.; Rickard, C. E. F.; Ware, D. C. *J. Chem. Soc., Dalton Trans.* **1990**, 1173-1178.

(9) (a) Bryan, J. C.; Mayer, J. M. *J. Am. Chem. Soc.* **1990**, *112*, 2298-2308. (b) Bryan, J. C.; Mayer, J. M. *J. Am. Chem. Soc.* **1987**, *109*, 2826-2828. (c) Bryan, J. C.; Geib, S. J.; Rheingold, A. L.; Mayer, J. M. *J. Am. Chem. Soc.* **1987**, *109*, 2826-2828. (d) Lichtenham, J. C.; Critchlow, S. C.; Doherty, N. M. *Inorg. Chem.* **1990**, *29*, 439-442.

(10) The synthesis of $WCl_4[N\text{-}2,6\text{-}C_6H_3\text{-}(i\text{-}Pr)_2]$ has been reported in refluxing *n*-octane. The poorer solubility of the product in *n*-octane as compared to *p*-xylene leads to greater ease of isolation, and therefore this method is preferred. See: Schrock, R. R.; DePue, R. T.; Feldman, J.; Yap, K. B.; Yang, D. C.; Park, L.; DiMare, M.; Schofield, M.; Anhaus, J.; Walborsky, E.; Evitt, E.; Kruger, C.; Betz, P. *Organometallics* **1990**, *9*, 2262-2275.

(11) Jernakoff, P.; Geoffroy, G. L.; Rheingold, A. L.; Geib, S. J. *J. Chem. Soc., Chem. Commun.* **1987**, 1610-1611.

(12) Ashcroft, B. R.; Clark, G. R.; Nielson, A. J.; Rickard, C. E. F. *Polyhedron* **1986**, *5*, 2081-2091.

(13) $WCl_2(N\text{-}2,6\text{-}C_6H_3\text{-}Me_2)(PMePh_2)_3$: ^1H (C_6D_6) δ 1.97 (s, 6, NAr: Me_2), 1.93 (br t, 6, mutually trans $P\mathit{Me}Ph_2$'s), 1.54 (d, 3, $J_{HP} = 7.81$ Hz, $PMePh_2$ trans to Cl).

(14) The occupation of a coordination site trans to an imido ligand by strong σ donor ligands such as phosphines is rare, due to the strong trans influence of the imido ligand. For discussions, see: (a) Ref. 7e. (b) Nielson, A. J. *Polyhedron* **1987**, *6*, 1647-1667. (c) Nugent, W. A.; Mayer, J. M. *Metal-Ligand Multiple Bonds*; John Wiley & Sons: New York, 1988; pp 156-157. (d) For a recent exception, see: Ref. 7b.

(15) Tolman, C. A., unpublished results.

(16) (a) Collman, J. P.; Hegedus, L. S.; Norton, J. R.; Finke, R. G. *Principles and Applications of Organotransition Metal Chemistry*; University Science Books: Mill Valley, CA, 1987; pp 66-72. (b) Crabtree, R. H. *The Organometallic Chemistry of the Transition Metals*; John Wiley & Sons: New York, 1988; pp 71-74. (c) Tolman, C. A. *Chem. Rev.* **1977**, *77*, 313-348. (d) Verkade, J. G. *Coord. Chem. Rev.* **1972/73**, *9*, 1-106.

(17) The synthesis of the analogous oxo complex $WCl_2(O)[P(OMe)_3]_3$ has been reported: Carmona, E.; Sanchez, L.; Poveda, M. L.; Jones, R. A.; Hefner, J. G. *Polyhedron* **1983**, *2*, 797-801.

(18) The structure of the analogous trimethylphosphine complex $WCl_2(NPh)(PMe_3)_3$ has been reported. See: Ref 6a.

(19) Detailed studies of π-complex formation have been published for $WCl_2(NPh)(PR_3)_3$ complexes (Ref. 7), and therefore the discussion here is limited to a comparison of the major similarities and differences of the reactivity of the phosphite analogues, with an emphasis on the points relavent to the cyclopropene reactions.

(20) $W(PhC{\equiv}CPh)Cl_2[N\text{-}2,6\text{-}C_6H_3\text{-}(i\text{-}Pr)_2][(P(OMe)_3]_2$ was observed in solution as a mixture of the bis- and mono(phosphite) adducts: $^{13}C(CD_2Cl_2)$ Bis$[P(OMe)_3]$ Adduct: δ 151.2 (t, $J_{CP} = 15.70$ Hz, $Ph\mathit{C}{\equiv}\mathit{C}Ph$); Mono$[P(OMe)_3]$ Adduct: δ 174.9 (d, $J_{CP} = 9.06$ Hz, $Ph\mathit{C}{\equiv}C'Ph$ cis to $P(OMe)_3$), 163.4 (d, $J_{CP} = 31.50$ Hz, $PhC{\equiv}\mathit{C}'Ph$ trans to $P(OMe)_3$); ^{31}P (tol-d_8) δ 140.7 (free $P(OMe)_3$), 123.9 ($J_{PW} = 336.9$ Hz, Mono$[P(OMe)_3]$ Adduct), 113.7 ($J_{PW} = 358.9$ Hz, Bis$[P(OMe)_3]$ Adduct).

(21) Preliminary experiments indicated that when sterically large acetylenes such as *t*-butylacetylene were used, mono(phosphine) adducts of acetylene complexes could also be observed. For example, $W(HC{\equiv}C\text{-}t\text{-}Bu)Cl_2(N\text{-}2,6\text{-}C_6H_3\text{-}Me_2)(PEt_2Ph)_2$ was observed as mainly the mono(PEt_2Ph) adduct in solution: ^1H (CD_2Cl_2) Bis(PEt_2Ph) Adduct δ 9.41 (dd, $J_{HP} = 22.36$ Hz (trans), 6.05 Hz (cis), $\mathit{H}C{\equiv}C\text{-}t\text{-}Bu$); Mono($PEt_2Ph$)

Adduct (d, J_{HP} = 18.05 Hz (trans), J_{HW} = 9.26 Hz, *H*C≡C-*t*-Bu); ^{31}P (CD_2Cl_2) 31.8 (J_{PW} = 190 Hz, Mono(PEt_2Ph) Adduct).

(22) Pedersen, S. F.; Schrock, R. R. *J. Am. Chem. Soc.* **1982**, *104*, 7483-7491.

(23) (a) Templeton, J. L.; Ward, B. C. *J. Am. Chem. Soc.* **1980**, *102*, 3288-3290. (b) Templeton, J. L. *Adv. Organomet. Chem.* **1989**, *29*, 1-100.

(24) 3,3-Diphenylcyclopropene was prepared following the synthesis developed by Dr. Jeff S. Moore, which was subsequently optimized by Sonbinh T. Nguyen (Moore, J. S.; Nguyen, S. T.; Grubbs, R. H., unpublished results). The synthesis is available upon request and was developed based upon the following literature references: (a) Skattebol, L. *Acta Chemica Scandinavica* **1963**, *17*, 1683-1693. (b) Hirao, T.; Masunaga, T.; Ohshiro, Y.; Agawa, T. *J. Org. Chem.* **1981**, *46*, 3745-3747. (c) Binger, P. *Synthesis* **1974**, 190-192.

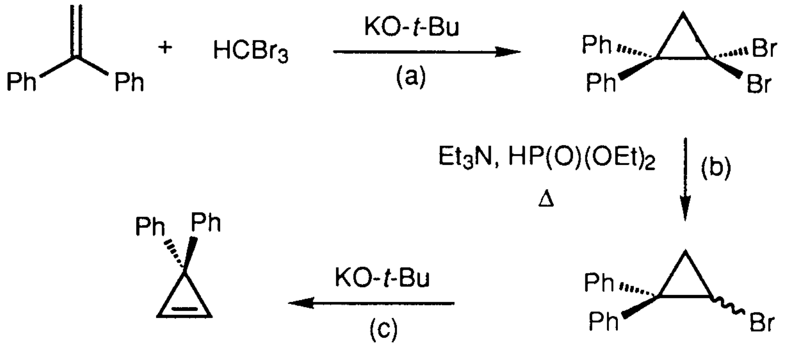

(25) For details of the synthesis and reactivity of 4,8-dioxaspiro[2.5]oct-1-ene (ketalcyclopropene), see: (a) Boger, D. L.; Brotherton, C. E.; Georg, G. I.; Davidsen, S. K.; Heathcock, C. H. *Organic Syntheses*; Vedejs, E., Ed.; Organic Syntheses, Inc.: USA, 1987; pp 32-41. (b) Boger, D. L.; Brotherton, C. E. *J. Am. Chem. Soc.* **1986**, *108*, 6695-6713. (c) Butler, G. B.; Herring, K. H.; Lewis, P. L.; Sharpe, V. V., III; Veazey, R. L. *J. Org. Chem.* **1977**, *42*, 679-682.

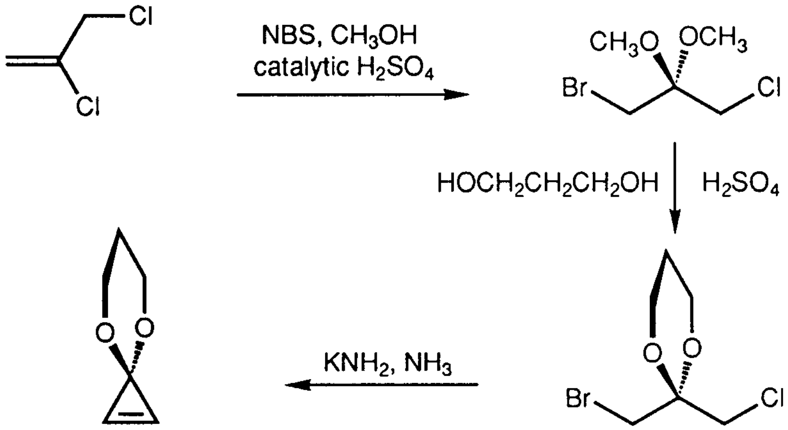

(26) Ketalcyclopropene forms an η^2-olefin complex upon reaction with $Cp_2Ti(PMe_3)_2$. See: Binger, P.; Muller, P.; Herrmann, A. T.; Philipps, P.; Gabor, B.; Langhauser, F.; Kruger, C. *Chem. Ber.* **1991**, *124*, 2165-2170.

(27) The reactivity of 3,3-dimethylcyclopropene with $WCl_2(NAr)[P(OMe)_3]_3$ complexes was briefly investigated. Although η^2-dimethylcyclopropene complexes and dimethylvinyl alkylidene complexes were observed, it was very difficult to drive the formation of these compounds to completion. That is, due to unidentified side reactions, some of the tris(phosphite) precursor always remained unreacted. The results of the reactions of the other two cyclopropenes indicated that the reactivity of 3,3-dimethylcyclopropene with the tris(phosphine) precursors, especially $WCl_2(N\text{-}2,6\text{-}C_6H_3\text{-}Me_2)(PEt_2Ph)_3$, may be more promising, but this was not investigated.

In addition, reactions of 3,3-dimethyl-, 3,3-diphenyl- and ketalcyclopropene with the tungsten(V) precursor $WCl_3[N\text{-}2,6\text{-}C_6H_3\text{-}(i\text{-}Pr)_2](PMe_3)_2$ (synthesis reported in the Experimental Section) were briefly investigated. The tungsten complex and the cyclopropene were dissolved in C_6D_6 and the tungsten complex was then reduced by an excess of 1% sodium amalgam. In all three cases, vinyl alkylidene formation was observed in low to moderate yields.

(28) Wiberg, K. B. In *The Chemistry of the Cyclopropyl Group*; Rappoport, A., Ed.; John Wiley & Sons: New York, 1987; Part 1, Chapter 1.

(29) Schrock, R. R. In *Reactions of Coordinated Ligands*; Braterman, P. S., Ed.; Plenum: New York, 1986; Vol. 1, pp 221-283.

(30) Schrock, R. R.; Crowe, W. E.; Bazan, G. C.; DiMare, M.; O'Regan, M. B.; Schofield, M. H. *Organometallics* **1991**, *10*, 1832-1843.

(31) (a) Collman, J. P.; Hegedus, L. S.; Norton, J. R.; Finke, R. G. *Principles and Applications of Organotransition Metal Chemistry*; University Science Books: Mill Valley, CA, 1987; 119-137. (b) Crabtree, R. H. *The Organometallic Chemistry of the Transition Metals*; John Wiley & Sons: New York, 1988; Chapter 11.

(32) (a) Bishop, K. C., III *Chem. Rev.* **1976**, *76*, 461-486. (b) Shirafuji, T.; Yamamoto, Y.; Nozaki, H. *Tetrahedron Lett.* **1971**, 4713-4714.

(33) (a) Padwa, A. *Org. Photochem.* **1979**, *4*, 261-326. (b) Padwa, A. *Acc. Chem. Res.* **1979**, *12*, 310-317. (c) Padwa, A.; Blacklock, T. J.; Cordova, D. M.; Loza, R. *J. Am. Chem. Soc.* **1980**, *102*, 5684-5656.

(34) Nugent, W. A.; Mayer, J. M. *Metal-Ligand Multiple Bonds*; John Wiley & Sons: New York, 1988; pp 35-36, and references therein.

(35) (a) Ref. 25b. (b) York, E. J.; Dittmar, W.; Stevenson, J. R.; Bergman, R. G. *J. Am. Chem. Soc.* **1973**, *95*, 5680-5687. (c) Davis, J. H.; Goddard, W. A., III; Bergman, R. G. *J. Am. Chem. Soc.* **1977**, *99*, 2427-2434.

(36) (a) Salaun, J. In *The Chemistry of the Cyclopropyl Group*; Rappoport, A., Ed.; John Wiley & Sons: New York, 1987; Part 2, Chapter 13. (b) Sarel, S. *Acc. Chem. Res.* **1978**, *11*, 204-211.

(37) $WOCl_4$ is available commercially or it may be readily synthesized from: (a) WO_3 and $SOCl_2$ (Nielson, A. J. In *Inorg Syn.*; Kirschner, S., Ed.; John Wiley & Sons: New York, 1985; pp 195-199), (b) WCl_6 and $MeOSiMe_3$ (Pedersen, S. F.; Schrock, R. R. *J. Am. Chem. Soc.* **1982**, *104*, 7483-7491), or (c) WCl_6 and $(Me_3Si)_2O$ (Gibson, V. C.; Kee, T. P.; Shaw, A. *Polyhedron* **1988**, *7*, 579-580).

(38) Churchill, M. R.; Lashewycz, R. A.; Rotella, F. J. *Inorg. Chem.* **1977**, *16*, 265-271.

(39) Nowacki, W.; Matsumoto, T.; Edenharter, A. *Acta Crystallogr.* **1967**, *22*, 935-940.

(40) UCLA Crystallographic Computing Package, University of California Los Angeles, 1981, C. Strouse; personal communication.

(41) Siemens Analytical X-Ray Instruments, Inc.; Madison, WI 1988.

(42) *International Tables for X-Ray Crystallography*, Kynoch Press: Birmingham, England, 1974; (a) pp 99-101; (b) pp 149-150.

Chapter 3

Alkylidene Transfer from Phosphoranes to Tungsten(IV) Imido Complexes

Introduction

The chemical reactivity and physical properties of phosphorus ylides, or phosphoranes, are dominated by the zwitterionic resonance structure A. The carbanionic nature of the ylide carbon is manifested in the diverse reactivity of phosphorus ylides with organometallic species.[1] For example, Figure 1 depicts reactions of phosphoranes involving the synthesis and/or transformation of transition-metal carbene/alkylidene complexes and their phosphine adducts. Phosphoranes act as bases in the deprotonation of alkylidene ligands to yield alkylidynes,[2] as nucleophiles in the transformation of carbene ligands to give olefins,[3] and as donor ligands in the reaction with metal centers to form metal-carbon bonds.[4]

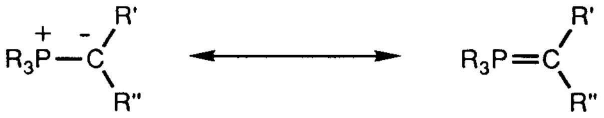

A B

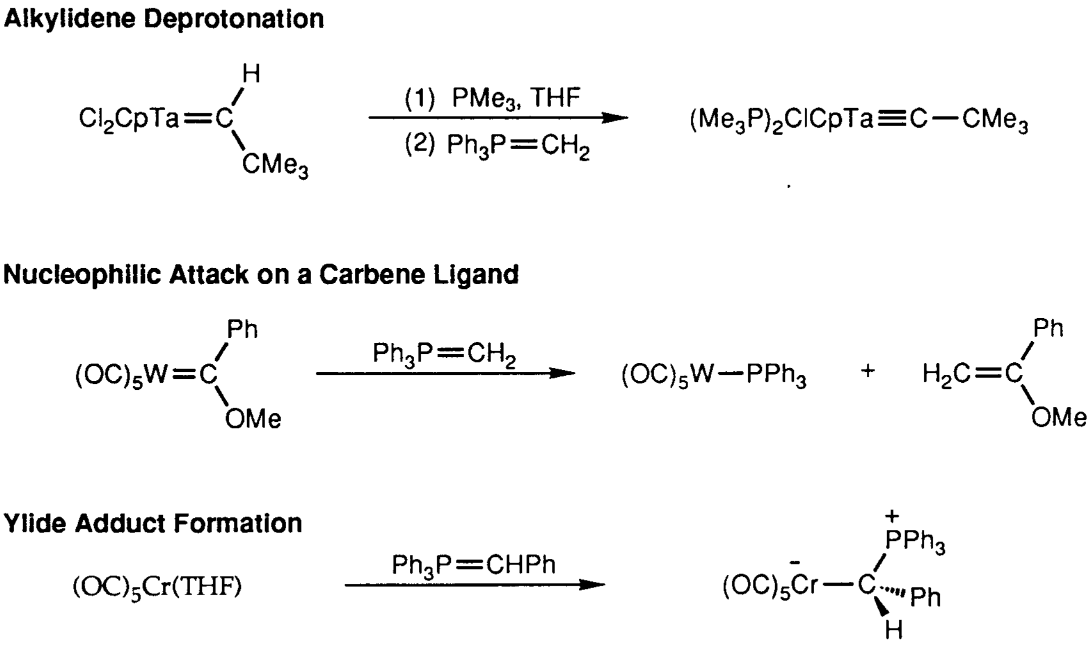

Alkylidene Deprotonation

Nucleophilic Attack on a Carbene Ligand

Ylide Adduct Formation

Figure 1. Examples of reactions of phosphoranes with transition-metal complexes.[2-4]

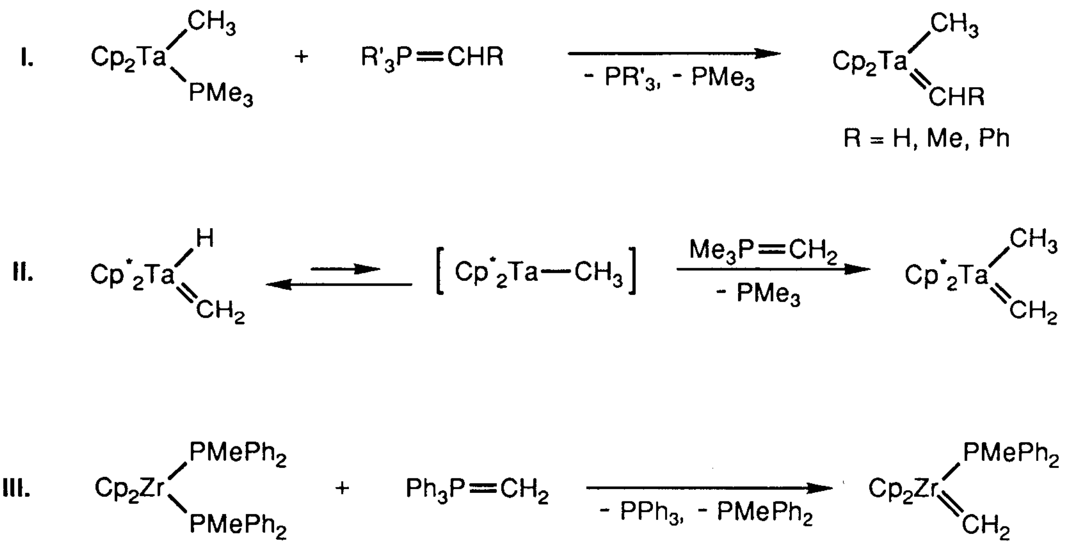

Figure 2. The three known examples of alkylidene transfer from phosphoranes to transition-metal centers.[5-7]

Although a myriad of transition-metal compounds with ylide donor ligands have been synthesized,[1] loss of phosphine to yield an alkylidene complex has rarely been observed. The three known examples are shown in Figure 2 and include the first synthesis of a terminal ethylidene complex.[5-7] In these examples, nucleophilic alkylidene ligands were formed, thus favoring loss of phosphine from the proposed intermediate ylide adducts.[5] The crowded coordination spheres of these intermediates may also have aided phosphine loss, as well as prevented alkylidene deprotonation by excess phosphorane.[5]

The further extension of this reaction would be desirable for the following reasons: (1) A wide variety of phosphorus ylides are easily synthesized and readily isolated, making them attractive precursors to metal alkylidenes. Upon development of suitable transition-metal precursors, phosphorus ylides could potentially enable the synthesis of alkylidene ligands incorporating a number of different substituents (eq 1). Variation of metal alkylidene substituents is important, as it would allow control of the polymer end-group in ring-opening metathesis polymerization (ROMP)[8] and the

$$L_nM \quad + \quad R''_3P{=}CRR' \xrightarrow[-\ PR''_3]{} L_nM{=}CRR' \qquad (1)$$

R, R' = H, alkyl, aryl, etc.

selection of the products obtained from the Wittig-type olefinations of carbonyl compounds, including esters and amides.[9] (2) In addition, the synthesis of di-initiators for ROMP can easily be envisioned via the use of bis(ylide) precursors (eq 2). A

$$2\ L_nM \quad + \quad R_3P{=}C(H){-}X{-}(H)C{=}PR_3 \xrightarrow[-\ 2\ PR_3]{} L_nM{=}C(H){-}X{-}(H)C{=}ML_n \qquad (2)$$

bis(titanacyclobutane) initiator **C** has already been reported, and its efficacy in the synthesis of block copolymers was demonstrated.[10] However, the isolable chain-carrying species of ROMP catalysts of later metals, for example, Groups VI and VII, are alkylidenes,[11] and di-initiators of these catalysts must be synthesized by different routes.

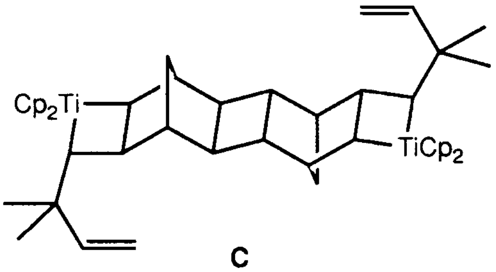

C

The promise of phosphorus ylides as precursors to metal alkylidenes prompted the following research, which involved an investigation of the reactivity of reduced tungsten imido complexes, including $WCl_2(NPh)(PMePh_2)_3$,[12] with phosphorus ylides. Impetus for the selection of this precursor was two-fold: (1) Following the loss of a phosphine ligand, $WCl_2(NPh)(PMePh_2)_3$ readily reacts with a number of π-acceptors (L), including carbon monoxide, isonitriles, aldehydes, olefins, and acetylenes, to give $WCl_2(L)(NPh)$-

$(PMePh_2)_2$,[13] and thus similar substitution reactions with phosphorus ylides to give $W(=CHR)Cl_2(NPh)(PMePh_2)_2$ complexes were likely. (2) Analogs of the expected alkylidene transfer products, for example, $W(=CH\text{-}t\text{-}Bu)Cl_2(NAr)(PR_3)_2$ (R = Me, Et), are known, and the nucleophilic alkylidene ligands of these stable compounds does not bind to phosphines.[14] Therefore, upon addition of the ylide carbon to tungsten, loss of phosphine and generation of a stable alkylidene was probable.

Results and Discussion

Reactions of Phosphoranes with $WCl_2(NAr)(PX_3)_3$ Complexes

Synthesis of $W(=CHR)Cl_2(NPh)(PMePh_2)_2$ Complexes. The reactions of $WCl_2(NPh)(PMePh_2)_3$ with a number of triphenylphosphoranes were surveyed, and clean alkylidene transfer was observed for variously substituted aryl ylides $Ph_3P=CHAr'$, where Ar' = C_6H_5, C_6H_4-*p*-Me, C_6H_4-*m*-Me, C_6H_4-*o*-Me, C_6H_4-*p*-OEt, C_6H_4-*o*-OMe, C_6F_5, *o*-Np, and *m*-Np, and also for the vinyl ylide $Ph_3P=CH\text{-}CH=CMe_2$ (eq 3). Several of these derivatives were synthesized on a preparatory scale, and selected NMR data for these complexes is listed in Table 1. Transfer of the alkylidene moiety from phosphorus to tungsten was clearly indicated by the downfield shifts of the alkylidene H_α and C_α resonances,[15] by the appearance of both of these resonances as triplets due to coupling with the mutually trans phosphine ligands, and also by the coupling of the alkylidene C_α resonance to tungsten.

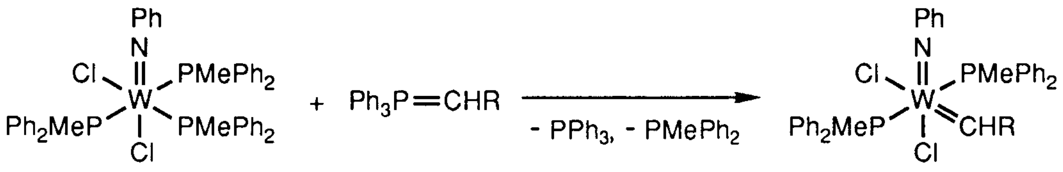

(3)

R = Ar' and CH=CMe$_2$

Table 1. Selected NMR Data for $W(=CHR)Cl_2(NPh)(PMePh_2)_2$ Complexes[a]

Cmpd	R	H_α	J_{HP}	C_α	J_{CH}	J_{CP}	J_{CW}
1	Ph	12.51[b]	4.77	290.9	126.5	12.0	132.8
2	C_6H_4-*p*-Me	12.12	4.64	290.7	126.7	—	—
3	C_6H_4-*p*-CF_3	12.13	4.63	288.3	128.6	12.2	131.6
4	2-Np	12.31	4.72	290.4	125.3	12.1	132.3
5	C_6F_5	11.71	4.12	261.5	133.9	12.0	146
6	$CH=CMe_2$ (syn)	12.22[c]	4.14	284.0	134.4	11.6	129.3
6	$CH=CMe_2$ (anti)	12.45[d]	4.35	274.2	126.3	11.9	—

[a] Spectra were acquired in CD_2Cl_2 unless indicated otherwise. [b] In C_6D_6. [c] δ 8.00 (H_β, $J_{H\alpha\text{-}H\beta}$ = 12.77 Hz). [d] δ 7.9 (H_β, $J_{H\alpha\text{-}H\beta}$ = 13.11 Hz).

X-ray Diffraction Study of $W(=CHC_6H_4$-*p*-$Me)Cl_2(NPh)(PMePh_2)_2$ (2). The structure of the alkylidene transfer products was further confirmed by an X-ray diffraction study of the *p*-methylbenzylidene complex **2**. An ORTEP diagram is shown in Figure 3, and selected bond lengths and angles are given in Table 2.[16] The geometry of the complex is a distorted octahedron in which C_α of the alkylidene moiety and the two phosphorus atoms all lie beneath the equatorial plane, on the side opposite to the imido ligand. The *p*-methylbenzylidene ring is syn to the imido ligand, and a roughly perpendicular arrangement of the two aryl rings minimizes steric interactions between the two groups. Steric interactions between the alkylidene and imido substituents are further minimized by the widening of the W(1) - C(1) - C(2) angle to 138.1(3)° and the bending of the imido ligand away from the alkylidene moiety at an angle of 168.8(2)° [W(1) - N(1) - C(9) angle].

Synthetic and Mechanistic Observations. The alkylidene tranfer reaction proceeded slowly at room temperature in C_6D_6 or tol-d_8, and the reactions could therefore be monitored by ^1H NMR spectroscopy. With the exception of the *o*-naphthyl and pentafluoroaryl alkylidenes, two alkylidene H_α resonances, consistent with the formation of both the syn and anti rotamers of the alkylidene ligand,[17] were initially

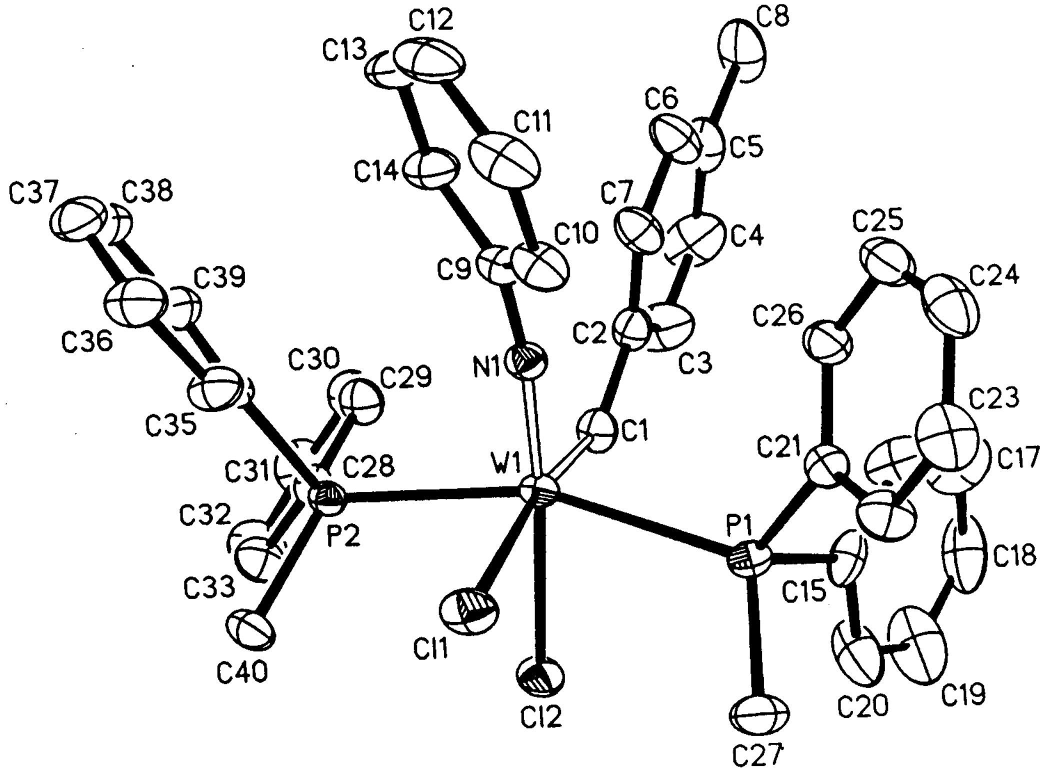

Figure 3. ORTEP plot of W(=CHC_6H_4-*p*-Me)Cl_2(NPh)($PMePh_2$)$_2$ (**2**). Thermal ellipsoids are drawn at the 50% probability level.

Table 2. Selected Bond Lengths and Angles for W(=CHC_6H_4-*p*-Me)Cl_2(NPh)-($PMePh_2$)$_2$ (**2**)

Bond Lengths (Å)

W(1) - Cl(1)	2.556(1)	W(1) - Cl(2)	2.490(1)
W(1) - P(1)	2.546(1)	W(1) - P(2)	2.538(1)
W(1) - N(1)	1.752(3)	W(1) - C(1)	1.975(3)

Bond Angles (°)

Cl(1) - W(1) - Cl(2)	84.7(1)	Cl(1) - W(1) - P(1)	83.4(1)
Cl(2) - W(1) - P(1)	81.4(1)	Cl(1) - W(1) - P(2)	85.8(1)
Cl(2) - W(1) - P(2)	80.7(1)	P(1) - W(1) - P(2)	159.8(1)
Cl(1) - W(1) - N(1)	89.5(1)	Cl(2) - W(1) - N(1)	173.5(1)
P(1) - W(1) - N(1)	100.9(1)	P(2) - W(1) - N(1)	96.1(1)
Cl(1) - W(1) - C(1)	170.8(1)	Cl(2) - W(1) - C(1)	86.9(1)
P(1) - W(1) - C(1)	91.8(1)	P(2) - W(1) - C(1)	96.3(1)
N(1) - W(1) - C(1)	99.1(1)	W(1) - N(1) - C(9)	168.8(2)
W(1) - C(1) - C(2)	138.1(3)		

observed in the ^1H NMR spectra for the aryl and vinyl alkylidenes. With time and heating, gradual conversion to one rotamer was observed. For the aryl alkylidenes, the downfield H_α resonance corresponded to the thermodynamic rotamer, whereas for the vinyl alkylidene complex **6**, the rotamer with the upfield H_α resonance was the thermodynamic product. Based on the X-ray diffraction study of **2**, the thermodynamic product is the syn rotamer.

NMR studies indicated that the transfer of aryl alkylidenes was hindered by the incorporation of *ortho* substituents (e.g., *o*-methyl, *o*-methoxy, and *o*-napthyl) on the benzylidene ring and also by the incorporation of electronegative substituents, as in the case of pentafluorobenzylidene. As the reaction progressed, the rate of alkylidene transfer was slowed by the build-up of free phosphine, and high temperatures (~60 - 80 °C for several h) were required to drive the reactions to completion.

Observation of the alkylidene transfer product depended markedly on the choice of solvent. Transfer was most favorable when the reaction was conducted in benzene and, to a slightly lesser extent, toluene. Formation of the tungsten alkylidene also occurred in THF-d_8, but at a much slower rate. In CD_2Cl_2, alkylidene transfer to tungsten was not observed, although the ylide did react relatively rapidly with the tungsten precursor. Identification of the products of the CD_2Cl_2 reaction was not pursued.

The aryl and vinyl phosphoranes, $Ph_3P{=}CHAr'$ and $Ph_3P{=}CH\text{-}CH{=}CMe_2$, are both partially resonance-stabilized ylides with moderate steric requirements. The larger, more nucleophilic ylides, $Ph_3P{=}CH\text{-}t\text{-}Bu$ and $Ph_3P{=}CHSiMe_3$, did not react with $WCl_2(NPh)(PMePh_2)_3$. Similar to $WCl_2(NPh)(PMePh_2)_3$, the 2,6-dimethylphenylimido complex $WCl_2(N\text{-}2,6\text{-}C_6H_3\text{-}Me_2)(PEt_2Ph)_3$ readily forms π-acceptor complexes upon displacement of a PEt_2Ph ligand at room temperature.[18] However, alkylidene transfer was not observed from $Ph_3P{=}CHAr'$ and $Ph_3P{=}CH\text{-}CH{=}CMe_2$ to this complex. According to ^1H NMR spectroscopy, alkylidene transfer from $Ph_3P{=}CH_2$ and $Ph_3P{=}CHMe$ to $WCl_2(NPh)(PMePh_2)_3$ and $WCl_2(N\text{-}2,6\text{-}C_6H_3\text{-}Me_2)(PEt_2Ph)_3$ occurred in low to moderate yields in THF-d_8; transfer was not as clean in C_6D_6 or tol-d_8.[19] These reactions were not pursued on a preparative scale due to their low yields and complex product mixtures.

All of the above observations are consistent with a mechanism in which loss of phosphine from the metal precursor precedes nucleophilic attack by the ylide carbon on the metal center of the 16-electron pentacoordinate intermediate **D** (Scheme 1). Addition of the ylide is thus slowed by excess phosphine, an increase in the steric bulk of the alkylidene or imido substituents, or a decrease in the nucleophilicity of the ylide carbon. In contrast to the metal precursors involved in previous examples of alkylidene transfer

Scheme 1. Proposed Mechanism for Alkylidene Transfer from $Ph_3P=CHR$ to $WCl_2(NPh)(PMePh_2)_3$

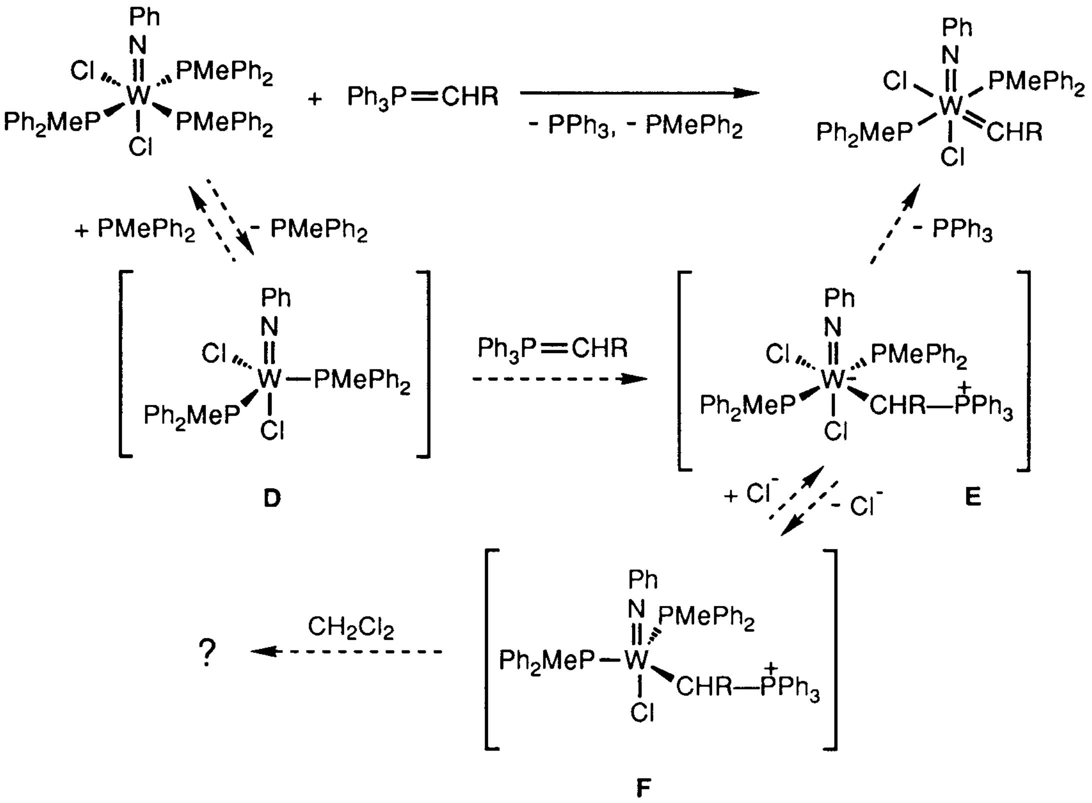

(Figure 2), $WCl_2(NPh)(PMePh_2)_3$ has readily substituted anionic ligands and therefore, two possible reactions, loss of triphenylphosphine or loss of a chloride ligand, would relieve the steric crowding of the zwitterionic ylide adduct **E**. In nonpolar solvents such as C_6D_6 and tol-d_8, loss of phosphine to generate $W(=CHR)Cl_2(NPh)(PMePh_2)_2$ should be favored. However, polar solvents such as THF-d_8 and CD_2Cl_2 should stabilize the zwitterionic intermediate **E**, thus slowing the rate of alkylidene transfer.

Loss of a chloride ligand to generate the pentacoordinate cationic complex **F**, which would be stabilized by strong donation by the phosphine and imido ligands, is highly probable in CD_2Cl_2 and may be the reason that alkylidene transfer was not observed in this solvent. Aside from the addition of the chloride ligand to regenerate the zwitterionic ylide adduct, several other transformations of this cationic complex are conceivable, including reactions with a second equivalent of ylide or trapping by free phosphine. The alkylidene ligand of this cationic complex may be electrophilic and thus form a stable phosphine adduct. In addition, steric crowding would be relieved by loss of a chloride ligand upon formation of **F** and would no longer provide a strong driving force for the loss of PPh_3.

Reactions of $W(=CHR)Cl_2(NPh)(PMePh_2)_2$ with Alkoxides. The alkylidene complexes synthesized in these studies are potential precursors to analogs of the arylimido metathesis catalysts $W(=CH\text{-}t\text{-}Bu)[N\text{-}2,6\text{-}C_6H_3\text{-}(i\text{-}Pr)_2](OR)_2$,[11a,c] and therefore the reactions of these complexes with alkoxides were investigated. Monitoring the reaction of the benzylidene complex $W(=CHPh)Cl_2(NPh)(PMePh_2)_2$ with two equivalents of $LiOCMe(CF_3)_2$ by ^1H NMR spectroscopy indicated that a chloride ligand was rapidly displaced by the first equivalent of alkoxide to yield $W(=CHPh)Cl(NPh)[OCMe(CF_3)_2](PMePh_2)$. Reaction with the second equivalent of alkoxide proceeded more slowly and resulted in the formation of $W(=CHPh)(NPh)[OCMe(CF_3)_2]_2(PMePh_2)$. Methyldiphenylphosphine was coordinated reversibly to this complex, and in donor solvents such as THF-d_8 and dioxane-d_8, the phosphine-free complex was also observed. The reversible coordination of $PMePh_2$ and the small steric bulk of the imido and alkylidene ligands resulted in the fairly rapid decomposition (~1 day) of the bis(alkoxide) complex in solution.[20] Only unidentified decomposition products were observed for the reaction of the same precursor with $LiOCMe_3$. Most likely, the formation of a more electron-rich metal center prevented strong donation by $PMePh_2$ and, hence, observation of the pentacoordinate intermediate. In general, these studies indicated that stronger donor ligands, such as PMe_3, are needed to stabilize the pentacoordinate base adduct and permit its isolation.

The use of larger alkoxides, such as $LiOC_6H_3\text{-}(i\text{-}Pr)_2$ and $LiOCEt_3$, enabled relatively clean formation of the tetracoordinate benzylidene and vinyl alkylidene compounds. For example, when two equivalents of $LiOC_6H_3\text{-}(i\text{-}Pr)_2$ in a small amount of THF-d_8, the dimethylvinyl alkylidene complex **6** in C_6D_6, and an excess of CuCl were mixed, sharp doublets for H_α (9.06 ppm, $J_{H\alpha - H\beta}$ = 16.11 Hz) and H_β (8.12 ppm, $J_{H\alpha - H\beta}$ = 16.12 Hz) were observed. A sharp singlet at 10.3 ppm was observed for the reaction of the benzylidene compound **1** with two equivalents of $LiOCEt_3$ in a mixture of C_6D_6 and dioxane-d_8. These results are very preliminary and first attempts to synthesize the tetracoordinate alkoxide complexes on a preparative scale in THF were unsuccessful. Two modes of decomposition are likely: (1) bimolecular decomposition upon solvent removal or (2) CuCl-catalyzed decomposition. If CuCl was responsible for the decomposition, perhaps a noncoordinating and less polar solvent than THF should be used in order to minimize the solubility of CuCl.

In Situ Trapping of Reduced Tungsten Complexes by Phosphoranes

The above examples of alkylidene transfer to $WCl_2(NPh)(PMePh_2)_3$ and the examples shown in Figure 2 all involved transfer to reduced metal complexes that were stabilized by donor ligands. Prior loss of a donor ligand was required for alkylidene transfer to occur, and therefore transfer was often slow and normally required high temperatures. A more attractive method of alkylidene synthesis would involve the in situ trapping of reduced metal species by phosphoranes, thereby eliminating the synthesis and isolation of reduced intermediates. In order to determine the viability of this method, the following study was undertaken.

$WCl_4(NAr)$ Precursors. Initial investigations involving $WCl_4(NAr)$ precursors were not promising. Benzylidene triphenylphosphorane reacted with these complexes in C_6D_6 to give an intractable precipitate. A green powder was formed when the reaction was carried out in CH_2Cl_2 and the solvent was removed in vacuo. Although the NMR of the product was broad and uninterpretable, initial displacement of a chloride ligand by the ylide is precedented.[21]

$WCl_2(NAr)[OCMe(CF_3)_2]_2(THF)$ Precursors. The increased steric stabiliza-

Table 3. Selected NMR Data for Alkylidene Complexes Prepared by the In Situ Trapping of Reduced Tungsten Species by Phosphoranes

Cmpd	Formula	H_α	C_α	J_{CH}	J_{CW}
11	W(CHPh)(N-2,6-C_6H_3-Me_2)[OCMe(CF_3)$_2$]$_2$(PMe_3)	12.16^a	266.5^a	144	154
12	W(=CHC_6H_4-*o*-OMe)(NPh)[OCMe(CF_3)$_2$]$_2$(THF)	10.46^b	246.4	149	161
13	W(=CHC_6H_4-*o*-OMe)(N-2,6-C_6H_3-Me_2)-[OCMe(CF_3)$_2$]$_2$(THF)	10.81^a	240.2^a	151	160
14	W(=CHC_6H_4-*o*-OMe)[N-2,6-C_6H_3-(*i*-Pr_2)]-[OCMe(CF_3)$_2$]$_2$(THF)	10.60^b	248.1^b	148	167
15	W(=CHC_6H_4-*o*-OMe)(N-2,6-C_6H_3-Me_2)[OCMe(CF_3)$_2$]$_2$(PMe_3)	12.48^c	259.5^c	147	148
16a	W(=CHC_6H_4-*o*-OMe)(N-2,6-C_6H_3-Me_2)[OCMe(CF_3)$_2$]$_2$	10.94^a	228.1^a	155	172
16b	W(=CHC_6H_4-*o*-OMe)[N-2,6-C_6H_3-(*i*-Pr_2)]-[OCMe(CF_3)$_2$]$_2$	10.79^c	229.4^c	155	176

^{a}In C_6D_6. ^{b}In THF-d_8. ^{c}In CD_2Cl_2.

tion of WCl_2(NAr)[OCMe(CF_3)$_2$]$_2$(THF) precursors [Ar = Ph (**7**), 2,6-C_6H_3-Me_2 (**8**), and 2,6-C_6H_3-(*i*-Pr)$_2$ (**9**)], which were synthesized by the addition of two equivalents of LiOCMe(CF_3)$_2$ to WCl_4(NAr), prevented their reaction with aryl ylides in the absence of a reducing agent and enabled the reduction of these complexes in the presence of a number of phosphoranes to be investigated. When the 2,6-dimethylphenylimido precursor **8** was reduced by an excess of 1% sodium amalgam in the presence of phosphoranes, alkylidene transfer (yields of 60 - 85% by ^{1}H NMR spectroscopy) from phosphorus to tungsten was observed for several aryl ylides Ph_3P=CHAr' (eq 5), where Ar' = Ph, C_6H_4-*p*-Me, C_6H_4-*m*-Me, C_6H_4-*o*-Me, and C_6H_4-*p*-OEt [**10(a - e)**], but not where Ar' = C_6F_5, 1-Np, and 2-Np. Alkylidene transfer from Ph_3P=CH-CH=CMe_2 and Ph_3P=CH_2 was also not observed, and Ph_3P=C_6H_4-*p*-CF_3 reacted with **8** prior to reduction.[22]

Yields of the tungsten alkylidene complexes were low for the reactions of Ph_3P=CHPh with the analogous phenyl- and 2,6-di-*i*-propylphenylimido precursors **7** and

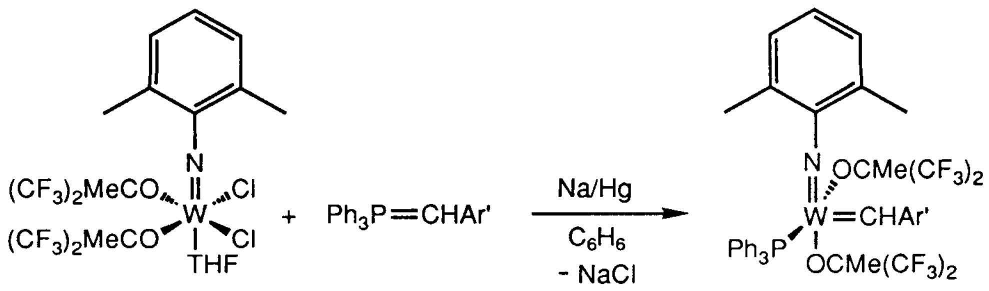

(5)

9. Also, reduction and alkylidene transfer were less favorable when alkoxide ligands other than hexafluoro-*t*-butoxide were used. For example, the bis(*t*-butoxide) complex $WCl_2(N\text{-}2,6\text{-}C_6H_3\text{-}Me_2)(O\text{-}t\text{-}Bu)_2$ was not measurably reduced by sodium amalgam under the standard conditions used for the alkylidene transfer reaction. Tungsten decomposition products and unreacted aryl ylides were observed when either two trifluoro-*t*-butoxide or substituted phenoxide [$O\text{-}2,6\text{-}C_6H_4\text{-}Me_2$ and $O\text{-}2,6\text{-}C_6H_4\text{-}(i\text{-}Pr)_2$] ligands were incorporated on the tungsten precursor. Apparently, the very electron-withdrawing hexafluoro-*t*-butoxide ligands enabled rapid reduction of the tunsten(IV) precursor, and the combined steric bulk of the alkoxide and the 2,6-dimethylphenylimido substituents was sufficient to stabilize the reduced intermediates, but not so great as to prevent alkylidene transfer.

Transfer of the benzylidenes to tungsten was indicated by the large downfield shifts of the H_α resonances (12.26 - 12.65 ppm) for complexes **10(a - e)**[15] and the coupling of these resonances to tungsten-coordinated PPh_3 (J_{HP} = 6.37 - 6.87 Hz). The imido methyl groups and the alkoxide ligands are inequivalent in these complexes, and comparisons with crystal structures of similar complexes suggest that the geometry shown in eq 5 is likely.[17,18] Triphenylphosphine was coordinated reversibly to these alkylidene complexes and could be removed from the metal center by the addition of one equivalent of CuCl, a phosphine sponge.[14] The alkylidene complexes were stable in solution in the presence of PPh_3, but not in its absence, and the isolation of these complexes required the addition of a stronger donor ligand to prevent decomposition

Scheme 2. Reaction Sequence for the Synthesis of *o*-Methoxybenzylidene Complexes

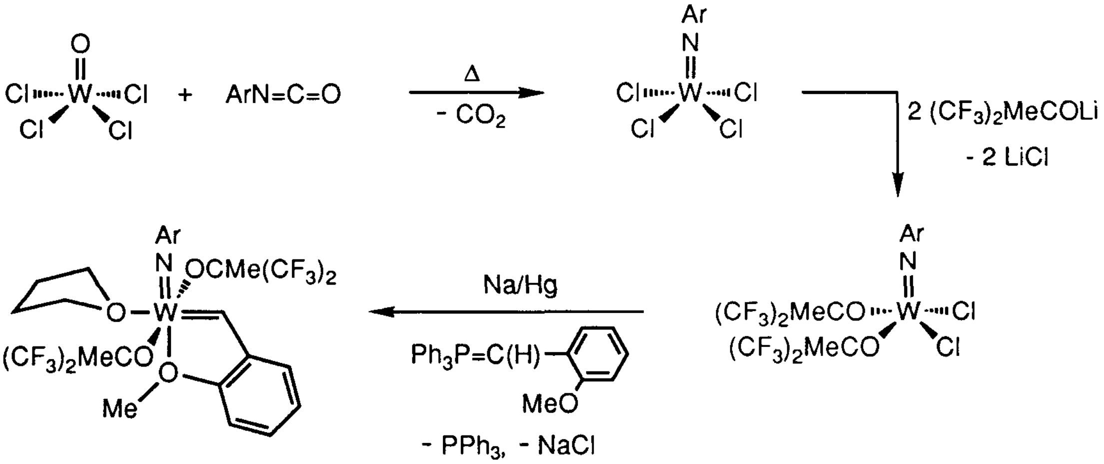

Ar = Ph (**12**), 2,6-C_6H_3-Me_2 (**13**), and 2,6-C_6H_3-(i-Pr)$_2$ (**14**)

upon solvent removal. For example, addition of PMe_3 to the final reaction mixture enabled the isolation of the benzylidene complex W(=CHPh)(N-2,6-C_6H_3-Me_2)[$OCMe(CF_3)_2$]$_2$-(PMe_3) (**11**) as an 18:1 mixture of rotamers.

Chelation by *o*-Methoxybenzylidene[23]

THF-Adducts of *o*-Methoxybenzylidene Complexes. In contrast to the reactivity of the other aryl ylides, alkylidene transfer from $Ph_3P=CHC_6H_4$-*o*-OMe to tungsten was observed in high yields for the phenyl- and 2,6-di-*i*-propylphenylimido precursors **7** and **9**, as well as for the 2,6-dimethylphenylimido precursor **8**, and stable alkylidene complexes that did not bind PPh_3 were isolated. Recrystallization of the complexes from Et_2O or pentane in the presence of THF yielded the yellow, crystalline THF adducts W(=CHC_6H_4-*o*-OMe)(NAr)[$OCMe(CF_3)_2$]$_2$(THF) [NAr = Ph (**12**), 2,6-C_6H_3-Me_2 (**13**), and 2,6-C_6H_3-(i-Pr)$_2$ (**14**)] in good yields. The reaction sequence for the syntheses of these complexes is shown in Scheme 2.

The structure of the 2,6-dimethylphenylimido complex **13** was determined by X-ray diffraction. An ORTEP diagram is included in Figure 4 and selected bond lengths

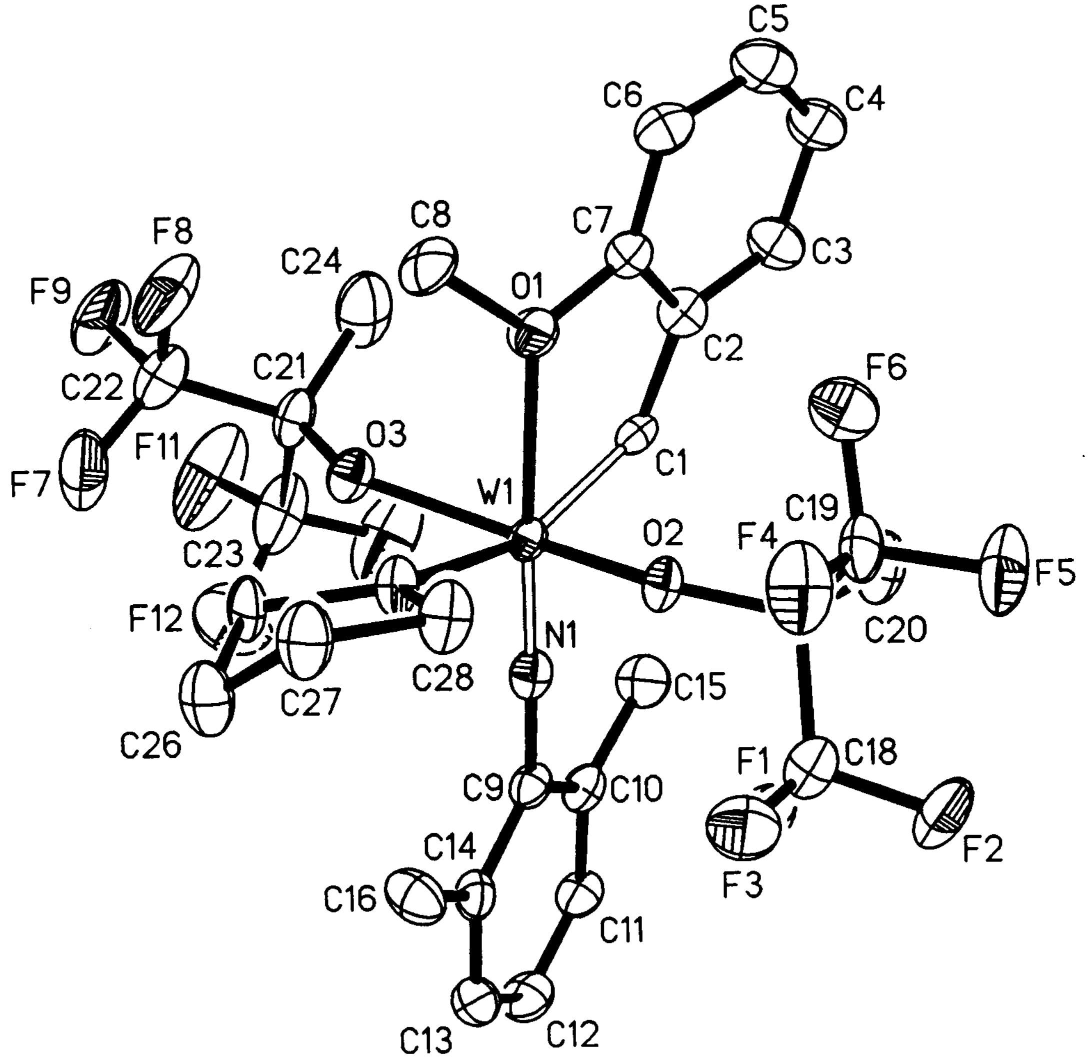

Figure 4. ORTEP plot of $W(=CHC_6H_4\text{-}o\text{-}OMe)(N\text{-}2,6\text{-}C_6H_3\text{-}Me_2)[OCMe(CF_3)_2]_2\text{-}(THF)$ (**13**). Thermal ellipsoids are drawn at the 50% probability level.

Table 4. Selected Bond Lengths and Angles for W(=CHC$_6$H$_4$-*o*-OMe)(N-2,6-C$_6$H$_3$-Me$_2$)[OCMe(CF$_3$)$_2$]$_2$(THF) (**13**)

Bond Lengths (Å)

W(1) - C(1)	1.943(5)	W(1) - N(1)	1.737(4)
W(1) - O(1)	2.346(3)	W(1) - O(2)	1.995(4)
W(1) - O(3)	1.995(3)	W(1) - O(4)	2.294(3)

Bond Angles (°)

C(1) - W(1) - N(1)	99.2(2)	C(1) - W(1) - O(1)	74.2(2)
N(1) - W(1) - O(1)	173.0(2)	C(1) - W(1) - O(2)	97.6(2)
N(1) - W(1) - O(2)	101.2(2)	O(1) - W(1) - O(2)	82.0(1)
C(1) - W(1) - O(3)	103.0(2)	N(1) - W(1) - O(3)	100.2(2)
O(1) - W(1) - O(3)	79.7(1)	O(2) - W(1) - O(3)	147.3(1)
C(1) - W(1) - O(4)	153.7(2)	N(1) - W(1) - O(4)	107.0(2)
O(1) - W(1) - O(4)	79.8(1)	O(2) - W(1) - O(4)	75.2(1)
O(3) - W(1) - O(4)	75.1(1)	W(1) - N(1) - C(9)	174.6(4)
W(1) - O(1) - C(7)	112.1(3)	W(1) - O(1) - C(8)	128.4(3)
W(1) - O(2) - C(17)	138.8(3)	W(1) - O(3) - C(21)	138.4(3)
W(1) - O(4) - C(25)	123.5(3)	W(1) - O(4) - C(28)	126.9(3)
W(1) - C(1) - C(2)	121.9(4)	C(1) - C(2) - C(7)	117.4(5)
C(2) - C(7) - O(1)	112.8(4)		

and angles are given in Table 4. In complex **13**, the geometry about the metal center is a distorted octahedron with the imido and alkylidene ligands lying in the expected cis orientation.[24] The methoxy group of the benzylidene ligand is coordinated to tungsten and occupies an axial site of the octahedron; the 2.346(3) Å W(1) - O(1) bond distance is comparable to the 2.294(3) Å W(1) - O(4) (THF) bond distance.[25] As a result of chelation by the methoxy group, the W(1) - C(1) - C(2) bond angle is approximately 16° and 23° smaller, respectively, than the analogous angles in W(=CHC$_6$H$_4$-*p*-Me)Cl$_2$(NPh)(PMePh$_2$)$_2$ (**2**) and W(=CHPh)(NAr)[OCMe(CF$_3$)$_2$]$_2$.[11a] The angle size is reflected in the respective C_α - H_α coupling constants of these three complexes: $J_{CH\alpha}$ = 151 Hz for **13**, 127 Hz for **2**, and 121 Hz for $W(=CHPh)(NAr)[OCMe(CF_3)_2]_2$.[11a]

Difference NOE and low-temperature spectra were consistent with the solid-state structure of **13**. Strong NOE enhancements, indicative of an anti orientation of the alkylidene substituents relative to the imido ligand, were observed between the methyl groups of the imido ligand and the alkylidene H_α resonance, and irradiation of the THF ether protons enhanced the *o*-methoxy resonance and the imido methyl resonance and vice versa. NOE enhancements were not observed in either direction between the methoxy group and the alkylidene α-proton, consistent with irreversible coordination by the *o*-methoxy group to tungsten. At room temperature, the arylimido ligand of **13** rotated freely, however, at -70 °C, two imido methyl groups were observed in the ^1H NMR spectrum, requiring that the aryl ring not lie in the RO-W(N)-OR plane.

THF Lability. The reversible coordination of THF to complexes **12** - **14** was demonstrated by the rapid exchange of *deuterio*-THF with coordinated *protio*-THF, the production of yellow $W(=CHC_6H_4\text{-}o\text{-}OMe)(N\text{-}2,6\text{-}C_6H_3\text{-}Me_2)[OCMe(CF_3)_2]_2(PMe_3)$ (**15**) upon treatment of **13** with PMe_3, and the formation of red, pentacoordinate, THF-free $W(=CHC_6H_4\text{-}o\text{-}OMe)(N\text{-}2,6\text{-}C_6H_3\text{-}Me_2)[OCMe(CF_3)_2]_2$ (**16a**) and $W(=CHC_6H_4\text{-}o\text{-}OMe)[N\text{-}2,6\text{-}C_6H_3\text{-}(i\text{-}Pr)_2][OCMe(CF_3)_2]_2$ (**16b**) upon heating toluene solutions of **13** and **14** under vacuum. An increase in solubility was noted upon loss of THF, and the downfield chemical shifts of the α-protons of the *o*-methoxybenzylidene ligands of **16a** and **16b** can be compared with the downfield shifts reported for alkylidene complexes coordinated by Lewis bases,[26] which suggests that in solution the methoxy groups of **16a** and **16b** coordinate to the tungsten metal centers. The continuum of the alkylidene C_α chemical shifts of **14** in THF-d_8 (248.1 ppm, sharp singlet, J_{CW} = 167 Hz) and CD_2Cl_2 (239.6 ppm, broad multiplet) and of **16b** in CD_2Cl_2 (229.4 ppm, sharp singlet, J_{CW} = 176 Hz) further demonstrates the reversible coordination of THF to **14**, and the increase in the

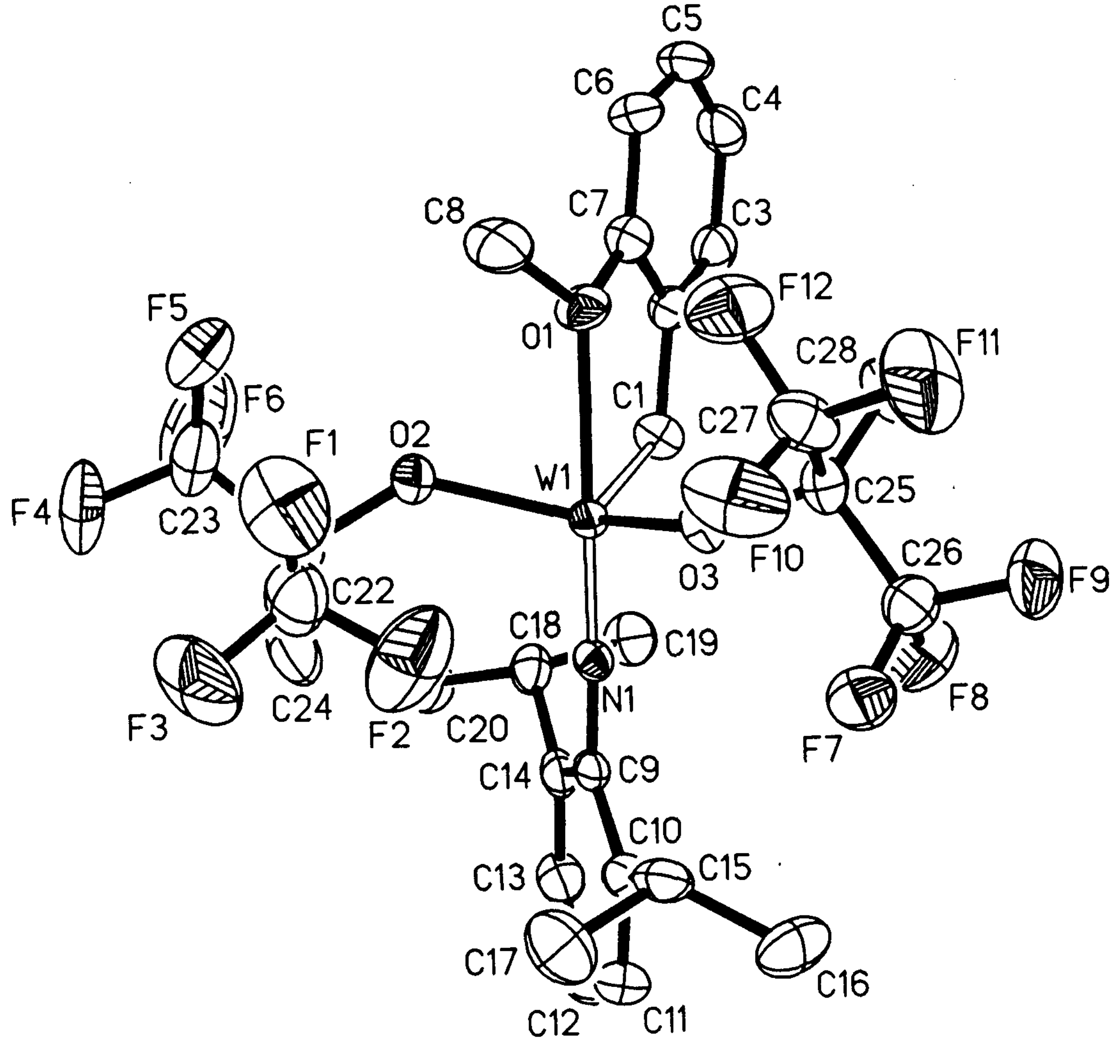

Figure 5. ORTEP plot of W(=CHC_6H_4-*o*-OMe)[N-2,6-C_6H_3-(*i*-Pr)$_2$][OCMe(CF_3)$_2$]$_2$ (**16b**). Thermal ellipsoids are drawn at the 50% probability level.

Table 5. Selected Bond Lengths and Angles for $W(=CHC_6H_4\text{-}o\text{-}OMe)[N\text{-}2,6\text{-}C_6H_3\text{-}(i\text{-}Pr)_2][OCMe(CF_3)_2]_2$ (**16b**)

Bond Lengths (Å)

W(1) - O(1)	2.352(3)	W(1) - O(2)	1.952(3)
W(1) - O(3)	1.923(3)	W(1) - N(1)	1.741(4)
W(1) - C(1)	1.939(5)		

Bond Angles (°)

O(1) - W(1) - O(2)	74.2(1)	O(1) - W(1) - O(3)	82.4(1)
O(2) - W(1) - O(3)	121.1(1)	O(1) - W(1) - N(1)	170.2(1)
O(2) - W(1) - N(1)	106.4(2)	O(3) - W(1) - N(1)	105.1(2)
O(1) - W(1) - C(1)	74.1(2)	O(2) - W(1) - C(1)	111.7(2)
O(3) - W(1) - C(1)	112.4(2)	N(1) - W(1) - C(1)	96.9(2)
W(1) - O(1) - C(7)	112.9(3)	W(1) - O(1) - C(8)	125.5(3)
W(1) - O(2) - C(21)	134.3(3)	W(1) - O(3) - C(25)	143.6(3)
W(1) - N(1) - C(9)	177.4(3)	W(1) - C(1) - C(2)	122.0(3)
C(1) - C(2) - C(7)	117.8(4)		

C_α - W coupling constant is indicative of a shortening of the C_α - W bond upon loss of THF.

The synthesis of the THF-free complexes **16(a - b)** was confirmed by an X-ray diffraction study of **16b**. Selected bond lengths and angles are given in Table 5 and an ORTEP diagram is shown in Figure 5. The complex is best described as a distorted trigonal bipyramid with the imido and *o*-methoxy groups occupying the axial positions. All of the equatorial ligands again lie on the opposite side of the plane from the arylimido ligand, thus relieving unfavorable steric interactions with the *i*-propyl groups, and a comparison with the structure of **13** indicates that the major adjustment upon loss of THF is a widening of the angles between the alkoxide and alkylidene ligands. A slight decrease in the W - C_α bond length is observed upon loss of THF, consistent with the trends noted previously for the W - C_α coupling constants.

Reactivity Studies. The potential of the *o*-methoxybenzylidene complexes to serve as metathesis catalysts was determined by studying the reactions of the 2,6-dimethylphenylimido THF-adduct **13** and its THF-free derivative **16a**. For [W] = 0.012 M and [norbornene] = 0.63 M, the THF-adduct **13** polymerized norbornene at a rate of 18 equiv/h at -40 °C [PDI = 1.5 (polydispersity index: M_w/M_n)], and THF-free **16a** polymerized norbornene at a rate of 17 equiv/h at -60 °C (PDI = 1.6). The latter rate is the same as that of the analogous neopentylidene complex,[11b] however, **16a** metathesized *cis*-2-pentene at a much slower rate (lower limit = 1.4 equiv/min) than the neopentylidene derivative.[11a] The molecular weights were obtained by GPC analysis vs. polystyrene standards, and the relatively broad polydispersities are typical of polymerizations initiated by hexafluoro-*t*-butoxide arylimido alkylidene catalysts.[11b] Analysis by ^{13}C NMR spectroscopy indicated that *cis*- polynorbornene was formed by the ROMP of norbornene initiated by both **13** and **16**,[27] again typical of hexafluoro-*t*-butoxide catalysts.[11b] Finally, complex **13** reacted in a Wittig-type fashion with carbonyl compounds, including esters and amides, in yields of 82 - 100% as measured by NMR spectroscopy.[9,28]

For practical applications, it is important to note that the reaction sequence shown in Scheme 2 requires the use of the hexafluoro-*t*-butoxide ligand. Arylimido metathesis catalysts incorporating this ligand are very active, but are not living,[11b] and therefore these catalysts are best utilized in the polymerization of relatively unstrained monomers, such as cyclooctatetraene.[29,30] For the living polymerization of strained monomers and corresponding control over molecular weights and polydispersities, the *t*-butoxide derivatives are needed.[11b] Clean substitution of the hexafluoro-*t*-butoxide ligands by two equivalents of the more donating *t*-butoxide moiety was observed. However, the addition of PMe_2Ph was necessary in order to separate the complex from free hexafluoro-*t*-

butoxide, and therefore, the living *t*-butoxide catalysts are best prepared by other methods.[11c]

Conclusions

In this investigation, several examples of successful alkylidene transfer from phosphorus to reduced arylimido tungsten complexes were observed, demonstrating that this is a viable method for synthesizing high-valent tungsten alkylidenes, as well as providing the first extension of this reaction to Group VI metals. Insights gained from this study include the following:

(a) Transfer of partially resonance-stabilized alkylidenes (e.g., $Ph_3P{=}CHPh$ and $Ph_3P{=}CH\text{-}CH{=}CMe_2$) is especially favorable, most likely for several reasons: (1) Stable alkylidene complexes are formed, as the substituents on the alkylidene ligand also stabilize the M^+—C^- resonance structure of the resulting nucleophilic tungsten alkylidene. (2) The steric requirements of these alkylidenes are moderate, enabling the ylide carbon to approach the metal center. (3) The nucleophilicity of the ylide carbon is sufficient to enable transfer to the metal, but not so great as to result in further side reactions, such as deprotonation of the metal alkylidene. For very sterically congested precursors, methylidene transfer from smaller and more nucleophilic $Ph_3P{=}CH_2$ is more likely, and in general, the results of this research suggest that survey reactions with three triphenylphosphoranes, $Ph_3P{=}CH_2$, $Ph_3P{=}CHPh$, and $Ph_3P{=}CHC_6H_4$-*o*-OMe, provide a good indication of whether alkylidene transfer to a given metal precursor is possible.

(b) Alkylidene transfer to complexes containing labile anionic ligands is possible with the proper choice of solvent and/or the incorporation of sufficient steric bulk around the metal center. For example, for the $WCl_2(NPh)(PMePh_2)_3$ precursors, alkylidene transfer was observed in nonpolar solvents, such as benzene and toluene, that disfavor formation of ionic intermediates, such as those resulting from displacement of a chloride ligand by the ylide. For the in situ reduction and trapping of reduced tungsten complexes by phosphoranes, the incorporation of bulky alkoxides on the metal precursor prevented displacement of its chloride ligands by the phosphorane prior to reduction.

(c) Transfer of the alkylidene is extremely sensitive to the steric congestion around the metal center, and therefore precursors with potentially variable structures are useful. In the present study, the steric bulk of the imido, alkoxide/chloride, and phosphine/phosphite ligands could all be varied, and it was this flexibility that enabled the alkylidene transfer reaction to be observed under several circumstances.

(d) Although the in situ reduction and trapping of the tungsten complex by the phosphorane provides a very efficient method for the synthesis of alkylidenes, the appropriate tuning of the steric and electronic properties of the metal precursor and the phosphorane is critical, since if the reduced metal species is not trapped immediately by the phosphorane, there are no stabilizing donor ligands to prevent it from undergoing detrimental side reactions. Therefore, the use of the chelating *o*-methoxybenzylidene was especially effective in this case, as coordination by the *o*-methoxy group greatly aided the transfer reaction and, in addition, stabilized the resulting product.

(e) One of the motivations of this study was the potential ability to synthesize a variety of metal alkylidene structures by alkylidene transfer from phosphorus. This goal was achieved by the successful synthesis of a number of new high-valent tungsten aryl and vinyl alkylidenes. Although there are some restrictions to the transfer reaction, these complexes may potentially be valuable catalysts for end-group control in ROMP or for

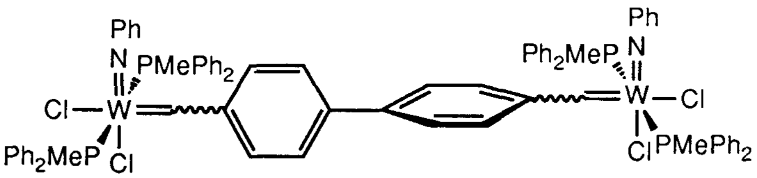

G

carbonyl olefinations in organic synthesis. Furthermore, the utility of the alkylidene transfer reaction in synthesizing a bis(initiator) **G** was recently demonstrated by Frey and Grubbs.[31]

Experimental Section

General Considerations

All manipulations of air- and/or water-sensitive compounds were performed using standard high-vacuum or Schlenk techniques. Argon was purified by passage through columns of BASF R3-11 catalyst (Chemalog) and 4 Å molecular sieves (Linde). Solid organometallic compounds were transferred and stored in a nitrogen-filled Vacuum Atmospheres drybox. NMR spectra were recorded with either a JEOL FX-90Q (89.60 MHz ^{1}H; 22.53 MHz ^{13}C; 36.20 MHz ^{31}P), a JEOL GX-400 (399.65 MHz ^{1}H; 100.40 MHz ^{13}C), or a QE-300 Plus (300.10 MHz ^{1}H; 75.49 MHz ^{13}C) spectrometer. All coupling constants are reported in Hz. Gel permeation chromatography was performed on a Waters GPC-120C, and molecular weights are reported relative to narrow molecular weight polystyrene standards.

Materials

Toluene, benzene, diethyl ether and tetrahydrofuran were distilled or vacuum-transferred from sodium-benzophenone ketyl. *p*-Xylene was dried over CaH_2 and distilled under argon. Pentane was stirred over concentrated H_2SO_4, dried over $MgSO_4$ and CaH_2, and then transferred onto sodium-benzophenone ketyl solubilized with tetraglyme. Benzene-d_6, toluene-d_8, and THF-d_8 were dried over sodium-benzophenone ketyl. Chloroform-*d* and methylene chloride-d_2 were dried over P_2O_5, vacuum-transferred, and then degassed by repeated freeze-pump-thaw cycles. Isocyanates were purified by fractional distillation under argon. $WCl_4(NAr)$ complexes and $(CF_3)_2CH_3COLi$ were synthesized as described in Chapter 2. Organic halides, which were used as precursors to the ylides, were purchased commercially with the exception of Me_3CCH_2I.[32] Phosphonium salts were generally synthesized by refluxing a 1:1 mixure of triphenylphosphine and the organic halide overnight in THF and then filtering. However, $Me_3CCH_2PPh_3I$ and $Me_3SiCH_2PPh_3I$ were synthesized by refluxing triphenylphosphine in a small excess of the corresponding halide.[33]

Table 6. Comparison of the Rates of Alkylidene Transfer from *ortho-*, *meta-*, and *para*-Substituted Aryl Ylides $Ph_3P{=}CHAr'$ to $WCl_2(NPh)(PMePh_2)_3$[a]

Time/Temp	Yield of $W({=}CHAr')Cl_2(NPh)(PMePh_2)_2$; Ar' =			
	C_6H_4-*p*-Me	C_6H_4-*m*-Me	C_6H_4-*o*-Me	C_6H_4-*o*-OMe
0.33 h/r.t.	6%	4%	0%	0%
3.33 h/r.t.	15%	10%	0%	0%
6.33 h/r.t.	19%	20%	0%	0%
24.33 h/r.t.	35%[b]	34%[c]	0%	0%
+ 8 h/ 70 °C	41%[d]	42%[e]	25%[f]	19%[g]

[a] General Procedure: Dissolved $WCl_2(NPh)(PMePh_2)_3$ (10 mg, 0.011 mmol, 0.018 M) in 600 µL of tol-d_8 (0.014 M in mesitylene internal standard) together with 1 equiv of the respective triphenylphosphorane. The solution was transferred to an NMR tube, the NMR tube was capped with a septum, and the septum was wrapped with Parafilm. The tube was rotated at room temperature for a total of 24.33 h; ^1H NMR spectra were acquired periodically. (All four reactions were run simultaneously, and the tubes were rotated together at the same rate.) Subsequently, the tube was heated in an oil bath at 70 °C without any external mixing for 8 h, and a ^1H NMR spectrum was then acquired and integrated. [b] δ 12.38 (t, J = 4.95, H_α, 21%); δ 12.42 (t, J = 4.58, H_α, 15%). [c] δ 12.39 (t, J = 4.55, H_α, 21%); δ 12.46 (t, J = 4.64, H_α, 13%). [d] 12.42 H_α resonance only. [e] 12.46 H_α resonance only. [f] δ 12.71 (t, J = 4.79, H_α, 25%). [g] δ 12.63 (t, J = 2.72, H_α, 10%); δ 13.14 (t, J = 5.25, H_α, 9%).

$CpFeC_5H_4CH_2PPh_3I$ was the gift of Dr. Seth R. Marder.[34] Ylides were synthesized by deprotonation of the phosphonium salt with an excess of NaH in refluxing THF until evolution of H_2 ceased. After filtering the solution, the ylide was recrystallized from THF or Et_2O at low temperature. Gifts of $Ph_3P{=}CH_2$ were received from Dr. David R. Wheeler and Dr. Scott C. Virgil.

$W({=}CHPh)Cl_2(NPh)(PMePh_2)_2$ (1)

An orange solution of $Ph_3P{=}CHPh$ (0.765 g, 2.17 mmol) in 60 mL of benzene was transferred via cannula into a Schlenk flask containing 2.05 g (2.17 mmol) of $WCl_2(NPh)(PMePh_2)_3$ dissolved in 40 mL of benzene. After refluxing for 21.5 h, the solvent was removed in vacuo, and the remaining brown oil was washed twice with 40 mL portions of pentane to yield a golden yellow powder. The powder was dissolved in 20 mL of toluene, and the resulting solution was filtered, layered with pentane, and

Table 7. Survey of the Reactivity of Phosphoranes with $WCl_2(NPh)(PMePh_2)_3$[a]

Triphenylphosphorane	Solvent/time color	Yield/^{1}H NMR Data for H_α of [W](=CHR)
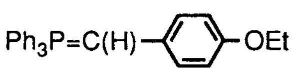	tol-d_8, 7 h yellow	69% δ 12.34 (t, J_{HP} = 4.6) 15% δ 12.26 (t, J_{HP} = 4.6) 16% $WCl_2(NPh)(PMePh_2)_3$ unreacted.
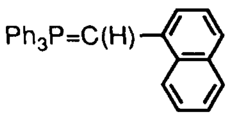	tol-d_8, 10 h orange	71% δ 13.46 (t, J_{HP} = 4.6) 25% $WCl_2(NPh)(PMePh_2)_3$ unreacted.
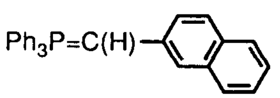	tol-d_8, 7 h yellow	~73% δ 12.59 (t, J_{HP} = 4.6) ~23% δ 12.47 (t, J_{HP} = 4.9) 4% $WCl_2(NPh)(PMePh_2)_3$ unreacted.
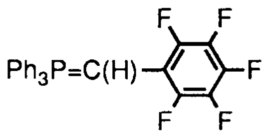	tol-d_8, 7 h yellow	70% δ 11.96 (br m) 33% $WCl_2(NPh)(PMePh_2)_3$ unreacted.
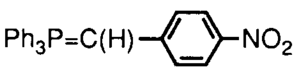	THF-d_8, min's	Not acquired—precipitate formed.
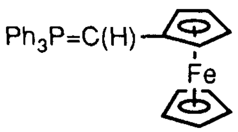	tol-d_8, 7 h magenta	12% δ 12.36 (t, J_{HP} = 4.15) Starting materials remained unreacted.
$Ph_3P{=}CH\text{-}t\text{-}Bu$	THF-d_8, 10 h yellow	No alkylidene observed—starting materials remained unreacted.
$Ph_3P{=}CHSiMe_3$	THF-d_8, 10 h yellow	No alkylidene observed—starting materials remained unreacted.
$Ph_3P{=}CH_2$	THF-d_8, 1 h yellow	20% δ 10.70 (m, C*H*H') δ 10.30 (m, CH*H'*) 23% $WCl_2(NPh)(PMePh_2)_3$ unreacted.
$Ph_3P{=}CHMe$	THF-d_8, 1 h red	1% δ 12.47 (m) 1% δ 12.15 (m) 7% δ 10.77 (m) 39% $WCl_2(NPh)(PMePh_2)_3$ unreacted.

[a] General Procedure: Dissolved $WCl_2(NPh)(PMePh_2)_3$ (10 mg, 0.011 mmol, 0.018 M) in 600 μL of solvent [either tol-d_8 (0.014 M in mesitylene internal standard) or THF-d_8 (0.0034 M in mesitylene internal standard)] together with 1 equiv of the respective triphenylphosphorane. The solution was transferred to an NMR tube, the NMR tube was capped with a septum, and the septum was wrapped with Parafilm. The tube was heated in an oil bath at 60 - 65 °C without any external mixing for several h, and a ^{1}H NMR spectrum was then acquired and integrated.

cooled to -50 °C. Yellow-brown crystals (1.1 g, 61%) were isolated: ^{1}H NMR (C_6D_6) δ 12.52 (t, 1, J_{HP} = 4.77, H_α), 7.8-6.5 (m, 30, H_{aryl}), 2.47 (t, 6, J_{HP} = 4.57, P*Me*Ph$_2$); ^{13}C NMR (CD_2Cl_2) δ 290.9 (t, J_{CH} = 126.5, J_{CP} = 12.0, J_{CW} = 132.8, C_α), 152.8 (t, J_{CP} = 1.9, J_{CW} = 37.6, NPh: C_{ipso}), 146.7 (t, J_{CP} = 3.0, CH*Ph*: C_{ipso}), 133.8 (t, J_{CP} = 23.4, PMe*Ph*Ph': C_{ipso}), 132.9 (t, J_{CP} = 5.1, PMe*Ph*Ph': C_o), 132.7 (t, J_{CP} = 21.2, PMePh*Ph'*: C_{ipso}), 132.5 (t, J_{CP} = 5.2, PMePh*Ph'*: C_o), 130.8 (CH*Ph*: C_o), 130.3 (PMe*Ph*Ph': C_p), 129.9 (PMePh*Ph'*: C_p), 129.6 (CH*Ph*: C_p), 128.04 (t, J_{CP} = 5.04, PMe*Ph*Ph': C_m), 127.97 (t, J_{CP} = 4.92, PMePh*Ph'*: C_m), 127.8 (CH*Ph*: C_m), 127.5 and 127.4 (NPh: C_o and C_m), 126.9 (NPh: C_p), 13.9 (t, J_{CP} = 16.4, P*Me*Ph$_2$); ^{31}P NMR (CD_2Cl_2) δ 11.9 (J_{PW} = 283.2). Anal. Calcd for ($C_{39}H_{37}Cl_2NP_2W$): C, 56.00; H, 4.46; N, 1.67. Found: C, 55.47; H, 4.32; N, 1.60.

W(=CHC$_6$H$_4$-*p*-Me)Cl$_2$(NPh)(PMePh$_2$)$_2$ (2)

In the drybox, WCl$_2$(NPh)(PMePh$_2$)$_3$ (1.98 g, 2.09 mmol) and Ph$_3$P=CHC$_6$H$_4$-*p*-Me (0.77 g, 2.09 mmol) were placed in a 250 mL round-bottom Schlenk flask that was equipped with a Teflon stir bar and a reflux condenser. The sealed apparatus was removed from the drybox and attached to a Schlenk line. Benzene (100 mL) was added via cannula to yield a deep red-brown solution. All solids were dissolved. With stirring, the reaction was heated in an oil bath at 80 °C for approximately 6 h to give a yellow-brown solution. The solvent was removed in vacuo, and the resulting orange-brown oil was left under dynamic vacuum for approximately 12 h. Upon addition of pentane, the oil solidified and formed a mustard-gold powder. The powder was washed twice (2 x 30 mL) with pentane, and the pale yellow pentane wash solution was discarded. The powder was dissolved in toluene (35 mL) and placed in a freezer to crystallize. Brown-orange crystals (1.04 g, 58.4%) were isolated: ^{1}H NMR (CD_2Cl_2) δ 12.21 (t, 1, J_{HP} = 4.64, H_α), 7.6-6.7 (m, 29, H_{aryl}), 2.53 (s, 3, CH*Ar'*: *p*-Me), 2.43 (t, 6, J_{HP} = 4.40, P*Me*Ph$_2$); ^{13}C NMR (CD_2Cl_2) δ 290.7 (m, J_{CH} = 126.7, C_α), 153.2 (t, J_{CP} = 2.3, NPh: C_{ipso}), 144.3 (t,

J_{CP} = 3.3, CH*Ar'*: C_{ipso}), 140.2 (CH*Ar'*: C_p), 134.1 (t, J_{CP} = 23.5, PMe*Ph*Ph': C_{ipso}), 133.1 (t, J_{CP} = 21.1, PMePh*Ph'*: C_{ipso}), 133.1 (t, J_{CP} = 5.1, PMe*Ph*Ph': C_o), 132.7 (t, J_{CP} = 5.1, PMePh*Ph'*: C_o), 130.4 (PMe*Ph*Ph': C_p), 130.0 (PMePh*Ph'*: C_p), 128.2 (t, J_{CP} = 5.1, PMe*PhPh'*: C_m), 131.2, 128.1, 128.0 and 127.7 (NPh: C_o, C_m and CH*Ar'*: C_o, C_m), 126.9 (NPh: C_p), 14.1 (t, J_{CP} =16.5, P*Me*Ph_2); ^{31}P NMR (CD_2Cl_2) δ 12.5 (J_{PW} = 283). Anal. Calcd for ($C_{40}H_{39}Cl_2NP_2W$): C, 56.49; H, 4.62; N, 1.65. Found: C, 56.79; H, 4.40; N, 1.32.

$W(=CHC_6H_4$-*p*-$CF_3)Cl_2(NPh)(PMePh_2)_2$ (3)

In the drybox, $WCl_2(NPh)(PMePh_2)_3$ (2.02 g, 2.13 mmol) and $Ph_3P=CHC_6H_4$-*p*-CF_3 (0.90 g, 2.13 mmol) were placed in a 250 mL round-bottom Schlenk flask that was equipped with a Teflon stir bar and a reflux condenser. The sealed apparatus was removed from the drybox and attached to a Schlenk line. Benzene (100 mL) was added via cannula to yield a deep red-brown solution. All solids were dissolved. With stirring, the reaction was heated in an oil bath at 80 °C for 6.5 h to give an orange-brown solution. The solvent was removed in vacuo, and the resulting orange-brown oil was left under dynamic vacuum for approximately 12 h. Upon addition of pentane, the brown oil partially solidified. The solid was washed twice (2 x 25 mL) with pentane. The powder was dissolved in toluene (30 mL) at 40 °C. The toluene solution was layered with pentane and cooled to -50 °C. Gold crystals (805 mg, 42%) were isolated: ^1H NMR (CD_2Cl_2) δ 12.13 (t, 1, J_{HP} = 4.63, H_α), 7.6-6.7 (m, 29, H_{aryl}), 2.43 (t, 6, J_{HP} = 4.46, P*Me*Ph_2); ^{13}C NMR (CD_2Cl_2) 288.3 (t, J_{CH} = 128.6, J_{CP} = 12.2, J_{CW} = 131.6, C_α), 152.4 (t, J_{CP} = 1.8, J_{CW} = 37.5, NPh: C_{ipso}), 149.8 (CH*Ar'*: C_{ipso}), 133.5 (t, J_{CP} = 21.8, PMe*Ph*Ph': C_{ipso}), 132.7 (t, J_{CP} = 5.1, PMe*Ph*Ph': C_o), 132.4 (t, J_{CP} = 5.1, PMePh*Ph'*: C_o), 132.2 (t, J_{CP} = 21.7, PMePh*Ph'*: C_{ipso}), 130.4 (PMe*Ph*Ph': C_p) 130.3 (PMePh*Ph'*: C_p), 129.9 (q, J_{CF} = 32.1, CH*Ar'*: C_p), 128.0 (t, J_{CP} = 5.0, PMe*Ph*Ph': C_m), 128.0 (t, J_{CP} = 4.9, PMePh*Ph'*: C_m), 129.9, 127.8, 127.6, 127.2 (NPh: C_o, C_m, C_p; CHAr': C_o), 124.1

(q, J_{CF} = 3.5, CH*Ar'*: C_m), 124.1 (q, J_{CF} = 271.8, *C*F$_3$); 13.8 (t, J_{CP} = 16.6, P*Me*Ph$_2$); ^{31}P NMR (CD_2Cl_2) δ 11.9 (J_{PW} = 280); ^{19}F NMR (CD_2Cl_2) δ -62.3 (CF_3). Anal. Calcd for ($C_{40}H_{36}Cl_2F_3NP_2W$): C, 53.12; H, 4.01; N, 1.55. Found: C, 53.09; H, 3.99; N, 1.44.

W[=CH(2-Np)]Cl$_2$(NPh)(PMePh$_2$)$_2$ (4)

In the drybox, WCl$_2$(NPh)(PMePh$_2$)$_3$ (3.09 g, 3.27 mmol) and Ph$_3$P=CH(2-Np) (1.50 g, 3.29 mmol) were placed in the same Schlenk tube. The mixture was dissolved in 60 mL of toluene and stirred for 4 h at 83 °C. After the solution was stored at -20 °C for 1 day, the supernatant was transferred into another Schlenk tube via a cannula equipped with a filter. Approximately 35 mL of the solvent was removed in vacuo, and the remaining brown solution was transferred via cannula into 150 mL of rapidly stirring pentane. Filtration yielded 2.58 g (89.0%) of yellow powder, which was dried in vacuo: ^{1}H NMR (CD_2Cl_2) δ 12.31 (t, 1, J_{HP} = 4.72, H_α), 7.8-6.6 (m, 32, H_{aryl}), 2.45 (t, 6, J_{HP} = 4.50, P*Me*Ph$_2$); ^{13}C NMR (CD_2Cl_2, not all aryl chemical shifts were assigned) δ 290.4 (t, J_{CH} = 125.3, J_{CP} = 12.1, J_{CW} = 132.3, C_α), 153.0 (t, J_{CP} = 1.9, J_{CW} = 37.6, NPh: C_{ipso}), 144.4 (t, J_{CP} = 3.2, CH*Ar'*: C_{ipso}), 133.9 (t, J_{CP} = 21.1, PMe*Ph*Ph': C_{ipso}), 133.9 (t, J_{CP} = 23.5, PMePh*Ph'*: C_{ipso}), 133.0 (t, J_{CP} = 5.1, PMe*Ph*Ph': C_o), 132.8 (t, J_{CP} = 5.1, PMePh*Ph'*: C_o), 130.4 (PMe*Ph*Ph': C_p), 130.0 (PMePh*Ph'*: C_p), 128.2 (t, J_{CP} = 5.1, PMe*Ph*Ph': C_m), 128.2 (t, J_{CP} = 4.9, PMePh*Ph'*: C_m), 14.2 (t, J_{CP} = 16.4, P*Me*Ph$_2$); ^{31}P NMR (CD_2Cl_2) 11.8 (J_{PW} = 281). Anal. Calcd for ($C_{43}H_{39}Cl_2NP_2W$): C, 58.26; H, 4.43; N, 1.58. Found: C, 57.95; H, 4.29; N, 1.64.

W(=CHC$_6$F$_5$)Cl$_2$(NPh)(PMePh$_2$) (5)

A mixture of WCl$_2$(NPh)(PMePh$_2$)$_3$ (3.07 g, 3.25 mmol) and Ph$_3$P=CHC$_6$F$_5$ (1.62 g, 3.67 mmol) was dissolved in 30 mL of benzene and stirred at 75 °C for 4.25 h. Most of the benzene (~23 mL) was removed in vacuo, and 150 mL of pentane was added to the reaction mixture. Upon vigorous stirring, a bright yellow powder formed, and the reaction mixture was then filtered. At this point, the ^{1}H NMR spectrum of the yellow powder indicated a 28:72 mixture of $WCl_2(NPh)(PMePh_2)_3$ and $W(=CHC_6F_5)Cl_2(NPh)(PMePh_2)_2$. The powder was redissolved in 30 mL of benzene together with 543 mg (1.23 mmol) of $Ph_3P=CHC_6F_5$, and the solution was stirred for 2 h at 75 °C. After removing benzene in vacuo, the yellow powder was washed with 30 mL of pentane and then dissolved in a mixture of 100 mL of toluene and 30 mL of pentane. This solution was filtered, and subsequent removal of the solvent in vacuo yielded an oil. The oil was partially dissolved in 17 mL of benzene. Slow addition of 50 mL of hexane and subsequent filtration resulted in the isolation of 1.78 g (56.7%) of yellow powder: ^{1}H NMR (CD_2Cl_2) δ 11.71 (t, 1, J_{HP} = 4.12, H_α), 7.69-6.51 (m, 25, H_{aryl}), 2.42 (t, 6, J = 4.55, P*Me*Ph_2); ^{13}C NMR (CD_2Cl_2) δ 261.5 (t, J_{CH} = 133.9, J_{CP} = 12.0, J_{CW} = 146, C_α), 152.3 (t, J_{CP} = 1.9, J_{CW} = 39, NPh: C_{ipso}), 133.0 (t, J_{CP} = 22.8, PMe*Ph*Ph': C_{ipso}), 132.8 (t, J_{CP} = 5.3, PMe*Ph*Ph': C_o), 132.7 (t, J_{CP} = 5.0, PMePh*Ph'*: C_o), 131.9 (t, J_{CP} = 22.6, PMePh*Ph'*: C_{ipso}), 130.5 (PMe*Ph*Ph': C_p), 130.0 (PMePh*Ph'*: C_p), 128.2 (t, J_{CP} = 4.9, PMe*Ph*Ph': C_m), 127.9 (t, J_{CP} = 4.8, PMePh*Ph'*: C_m), 127.74, 127.69, and 127.67 (NPh: C_o, C_m, and C_p), 14.9 (t, J_{CP} = 16.8, P*Me*Ph_2), (multiplets for the CHC_6F_5 ring carbons were observed between 124-145 ppm); ^{19}F NMR (CD_2Cl_2) δ -136.68 (d, J_{FF} = 25.7, F_o), -158.13 (t, J_{FF} = 20.1, F_p), -164.87 (t, J_{FF} = 22.0, F_m); ^{31}P NMR (CD_2Cl_2) δ 13.7 (J_{PW} = 280). Anal. Calcd for $[C_{32}H_{32}Cl_2F_5NP_2W \cdot 1/2(C_6H_6)]$: C, 52.25; H, 3.65; N, 1.45. Found: C, 51.94; H, 3.29; N, 1.27. (Inclusion of one-half of a molecule of benzene was supported by the ^{1}H and ^{13}C NMR spectra.)

$W(=CH\text{-}CH=CMe_2)Cl_2(NPh)(PMePh_2)_2$ (6)

$WCl_2(NPh)(PMePh_2)_3$ (10.24 g, 10.82 mmol) and $Ph_3P=CH\text{-}CH=CMe_2$ (3.66 g, 11.1 mmol) were placed together in a Schenk flask equipped with a reflux condenser, dissolved in 150 mL of benzene, and stirred for 20.5 h at 90 °C. After ~40 mL of benzene was removed in vacuo, the solution was transferred via a cannula equipped with a filter into 300 mL of rapidly stirring pentane. A golden-yellow powder (7.24 g, 82.2%) precipitated and was filtered away from the pentane solution. The complex was always isolated as a mixture of syn and anti rotamers of the alkylidene ligand, the relative amounts of which varied according to the reaction time. The thermodynamic rotamer with the more upfield H_α resonance is tentatively assigned as the syn rotamer on the basis of comparisons with the chemical shifts of the rotamers of $W(=CH\text{-}CH=CPh_2)Cl_2(N\text{-}2,6\text{-}C_6H_3\text{-}Me_2)(PEt_2Ph)_2$, which were assigned on the basis of difference NOE measurements, and comparisons with the analogous aryl alkylidenes, for which the thermodynamic rotamer was determined by an X-ray diffraction study to be the syn isomer: ^1H NMR (CD_2Cl_2) Syn Rotamer: δ 12.22 (d of t, 1, J_{HH} = 12.77, J_{HP} = 4.14, H_α), 8.00 (d, 1, J_{HH} = 12.73, H_β), 7.7-6.8 (m, 25, H_{aryl}), 2.44 (t, 6, J_{HP} = 4.39, P*Me*Ph$_2$), 2.30 (s, 3, =C*Me*Me'), 1.90 (s, 3, =CMe*Me'*); Anti Rotamer: δ 12.45 (d of t, 1, J_{HH} = 13.11, J_{HP} = 4.35, H_α), 7.9 (d, 1, H_β), 2.41 (t, 6, J_{HP} = 4.32, P*Me*Ph$_2$), 2.15 (s, 3, =C*Me*Me'), 1.98 (s, 3, =CMe*Me'*); ^{13}C NMR (CD_2Cl_2) Syn Rotamer: δ 284.0 (t, J_{CH} = 134.4, J_{CP} = 11.6, J_{CW} = 129.3, C_α), 153.2 (t, J_{CP} = 1.9, J_{CW} = 38.2, NPh: C_{ipso}), 140.0 (t, J_{CH} = 155.6, J_{CP} = 3.9, C_β), 138.7 (t, J_{CP} = 3.7, C_γ), 134.4 (t, J_{CP} = 23.3, PMe*Ph*Ph': C_{ipso}), 133.3 (t, J_{CP} = 21.1, PMePh*Ph'*: C_{ipso}), 132.8 (t, J_{CP} = 5.1, PMe*Ph*Ph': C_o), 132.7 (t, J_{CP} = 5.2, PMePh*Ph'*: C_o), 130.0 (PMe*Ph*Ph': C_p), 129.8 (PMePh*Ph'*: C_p), 128.1 (t, J_{CP} = 4.9, PMe*Ph*Ph': C_m), 128.0 (t, J_{CP} = 4.8, PMePh*Ph'*: C_m), 127.9 and 127.8 (NPh: C_o and C_m), 126.5 (NPh: C_p), 25.2 (=C*Me*Me'), 18.0 (=CMe*Me'*), 13.6 (t, J_{CP} = 16.0, P*Me*Ph$_2$); Anti Rotamer (only selected C_{aryl} chemical shifts listed): δ 274.2 (t, J_{CH} = 126.3, J_{CP} = 11.9, C_α), 153.9 (t, J_{CP} = 1.7, NPh: C_{ipso}), 138.1 (C_γ), 136.9 (J_{CH} = 159.7, C_β), 24.9 (=C*Me*Me'), 17.8 (=CMe*Me'*), 13.4 (t, J_{CP} = 18.2, PMePh$_2$); ^{31}P NMR (CD_2Cl_2) δ 12.0 (J_{PW} = 283, Syn Rotamer), 11.5 (J_{PW} = 276, Anti Rotamer). Anal. Calcd for ($C_{37}H_{39}Cl_2NP_2W$): C, 54.57; H, 4.83; N, 1.72. Found: C, 54.56; H, 4.60; N, 1.45.

Observation of $W(=CHPh)(NPh)[OCMe(CF_3)_2]_2(PMePh_2)$

A 20 mL THF solution of 180 mg of $(CF_3)_2MeCOLi$ (0.90 mmol) was transferred via cannula into a 10 mL THF solution of 380 mg of **1** (0.45 mmol). After the reaction mixture was stirred at room temperature for 14 h, the THF was removed in vacuo: ^1H NMR (dioxane-d_8) δ 11.07 (d, J_{HP} = 2.93, H_α), 11.06 (d, J_{HP} = 2.93, H_α). [Note: After the addition of one equiv of $(CF_3)_2MeCOLi$ to tungsten, loss of one $PMePh_2$ ligand was observed, and the H_α resonance appeared as a doublet at 11.86 ppm in dioxand-d_8.]

Reaction of $W(=CHPh)(NPh)[OCMe(CF_3)_2]_2(PMePh_2)$ with CuCl

$W(=CHPh)(NPh)[OCMe(CF_3)_2]_2(PMePh_2)$ was generated in dioxane-d_8 by the addition of excess $(CF_3)_2MeCOLi$ to **1**. Addition of CuCl resulted in the observation of two singlet H_α resonances at 9.95 and 9.75 ppm. A small singlet at 9.9 ppm was observed even before the addition of CuCl.

$WCl_2(NPh)[OCMe(CF_3)_2]_2(THF)$ (7)

A solution of $(CF_3)_2CH_3COLi$ (18.72 g, 99.55 mmol) in 120 mL of THF was added via cannula over a 15 minute period to a suspension of $WCl_4(NPh)$ (20.74 g, 47.74 mmol) in 120 mL of THF cooled to 0 °C. After stirring the solution for 16 h at room temperature, the solvent was removed in vacuo, and the product was dissolved in 90 mL of Et_2O. The solution was filtered and then cooled to -50 °C to afford 34.89 g of bright orange crystals (93.7%, 3 crops): ^1H NMR (CD_2Cl_2) δ 7.63 (dd, 2, H_m), 7.30 (d, 2, J = 7.57, H_o), 7.14 (t, 1, J = 7.57, H_p), 4.40 (m, 4, THF), 2.06 (m, 4, THF), 1.75 (s, 6, $OC\mathit{Me}(CF_3)_2$); ^{13}C NMR (CD_2Cl_2) δ 150.7 (C_{ipso}), 132.3, 128.6, and 128.3 (C_{aryl}), 123.7 (q, J_{CF} = 290, CF_3), 86.2 (septet, J_{CF} = 30, $O\mathit{C}Me(CF_3)_2$), 73.0 (THF), 25.9 (THF), 17.7 ($OC\mathit{Me}(CF_3)_2$). Anal. Calcd for ($C_{18}H_{19}Cl_2F_{12}NO_3W$): C, 27.71; H, 2.46; N, 1.80. Found: C, 27.84; H, 2.47; N, 1.83.

$WCl_2(N-2,6-C_6H_3-Me_2)[OCMe(CF_3)_2]_2(THF)$ (8)

Two equivalents of $(CF_3)_2MeCOLi$ (17.14 g, 91.17 mmol) were dissolved in 90 mL of THF. The resulting solution was added slowly via cannula to a -78 °C solution of $WCl_4(N-2,6-C_6H_3-Me_2)(Et_2O)$ (23.24 g, 44.79 mmol) in 60 mL of THF. After warming to room temperature, the solution was stirred for 19 h before the solvent was removed in vacuo. The red powder was then dissolved in 150 mL of Et_2O, and the solution was filtered. Recrystallization at -50 °C afforded red crystals in 93.4% yield (33.8 g, 2 crops): ^1H NMR (C_6D_6) δ 6.80 (d, 2, J = 7.6, H_m), 6.35 (t, 1, J = 7.6, H_p), 4.25 (m, 4, THF), 2.93 (s, 6, NAr: Me), 1.54 (s, 6, $OCMe(CF_3)_2$), 1.29 (m, 4, THF); ^{13}C NMR (C_6D_6) δ 148.7 (C_{ipso}), 144.9 (C_o), 131.5 and 127.8 (C_m and C_p), 123.8 (q, J_{CF} = 288, CF_3), 85.8 (septet, J_{CF} = 30, $O\mathit{C}Me(CF_3)_2$), 72.2 (THF), 25.1 (THF), 19.8 and 16.4 (NAr: Me and $OC\mathit{Me}(CF_3)_2$). Anal. Calcd for ($C_{20}H_{23}Cl_2F_{12}NO_3W$): C, 29.73; H, 2.87; N, 1.73. Found: C, 29.72; H, 2.86; N, 1.76.

$WCl_2[N-2,6-C_6H_3-(i-Pr)_2][OCMe(CF_3)_2]_2(THF)$ (9)

Two equivalents of $(CF_3)_2CH_3COLi$ (7.20 g, 38.3 mmol) were dissolved in 40 mL of THF. The resulting solution was added over a period of 10 minutes to a suspension of $WCl_4[N-2,6-C_6H_3-(i-Pr)_2]$ (9.59 g, 19.1 mmol) in 40 mL of THF at 0 °C. After warming to room temperature, the solution was stirred for 15 h before the solvent was removed in vacuo. The red solid was dissolved in pentane, and the solution was filtered and slowly cooled to -50 °C. Red crystals (13.68 g) were isolated in 82.7% yield (2 crops): ^1H NMR (C_6D_6) δ 7.07 (d, 2, J = 8.06, H_m), 6.57 (t, 1, J = 8.06, H_p), 4.61 (septet, 2, J = 6.59, $C\mathit{H}Me_2$), 4.25 (m, 4, THF), 1.58 (s, 6, $OCMe(CF_3)_2$), 1.29 (m, 4, THF), 1.28 (d, 12, J = 6.59, $CH\mathit{Me}_2$); ^{13}C NMR (C_6D_6) δ 154.1 (C_o), 146.6 (C_{ipso}), 132.1 and 123.5 (C_m and C_p), 123.8 (q, J_{CF} = 288, CF_3), 86.5 (septet, J_{CF} = 30, $O\mathit{C}Me(CF_3)_2$), 72.1 (THF), 27.6 ($\mathit{C}H(CH_3)_2$), 25.1 (THF), 24.9 ($CH(\mathit{C}H_3)_2$), and 17.1

(OCMe(CF_3)$_2$). Anal. Calcd for ($C_{24}H_{31}Cl_2F_{12}NO_3W$): C, 33.35; H, 3.62; N, 1.62. Found: C, 33.60; H, 3.65; N, 1.75.

W(=CHAr')(N-2,6-C_6H_3-Me_2)[OCMe(CF_3)$_2$]$_2$(PPh_3) (10)

Representative Procedure: A 600 μL C_6D_6 solution of WCl_2(N-2,6-C_6H_3-Me_2)[OC*Me*(CF_3)$_2$]$_2$(THF) (30 mg, 0.037 mmol) and one equivalent of Ph_3P=CHAr' was added to an excess (~6 - 8 equiv) of 1% Na(Hg) in an NMR tube in the drybox. The NMR tube was capped with a septum, the septum was wrapped with Parafilm, and the tube was then rotated for 4 h. The NMR tube was returned to the drybox and the reaction mixture was poured into a vial. After allowing the salts to settle, the orange-brown solution was transferred via pipet off of the spent sodium amalgam and placed in the NMR tube again. ^1H and ^{31}P NMR spectra of the product were then acquired.

W(=CHPh)(N-2,6-C_6H_3-Me_2)[OCMe(CF_3)$_2$]$_2$(PPh_3) (10a): ^1H NMR (C_6D_6) δ 12.32 (d, 1, J_{HP} = 6.87, H_α), 7.5 - 6.5 (m, H_{aryl}), 2.63 (s, 3, NAr: Me), 2.16 (s, 3, OC*Me*(CF_3)$_2$), 1.80 (s, 3, NAr: Me), 1.44 (s, 3, OC*Me*(CF_3)$_2$); ^{31}P NMR (C_6D_6) δ 37.4 (J_{PW} = 284, PPh_3).

W(=CHC_6H_4-*p*-Me)(N-2,6-C_6H_3-Me_2)[OCMe(CF_3)$_2$]$_2$(PPh_3) (10b): ^1H NMR (C_6D_6) δ 12.31 (d, 1, J_{HP} = 6.87, H_α), 8.0 - 6.5 (m, H_{aryl}), 2.63 (s, 3, NAr: Me), 2.36 (s, 3, CHAr': Me), 2.19 (s, 3, OC*Me*(CF_3)$_2$), 1.81 (s, 3, NAr: Me), 1.45 (s, 3, OC*Me*(CF_3)$_2$); ^{31}P NMR (C_6D_6) δ 35.7 (J_{PW} = 283, PPh_3).

W(=CHC_6H_4-*m*-Me)(N-2,6-C_6H_3-Me_2)[OCMe(CF_3)$_2$]$_2$(PPh_3) (10c): ^1H NMR (C_6D_6) δ 12.32 (d, 1, J_{HP} = 6.87, H_α), 7.9 - 6.2 (m, H_{aryl}), 2.64 (s, 3, NAr: Me), 2.27 (s, 3, CHAr': Me), 2.19 (s, 3, OC*Me*(CF_3)$_2$), 1.82 (s, 3, NAr: Me), 1.45 (s, 3, OC*Me*(CF_3)$_2$); ^{31}P NMR (C_6D_6) δ 37.6 (J_{PW} = 283, PPh_3).

W(=CHC_6H_4-*o*-Me)(N-2,6-C_6H_3-Me_2)[OCMe(CF_3)$_2$]$_2$(PPh_3) (10d): ^1H NMR (C_6D_6) δ 12.65 (d, 1, J_{HP} = 6.84, H_α). [Not as stable as the other derivatives—decomposes within ~ 12 h.]

$\mathrm{W(=CHC_6H_4\text{-}\mathit{p}\text{-}OEt)(N\text{-}2,6\text{-}C_6H_3\text{-}Me_2)[OCMe(CF_3)_2]_2(PPh_3)}$ (10e): ^{1}H NMR (C_6D_6) δ 12.26 (d, 1, J_{HP} = 6.37, H_α), 8 - 6 (m, H_{aryl}), 3.61 (q, 2, J = 6.87, $\mathrm{O}\mathit{CH}_2\mathrm{CH}_3$), 2.64 (s, 3, NAr: Me), 2.19 (s, 3, $\mathrm{OC}\mathit{Me}\mathrm{(CF_3)_2}$), 1.81 (s, 3, NAr: Me), 1.49 (s, 3, $\mathrm{OC}\mathit{Me}\mathrm{(CF_3)_2}$), 1.12 (t, 3, J = 6.87, $\mathrm{OCH_2}\mathit{CH}_3$); ^{31}P NMR ($C_6D_6$) δ 35.8 ($J_{PW}$ = 283, PPh_3).

$\mathrm{W(CHPh)(N\text{-}2,6\text{-}C_6H_3\text{-}Me_2)[OCMe(CF_3)_2]_2(PMe_3)}$ (11)

A solution of $Ph_3P{=}CHPh$ (2.25 g, 6.38 mmol) and $\mathrm{WCl_2(N\text{-}2,6\text{-}C_6H_3\text{-}Me_2)[OCMe(CF_3)_2]_2(THF)}$ (5.05 g, 6.25 mmol) in 50 mL of benzene was added to a 1% sodium amalgam (1.47 g Na, 64.1 mmol) and stirred for 3 h. After adding 1.98 mL of PMe_3 (3 equiv, 19.1 mmol) via syringe and stirring for an additional 16 h, the mixture was allowed to settle. The golden brown solution was separated from the residual sodium amalgam, which was then washed with 45 mL of benzene. The solvent was removed in vacuo, and the brown residue was dissolved in 90 mL of Et_2O. After filtering the solution, it was added via cannula to 0.66 g (6.6 mmol) of CuCl and stirred for 15 h. The Et_2O was removed in vacuo and the solid was extracted with 230 mL of pentane to give a yellow-brown solution. After the solution was filtered and concentrated, recrystallization at -50 °C afforded 2.51 g of yellow-brown crystals (48.3%): (This complex was isolated as an 18:1 ratio of isomers. Spectroscopic data for the major isomer is reported here.) ^{1}H NMR (C_6D_6) δ 12.16 (d, 1, J_{HP} = 9.59, H_α), 7.27 (t, 2, J = 7.57, H_{aryl}), 7.13 (m, 2, H_{aryl}), 6.91 (d, 2, J = 7.57, H_{aryl}), 6.78 (m, 1, H_{aryl}), 6.73 (t, 1, J = 7.57, H_{aryl}), 2.54 (s, 3, NAr: Me), 2.43 (s, 3, NAr: Me), 2.14 (s, 3, $\mathrm{OC}\mathit{Me}\mathrm{(CF_3)_2}$), 1.40 (s, 3, $\mathrm{OC}\mathit{Me}\mathrm{(CF_3)_2}$), 0.79 (d, 9, J_{HP} = 9.28, PMe_3); ^{13}C NMR (C_6D_6) δ 266.5 (J_{CH} = 144, J_{CW} = 154, J_{CP} = 14, C_α), 153.8 (NAr: C_{ipso}), 141.09 and 136.7 ($\mathrm{CH}\mathit{Ph}$: C_{ipso} and NAr: C_o), 134.4, 128.7, 128.1, 127.9, and 126.7 (all C_{aryl}), 125.7 (q, J_{CF} = 289, CF_3), 125.1 (q, J_{CF} = 289, CF_3), 82.8 (septet, J_{CF} = 29, $\mathrm{O}\mathit{C}\mathrm{Me(CF_3)_2}$), 80.4 (septet, J_{CF} = 28, $\mathrm{O}\mathit{C}\mathrm{Me(CF_3)_2}$), 19.2, 18.7, and 17.4 (NAr: Me and $\mathrm{OC}\mathit{Me}\mathrm{(CF_3)_2}$), 14.2 (d, J_{CP} = 29, PMe_3); ^{31}P NMR (CD_2Cl_2) δ 12.7

(J_{PW} = 318, PMe_3). Anal. Calcd for ($C_{26}H_{30}F_{12}NO_2PW$): C, 37.56; H, 3.64; N, 1.68. Found: C, 37.74; H, 3.69; N, 1.84.

W(=CHC$_6$H$_4$-*o*-OMe)(NPh)[OCMe(CF$_3$)$_2$]$_2$(THF) (12)

A solution of $Ph_3P=CHC_6H_4$-*o*-OMe (7.82 g, 20.5 mmol) and WCl_2(NPh)[OCMe(CF_3)$_2$]$_2$(THF) (15.49 g, 19.85 mmol) in 160 mL of benzene and 5 mL of THF was added to a 1% sodium amalgam (3.66 g Na, 8.02 equiv) and then stirred for 4.5 h. After the mixture settled, the solution was added via cannula to 2.07 g (20.9 mmol) of CuCl, and the residual sodium amalgam was washed with 60 mL of benzene. The combined benzene solutions were stirred with CuCl for 13 h before the solvent was removed in vacuo, and the brown solid was then extracted with 135 mL of pentane. THF (4 mL) was added to the red solution, which was then filtered and slowly cooled to -50 °C. Burnt-orange crystals (10.5 g, 63.8%) were obtained: ^{1}H NMR (THF-d_8) δ 10.46 (s, 1, H_α), 7.38 (dd, 2, NPh: H_m), 7.23 (d, 2, J = 7.69, NPh: H_o), 7.11 (m, 3, H_{aryl}), 6.68 (t, 1, J = 7.69, H_{aryl}), 6.39 (d, 1, J = 7.69, Ar': H_m), 4.09 (s, 3, OMe), 3.61 (m, 4, THF), 1.78 (m, 4, THF), 1.14 (s, 6, OC*Me*(CF_3)$_2$); ^{13}C NMR (THF-d_8) δ 246.4 (J_{CH} = 149, J_{CW} = 161, C_α), 159.6 and 156.2 (Ar': *C*OMe and NPh: C_{ipso}), 133.5 (CH*Ar'*: C_{ipso}), 129.0, 128.8, 126.5, 126.3 125.0, and 122.6 (all C_{aryl}), 108.4 (1, CH*Ar'*: C_m), 125.6 (q, J_{CF} = 288, CF_3), 80.9 (septet, J_{CF} = 28, O*C*Me(CF_3)$_2$), 68.2 (THF), 57.1 (OMe), 26.4 (THF), 18.0 (OC*Me*(CF_3)$_2$). Anal. Calcd for ($C_{26}H_{27}F_{12}NO_4W$): C, 37.66; H, 3.28; N, 1.69. Found: C, 37.93; H, 3.45; N, 2.16.

W(=CHC$_6$H$_4$-*o*-OMe)(N-2,6-C$_6$H$_3$-Me$_2$)[OCMe(CF$_3$)$_2$]$_2$(THF) (13)

WCl_2(N-2,6-C_6H_3-Me_2)[OCMe(CF_3)$_2$]$_2$(THF) (16.0 g, 19.8 mmol) and $Ph_3P=CHC_6H_4$-*o*-OMe (7.78 g, 20.3 mmol) were dissolved in 160 mL of benzene and 2.5 mL of THF, and the solution was added to a 1% sodium amalgam (3.59 g of Na, 7.90 equiv). After being stirred for 8 h at room temperature, the mixture was allowed to settle, and the orange-brown supernatant was added via cannula to 2.07 g of CuCl (20.9 mmol). The residual sodium amalgam was washed with a total of 120 mL of Et_2O, and the combined benzene/Et_2O solution was stirred with CuCl for 12 h before removing the solvent in vacuo. The brown solid was then extracted with 260 mL of Et_2O. After 2 mL of THF was added to the extract, the solution was filtered and then slowly cooled to -50 °C to give 12.0 g (70.6%) of an olive-yellow powder: ^1H NMR (C_6D_6) δ 10.81 (s, 1, H_α), 6.96 (m, 1, H_{aryl}), 6.95 (d, 2, J = 8.06, NAr: H_m), 6.75 (m, 1, H_{aryl}), 6.53 (d, 1, J = 7.32, CH*Ar'*: H), 6.48 (m, 1, H_{aryl}), 6.26 (d, 1, J = 7.32, CH*Ar'*: H_m), 3.93 (m, 4, THF), 3.59 (s, 3, OMe), 2.66 (s, 6, Ar: Me), 1.37 (m, 4, THF), 1.19 (s, 6, OC*Me*$(CF_3)_2$). Difference NOE experiments: irrad. of δ 10.81 enhances δ 6.26, 2.66; irrad. of δ 3.93 enhances δ 3.59, 2.66, 1.37; irrad. of δ 3.59 enhances δ 6.53, 3.93; irrad. of δ 2.66 enhances δ 10.81, 6.95, 3.93; irrad. of δ 1.19 enhances δ 10.81. ^{13}C NMR (C_6D_6) δ 240.2 (J_{CH} = 151, J_{CW} = 160, C_α), 158.0 (CHAr': *C*OMe), 153.5 (NAr: C_{ipso}), 134.9 and 132.5 (CH*Ar'*: C_{ipso} and NAr: C_o), 128.0, 127.8, 125.6, 124.3, and 122.3 (all C_{aryl}), 107.8 (CH*Ar'*: C_m), 124.8 (q, J_{CF} = 291, CF_3), 124.6 (q, J_{CF} = 290, CF_3), 81.0 (septet, J_{CF} = 28, O*C*Me$(CF_3)_2$), 70.3 (THF), 56.1 (OMe), 25.6 (THF), 18.9 and 18.1 (NAr: Me and OC*Me*$(CF_3)_2$). Anal. Calcd for ($C_{28}H_{31}F_{12}NO_4W$): C, 39.22; H, 3.64; N, 1.63. Found: C, 39.33; H, 3.71; N, 1.65.

^1H NMR (-70 °C, tol-d_8) δ 10.78 (s, 1, H_α), 6.99 (m, 3, H_{aryl}), 6.80 (m, 1, H_{aryl}), 6.48 (m, 2, H_{aryl}), 6.11 (d, 1, J = 7.32, H_{aryl}), 4.11 (br s, 4, THF), 3.40 (s, 3, OMe), 2.92 (s, 3, NAr: Me), 2.37 (s, 3, NAr: Me), 1.25 (s, 6, OC*Me*$(CF_3)_2$), 1.22 (br s, 4, THF).

W(=CHC$_6$H$_4$-*o*-OMe)[N-2,6-C$_6$H$_3$-(*i*-Pr)$_2$][OCMe(CF$_3$)$_2$]$_2$(THF) (14)

A solution of Ph_3P=CHC_6H_4-*o*-OMe (7.12 g, 18.6 mmol) and WCl_2[N-2,6-C_6H_3-(*i*-Pr)$_2$][OCMe$(CF_3)_2$]$_2$(THF) (15.16 g, 17.54 mmol) in 150 mL of benzene and 4 mL of THF was added via cannula to a 1% sodium amalgam (3.37 g Na, 8.35 equiv) and stirred for 8 h at room temperature. After the mixture settled, the orange-brown supernatant was added via cannula to CuCl (1.79 g, 18.1 mmol). Next, the residual sodium amalgam was washed with a total of 120 mL of benzene, and the combined benzene solutions were stirred with the CuCl for 12 h before the solvent was removed in vacuo. Diethyl ether (330 mL) was used to extract the product from the brown solid. After being filtered, the Et_2O solution was cooled to -50 °C to yield 7.3 g of golden crystals (46%): ^1H NMR (THF-d_8) δ 10.60 (s, 1, H_α), 7.17 (d, 2, J = 7.69, NAr: H_m), 7.13 (m, 2, H_{aryl}), 6.98 (t, 1, J = 7.69, NAr: H_p), 6.72 (m, 1, H_{aryl}), 6.41 (d, 1, J = 7.33, CH*Ar'*: H_m), 4.03 (s, 3, OMe), 3.63 (m, 4, THF), 3.62 (m, 2, C*H*(CH_3)$_2$), 1.78 (m, 4, THF), 1.34 (br s, 2, CH*(CH_3)$_2$*), 1.18 (s, 6, OC*Me*(CF_3)$_2$); ^{13}C NMR (THF-d_8) δ 248.1 (J_{CH} = 148, J_{CW} = 167, C_α), 159.8 (CH*Ar'*: *C*OMe), 151.3 (NAr: C_{ipso}), 145.8 and 133.1 (CH*Ar'*: C_{ipso} and NAr: C_o), 129.3, 126.2, 125.2, 123.3, and 122.4 (all C_{aryl}), 108.7 (CH*Ar'*: C_m), 125.6 (q, J_{CF} = 290, CF_3), 125.4 (q, J_{CF} = 291, CF_3), 80.8 (septet, J_{CF} = 28.3, O*C*Me(CF_3)$_2$), 68.1 (THF), 56.9 (OMe), 28.6 (*C*H(CH_3)$_2$), 26.4 (THF), 24.4 (CH(*C*H_3)$_2$), 18.0 (OC*Me*(CF_3)$_2$). Anal. Calcd for ($C_{32}H_{39}F_{12}NO_4W$): C, 42.08; H, 4.30; N, 1.53. Found: C, 42.22; H, 4.33; N, 1.82.

$W(=CHC_6H_4$-*o*-$OMe)(N$-2,6-C_6H_3-$Me_2)[OCMe(CF_3)_2]_2(PMe_3)$ (15)

$W(=CHC_6H_4$-*o*-$OMe)(N$-2,6-C_6H_3-$Me_2)[OCMe(CF_3)_2]_2(THF)$ (2.01 g, 2.34 mmol) was dissolved in 50 mL of benzene. Three equivalents of PMe_3 (0.73 mL, 7.1 mmol) were added, and the red solution turned golden brown within a few minutes. After the reaction mixture was stirred for 12 h, the solvent was removed in vacuo, and the product was recrystallized from pentane at -50 °C to give 1.44 g of golden crystals (71.4%): (This complex was isolated as a 12:1 ratio of isomers. Spectroscopic data for the major isomer is reported here.) ^1H NMR (CD_2Cl_2) δ 12.48 (d, 1, J_{HP} = 7.08, H_α), 7.32 (d, 1, J = 7.57, H_{aryl}), 7.22 (d, 2, J = 7.57, NAr: H_m), 7.18 (m, 1, H_{aryl}), 7.04 (m, 3, H_{aryl}), 4.05 (s, 3, OMe), 2.79 (s, 6, NAr: Me), 2.07 (s, 3, OC*Me*(CF_3)$_2$), 1.45 (s, 3, OC*Me*(CF_3)$_2$), 1.37 (d, 9, J_{HP} = 9.52, PMe_3); ^{13}C NMR (CD_2Cl_2) δ 259.5 (J_{CH} = 147,

J_{CW} = 148, J_{CP} = 15, C_α), 154.3 and 153.9 (CH*Ar'*: *C*OMe and NAr: C_{ipso}), 136.4 and 132.4 (CH*Ar'*: C_{ipso} and NAr: C_o), 131.4, 130.3, 128.5, 126.8, and 121.1 (all C_{aryl}), 109.9 (CH*Ar'*: C_m), 125.9 (q, J_{CF} = 290, CF_3), 125.3 (q, J_{CF} = 289, CF_3), 82.4 (septet, J_{CF} = 28, O*C*Me(CF_3)$_2$), 80.6 (septet, J_{CF} = 28, O*C*Me(CF_3)$_2$), 56.6 (OMe), 19.7, 19.4, and 18.2 (NAr: Me and OC*Me*(CF_3)$_2$), 15.3 (d, J_{CP} = 29, PMe_3); ^{31}P NMR (CD_2Cl_2) δ 11.0 (J_{PW} = 324). Anal. Calcd for ($C_{27}H_{32}F_{12}NO_3PW$): C, 37.65; H, 3.74; N, 1.63. Found: C, 37.89; H, 3.79; N, 1.56.

W(=CHC$_6$H$_4$-*o*-OMe)(NAr)[OCMe(CF$_3$)$_2$]$_2$ (16)

W(=CHC$_6$H$_4$-*o*-OMe)(N-2,6-C$_6$H$_3$-Me$_2$)[OCMe(CF$_3$)$_2$]$_2$ (16a). A 150 mL toluene solution of the THF adduct W(=CHC$_6$H$_4$-*o*-OMe)(N-2,6-C$_6$H$_3$-Me$_2$)[OCMe(CF$_3$)$_2$]$_2$(THF) (7.92 g, 9.17 mmol) was heated to 50 °C as the solvent was removed in vacuo. The resulting red powder was dissolved in 30 mL of toluene, and the solution was filtered, layered with 120 mL of pentane, and cooled to -10 °C to give red crystals in 73% yield (5.2 g, 2 crops): ^1H NMR (C_6D_6) δ 10.94 (s, 1, H_α), 6.93 (m, 1, H_{aryl}), 6.90 (d, 2, J = 7.69, NAr: H_m), 6.73 (t, 1, J = 7.69, NAr: H_p), 6.49 (m, 2, H_{aryl}), 6.37 (d, 1, J = 6.96, CH*Ar'*: H_m), 3.75 (s, 3, OMe), 2.69 (s, 6, Ar: Me), 1.11 (s, 6, OC*Me*(CF_3)$_2$); ^{13}C NMR (C_6D_6) δ 228.1 (J_{CH} = 155, J_{CW} = 172, C_α), 156.3 (CH*Ar'*: *C*OMe), 153.0 (NAr: C_{ipso}), 135.6 and 132.4 (CH*Ar'*: C_{ipso} and NAr: C_o), 127.9, 126.8, 126.6, 123.6, and 122.6 (all C_{aryl}), 107.6 (CH*Ar'*: C_m), 124.0 (q, J_{CF} = 288, CF_3), 82.3 (septet, J = 29, O*C*Me(CF_3)$_2$), 56.7 (OMe), 18.73 and 18.66 (NAr: Me and OC*Me*(CF_3)$_2$). Anal. Calcd for ($C_{24}H_{23}F_{12}NO_3W$): C, 36.71; H, 2.95; N, 1.78. Found: C, 36.90; H, 3.03; N, 1.70.

W(=CHC$_6$H$_4$-*o*-OMe)[N-2,6-C$_6$H$_3$-(*i*-Pr)$_2$][OCMe(CF$_3$)$_2$]$_2$ (16b). Removal of THF from W(=CHC$_6$H$_4$-*o*-OMe)[N-2,6-C$_6$H$_3$-(*i*-Pr)$_2$][OCMe(CF$_3$)$_2$]$_2$(THF) was much more difficult than for the dimethylphenylimido analogue. After the above procedure was repeated twice, the product was dissolved in pentane, filtered, and cooled to -10 °C.

Red single crystals of **16b** precipitated from solution, but a small amount of yellow single crystals of the THF-adduct **14** also precipitated. Due to the differences in color, the crystals were easily separated by hand, and pure **16b** was then characterized: ^{1}H NMR (CD_2Cl_2) δ 10.79 (s, 1, H_α), 7.28 (d, 2, J = 8.06, NAr: H_m), 7.18 (t, 1, J = 6.96, H_{aryl}), 7.14 (t, 1, J = 7.70, H_{aryl}), 7.09 (d, 1, J = 8.06, CH*Ar'*: H_o), 6.81 (t, 1, J = 7.89, H_{aryl}), 6.59 (d, 1, J = 7.33, CH*Ar'*: H_m), 4.22 (s, 3, OMe), 4.06 (septet, 2, J = 6.96, *CH*$(CH_3)_2$), 1.34 (d, 2, J = 6.96, CH*(CH*$_3$*)*$_2$), 1.29 (s, 6, OC*Me*$(CF_3)_2$); ^{13}C NMR (CD_2Cl_2) δ 229.4 (J_{CH} = 155, J_{CW} = 176, C_α), 156.6 (CH*Ar': C*OMe), 150.4 (NAr: C_{ipso}), 146.4 and 132.4 (CH*Ar':* C_{ipso} and NAr: C_o), 127.5, 127.0, 123.9, 123.1, and 122.8 (all C_{aryl}), 107.9 (CH*Ar'*: C_m), 124.0 (q, J_{CF} = 289, CF_3), 123.9 (q, J_{CF} = 289, CF_3), 82.5 (septet, J_{CF} = 29.3, O*C*Me$(CF_3)_2$), 57.4 (OMe), 28.6 (*C*H$(CH_3)_2$), 24.3 (CH(*C*$H_3)_2$), 19.0 (OC*Me*$(CF_3)_2$). Anal. Calcd for ($C_{28}H_{31}F_{12}NO_3W$): C, 39.97; H, 3.71; N, 1.66. Found: C, 40.11; H, 3.73; N, 1.82.

W(=CHC_6H_4-*o*-OMe)(N-2,6-C_6H_3-Me_2)(O-*t*-Bu)$_2$(PMe_2Ph)

(General Procedure.) W(=CHC_6H_4-*o*-OMe)(N-2,6-C_6H_3-Me_2)(O-*t*-Bu)$_2$ was formed upon mixing **13** with 2 equiv of NaO-*t*-Bu, but numerous difficulties were encountered in separating this complex from free $LiOCMe(CF_3)_2$. After several manipulations of the product, it was discovered that the addition of PMe_2Ph, which binds reversibly to tungsten, to a pentane solution of the t-butoxide complex and subsequent filtration enabled the removal of the free alkoxide. The PMe_2Ph adduct was then recrystallized from pentane. Due to the number of manipulations that were carried out on the reaction product prior to the addition of PMe_2Ph, it is not possible to report a more specific procedure or the reaction yield here: ^{1}H NMR (C_6D_6) δ 10.55 (br s, 1, H_α), 7.35 - 6.54 (m, 12, H_{aryl}), 3.72 (s, 3, OMe), 2.79 (s, 6, NAr: *Me*$_2$), 1.18 (s, 18, OC*Me*$_3$), 1.07 (s, 6, P*Me*$_2$Ph); ^{13}C NMR (CD_2Cl_2, selected C_{aryl} only) δ 208 (br, C_α), 155.4 (br, CH*Ar'*:

*C*OMe), 154.0 (NAr: C_{ipso}), 136.4 (br, CH*Ar'*: C_{ipso}), 134.7 (NAr: C_o), 107.9 (CH*Ar'*: C_m), 80.0 (O*C*Me_3), 56.3 (OMe), 32.6 (OCMe_3), 19.4 (NAr: Me_2), 14.6 (PMe_2Ph).

Polymerization of Norbornene by 13. Norbornene (35.9 mg, 0.381 mmol) was dissolved in 300 μL of tol-d_8 and transferred via pipet into a small flask equipped with a Kontes valve. Complex **13** (6.3 mg, 0.0073 mmol) and 4.9 mg (0.041 mmol) of mesitylene were dissolved in 300 μL of tol-d_8 and transferred via pipet into a sealable NMR tube. After both solutions were freeze-pump-thaw-degassed several times, the tol-d_8 solution of norbornene was vacuum-transferred onto the solution of **13** ([**13**] = 0.012 M; [norbornene] = 0.635 M, 52.9 equiv), and the tube was sealed and then stored in liquid nitrogen before it was placed in the probe of the 400 MHz NMR at -82 °C. After an initial spectrum was acquired at -82 °C, the probe was warmed to -61 °C and the polymerization was monitored at this temperature for 50 min. After 50 min, integration versus the mesitylene internal standard indicated that [norbornene] = 0.606 M and [polynorbornene] = 0.002 M. The probe was then warmed to -40 °C, and the polymerization was again monitored for 80 min. A plot of the rate of disappearance of norbornene versus time was linear with rate = 17.5 equiv/h.

Polymerization at -40 °C by 13

Time (min)	[Norbornene] (M)	[Polynorbornene] (M)
0	0.590	0.007
10.23	0.559	0.036
20.03	0.514	0.077
30.01	0.478	0.121
40.01	0.433	0.158
49.96	0.404	0.196
60.08	0.372	0.227
70.06	0.341	0.251
79.99	0.319	0.277

Polymerization of Norbornene by 16a. Norbornene (35.6 mg, 0.378 mmol) was dissolved in 300 µL of tol-d_8 and transferrred via pipet into a small flask equipped with a Kontes valve. Complex **16a** (5.7 mg, 0.0073 mmol) and 4.5 mg (0.037 mmol) of mesitylene were dissolved in 300 µL of tol-d_8 and transferred via pipet into a sealable NMR tube. After both solutions were freeze-pump-thaw-degassed several times, the tol-d_8 solution of norbornene was vacuum-transferred onto the solution of **16a** ([**16a**] = 0.012 M; [norbornene] = 0.630 M, 52.5 equiv), and the tube was sealed and then stored in liquid nitrogen before it was placed in the probe of the 400 MHz NMR at -82 °C. After an initial spectrum was acquired at -82 °C, the probe was warmed to -61 °C and the polymerization was monitored at this temperature for 120 min. A plot of the rate of disappearance of norbornene versus time was linear with rate = 16.5 equiv/h. (Note: The starting alkylidene peak disappeared during the polymerization at low temperature and then reappeared when the solution was warmed to room temperature. This observation, together with the occurrence of a doublet at 4.77 ppm and a triplet at 0.65 ppm, may indicate that the resting state of the catalyst is the norbornene metallacycle at low temperature.]

Polymerization at -61 °C by 16a

Time (min)	[Norbornene] (M)	[Polynorbornene] (M)
0	0.630	0.004
9.98	0.606	0.023
20.02	0.590	0.052
29.97	0.546	0.084
40.05	0.516	0.121
50.02	0.480	0.158
60.00	0.432	0.188
70.03	0.405	0.233
80.03	0.367	0.273
110.02	0.269	0.377
120.02	0.234	0.400

General Procedure for the Olefination of Carbonyl Compounds by 13. A small excess of the carbonyl compound and 25 mg of **13** were dissolved together in 600 µL of C_6D_6, and the reaction was monitiored by ^1H NMR spectroscopy. The reactions were carried out at room temperature unless specified otherwise for the following: EtC(O)H, PhC(O)H, PhC(O)Me, PhC(O)Ph, MeC(O)OEt (65 °C), and $MeC(O)NMe_2$ (65 °C). A mixture of trans and cis isomers was observed in all cases for the alkene products.

Isomerization of *cis*-2-Pentene by 16a. Complex **16a** (1.4 mg, .0018 mmol, 0.0030 M), *cis*-2-pentene (17.5 mg, 0.250 mmol, 0.416 M, 140 equiv), and mesitylene (internal standard, 2.8 mg, 0.023 mmol) were dissolved together in 600 µL of tol-d_8, and the reaction was monitored by ^1H NMR spectroscopy. An equilibrium mixture of *cis*- and *trans*-2-pentene was obtained within 75 min, establishing a lower limit of 1.4 equiv/min for the metathesis of *cis*-2-pentene by **16a**.

time (min)	[*cis*-2-pentene] (M)	time (min)	[*cis*-2-pentene] (M)
0	0.416	65.5	0.114
10.4	0.372	75.0	0.100
23.7	0.319	85.4	0.095
34.8	0.283	106.1	0.089
49.2	0.176	128.7	0.091
57.0	0.136		

X-ray Data Collection, Structure Determination and Refinement for $W(=CHC_6H_4\text{-}p\text{-}Me)Cl_2(NPh)(PMePh_2)_2$

A yellow crystal of approximate dimensions 0.23 x 0.40 x 0.47 mm was oil-mounted on a glass fiber and transferred to the Siemens P3 diffractometer which is equipped with a modified LT-2 low temperature system. Determination of Laue symmetry, crystal class, unit cell parameters and the crystal's orientation matrix were carried out by previously described techniques similar to those of Churchill.[35] Low temperature (168 K) intensity data were collected via a θ-2θ scan technique with MoKα radiation under the conditions given in Table E-1 (Appendix).

All 8664 data were corrected for absorption and for Lorentz and polarization effects and placed on an approximately absolute scale. Any reflection with I(net) < 0 was assigned the value $|F_o| = 0$. There were no systematic extinctions nor any diffraction symmetry other than the Friedel condition. The two possible triclinic space groups are the noncentrosymmetric P1 [C_1^1; No.1] or the centrosymmetric $P\bar{1}$ [C_i^1; No.2]. With Z = 2 and no expectation of a resolved chiral molecule, the latter centrosymmetric space group is far more probable,[36] and was later shown to be the correct choice.

All crystallographic calculations were carried out using either the UCI modified version of the UCLA Crystallographic Computing Package[37] or the SHELXTL PLUS program set.[38] The analytical scattering factors for neutral atoms were used throughout the analysis;[39a] both the real ($\Delta f'$) and imaginary ($i\Delta f''$) components of anomalous dispersion[39b] were included. The quantity minimized during least-squares analysis was $\Sigma w(|F_o| - |F_c|)^2$ where $w^{-1} = \sigma^2(|F_o| + 0.0010(|F_o|)^2$.

The structure was solved by direct methods (SHELXTL PLUS); and refined by full-matrix least-squares techniques. Hydrogen atoms were included using a riding model with d(C-H) = 0.96 Å and U(iso) = 0.08 Å^2. Refinement of the model led to convergence with $R_F = 3.0\%$, $R_{wF} = 4.1\%$ and GOF = 1.08 for 415 variables refined against those 7811 data with $|F_o| > 3.0\sigma(|F_o|)$. A final difference-Fourier map yielded $\rho(\max) = 1.25$ eÅ^{-3} at a distance of 1.53 Å from tungsten.

X-ray Data Collection, Structure Determination and Refinement for W(=CHC$_6$H$_4$-*o*-OMe)(N-2,6-C$_6$H$_3$-Me$_2$)[OCMe(CF$_3$)$_2$]$_2$(THF)

A yellow/gold crystal of approximate dimensions 0.32 x 0.34 x 0.40 mm was immersed in Paratone-N (lube-oil additive), mounted on a glass fiber and transferred to the Nicolet P3 diffractometer which is equipped with a modified LT-2 low temperature system. Determination of Laue symmetry, crystal class, unit cell parameters and the crystal's orientation matrix were carried out by previously described techniques similar to those of Churchill.[35] Low temperature (173 K) intensity data were collected via a θ-2θ scan technique with MoKα radiation under the conditions given in Table F-1 (Appendix).

All 6054 data were corrected for absorption and for Lorentz and polarization effects and placed on an approximately absolute scale. Any reflection with I(net) < 0 was assigned the value $|F_o| = 0$. The systematic extinctions observed were $0k0$ for $k = 2n + 1$ and $h0l$ for $l = 2n + 1$; the diffraction symmetry was 2/m. The centrosymmetric monoclinic space group $P2_1/c$ [C_{2h}^5; No. 14] is thus uniquely defined.

All crystallographic calculations were carried out using either the UCI modified version of the UCLA Crystallographic Computing Package[37] or the SHELXTL PLUS program set.[38] The analytical scattering factors for neutral atoms were used throughout the analysis;[39a] both the real ($\Delta f'$) and imaginary ($i\Delta f''$) components of anomalous dispersion[39b] were included. The quantity minimized during least-squares analysis was $\Sigma w(|F_o| - |F_c|)^2$ where $w^{-1} = \sigma^2(|F_o| + 0.0005(|F_o|)^2$.

The structure was solved via an automatic Patterson routine (SHELXTL PLUS); and refined by full-matrix least-squares techniques. Hydrogen atoms were included using a riding model with d(C-H) = 0.96 Å and U(iso) = 0.08 Å^2. Refinement of positional and anisotropic thermal parameters led to convergence with $R_F = 3.8\%$, $R_{wF} = 4.4\%$ and GOF = 1.39 for 415 variables refined against all 5269 unique data with $|F_o| > 0$; ($R_F = 3.1\%$, $R_{wF} = 4.1\%$ for those 4576 data with $|F_o| > 6.0\sigma(|F_o|)$). A final difference-Fourier map yielded $\rho(\max) = 2.29$ eÅ^{-3} at a distance of 0.95 Å from tungsten.

X-ray Data Collection, Structure Determination and Refinement for W(=CHC$_6$H$_4$-*o*-OMe)[2,6-C$_6$H$_3$-(*i*-Pr)$_2$][OCMe(CF$_3$)$_2$]$_2$

A bright red crystal of approximate dimensions 0.20 x 0.30 x 0.32 mm was immersed in Paratone-N (lube-oil additive), mounted on a glass fiber and transferred to the Syntex $P2_1$ diffractometer which is equipped with a modified LT-1 low temperature system. Determination of Lau symmetry, crystal class, unit cell parameters and the crystal's orientation matrix were carried out by previously described techniques similar to those of Churchill.[35] Low temperature (183 K) intensity data were collected via a θ-2θ scan technique with Mo$K\alpha$ radiation under the conditions given in Table G-1 (Appendix).

All 6092 data were corrected for absorption and for Lorentz and polarization effects and placed on an approximately absolute scale. Any reflection with I(net) < 0 was assigned the value $|F_o| = 0$. The systematic extinctions observed were $0k0$ for $k = 2n + 1$ and $h0l$ for $l = 2n + 1$; the diffraction symmetry was 2/m. The centrosymmetric monoclinic space group $P2_1/c$ [C_{2h}^5; No. 14] is thus uniquely defined.

All crystallographic calculations were carried out using either the UCI modified version of the UCLA Crystallographic Computing Package[37] or the SHELXTL PLUS program set.[38] The analytical scattering factors for neutral atoms were used throughout the analysis;[39a] both the real ($\Delta f'$) and imaginary ($i\Delta f''$) components of anomalous dispersion[39b] were included. The quantity minimized during least-squares analysis was $\Sigma w(|F_o| - |F_c|)^2$ where $w^{-1} = \sigma^2(|F_o|) + 0.0010(|F_o|)^2$.

The structure was solved via an automatic Patterson routine (SHELXTL PLUS); and refined by full-matrix least-squares techniques. All hydrogen atoms were located from a series of difference-Fourier syntheses and included in the refinement with isotropic temperature factors. Full-matrix least-squares refinement of the model led to convergence with $R_F = 3.4\%$, $R_{wF} = 4.1\%$ and GOF = 1.00 for 530 variables refined against all 5195 unique data with $|F_o| > 0$; ($R_F = 2.5\%$, $R_{wF} = 3.7\%$ for those 4434 data with $|F_o| > 6.0\sigma(|F_o|)$). A final difference-Fourier map showed no significant features, $\rho(\max) = 1.17$ eÅ^{-3} at a distance of 1.06 Å from tungsten.

References and Notes

(1) (a) Schmidbaur, H. *Acc. Chem. Res.* **1975**, *8*, 62-70. (b) Schmidbaur, H. *Adv. Organomet. Chem.* **1976**, *14*, 205-243. (c) Schmidbaur, H.; Jeong, J.; Schier, A.; Graf, W.; Wilkinson, D. L.; Muller, G. *New. J. Chem.* **1989**, *13*, 341-352. (d) Schmidbaur, H. *Angew. Chem., Int. Ed. Engl.* **1983**, *22*, 907-927. (e) Kaska, W. C. *Coord. Chem. Rev.* **1983**, *48*, 1-58. (f) Schmidbaur, H. *Pure & Appl. Chem.* **1978**, *50*, 19-25.

(2) McLain, S. J.; Wood, C. D.; Messerle, L. W.; Schrock, R. R.; Hollander, F. J.; Youngs, W. J.; Churchill, M. R. *J. Am. Chem. Soc.* **1978**, *100*, 5962-5964.

(3) Casey, C. P.; Burkhardt, T. J. *J. Am. Chem. Soc.* **1972**, *94*, 6543-6544.

(4) Knoll, L. *J. Organomet. Chem.* **1978**, *148*, C25-C26.

(5) Sharp, P. R.; Schrock, R. R. *J. Organomet. Chem.* **1979**, *171*, 43-51.

(6) Schwartz, J.; Gell, K. I. *J. Organomet. Chem.* **1980**, *184*, C1-C2.

(7) van Asselt, A.; Burger, B. J.; Gibson, V. C.; Bercaw, J. E. *J. Am. Chem. Soc.* **1986**, *108*, 5347-5349.

(8) (a) Cannizzo, L. F.; Grubbs, R. H. *Macromolecules* **1987**, *20*, 1488-1490. (b) Risse, W.; Grubbs, R. H. *Macromolecules* **1989**, *22*, 1558-1562. (c) Mitchell, J. P.; Gibson, V. C.; Schrock, R. R. *Macromolecules* **1991**, *24*, 1220-1221.

(9) (a) Brown-Wensley, K. A.; Buchwald, S. L.; Cannizzo, L.; Clawson, L.; Ho, S.; Meinhardt, D.; Stille, J. R.; Straus, D.; Grubbs, R. H. *Pure & Appl. Chem.* **1983**, *55*, 1733-1744. (b) Pine, S. H.; Zahler, R.; Evans, D. A.; Grubbs, R. H. *J. Am. Chem. Soc.* **1980**, *102*, 3270-3272. (c) Aguero, A.; Kress, J.; Osborn, J. A. *J. Chem. Soc., Chem. Commun.* **1986**, 531-533. (d) Heppert, J. A.; Dietz, S. D.; Morton, M. D. *Abstracts of Papers*, 199th National Meeting of the American Chemical Society, Boston, MA; American Chemical Society: Washington, DC, 1990; INOR 262. (e) Bazan, G. C.; Schrock, R. R.; O'Regan, M. B. *Organometallics* **1991**, *10*, 1062-1067.

(10) Risse, W.; Wheeler, D. R.; Cannizzo, L. F.; Grubbs, R. H. *Macromolecules* **1989**, *22*, 3205-3210.

(11) See, for example: (a) Schrock, R. R.; DePue, R. T.; Feldman, J.; Schaverien, C. J.; Dewan, J. C.; Liu, A. H. *J. Am. Chem. Soc.* **1988**, *110*, 1423-1435. (b) Schrock, R. R.; Feldman, J.; Cannizzo, L. F.; Grubbs, R. H. *Macromolecules* **1987**, *20*, 1169-1172. (c) Schrock, R. R.; DePue, R. T.; Feldman, J.; Yap, K. B.; Yang, D. C.; Park, L.; DiMare, M.; Schofield, M.; Anhaus, J.; Walborsky, E.; Evitt, E.; Kruger, C.; Betz, P. *Organometallics* **1990**, *9*, 2262-2275. (d) Schrock, R. R. *Acc. Chem. Res.* **1990**, *23*, 158-165. (e) Kress, J.; Aguero, A.; Osborn, J. A. *J. Mol. Catal.* **1986**, *36*, 1-12. (f) Kress, J.; Osborn, J. A.; Greene, R. M. E.; Ivin, K. J.; Rooney, J. J. *J. Am. Chem. Soc.* **1987**, *109*, 899-901. (g) Quignard, F.; Leconte, M.; Basset, J. M. *J. Mol. Catal.* **1986**, *36*, 13-29. (h) Quignard, F.; Leconte, M.; Basset, J.-M. *J. Chem. Soc., Chem. Commun.* **1985**, 1816-1817. (i) Blosch, L. L.; Abboud, K.; Boncella, J. M. *J. Am. Chem. Soc.* **1991**, *113*, 7066-7068. (j) Murdzek, J. S.; Schrock, R. R. *Organometallics* **1987**, *6*, 1373-1374. (k) Murdzek, J. S.; Schrock, R. R. *Macromolecules* **1987**, *20*, 2640-2642. (l) Schrock, R. R.; Murdzek, J. S.; Bazan, G. C.; Robbins, J.; DiMare, M.; O'Regan, M. *J. Am. Chem. Soc.* **1990**, *112*, 3875-3886. (m) Bazan, G. C.; Oskam, J. H.; Cho, H.-N.; Park, L. Y.; Schrock, R. R. *J. Am. Chem. Soc.* **1991**, *113*, 6899-6907. (n) Toreki, R.; Schrock, R. R.

J. Am. Chem. Soc. **1990,** *112,* 2448-2449. (o) Schofield, M. H.; Schrock, R. R.; Park, L. Y. *Organometallics* **1991,** *10,* 1844-1855. (p) Nguyen, S. T.; Johnson, L. K.; Grubbs, R. H.; Ziller, J. W. *J. Am. Chem. Soc.* **1992,** *114,* 3974-3975.

(12) (a) Bradley, D. C.; Hursthouse, M. B.; Malik, K. M. A.; Nielson, A. J.; Short, R. L. *J. Chem. Soc., Dalton Trans.* **1983**, 2651-2656. (b) Nielson, A. J.; McCarley, R. E.; Laughlin, S. L.; Carlson, C. D. In *Inorg. Syn.*; Schreeve, J. M., Ed.; John Wiley & Sons: New York, 1986; Vol. 24, pp 194-200.

(13) Su, F.-M.; Bryan, J. C.; Jang, S.; Mayer, J. M. *Polyhedron* **1989,** *8,* 1261-1277.

(14) Pedersen, S. F.; Schrock, R. R. *J. Am. Chem. Soc.* **1982,** *104,* 7483-7491.

(15) Schrock, R. R. In *Reactions of Coordinated Ligands*; Braterman, P. S., Ed.; Plenum: New York, 1986; Vol. 1, pp 221-283.

(16) This structure may be compared with that of $W(=CH\text{-}t\text{-}Bu)Cl_2(O)(PMe_3)_2$. In this molecule, the alkylidene substituent lies syn to the oxo ligand, the W=C distance is 1.986(21) Å, and the W(1) - C(1) - C(2) angle is 142.4(19)°. See: Churchill, M. R.; Rheingold, A. R. *Inorg. Chem.* **1982,** *21,* 1357-1359.

(17) In order to maximize π-bonding, the alkylidene substituent must lie in the N - W - C_α plane. Two isomers are then possible: (1) a syn rotamer, in which the alkylidene substituent points toward the imido ligand, and (2) an anti rotamer, in which the alkylidene substitutent points away from the imido ligand. Detailed studies of syn and anti rotamers of arylimido alkylidene complexes have been reported by Schrock and coworkers: Schrock, R. R.; Crowe, W. E.; Bazan, G. C.; DiMare, M.; O'Regan, M. B.; Schofield, M. H. *Organometallics* **1991,** *10,* 1832-1843.

(18) Please see Chapter 2 of this thesis.

(19) The reactions were carried out at room temperature in THF-d_8 using stoichiometric amounts of the tungsten(IV) precursors and $Ph_3P{=}CH_2$ or $Ph_3P{=}CHMe$. The resulting ^1H NMR spectra of the products were complicated and difficult to completely analyze. Downfield peaks were observed, and it was on this basis that alkylidene transfer was believed to have occurred. Given the high nucleophilicity and small size of the methylidene and ethylidene ylides, displacement of a chloride ligand by the ylide and formation of a zwitterionic ylide adduct with tungsten is likely, and the observation of several H_α resonances in some cases may be an indication that this occurred.* ^1H NMR Data: $WCl_2(NPh)(PMePh_2)_3$ + $Ph_3P{=}CH_2$ (yellow, THF-d_8) δ 10.7, 10.3, 9.6, 9.3 (m, H_α); $WCl_2(N\text{-}2,6\text{-}C_6H_3\text{-}Me_2)(PEt_2Ph)_3$ + $Ph_3P{=}CH_2$ (yellow, THF-d_8) δ 11.7, 11.2, 10.6 (m, H_α); $WCl_2(NPh)(PMePh_2)_3$ + $Ph_3P{=}CHMe$ (orange, THF-d_8) δ 10.8 (m, H_α); $WCl_2(N\text{-}2,6\text{-}C_6H_3\text{-}Me_2)(PEt_2Ph)_3$ + $Ph_3P{=}CHMe$ (red, THF-d_8) 12.5 (m, H_α).
[*Note: The reaction between $WCl_2(N\text{-}2,6\text{-}C_6H_3\text{-}Me_2)[P(OMe)_3]_3$ and 2.5 equiv of $Ph_3P{=}CH_2$ was quite clean and preliminary analysis (^1H, ^{13}C, and ^{31}P NMR spectroscopy and the low solubility of the complex in nonpolar solvents) point toward the formation of ethylene and an alkylidene transfer product that is modified, perhaps, by the displacement of chloride ligands by excess phosphorane to yield zwitterionic ylide adducts. Downfield multiplets were also observed in the ^1H NMR spectra of preliminary reactions involving the simultaneous mixing of $WCl_2[N\text{-}2,6\text{-}C_6H_3\text{-}(i\text{-}Pr)_2][P(OMe)_3]_3$ and one equiv of $Ph_3P{=}CH_2$ in the presence of 2 equiv of $LiOMe(CF_3)_2$ or $LiO\text{-}2,6\text{-}C_6H_3\text{-}(i\text{-}Pr)_2$.]

(20) The tetracoordinate complex W(=CH-*t*-Bu)[N-2,6-C_6H_3-(*i*-Pr)$_2$][OCMe(CF_3)$_2$]$_2$ is isolable due to stabilization by the substantial steric bulk of the alkylidene, alkoxide, and imido ligands. A decrease in size of any one of these ligands generally renders analogues of this compound unstable in the absence of a strong Lewis base.[11a,c]

(21) See reference 1 for examples. Also, see: Finch, W. Ph. D. Thesis, California Institute of Technology, 1986.

(22) A bright magenta solution formed upon reaction of **8** with Ph_3P=CHC_6H_4-*p*-CF_3, and very tentatively, the ^{1}H NMR spectrum appeared consistent with the displacement of a chloride ligand and formation of an ylide adduct: ^{1}H(C_6D_6) δ 5.15 (d, J_{HP} = 16 Hz, C(*H*)(Ar)(PPh_3)), 3.29 (s, NAr: Me_2), 2.13 (s, OCMe(CF_3)$_2$).

(23) A preliminary account of this research has been published: Johnson, L. K.; Virgil, S. C.; Grubbs, R. H.; Ziller, J. W. *J. Am. Chem. Soc.* **1990**, *112*, 5384-5385.

(24) Nugent, W. A.; Mayer, J. M. *Metal-Ligand Multiple Bonds*; John Wiley & Sons: New York, 1988; pp 35-36, and references therein.

(25) (a) According to an X-ray diffraction study, the methoxy group coordinates to chromium in (OC)$_4$Cr[=C(OMe)(*o*-C_6H_4-OMe). See: Dotz, K. H.; Sturm, W.; Popall, M.; Riede, J. *J. Organomet. Chem.* **1984**, *277*, 267-275. (b) For information on analogous tungsten complexes, see: Dotz, K. H.; Erben, H.-G., Staudacher, W.; Harms, K.; Muller, G.; Riede, J. *J. Organomet. Chem.* **1988**, *355*, 177-191.

(26) For examples, see references 11a, 14, 17, and 18.

(27) Ivin, K. J.; Laverty, D. T.; Rooney, J. J. *Makromol. Chem.* **1977**, *178*, 1545-1559.

(28) More detailed studies of the olefinations of carbonyl compounds by the alkylidene complexes reported in this chapter have been undertaken: Ulibarri, T. A.; France, M. B.; Fu, G. C.; Grubbs, R. H., unpublished results.

(29) (a) Klavetter, F. L.; Grubbs, R. H. *J. Am. Chem. Soc.* **1988**, *110*, 7807-7813. (b) Ginsburg, E. J.; Gorman, C. B.; Marder, S. R.; Grubbs, R. H. *J. Am. Chem. Soc.* **1989**, *11*, 7621-7622. (c) Gorman, C. B.; Ginsburg, E. J.; Marder, S. R.; Grubbs, R. H. *Angew. Chem., Int. Ed. Engl.* **1989**, *101*, 1603-1606.

(30) The use of the *o*-methoxybenzylidene catalyst for polymerizing COT monomers has been reported: (a) Moore, J. S.; Gorman, C. B.; Grubbs, R. H. *J. Am. Chem. Soc.* **1991**, *113*, 1704-1712. (b) Gorman, C. B. Ph.D. Thesis, California Institute of Technology, 1992.

(31) Frey, M.; Grubbs, R. H., unpublished results.

(32) Landauer, S. R.; Rydon, H. N. *J. Chem. Soc.* **1953**, 2224-2234.

(33) Seyferth, D.; Singh, G. *J. Am. Chem. Soc.* **1965**, *87*, 4156-4162.

(34) Paulson, P. L.; Watts, W. E. *J. Chem. Soc.* **1963**, 2990-2996.

(35) Churchill, M. R.; Lashewycz, R. A.; Rotella, F. J. *Inorg. Chem.* **1977**, *16*, 265-271.

(36) Nowacki, W.; Matsumoto, T.; Edenharter, A. *Acta Crystallogr.* **1967**, *22*, 935-940.

(37) UCLA Crystallographic Computing Package, University of California Los Angeles, 1981, C. Strouse; personal communication.

(38) Siemens Analytical X-Ray Instruments, Inc.; Madison, WI 1988.

(39) *International Tables for X-Ray Crystallography*, Kynoch Press: Birmingham, England, 1974; (a) pp 99-101; (b) pp 149-150.

Chapter 4

Reactions of $WCl_2(NAr)(PX_3)_3$ [$PX_3 = PR_3$, $P(OMe)_3$] Complexes with *exo*-5,6-Dimethoxymethyl-7-Oxanorbornene

Introduction

Aqua ruthenium complexes of 7-oxanorbornenes rapidly initiate the ring-opening metathesis polymerization (ROMP) of strained, cyclic olefins (eq 1).[1] These catalysts are active in protic solvents, including water, and are able to metathesize monomers incorporating a number of functional groups. However, the small percentage of ruthenium that actually initiates the polymerization has thus far prevented a detailed understanding of the polymerization mechanism, although evidence in support of a ruthenium carbene intermediate now exists.[2] In the following study, the reactions of *exo*-5,6-dimethoxymethyl-7-oxanorbornene (7-oxanorbornene) with $WCl_2(NAr)(PX_3)_3$ complexes were investigated in order to gain further insight into the modes of reactivity of this olefin with transition metals.

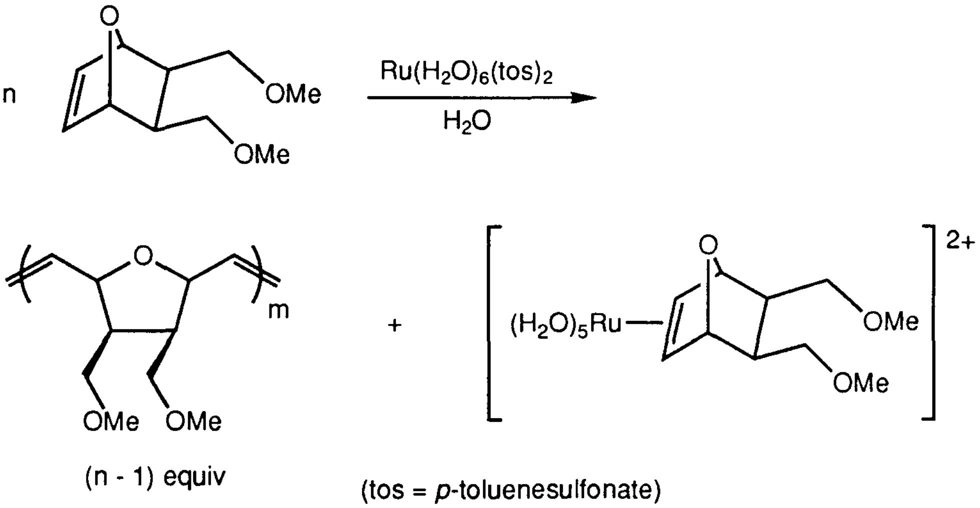

(tos = *p*-toluenesulfonate)

(1)

Results

η²-(7-Oxanorbornene) Complexes. The phenyl- and 2,6-dimethylphenylimido tungsten(IV) precursors $WCl_2(NPh)(PMePh_2)_3$, $WCl_2(NPh)[P(OMe)_3]_3$, and $WCl_2(N\text{-}2,6\text{-}C_6H_3\text{-}Me_2)(PEt_2Ph)_3$ reacted at room temperature with 7-oxanorbornene to form the corresponding η^2-olefin complexes (eq 2).[3-5] Large upfield shifts of the olefinic proton and carbon resonances, characteristic of η^2-complex formation, were observed by NMR spectroscopy.[6] These resonances appeared as triplets due to coupling with the two trans phosphine/phosphite ligands (Table 1). Upon irradiation of the *ortho* proton of the phenylimido ligand of $W[\eta^2\text{-(7-oxanorbornene)}]Cl_2(NPh)[P(OMe)_3]_2$, NOE enhancements were observed for the bridgehead and ether proton resonances, but not for the olefinic proton resonance. These observations are consistent with a syn orientation of the imido ligand and the oxo substituent of the olefin, as depicted in eq 2.

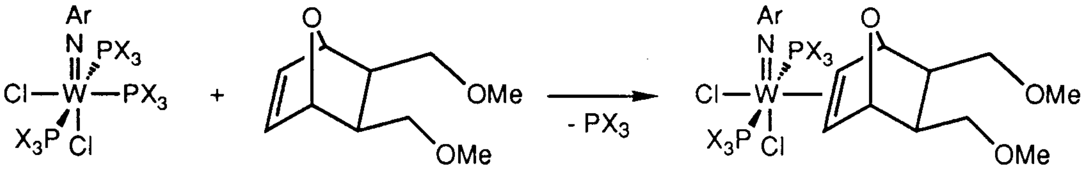

(2)

Oxo Abstraction. In the reaction of 7-oxanorbornene with the 2,6-di-*i*-propylphenylimido precursor $WCl_2[N\text{-}2,6\text{-}C_6H_3\text{-}(i\text{-}Pr)_2][P(OMe)_3]_3$, an upfield triplet indicative of an η^2-olefin complex was not observed in the ^1H NMR spectrum; instead, two olefinic multiplets were observed between 5.5 and 6 ppm. The volatile components of the reaction mixture were identified by ^1H, ^{13}C, and GC-mass spectral data as $P(OMe)_3$ and 5,6-dimethoxymethylcyclohexadiene, the product of oxygen abstraction from 7-oxanorbornene (eq 3). The organometallic products were not identified, although the ^{31}P NMR spectrum of the original reaction mixture indicated the presence of only

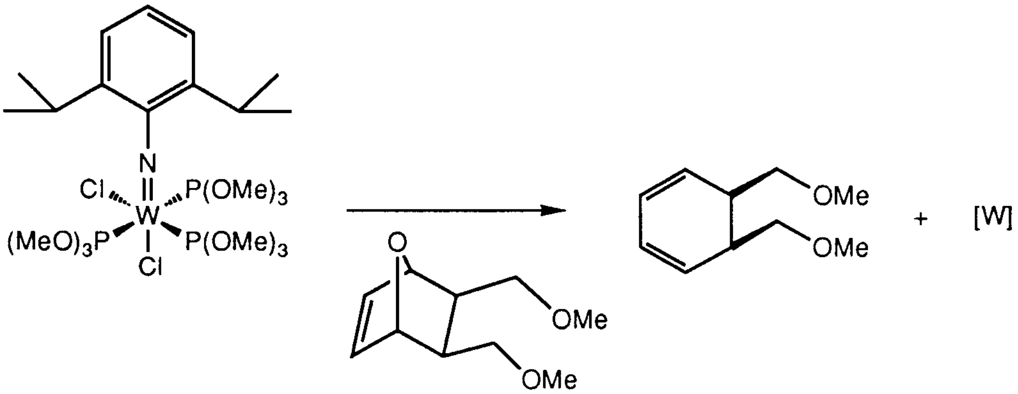

(3)

Table 1. Selected NMR Spectral Data for η^2-(*exo*-5,6-Dimethoxymethyl-7-Oxanorbornene) Complexes[a]

η^2-(7-Oxanorbornene) Complex	^{1}H (t, *H*C=C*H*)[b]		^{13}C (t, H*C*=*C*H)[c]				^{31}P	
	δ	J_{HP}	δ	J_{CH}	J_{CP}	J_{CW}	δ	J_{PW}
W[η^2-(7-oxanorbornene)]Cl_2(NPh)$(PMePh_2)_2$[12]	2.77	4.64	—	—	—	—	—	—
W[η^2-(7-oxanorbornene)]Cl_2(NPh)$[P(OMe)_3]_2$	3.97[d]	5.13	61.7	167	8.5	25.2	119.9[c]	374
W[η^2-(7-oxanorbornene)]Cl_2(N-2,6-C_6H_3-Me_2)$(PEt_2Ph)_2$	*e*	*e*	67.8	167	—	—	4.2[b]	212

[a]Uncomplexed *exo*-5,6-dimethoxymethyl-7-oxanorbornene: ^{1}H (C_6D_6) δ 5.96 (s, *H*C=C*H*); ^{13}C (CD_2Cl_2) δ 135.8 (J_{CH} = 177.6, H*C*=*C*H). [b]In C_6D_6. [c]In CD_2Cl_2. [d]J_{HW} = 5.26, *H*C=C*H*. [e]Overlaps with other resonances.

free P(OMe)$_3$ and tungsten-complexed P(OMe)$_3$ [123.8 ppm, J_{PW} = 451.6 Hz] in a roughly 3:2 ratio. In addition to the η^2-olefin complex, a small amount of 5,6-dimethoxymethylcyclohexadiene was also observed for the room temperature reaction of 7-oxanorbornene and WCl$_2$(NPh)(PMePh$_2$)$_3$ in C$_6$D$_6$.

Discussion

Paralleling the trends observed for the formation of η^2-(3,3-disubstituted)cyclopropene complexes, the observation of η^2-olefin complexes upon reaction of 7-oxanorbornene with WCl$_2$(NAr)(PX$_3$)$_3$ precursors is dependent on the steric bulk of the imido ligand.[7] Use of phenyl- and 2,6-dimethylphenylimido precursors enables the rapid formation of η^2-(7-oxanorbornene) complexes. The orientation of the olefinic substituents syn to the imido ligand, as indicated by difference NOE spectroscopy, is the same orientation that was confirmed by an X-ray crystallographic study for the analogous complex of 3,3-diphenylcyclopropene.[7]

Use of the more bulky 2,6-di-*i*-propylphenylimido precursor enables the observation of an oxygen-abstraction reaction. The lack of formation of OP(OMe)$_3$ and the occurrence of the reaction at room temperature suggest that the oxo abstraction from 7-oxanorbornene is not catalyzed by P(OMe)$_3$, although the deoxygenation of epoxides by P(OEt)$_3$ to form OP(OEt)$_3$ and the corresponding olefins has been observed at high temperatures.[8] It is more likely that the abstraction of oxygen is catalyzed by tungsten, which would be consistent with previous demonstrations of epoxide deoxygenation by several reduced tungsten species.[9] Unfavorable steric interactions between the *i*-propyl substituents of the arylimido ligand and the 7-oxanorbornene substituents probably prevent formation of a stable η^2-olefin complex and instead allow observation of the products resulting from the coordination and subsequent reaction of the oxo functionality with tungsten.

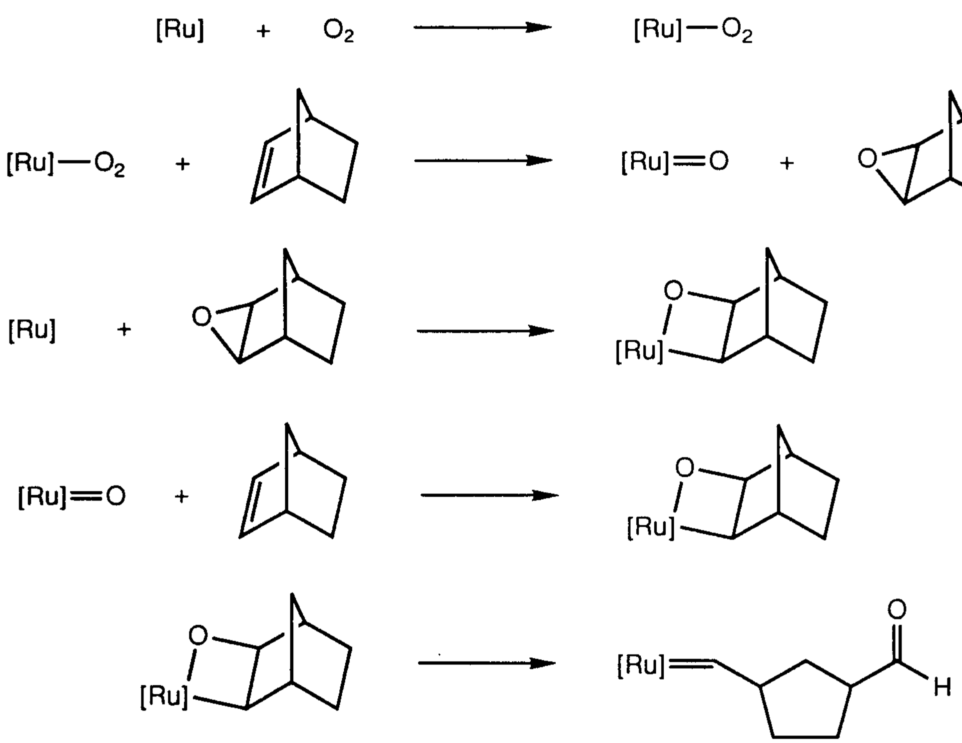

Figure 1. Proposed activation of metathesis catalyst precursors by oxygen.[10]

Further investigations, including the clean isolation of 5,6-dimethoxymethylcyclohexadiene, the identification of the tungsten product, and additional NMR studies, are needed in order to confirm oxo-abstraction by tungsten and to determine the mechanism of this reaction. However, the isolation of 5,6-dimethoxymethylcyclohexadiene strongly indicates that 7-oxanorbornene is a potential source of oxo ligands for transition metals. This observation is of interest as oxo ligands have been implicated in the initiation of ROMP by late-metal systems. For example, in a study involving two ruthenium(II) complexes $RuCl_2(PPh_3)_4$ and $RuCl_2(py)_2(PPh_3)_2$, it was noted that addition of O_2 to solutions of these catalyst precursors and norbornene greatly increased the rate of ROMP.[10] *exo*-2,3-Epoxynorbornene, a reaction product, activated the catalysts in the absence of oxygen. A mechanism involving both ruthenium oxo and metallaoxetane intermediates was suggested (Figure 1). The relevance of these studies to the mechanism of ROMP initiation by aqueous η^2-(7-oxanorbornene) ruthenium(II) catalyst precursors is being investigated.[11]

Experimental Section

General Considerations

All manipulations of air- and/or water-sensitive compounds were performed using standard high-vacuum or Schlenk techniques. Argon was purified by passage through columns of BASF R3-11 catalyst (Chemalog) and 4 Å molecular sieves (Linde). Solid organometallic compounds were transferred and stored in a nitrogen-filled Vacuum Atmospheres drybox. NMR spectra were recorded with either a JEOL FX-90Q (89.60 MHz ^1H; 22.53 MHz ^{13}C; 36.20 MHz ^{31}P), a JEOL GX-400 (399.65 MHz ^1H; 100.40 MHz ^{13}C), or a QE-300 Plus (300.10 MHz ^1H; 75.49 MHz ^{13}C) spectrometer. All coupling constants are reported in Hz.

Materials

Toluene, benzene, diethyl ether, tetrahydrofuran, and pentane were distilled or vacuum-transferred from sodium-benzophenone ketyl. Pentane was first stirred over concentrated H_2SO_4 and dried over $MgSO_4$ and CaH_2 before being transferred onto sodium-benzophenone ketyl solubilized with tetraglyme. Benzene-d_6, toluene-d_8, and THF-d_8 were dried over sodium-benzophenone ketyl. Methylene chloride and methylene chloride-d_2 were dried over CaH_2, vacuum-transferred, and then degassed by repeated freeze-pump-thaw cycles. *exo*-5,6-Dimethoxymethyl-7-oxanorbornene was the generous gift of Pui Tong Ho, $WCl_2(NPh)(PMePh_2)_3$ was synthesized according to the published procedure,[13] and $WCl_2(NPh)[P(OMe)_3]_3$, $WCl_2(N\text{-}2,6\text{-}C_6H_3\text{-}Me_2)(PEt_2Ph)_3$, and $WCl_2[N\text{-}2,6\text{-}C_6H_3\text{-}(i\text{-}Pr)_2][P(OMe)_3]_3$ were synthesized as previously described.[7]

W[η^2-(*exo*-5,6-Dimethoxymethyl-7-oxanorbornene)]$Cl_2(NPh)[P(OMe)_3]_2$

A 6 mL Et_2O solution of *exo*-5,6-dimethoxymethyl-7-oxanorbornene (347.8 mg, 1.89 mmol) was added to an 8 mL Et_2O suspension of $WCl_2(NPh)[P(OMe)_3]_3$ (1.31 g, 1.83 mmol). A yellow precipitate formed as the reaction mixture was stirred for 22.5 h.

Following the addition of 20 mL of pentane, the suspension was filtered to yield 1.25 g (87.7%) of pale yellow powder: ^{1}H (C_6D_6) δ 7.76 (d, 2, J = 7.45, NPh: H$_o$), 6.91 (t, 2, J = 7.69, NPh: H$_m$), 6.76 (t, 1, J = 7.42, NPh: H$_p$), 5.04 (s, 2, =CH-C*H*), 3.97 (t, 2, J_{HP} = 5.13, J_{HW} = 5.26, HC=CH), 3.63 (t, 18, J_{HP} = 5.23, P(OMe)$_3$), 3.34 (m, 4, CHC*H*$_2$OMe), 3.12 (s, 6, CHCH$_2$O*Me*), 2.58 (m, 2, C*H*CH$_2$OMe); ^{13}C (CD_2Cl_2) δ 153.7 (t, J_{CP} = 2.8, J_{CW} = 36, NPh: C$_{ipso}$), 127.4 (NPh: C$_m$), 126.7 (t, J_{CP} = 2.6, NPh: C$_o$), 126.2 (NPh: C$_p$), 83.0 (=CH-*C*H), 71.5 (CH*C*H$_2$OMe), 61.7 (t, J_{CH} = 167.0, J_{CP} = 8.5, J_{CW} = 25.2, HC=CH), 57.9 (CHCH$_2$O*Me*), 53.3 (t, J_{CP} = 3.19, P(OMe)$_3$), 47.2 (*C*HCH$_2$OMe); ^{31}P (CD_2Cl_2) δ 119.9 (J_{PW} = 374); NOEDS (C_6D_6) irradiation at 7.76 ppm, δ 6.91 (11.7% NOE), 5.04 (1.8% NOE), 3.63 (1.1% NOE), 3.34 (0.5% NOE), 3.12 (1.2% NOE); irradiation at 5.04, δ 7.76 (2.7% NOE), 3.97 (4.5% NOE), 2.58 (2.9% NOE); irradiation at 3.97, δ 5.04 (5.2% NOE), 3.12 (0.7% NOE), 2.58 (6.6% NOE); irradiation at 3.34, δ 5.04 (7.2% NOE), 3.12 (3.2% NOE); irradiation at 3.12, δ 5.04 (1.9% NOE), 3.63 (0.3% NOE), 2.58 (1.7% NOE).

W[η^2-(*exo*-5,6-Dimethoxymethyl-7-oxanorbornene)]Cl$_2$(N-2,6-C$_6$H$_3$-Me$_2$)(PEt$_2$Ph)$_2$

A 7 mL Et$_2$O solution of *exo*-5,6-dimethoxymethyl-7-oxanorbornene (317 mg, 1.72 mmol) was added to 1.50 g (1.72 mmol) of solid WCl$_2$(N-2,6-C$_6$H$_3$-Me$_2$)(PEt$_2$Ph)$_3$, and the reaction mixture was stirred for 17.5 h. Next, 30 mL of pentane was added to the reaction mixture, and the resulting suspension was filtered. The tan product was washed with an additional 15 mL of pentane before it was dried under vacuum (837 mg, 54.6%): ^{1}H (C_6D_6) δ 7.6 - 6.7 (m, 13, H$_{aryl}$), 4.14 (s, 2, =CH-C*H*), 3.3 - 2.1 (m's, 16, *H*C=C*H*, C*H*C*H*$_2$OMe), P(C*H*$_2$CH$_3$)$_2$Ph), 3.04 (s, 6, CHCH$_2$O*Me*), 2.55 (s, 6, NAr: Me$_2$), 1.12 (m, 6, P(CH$_2$C*H*$_3$)(CH$_2$CH$_3$)'Ph), 0.92 (m, 6, P(CH$_2$CH$_3$)(CH$_2$C*H*$_3$)'Ph); ^{13}C (CD_2Cl_2) δ 152.2 (J_{CW} = 37.7, NAr: C$_{ipso}$), 137.7 (NAr: C$_o$), 132.0 (PEt$_2$*Ph*: C$_o$), 131.7 (t, J_{CP} = 19.5, PEt$_2$*Ph*: C$_{ipso}$), 129.4 (PEt$_2$*Ph*: C$_p$), 127.9 (PEt$_2$*Ph*: C$_m$ and NAr: C$_m$), 126.0 (NAr: C$_p$), 82.3 (=CH-*C*H), 71.7 (CH*C*H$_2$OMe), 67.8 (J_{CH} = 167.3, HC=CH), 58.3

($CHCH_2OMe$), 47.8 ($CHCH_2OMe$), 21.1 (NAr: Me_2), 16.2 (t, J_{CP} = 11.2, $P(CH_2CH_3)$-$(CH_2CH_3)'Ph$), 15.1 (t, J_{CP} = 13.2, $P(CH_2CH_3)(CH_2CH_3)'Ph$), 8.8 ($P(CH_2CH_3)$-$(CH_2CH_3)'Ph$), 8.3 $P(CH_2CH_3)(CH_2CH_3)'Ph$); ^{31}P (C_6D_6) δ 4.2 (J_{PW} = 212).

Observation of the Reaction of *exo*-5,6-Dimethoxymethyl-7-Oxanorbornene with $WCl_2[N\text{-}2,6\text{-}C_6H_3\text{-}(i\text{-}Pr)_2][P(OMe)_3]_3$

The tungsten complex $WCl_2[N\text{-}2,6\text{-}C_6H_3\text{-}(i\text{-}Pr)_2][P(OMe)_3]_3$ and a slight excess of *exo*-5,6-dimethoxymethyl-7-oxanorbornene were dissolved in CD_2Cl_2 and then mixed. After ~12 h, ^1H and ^{31}P NMR spectra were acquired. (Prior monitoring of the same reaction in C_6D_6 had indicated that the reaction was only 50% complete after 4 h at room temperature.) The ^{31}P NMR spectrum indicated that $WCl_2[N\text{-}2,6\text{-}C_6H_3\text{-}(i\text{-}Pr)_2][P(OMe)_3]_3$ was completely consumed and that free $P(OMe)_3$ (141.5 ppm) and a new tungsten species (123.8 ppm, J_{PW} = 451.6 Hz) were formed in roughly a 3:2 ratio. According to the ^1H NMR spectrum, a small amount of 7-oxanorbornene (~5%) remained unreacted, and new olefinic multiplets appeared at 5.5 - 6.0 ppm. In order to identify the organic products, the reaction was repeated on a preparative scale and the volatile components were vacuum-transferred. Spectrocopic data was consistent with the presence of free $P(OMe)_3$ and 5,6-dimethoxymethylcyclohexadiene. Spectroscopic data for the latter compound follow: LRMS: m/e 168 (M^+); ^1H (C_6D_6) δ 5.85 (m, 2, =CH-CH=), 5.76 (m, 2, CH-CH=CH), 3.41 (dd, 2, J = 9.16, 6.65, OCHH'), 3.24 (dd, 2, J = 9.10, 7.17, OCHH'), 3.07 (s, 6, OCH_3), 2.78 (m, 2, CH_2CH); ^{13}C (C_6D_6) δ 128.59 (J_{CH} = 163.5, =CH-CH=), 124.6 (J_{CH} = 158.7, CH-CH=CH), 72.0 (J_{CH} = 143.7, OCH_2), 58.4 (J_{CH} = 140.1, OCH_3), 36.5 (J_{CH} = 129.3, CH_2CH).

References and Notes

(1) (a) Novak, B. M.; Grubbs, R. H. *J. Am. Chem. Soc.* **1988**, *110*, 7542-7543. (b) Novak, B. M.; Grubbs, R. H. *J. Am. Chem. Soc.* **1988**, *110*, 960-961. (c) Hillmyer, M. A.; Lepetit, C.; McGrath, D. V.; Novak, B. M.; Grubbs, R. H. *Macromolecules* **1992**, in press.

(2) France, M. B.; McGrath, D. V.; Paciello, R. A.; Grubbs, R. H., paper to be submitted to *Macromolecules*. (b) France, M. B.; Paciello, R. A.; Grubbs, R. H., paper to be submitted to *Macromolecules*.

(3) For additional examples of π-complex formation involving precursors of this type, please see Chapter 2 of this thesis and references 4 and 5.

(4) (a) Nielson, A. J.; Ware, D. C. *Polyhedron* **1990**, *9*, 603-610. (b) Clark, G. R.; Nielson, A. J.; Rickard, C. E. F.; Ware, D. C. *J. Chem. Soc., Dalton Trans.* **1990**, 1173-1178. (c) Clark, G. R.; Nielson, A. J.; Rickard, C. E. F.; Ware, D. C. *J. Chem. Soc., Chem. Commun.* **1989**, 343-345. (d) Clark, G. R.; Nielson, A. J.; Rickard, C. E. F. *J. Chem. Soc., Chem. Commun.* **1989**, 1157-1159.

(5) (a) Su, F.-M.; Cooper, C.; Geib, S. J.; Rheingold, A. L.; Mayer, J. M. *J. Am. Chem. Soc.* **1986**, *108*, 3545-3547. (b) Su, F.-M.; Bryan, J. C.; Jang, S.; Mayer, J. M. *Polyhedron* **1989**, *8*, 1261-1277. (c) Bryan, J. C.; Mayer, J. M. *J. Am. Chem. Soc.* **1990**, *112*, 2298-2308. (d) Bryan, J. C.; Geib, S. J.; Rheingold, A. L.; Mayer, J. M. *J. Am. Chem. Soc.* **1987**, *109*, 2826-2828.

(6) (a) Crabtree, R. H. *The Organometallic Chemistry of the Transition Metals*; John Wiley & Sons: New York, 1988; Chapter 5. (b) Collman, J. P.; Hegedus, L. S.; Norton, J. R.; Finke, R. G. *Principles and Applications of Organotransition Metal Chemistry*; University Science Books: Mill Valley, CA, 1987; pp 149-155.

(7) Please see Chapter 2 of this thesis.

(8) Scott, C. B. *J. Org. Chem.* **1957**, *22*, 1118-1119.

(9) (a) Sharpless, K. B.; Umbreit, M. A.; Nieh, M. T.; Flood, T. C. *J. Am. Chem. Soc.* **1972**, 6538-6540. (b) Sattar, A.; Forrester, J.; Moir, M.; Roberts, J. S.; Parker, W. *Tetrahedron Lett.* **1976**, 1405-1406. (c) Bryan, J. C.; Geib, S. J.; Rheingold, A. L.; Mayer, J. M. *J. Am. Chem. Soc.* **1987**, *109*, 2826-2828. (d) Su, F.-M.; Bryan, J. C.; Jang, S.; Mayer, J. M. *Polyhedron* **1989**, *8*, 1261-1277. (e) Berry, M.; Davies, S. G.; Green, M. L. H. *J. Chem. Soc., Chem. Commun.* **1978**, 99-100.

(10) Ivin, K. J.; Reddy, B. S. R.; Rooney, J. J. *J. Chem. Soc., Chem. Commun.* **1981**, 1062-1064.

(11) France, M. B.; Nguyen, S. T.; Grubbs, R. H., unpublished results.

(12) A preparative-scale synthesis of this η^2-olefin complex has been completed: Flatt, B. T.; Grubbs, R. H., unpublished results.

(13) (a) Bradley, D. C.; Hursthouse, M. B.; Malik, K. M. A.; Nielson, A. J.; Short, R. L. *J. Chem. Soc., Dalton Trans.* **1983**, 2651-2656. (b) Nielson, A. J.; McCarley, R. E.;

Laughlin, S. L.; Carlson, C. D. In *Inorg. Syn.*; Schreeve, J. M., Ed.; John Wiley & Sons: New York, 1986; Vol. 24, pp 194-200.

Appendix

Data for X-ray Diffraction Studies

A. X-ray Diffraction Study of $WCl_2[N\text{-}2,6\text{-}C_6H_3\text{-}(i\text{-}Pr)_2][P(OMe)_3]_3$

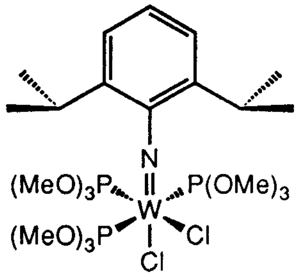

(See Chapter 2, Figure 1 for the ORTEP plot.)

Table A-1. Experimental Data for the X-ray Diffraction Study of $WCl_2[N\text{-}2,6\text{-}C_6H_3\text{-}(i\text{-}Pr)_2][P(OMe)_3]_3$

Formula: $C_{21}H_{44}NO_9P_3Cl_2W$	Fw: 802.2
Temperature (K): 158	Crystal System: Monoclinic
Space Group: $P2_1/c$	Z = 4
a = 10.891(2) Å	V = 3276.2(9) $Å^3$
b = 15.477(2) Å	β = 91.071(12)°
c = 19.439(3) Å	D_{calcd}, Mg/m^3 = 1.626
Radiation: MoKα (λ = 0.710730 Å)	Diffractometer: Siemens P3 (R3m/V System)
Data Collected: $+h$, $+k$, $\pm l$	Monochromator: Highly oriented graphite
Scan Range: 1.20° plus Kα-separation	Scan Type: θ-2θ
2θ Range: 4.0 to 55.0°	Scan Speed: 3.0 deg min^{-1} (in ω)
Absorption Correction:	μ(MoKα), mm^{-1} = 3.95
Semi-empirical (ψ-scan method)	Reflections Collected: 7579
No. of Variables: 334	Reflections with $\lvert F_o \rvert > 3.0\sigma(\lvert F_o \rvert)$: 6690
Goodness of Fit: 1.26	R_F = 2.8%, R_{wF} = 3.2%

Table A-2. Atomic Coordinates (x 10^4) and Equivalent Isotropic Displacement Coefficients ($Å^2$ x 10^4)[a]

	x	y	z	U(eq)
W(1)	8221(1)	7938(1)	1328(1)	147(1)
Cl(1)	7782(1)	8687(1)	2433(1)	224(2)
Cl(2)	9983(1)	8943(1)	1265(1)	240(2)
P(1)	9120(1)	7536(1)	227(1)	217(3)
P(2)	9486(1)	6975(1)	2079(1)	177(2)
P(3)	6941(1)	9034(1)	701(1)	220(3)
N(1)	6992(2)	7193(2)	1334(1)	163(7)
O(1)	8996(3)	8210(2)	-398(1)	330(9)
O(2)	8400(3)	6748(2)	-111(1)	387(10)
O(3)	10541(3)	7336(3)	123(2)	518(12)
O(4)	8989(2)	6753(2)	2829(1)	246(7)
O(5)	9754(2)	6055(2)	1752(1)	231(7)
O(6)	10832(2)	7277(2)	2308(1)	224(7)
O(7)	5768(3)	8663(2)	288(2)	374(9)
O(8)	7676(2)	9631(2)	194(1)	340(9)
O(9)	6111(3)	9699(2)	1123(2)	380(9)
C(1)	5980(3)	6646(2)	1410(2)	182(9)
C(2)	6045(3)	5766(2)	1208(2)	201(9)
C(3)	5022(3)	5244(3)	1312(2)	272(11)
C(4)	3966(3)	5564(3)	1601(2)	291(11)
C(5)	3903(3)	6421(3)	1792(2)	264(11)
C(6)	4900(3)	6977(2)	1709(2)	213(10)
C(7)	7168(3)	5374(2)	883(2)	235(10)
C(8)	6877(4)	5092(3)	146(2)	352(13)
C(9)	7666(4)	4611(3)	1304(2)	353(13)
C(10)	4794(3)	7904(2)	1964(2)	259(11)
C(11)	3740(4)	8383(3)	1608(2)	354(13)
C(12)	4666(4)	7922(3)	2751(2)	361(13)
C(13)	9895(4)	8849(3)	-566(2)	397(14)
C(14)	8674(5)	6472(3)	-811(2)	547(18)
C(15)	11368(4)	6967(3)	595(2)	457(16)

Table A-2 (cont'd). Atomic Coordinates (x 10^4) and Equivalent Isotropic Displacement Coefficients (Å^2 x 10^4)^a

	x	y	z	U(eq)
C(16)	7743(3)	6476(3)	2929(2)	319(12)
C(17)	10441(4)	5399(3)	2133(2)	326(12)
C(18)	10982(3)	7970(3)	2808(2)	307(11)
C(19)	5828(4)	7954(3)	-180(2)	409(14)
C(20)	7063(4)	10242(3)	-265(2)	447(15)
C(21)	6738(5)	10389(3)	1495(3)	551(19)

^{a}Equivalent isotropic U defined as one third of the trace of the orthogonalized U_{ij} tensor.

Table A-3. Interatomic Distances (Å) with Esd's

W(1) - Cl(1)	2.495(1)	W(1) - Cl(2)	2.475(1)
W(1) - P(1)	2.451(1)	W(1) - P(2)	2.486(1)
W(1) - P(3)	2.497(1)	W(1) - N(1)	1.767(3)
P(1) - O(1)	1.605(3)	P(1) - O(2)	1.586(3)
P(1) - O(3)	1.595(3)	P(2) - O(4)	1.600(3)
P(2) - O(5)	1.589(3)	P(2) - O(6)	1.594(2)
P(3) - O(7)	1.604(3)	P(3) - O(8)	1.579(3)
P(3) - O(9)	1.605(3)	N(1) - C(1)	1.400(4)
O(1) - C(13)	1.434(5)	O(2) - C(14)	1.462(5)
O(3) - C(15)	1.397(6)	O(4) - C(16)	1.440(5)
O(5) - C(17)	1.456(5)	O(6) - C(18)	1.455(5)
O(7) - C(19)	1.428(5)	O(8) - C(20)	1.454(5)
O(9) - C(21)	1.453(6)	C(1) - C(2)	1.420(5)
C(1) - C(6)	1.418(5)	C(2) - C(3)	1.394(5)
C(2) - C(7)	1.514(5)	C(3) - C(4)	1.382(5)
C(4) - C(5)	1.380(6)	C(5) - C(6)	1.397(5)
C(6) - C(10)	1.523(5)	C(7) - C(8)	1.526(5)
C(7) - C(9)	1.530(5)	C(10) - C(11)	1.522(5)
C(10) - C(12)	1.540(6)		

Table A-4. Interatomic Angles (Deg.) with Esd's

Cl(1) - W(1) - Cl(2)	85.0(1)	Cl(1) - W(1) - P(1)	163.0(1)
Cl(2) - W(1) - P(1)	78.1(1)	Cl(1) - W(1) - P(2)	83.4(1)
Cl(2) - W(1) - P(2)	89.1(1)	P(1) - W(1) - P(2)	97.7(1)
Cl(1) - W(1) - P(3)	89.5(1)	Cl(2) - W(1) - P(3)	88.6(1)
P(1) - W(1) - P(3)	88.6(1)	P(2) - W(1) - P(3)	172.7(1)
Cl(1) - W(1) - N(1)	98.0(1)	Cl(2) - W(1) - N(1)	177.0(1)
P(1) - W(1) - N(1)	98.9(1)	P(2) - W(1) - N(1)	90.9(1)
P(3) - W(1) - N(1)	91.8(1)		

W(1) - P(1) - O(1)	117.8(1)	W(1) - P(1) - O(2)	110.8(1)
O(1) - P(1) - O(2)	98.8(2)	W(1) - P(1) - O(3)	124.4(1)
O(1) - P(1) - O(3)	95.6(2)	O(2) - P(1) - O(3)	105.8(2)
W(1) - P(2) - O(4)	118.0(1)	W(1) - P(2) - O(5)	114.0(1)
O(4) - P(2) - O(5)	103.9(1)	W(1) - P(2) - O(6)	119.0(1)
O(4) - P(2) - O(6)	97.7(1)	O(5) - P(2) - O(6)	101.5(1)
W(1) - P(3) - O(7)	115.7(1)	W(1) - P(3) - O(8)	114.7(1)
O(7) - P(3) - O(8)	107.8(2)	W(1) - P(3) - O(9)	120.1(1)
O(7) - P(3) - O(9)	92.0(2)	O(8) - P(3) - O(9)	103.9(2)
W(1) - N(1) - C(1)	173.5(2)	P(1) - O(1) - C(13)	124.9(3)
P(1) - O(2) - C(14)	120.1(3)	P(1) - O(3) - C(15)	127.7(3)
P(2) - O(4) - C(16)	121.5(2)	P(2) - O(5) - C(17)	121.2(2)
P(2) - O(6) - C(18)	119.6(2)	P(3) - O(7) - C(19)	123.3(3)
P(3) - O(8) - C(20)	122.1(3)	P(3) - O(9) - C(21)	117.5(3)
N(1) - C(1) - C(2)	120.6(3)	N(1) - C(1) - C(6)	119.0(3)
C(2) - C(1) - C(6)	120.4(3)	C(1) - C(2) - C(3)	118.2(3)
C(1) - C(2) - C(7)	123.0(3)	C(3) - C(2) - C(7)	118.9(3)
C(2) - C(3) - C(4)	121.7(4)	C(3) - C(4) - C(5)	120.0(4)
C(4) - C(5) - C(6)	121.2(3)	C(1) - C(6) - C(5)	118.5(3)
C(1) - C(6) - C(10)	122.8(3)	C(5) - C(6) - C(10)	118.6(3)
C(2) - C(7) - C(8)	110.6(3)	C(2) - C(7) - C(9)	111.6(3)
C(8) - C(7) - C(9)	110.3(3)	C(6) - C(10) - C(11)	111.8(3)
C(6) - C(10) - C(12)	110.5(3)	C(11) - C(10) - C(12)	111.1(3)

Table A-5. Anisotropic Displacement Coefficients (Å^{2} x 10^{4})[a]

	U_{11}	U_{22}	U_{33}	U_{12}	U_{13}	U_{23}
W(1)	148(1)	151(1)	144(1)	5(1)	3(1)	7(1)
Cl(1)	242(4)	234(4)	196(4)	13(3)	10(3)	-46(3)
Cl(2)	230(4)	228(4)	264(4)	-65(3)	18(3)	12(3)
P(1)	223(4)	247(5)	182(4)	2(4)	35(3)	-13(4)
P(2)	168(4)	192(4)	169(4)	19(3)	-8(3)	11(3)
P(3)	212(4)	224(5)	224(4)	38(3)	-7(3)	39(3)
N(1)	149(12)	177(14)	163(12)	9(11)	-3(10)	-2(11)
O(1)	382(15)	362(16)	248(13)	-56(13)	44(11)	40(12)
O(2)	564(19)	364(16)	238(14)	-195(15)	136(13)	-123(12)
O(3)	329(16)	929(29)	299(15)	218(17)	75(13)	-10(17)
O(4)	202(12)	334(14)	202(12)	17(11)	-3(10)	78(11)
O(5)	244(12)	174(12)	275(13)	29(10)	-28(10)	5(10)
O(6)	185(12)	257(14)	230(12)	14(10)	-8(9)	-36(10)
O(7)	273(14)	442(18)	402(16)	47(13)	-105(12)	27(14)
O(8)	262(14)	363(16)	395(16)	75(12)	46(12)	203(13)
O(9)	405(16)	374(17)	363(16)	187(14)	40(13)	53(13)
C(1)	163(15)	225(18)	157(15)	-13(13)	-30(12)	25(13)
C(2)	216(16)	203(17)	184(16)	-18(13)	-28(13)	3(13)
C(3)	289(19)	262(20)	263(18)	-78(15)	-20(15)	6(15)
C(4)	271(19)	296(20)	308(20)	-109(16)	19(15)	10(16)
C(5)	196(17)	334(21)	263(18)	-41(15)	24(14)	-6(16)
C(6)	206(16)	243(19)	188(16)	-3(14)	-6(13)	31(13)
C(7)	241(17)	183(17)	280(18)	12(14)	-2(14)	8(14)
C(8)	377(22)	372(24)	308(21)	-50(18)	38(17)	-110(18)
C(9)	295(20)	268(21)	496(25)	35(17)	16(18)	77(18)
C(10)	211(17)	260(19)	307(19)	16(15)	60(14)	-9(15)
C(11)	282(20)	331(23)	451(24)	66(17)	79(18)	36(19)
C(12)	336(21)	423(25)	327(21)	34(19)	71(17)	-111(19)
C(13)	508(26)	355(23)	330(21)	-174(20)	90(19)	30(18)
C(14)	833(38)	582(33)	233(21)	-238(28)	175(22)	-156(21)
C(15)	294(22)	709(36)	370(23)	174(22)	70(18)	78(22)

Table A-5 (cont'd). Anisotropic Displacement Coefficients ($Å^2$ x 10^4)[a]

	U_{11}	U_{22}	U_{33}	U_{12}	U_{13}	U_{23}
C(16)	280(19)	440(24)	239(18)	-31(17)	59(15)	62(17)
C(17)	322(21)	252(20)	402(22)	84(16)	-79(17)	64(17)
C(18)	240(18)	395(23)	285(19)	-43(17)	-20(15)	-123(17)
C(19)	409(24)	486(27)	326(21)	-18(21)	-123(18)	-88(20)
C(20)	451(26)	423(27)	469(26)	123(21)	38(20)	277(22)
C(21)	971(44)	314(26)	366(25)	170(27)	-61(26)	-11(20)

[a] The anisotropic displacement exponent takes the form: $-2\pi^2(h^2a^{*2}U_{11} + \ldots + 2hka^*b^*U_{12})$.

Table A-6. H-Atom Coordinates (x10^4) and Isotropic Displacement Coefficients (Å^2 x 10^4)

	x	y	z	U
H(3A)	5097	4633	1237	600
H(4A)	3303	5185	1717	600
H(5A)	3158	6650	1975	600
H(7A)	7840	5772	852	600
H(8A)	6585	5577	-119	600
H(8B)	7663	4904	-14	600
H(8C)	6263	4648	157	600
H(9A)	7778	4783	1775	600
H(9B)	7088	4144	1319	600
H(9C)	8479	4450	1171	600
H(10A)	5525	8217	1852	600
H(11A)	3834	8364	1119	600
H(11B)	2974	8088	1668	600
H(11C)	3721	8980	1744	600
H(12A)	5281	7616	3015	600
H(12B)	4697	8508	2912	600
H(12C)	3924	7635	2880	600
H(13A)	9647	9192	-956	600
H(13B)	9991	9253	-195	600
H(13C)	10620	8563	-724	600
H(14A)	7872	6318	-984	600
H(14B)	8609	6945	-1129	600
H(14C)	9304	6044	-748	600
H(15A)	12188	6947	423	600
H(15B)	11321	7281	1020	600
H(15C)	11143	6401	749	600
H(16A)	7627	6365	3409	600
H(16B)	7131	6848	2727	600
H(16C)	7642	5914	2727	600
H(17A)	10508	4889	1854	600
H(17B)	11270	5591	2213	600

Table A-6 (cont'd). H-Atom Coordinates (x10^4) and Isotropic Displacement Coefficients ($Å^2$ x 10^4)

	x	y	z	U
H(17C)	10032	5204	2537	600
H(18A)	11701	8276	2666	600
H(18B)	10290	8355	2797	600
H(18C)	10967	7725	3261	600
H(19A)	5098	7871	-457	600
H(19B)	6446	8162	-484	600
H(19C)	6246	7489	53	600
H(20A)	7647	10661	-419	600
H(20B)	6608	9929	-611	600
H(20C)	6355	10539	-99	600
H(21A)	6355	10504	1926	600
H(21B)	7513	10219	1695	600
H(21C)	6701	10843	1158	600

B. X-ray Diffraction Study of $W(HC{=}CH{-}CPh_2)Cl_2(NPh)[P(OMe)_3]_2$

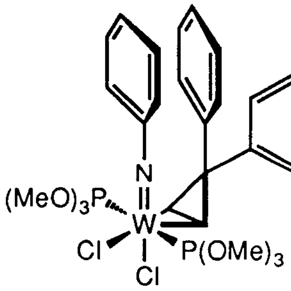

(See Chapter 2, Figure 2 for the ORTEP plot.)

Table B-1. Experimental Data for the X-ray Diffraction Study of $W(HC{=}CH{-}CPh_2)$-$Cl_2(NPh)[P(OMe)_3]_2$

Formula: $C_{27}H_{35}NO_6P_2Cl_2W \cdot 1/2(C_6H_6)$	Fw: 825.3
Temperature (K): 183	Crystal System: Monoclinic
Space Group: $P2_1/c$	Z = 4
$\underline{a}$ = 18.406(2) Å	$\underline{V}$ = 3359.3(5) Å^3
$\underline{b}$ = 9.9413(7) Å	β = 98.026(7)°
$\underline{c}$ = 18.5405(14) Å	D_{calcd}, Mg/m^3 = 1.632
Radiation: MoKα ($\bar{\lambda}$ = 0.710730 Å)	Diffractometer: Syntex $P2_1$ (Siemens R3m/V)
Data Collected: $+h$, $+k$, $\pm l$	Monochromator: Highly oriented graphite
Scan Range: 1.20° plus Kα-separation	Scan Type: θ-2θ
2θ Range: 4.0 to 45.0°	Scan Speed: 3.0 deg min^{-1} (in ω)
Absorption Correction: Semi-empirical (ψ-scan method)	μ(MoKα), mm^{-1} = 3.806
	Reflections Collected: 4899
No. of Variables: 364	Reflections with $\lvert F_o \rvert > 3.0\sigma(\lvert F_o \rvert)$: 3721
Goodness of Fit: 1.45	R_F = 4.5%, R_{wF} = 6.0%

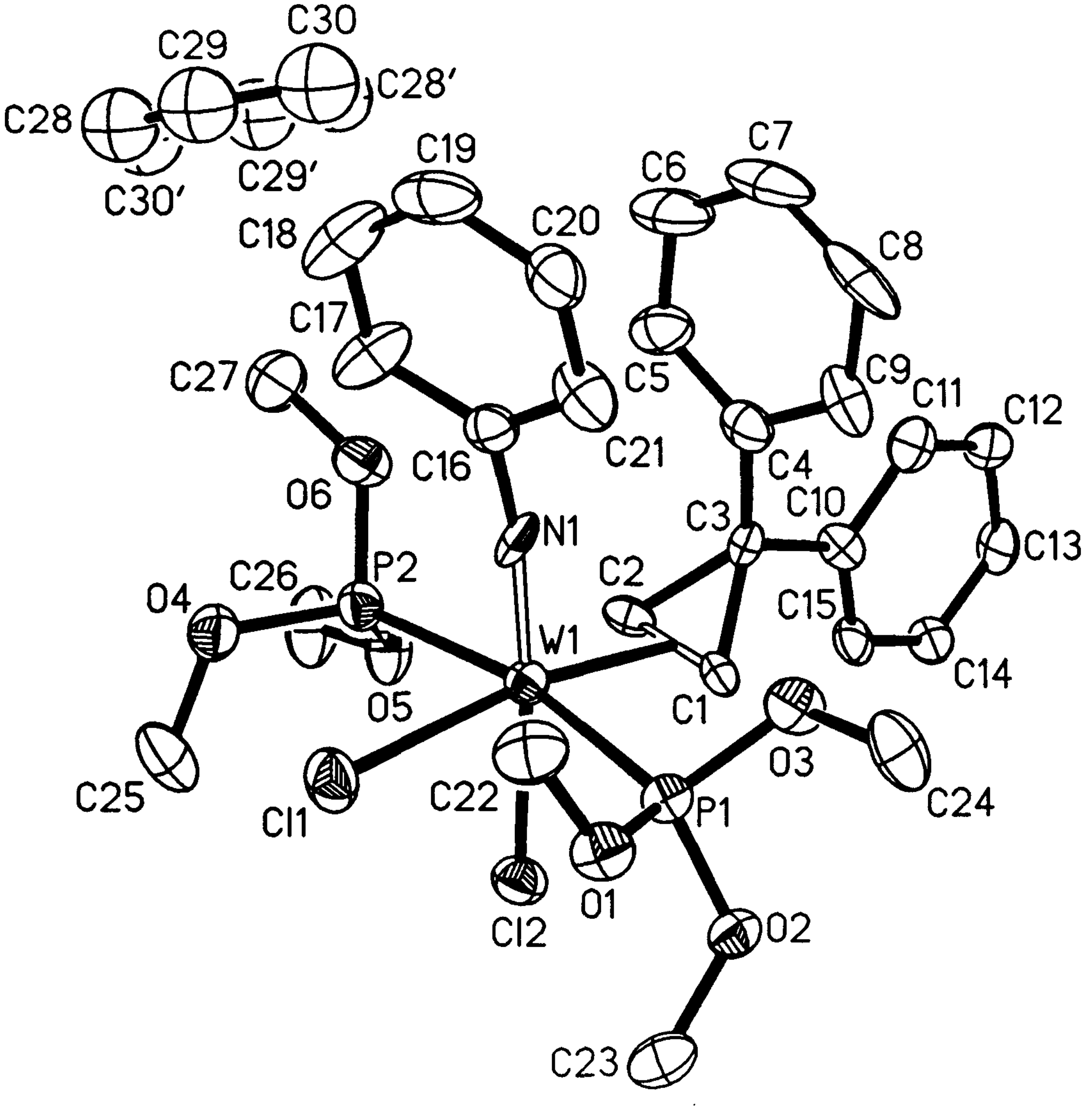

Figure B-1. ORTEP plot of W(H$\overline{\text{C=CH-C}}$Ph$_2$)Cl$_2$(NPh)[P(OMe)$_3$]$_2$ showing the inclusion of a benzene molecule at the inversion center. Thermal ellipsoids are drawn at the 50% probability level.

Table B-2. Atomic Coordinates (x 10^4) and Equivalent Isotropic Displacement Coefficients (Å^2 x 10^4)^a

	x	y	z	U(eq)
W(1)	1986(1)	528(1)	1799(1)	224(2)
Cl(1)	967(1)	2126(3)	1415(2)	376(9)
Cl(2)	2266(1)	854(3)	540(1)	327(8)
P(1)	1060(1)	-1241(3)	1332(1)	250(8)
P(2)	2732(1)	2638(3)	2113(2)	287(8)
O(1)	201(4)	-911(7)	1228(4)	320(23)
O(2)	1113(3)	-1845(6)	555(3)	271(22)
O(3)	1162(3)	-2517(7)	1845(3)	323(23)
O(4)	2380(4)	4098(7)	1999(4)	353(24)
O(5)	3439(4)	2725(6)	1722(4)	383(25)
O(6)	2970(4)	2633(7)	2959(4)	413(25)
N(1)	1735(4)	431(7)	2672(4)	261(27)
C(1)	2638(5)	-1280(9)	1744(5)	200(29)
C(2)	3110(5)	-160(10)	2004(5)	233(30)
C(3)	3172(5)	-1451(9)	2446(5)	231(30)
C(4)	2939(5)	-1594(11)	3176(5)	307(33)
C(5)	3144(6)	-647(11)	3724(6)	378(38)
C(6)	2991(7)	-877(15)	4420(6)	562(51)
C(7)	2662(7)	-2018(15)	4589(6)	536(49)
C(8)	2447(6)	-2978(13)	4055(7)	511(47)
C(9)	2578(5)	-2747(10)	3363(6)	368(37)
C(10)	3842(5)	-2300(9)	2334(5)	241(31)
C(11)	4233(5)	-3026(10)	2919(6)	310(34)
C(12)	4855(5)	-3748(10)	2834(5)	290(33)
C(13)	5109(5)	-3786(10)	2157(6)	317(35)
C(14)	4738(5)	-3060(9)	1596(5)	264(32)
C(15)	4116(5)	-2329(9)	1696(5)	278(33)
C(16)	1439(5)	491(9)	3330(5)	267(32)
C(17)	1509(6)	1692(12)	3729(6)	442(41)
C(18)	1213(6)	1733(15)	4379(7)	571(49)
C(19)	846(6)	618(14)	4616(6)	505(46)

Table B-2 (cont'd). Atomic Coordinates (x 10^4) and Equivalent Isotropic Displacement Coefficients (Å^2 x 10^4)^a

	x	y	z	U(eq)
C(20)	759(7)	-521(11)	4205(6)	440(41)
C(21)	1071(6)	-617(11)	3551(6)	402(40)
C(22)	-141(6)	-417(11)	1831(6)	387(38)
C(23)	787(6)	-1171(11)	-96(5)	390(38)
C(24)	653(6)	-3653(11)	1713(6)	423(40)
C(25)	2233(7)	4642(11)	1257(7)	493(44)
C(26)	3937(6)	3864(11)	1774(8)	543(48)
C(27)	3308(7)	3720(11)	3408(6)	540(46)
C(28)	4583(9)	6065(16)	4924(8)	773(44)
C(29)	4277(9)	4931(17)	5050(8)	785(44)
C(30)	4670(9)	3734(18)	5171(9)	878(49)

^{a}Equivalent isotropic U defined as one third of the trace of the orthogonalized U_{ij} tensor.

Table B-3. Interatomic Distances (Å) with Esd's

W(1) - Cl(1)	2.486(3)	W(1) - Cl(2)	2.482(3)
W(1) - P(1)	2.517(2)	W(1) - P(2)	2.530(3)
W(1) - N(1)	1.747(8)	W(1) - C(1)	2.171(9)
W(1) - C(2)	2.160(9)	W(1) - Cnt[a]	2.040
P(1) - O(1)	1.601(7)	P(1) - O(2)	1.576(7)
P(1) - O(3)	1.581(7)	P(2) - O(4)	1.591(7)
P(2) - O(5)	1.578(8)	P(2) - O(6)	1.568(7)
O(1) - C(22)	1.444(13)	O(2) - C(23)	1.437(12)
O(3) - C(24)	1.465(12)	O(4) - C(25)	1.468(14)
O(5) - C(26)	1.452(13)	O(6) - C(27)	1.449(13)
N(1) - C(16)	1.404(13)	C(1) - C(2)	1.452(12)
C(1) - C(3)	1.526(12)	C(2) - C(3)	1.518(13)
C(3) - C(4)	1.484(14)	C(3) - C(10)	1.531(13)
C(4) - C(5)	1.397(14)	C(4) - C(9)	1.393(15)
C(5) - C(6)	1.378(16)	C(6) - C(7)	1.344(20)
C(7) - C(8)	1.393(18)	C(8) - C(9)	1.357(17)
C(10) - C(11)	1.414(13)	C(10) - C(15)	1.349(14)
C(11) - C(12)	1.379(14)	C(12) - C(13)	1.399(15)
C(13) - C(14)	1.368(13)	C(14) - C(15)	1.391(14)
C(16) - C(17)	1.401(15)	C(16) - C(21)	1.385(15)
C(17) - C(18)	1.392(17)	C(18) - C(19)	1.400(19)
C(19) - C(20)	1.363(17)	C(20) - C(21)	1.416(17)
C(28) - C(29)	1.295(23)	C(28) - C(30')	1.425(24)
C(29) - C(30)	1.394(24)		

[a] Cnt is the centroid of the C(1) - C(2) bond.

Table B-4. Interatomic Angles (Deg.) with Esd's

Cl(1) - W(1) - Cl(2)	83.9(1)	Cl(1) - W(1) - P(1)	84.3(1)
Cl(2) - W(1) - P(1)	89.3(1)	Cl(1) - W(1) - P(2)	84.2(1)
Cl(2) - W(1) - P(2)	86.1(1)	P(1) - W(1) - P(2)	168.0(1)
Cl(1) - W(1) - N(1)	90.8(2)	Cl(2) -W(1) - N(1)	174.6(2)
P(1) - W(1) - N(1)	91.5(2)	P(2) - W(1) - N(1)	92.1(2)
Cl(1) - W(1) - C(1)	156.3(2)	Cl(2) - W(1) - C(1)	82.9(2)
P(1) - W(1) - C(1)	76.0(2)	P(2) - W(1) - C(1)	114.3(2)
N(1) - W(1) - C(1)	102.5(3)	Cl(1) - W(1) - C(2)	156.7(3)
Cl(2) - W(1) - C(2)	83.6(2)	P(1) - W(1) - C(2)	115.1(3)
P(2) - W(1) - C(2)	75.3(3)	N(1) - W(1) - C(2)	101.0(3)
C(1) - W(1) - C(2)	39.2(3)	Cnt - W(1) - N(1)[a]	102.5
Cnt - W(1) - P(1)[a]	95.5	Cnt - W(1) - P(2)[a]	94.9
Cnt - W(1) - Cl(1)[a]	166.7	Cnt - W(1) - Cl(2)[a]	82.8
W(1) - P(1) - O(1)	120.5(3)	W(1) - P(1) - O(2)	117.1(3)
O(1) - P(1) - O(2)	98.8(3)	W(1) - P(1) - O(3)	109.6(2)
O(1) - P(1) - O(3)	105.6(4)	O(2) - P(1) - O(3)	103.2(4)
W(1) - P(2) - O(4)	121.9(3)	W(1) - P(2) - O(5)	113.3(3)
O(4) - P(2) - O(5)	103.6(4)	W(1) - P(2) - O(6)	107.1(3)
O(4) - P(2) - O(6)	100.8(4)	O(5) - P(2) - O(6)	109.0(4)
P(1) - O(1) - C(22)	120.5(6)	P(1) - O(2) - C(23)	121.2(6)
P(1) - O(3) - C(24)	119.9(6)	P(2) - O(4) - C(25)	118.6(7)
P(2) - O(5) - C(26)	124.5(7)	P(2) - O(6) - C(27)	127.5(7)
W(1) - N(1) - C(16)	170.8(6)	W(1) - C(1) - C(2)	70.0(5)
W(1) - C(1) - C(3)	110.3(6)	C(2) - C(1) - C(3)	61.3(6)
W(1) - C(2) - C(1)	70.8(5)	W(1) - C(2) - C(3)	111.1(6)
C(1) - C(2) - C(3)	61.8(6)	C(1) - C(3) - C(2)	57.0(6)
C(1) - C(3) - C(4)	123.7(8)	C(2) - C(3) - C(4)	124.3(8)
C(1) - C(3) - C(10)	112.4(7)	C(2) - C(3) - C(10)	113.2(8)
C(4) - C(3) - C(10)	114.3(8)	C(3) - C(4) - C(5)	121.0(9)
C(3) - C(4) - C(9)	121.0(9)	C(5) - C(4) - C(9)	117.7(10)
C(4) - C(5) - C(6)	119.9(11)	C(5) - C(6) - C(7)	121.2(12)

Table B-4 (cont'd). Interatomic Angles (Deg.) with Esd's

C(6) - C(7) - C(8)	120.3(12)	C(7) - C(8) - C(9)	119.1(11)
C(4) - C(9) - C(8)	121.9(10)	C(3) - C(10) - C(11)	120.8(9)
C(3) - C(10) - C(15)	122.5(8)	C(11) - C(10) - C(15)	116.6(9)
C(10) - C(11) - C(12)	121.4(10)	C(11) - C(12) - C(13)	120.2(9)
C(12) - C(13) - C(14)	118.3(9)	C(13) - C(14) - C(15)	120.4(9)
C(10) - C(15) - C(14)	123.0(9)	N(1) - C(16) - C(17)	118.5(9)
N(1) - C(16) - C(21)	119.2(9)	C(17) - C(16) - C(21)	122.3(10)
C(16) - C(17) - C(18)	117.6(11)	C(17) - C(18) - C(19)	120.9(12)
C(18) - C(19) - C(20)	120.4(11)	C(19) - C(20) - C(21)	120.4(11)
C(16) - C(21) - C(20)	118.3(10)	C(29) - C(28) - C(30A)	126.6(16)
C(28) - C(29) - C(30)	122.9(16)	C(29) - C(30) - C(28A)	110.4(15)

[a] Cnt is the centroid of the C(1) - C(2) bond.

Table B-5. Anisotropic Displacement Coefficients (Å^2 x 10^4)^a

	U_{11}	U_{22}	U_{33}	U_{12}	U_{13}	U_{23}
W(1)	230(3)	210(3)	228(3)	-7(2)	14(2)	1(2)
Cl(1)	300(14)	320(14)	483(17)	71(11)	-35(12)	-1(12)
Cl(2)	365(14)	344(14)	270(13)	-5(11)	37(11)	45(11)
P(1)	248(14)	263(14)	239(14)	-6(11)	34(11)	-18(11)
P(2)	316(15)	224(14)	309(15)	-6(12)	8(12)	8(12)
O(1)	246(37)	391(40)	321(40)	5(31)	31(31)	-26(32)
O(2)	285(37)	277(37)	248(37)	-45(29)	29(29)	-40(29)
O(3)	277(37)	342(40)	341(40)	-62(32)	12(31)	36(33)
O(4)	359(41)	316(38)	381(43)	39(33)	37(34)	-21(33)
O(5)	312(40)	216(37)	636(51)	-88(32)	123(36)	-9(35)
O(6)	546(47)	282(40)	350(41)	-170(36)	-155(36)	23(33)
N(1)	244(44)	210(44)	322(49)	5(34)	20(37)	-164(35)
C(1)	217(50)	173(49)	213(50)	33(40)	48(39)	58(40)
C(2)	137(47)	333(57)	214(51)	30(42)	-27(38)	51(43)
C(3)	294(53)	154(46)	245(51)	6(42)	40(41)	-48(41)
C(4)	287(55)	357(59)	287(56)	136(49)	78(44)	67(49)
C(5)	322(61)	501(70)	292(62)	68(52)	-23(48)	-39(53)
C(6)	666(90)	808(10)	231(66)	60(76)	127(61)	78(63)
C(7)	500(76)	907(10)	225(65)	236(74)	130(56)	212(70)
C(8)	390(68)	592(83)	603(86)	145(60)	255(62)	473(72)
C(9)	297(58)	277(58)	547(73)	39(47)	114(53)	166(52)
C(10)	178(48)	264(53)	279(55)	-12(41)	24(42)	54(44)
C(11)	259(56)	281(56)	392(61)	-62(46)	54(47)	-39(47)
C(12)	223(54)	314(57)	307(58)	-8(45)	-55(44)	-26(45)
C(13)	257(56)	264(55)	436(66)	115(45)	71(49)	-37(48)
C(14)	274(54)	282(54)	260(54)	33(45)	124(44)	22(44)
C(15)	333(57)	182(50)	313(58)	-52(44)	25(46)	60(43)
C(16)	230(52)	324(58)	237(54)	66(45)	1(42)	-2(45)
C(17)	335(62)	570(75)	442(69)	-138(57)	129(53)	-246(61)
C(18)	392(70)	721(94)	593(84)	-30(68)	44(63)	-399(75)

Table B-5 (cont'd). Anisotropic Displacement Coefficients ($Å^2$ x 10^4)[a]

	U_{11}	U_{22}	U_{33}	U_{12}	U_{13}	U_{23}
C(19)	385(69)	843(99)	261(62)	236(71)	-49(52)	9(67)
C(20)	584(78)	402(67)	377(66)	243(59)	218(58)	86(56)
C(21)	343(63)	418(68)	477(71)	112(52)	172(54)	149(55)
C(22)	341(61)	498(70)	337(61)	-9(53)	101(49)	-27(53)
C(23)	418(65)	486(69)	283(61)	-3(55)	105(50)	-107(52)
C(24)	348(63)	337(64)	597(77)	-44(51)	111(55)	211(55)
C(25)	453(72)	374(68)	618(83)	-16(55)	-49(61)	210(59)
C(26)	400(70)	300(64)	931(14)	-127(55)	100(68)	-48(65)
C(27)	735(88)	363(71)	483(76)	-67(64)	-56(65)	-72(59)

[a] The anisotropic displacement exponent takes the form: $-2\pi^2(h^2a^{*2}U_{11} + \ldots + 2hka^*b^*U_{12})$.

Table B-6. H-Atom Coordinates (x10^4) and Isotropic Displacement Coefficients (Å^2 x 10^4)

	x	y	z	U
H(1A)	2673	-1760	1301	800
H(2A)	3493	190	1756	800
H(5A)	3409	148	3623	800
H(6A)	3105	-206	4791	800
H(7A)	2565	-2183	5077	800
H(8A)	2224	-3809	4171	800
H(9A)	2418	-3367	2976	800
H(11A)	4073	-2980	3390	800
H(12A)	5115	-4241	3235	800
H(13A)	5550	-4269	2103	800
H(14A)	4883	-3129	1119	800
H(15A)	3874	-1786	1307	800
H(17A)	1756	2467	3572	800
H(18A)	1244	2545	4662	800
H(19A)	655	655	5072	800
H(20A)	503	-1287	4359	800
H(21A)	1027	-1414	3255	800
H(22A)	-652	-256	1670	800
H(22B)	-90	-1087	2208	800
H(22C)	88	403	2017	800
H(23A)	880	-1675	-515	800
H(23B)	267	-1128	-84	800
H(23C)	978	-276	-123	800
H(24A)	793	-4341	2069	800
H(24B)	165	-3352	1752	800
H(24C)	668	-4008	1234	800
H(25A)	2025	5526	1269	800
H(25B)	2684	4689	1052	800
H(25C)	1895	4062	964	800
H(26A)	4324	3688	1489	800

Table B-6 (cont'd). H-Atom Coordinates (x10^4) and Isotropic Displacement Coefficients (Å^2 x 10^4)

	x	y	z	U
H(26B)	3676	4659	1594	800
H(26C)	4143	3995	2274	800
H(27A)	3386	3441	3908	800
H(27B)	3771	3919	3250	800
H(27C)	3004	4508	3359	800
H(28A)	4245	6800	4827	800
H(29A)	3765	4929	5100	800
H(30A)	4472	2862	5250	800

C. X-ray Diffraction Study of W(=CH-CH=CPh$_2$)[N-2,6-C$_6$H$_3$-(*i*-Pr)$_2$][OCMe(CF$_3$)$_2$]$_2$[P(OMe)$_3$]

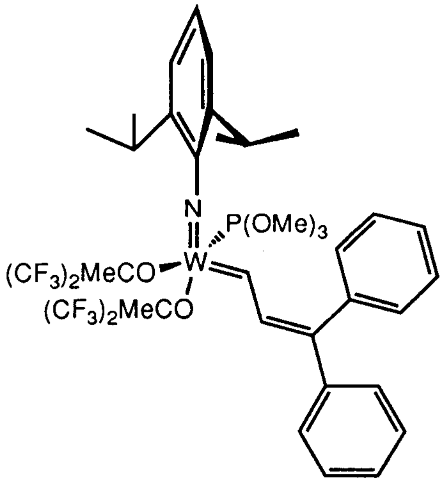

(See Chapter 2, Figure 3 for the ORTEP plot.)

Table C-1. Experimental Data for the X-ray Diffraction Study of W(=CH-CH=CPh$_2$)[N-2,6-C$_6$H$_3$-(*i*-Pr)$_2$][OCMe(CF$_3$)$_2$]$_2$[P(OMe)$_3$].

Formula: $C_{38}H_{44}NO_5F_{12}PW$
Temperature (K): 158
Space Group: $P\bar{1}$
$\underline{a}$ = 9.8392(15) Å
$\underline{b}$ = 11.317(2) Å
$\underline{c}$ = 20.184(4) Å
$\underline{V}$ = 2093.5(6) Å^3
Radiation: MoKα ($\bar{\lambda}$ = 0.710730 Å)
Data Collected: +*h*, ±*k*, ±*l*
Scan Range: 1.20° plus Kα-separation
2θ Range: 4.0 to 48.0°
Absorption Correction:
Semi-empirical (ψ-scan method)
No. of Variables: 699
Goodness of Fit: 1.64

Fw: 1037.6
Crystal System: Triclinic
Z = 2
α = 82.610(13)°
β = 89.708(13)°
γ = 70.074(12)°
D_{calcd}, Mg/m^3 = 1.65
Diffractometer: Siemens P3(R3m/V System)
Monochromator: Highly oriented graphite
Scan Type: θ-2θ
Scan Speed: 3.0 deg min^{-1} (in ω)
μ(MoKα), mm^{-1} = 2.95
Reflections Collected: 6801
Reflections with $|F_o| > 2.0\sigma(|F_o|)$: 6200
R_F = 3.4%, R_{wF} = 3.7%

Table C-2. Atomic Coordinates (x 10^4) and Equivalent Isotropic Displacement Coefficients ($Å^2$ x 10^4)^a

	x	y	z	U(eq)
W(1)	1715(1)	2383(1)	2809(1)	165(1)
P(1)	-243(1)	3907(1)	3386(1)	226(5)
O(1)	856(4)	1167(3)	3260(2)	262(13)
O(2)	3271(3)	837(3)	2583(2)	214(12)
O(3)	51(4)	4072(3)	4139(2)	333(15)
O(4)	-468(4)	5288(3)	3022(2)	321(14)
O(5)	-1786(4)	3781(4)	3461(2)	361(15)
N(1)	2639(4)	3434(3)	2899(2)	174(14)
F(1)	2115(4)	-1678(3)	4411(2)	599(16)
F(2)	1758(6)	226(4)	4559(2)	782(21)
F(3)	3366(4)	-667(4)	3904(2)	662(18)
F(4)	-629(4)	-1106(3)	3993(2)	576(16)
F(5)	-1057(5)	807(3)	4174(2)	679(19)
F(6)	-1493(4)	438(4)	3207(2)	676(19)
F(7)	5989(3)	-280(3)	3133(2)	459(14)
F(8)	6856(3)	-901(3)	2216(2)	437(13)
F(9)	5284(3)	-1599(3)	2695(2)	436(13)
F(10)	2937(4)	1126(3)	1183(2)	601(16)
F(11)	5035(4)	-272(3)	1132(2)	458(14)
F(12)	3400(4)	-759(3)	1668(2)	462(15)
C(1)	3321(5)	4224(4)	3113(2)	164(16)
C(2)	3444(5)	5220(4)	2637(2)	209(17)
C(3)	4065(6)	6033(5)	2855(3)	282(20)
C(4)	4549(6)	5886(5)	3512(3)	314(21)
C(5)	4446(6)	4908(5)	3964(3)	309(21)
C(6)	3816(5)	4055(4)	3781(3)	235(18)
C(7)	2924(6)	5398(5)	1911(3)	236(19)
C(8)	1603(8)	6587(7)	1748(4)	453(28)
C(9)	4119(8)	5407(7)	1437(3)	429(28)
C(10)	3769(6)	2938(5)	4274(3)	283(20)
C(11)	3553(10)	3222(7)	4989(3)	488(31)

Table C-2 (cont'd). Atomic Coordinates (x 10^4) and Equivalent Isotropic Displacement Coefficients (Å^2 x 10^4)[a]

	x	y	z	U(eq)
C(12)	5132(9)	1794(7)	4233(4)	481(29)
C(13)	626(5)	3229(5)	1977(3)	224(18)
C(14)	-243(6)	2675(5)	1628(3)	245(19)
C(15)	-1169(5)	3229(5)	1088(2)	220(18)
C(16)	-1551(5)	4582(5)	812(3)	234(18)
C(17)	-1645(6)	4970(5)	119(3)	273(20)
C(18)	-1984(6)	6218(5)	-144(3)	319(21)
C(19)	-2255(6)	7139(6)	285(3)	376(23)
C(20)	-2193(6)	6794(5)	959(3)	371(22)
C(21)	-1869(6)	5541(5)	1227(3)	292(21)
C(22)	-1822(6)	2441(5)	759(3)	250(19)
C(23)	-3208(6)	2961(6)	455(3)	297(21)
C(24)	-3834(7)	2221(7)	158(3)	379(25)
C(25)	-3090(8)	946(6)	150(3)	446(28)
C(26)	-1723(8)	416(6)	444(3)	481(28)
C(27)	-1079(7)	1152(5)	745(3)	372(23)
C(28)	-208(11)	3283(8)	4704(4)	555(35)
C(29)	-1348(12)	6418(7)	3288(5)	604(35)
C(30)	-2537(7)	3498(7)	2921(3)	351(24)
C(31)	960(5)	-69(4)	3503(3)	245(18)
C(32)	2036(7)	-549(5)	4093(3)	401(24)
C(33)	-563(7)	21(6)	3730(3)	413(24)
C(34)	1408(9)	-963(6)	2979(3)	377(26)
C(35)	4421(5)	558(4)	2170(3)	232(18)
C(36)	5642(6)	-559(5)	2549(3)	272(19)
C(37)	3960(6)	149(5)	1539(3)	308(20)
C(38)	4995(7)	1655(5)	1968(4)	363(24)

[a] Equivalent isotropic U defined as one third of the trace of the orthogonalized U_{ij} tensor.

Table C-3. Interatomic Distances (Å) with Esd's

W(1) - P(1)	2.505(1)	W(1) - O(1)	1.975(4)
W(1) - O(2)	1.996(3)	W(1) - N(1)	1.753(4)
W(1) - C(13)	1.947(5)		
P(1) - O(3)	1.594(4)	P(1) - O(4)	1.582(4)
P(1) - O(5)	1.577(4)	O(1) - C(31)	1.391(6)
O(2) - C(35)	1.374(6)	O(3) - C(28)	1.433(9)
O(4) - C(29)	1.447(9)	O(5) - C(30)	1.448(9)
N(1) - C(1)	1.394(7)	F(1) - C(32)	1.331(7)
F(2) - C(32)	1.331(8)	F(3) - C(32)	1.328(8)
F(4) - C(33)	1.339(8)	F(5) - C(33)	1.317(8)
F(6) - C(33)	1.327(8)	F(7) - C(36)	1.334(7)
F(8) - C(36)	1.331(6)	F(9) - C(36)	1.337(7)
F(10) - C(37)	1.340(6)	F(11) - C(37)	1.330(6)
F(12) - C(37)	1.320(8)	C(1) - C(2)	1.421(7)
C(1) - C(6)	1.403(7)	C(2) - C(3)	1.380(9)
C(2) - C(7)	1.520(7)	C(3) - C(4)	1.381(8)
C(4) - C(5)	1.372(8)	C(5) - C(6)	1.398(9)
C(6) - C(10)	1.519(7)	C(7) - C(8)	1.519(8)
C(7) - C(9)	1.513(9)	C(10) - C(11)	1.518(9)
C(10) - C(12)	1.524(8)	C(13) - C(14)	1.450(9)
C(14) - C(15)	1.363(7)	C(15) - C(16)	1.479(7)
C(15) - C(22)	1.483(9)	C(16) - C(17)	1.404(7)
C(16) - C(21)	1.406(8)	C(17) - C(18)	1.370(8)
C(18) - C(19)	1.395(9)	C(19) - C(20)	1.362(9)
C(20) - C(21)	1.379(8)	C(22) - C(23)	1.397(7)
C(22) - C(27)	1.395(7)	C(23) - C(24)	1.386(11)
C(24) - C(25)	1.380(9)	C(25) - C(26)	1.373(10)
C(26) - C(27)	1.400(11)	C(31) - C(32)	1.512(8)
C(31) - C(33)	1.539(9)	C(31) - C(34)	1.517(9)
C(35) - C(36)	1.534(6)	C(35) - C(37)	1.530(8)
C(35) - C(38)	1.540(9)		

Table C-4. Interatomic Angles (Deg.) with Esd's

P(1) - W(1) - O(1)	81.8(1)	P(1) - W(1) - O(2)	163.7(1)
O(1) - W(1) - O(2)	84.6(1)	P(1) - W(1) - N(1)	83.6(1)
O(1) - W(1) - N(1)	146.9(2)	O(2) - W(1) - N(1)	103.3(2)
P(1) - W(1) - C(13)	86.7(1)	O(1) - W(1) - C(13)	109.8(2)
O(2) - W(1) - C(13)	106.4(2)	N(1) - W(1) - C(13)	98.2(2)
W(1) - P(1) - O(3)	119.0(1)	W(1) - P(1) - O(4)	107.4(1)
O(3) - P(1) - O(4)	100.6(2)	W(1) - P(1) - O(5)	121.4(2)
O(3) - P(1) - O(5)	98.8(2)	O(4) - P(1) - O(5)	107.4(2)
W(1) - O(1) - C(31)	150.4(3)	W(1) - O(2) - C(35)	137.5(3)
P(1) - O(3) - C(28)	122.9(5)	P(1) - O(4) - C(29)	122.4(4)
P(1) - O(5) - C(30)	122.5(4)	W(1) - N(1) - C(1)	168.0(3)
N(1) - C(1) - C(2)	117.6(4)	N(1) - C(1) - C(6)	120.4(4)
C(2) - C(1) - C(6)	121.9(5)	C(1) - C(2) - C(3)	117.6(5)
C(1) - C(2) - C(7)	122.1(5)	C(3) - C(2) - C(7)	120.3(5)
C(2) - C(3) - C(4)	121.3(5)	C(3) - C(4) - C(5)	120.6(6)
C(4) - C(5) - C(6)	121.3(5)	C(1) - C(6) - C(5)	117.3(5)
C(1) - C(6) - C(10)	121.5(5)	C(5) - C(6) - C(10)	121.1(5)
C(2) - C(7) - C(8)	111.3(5)	C(2) - C(7) - C(9)	111.6(5)
C(8) - C(7) - C(9)	111.1(5)	C(6) - C(10) - C(11)	113.9(5)
C(6) - C(10) - C(12)	109.9(5)	C(11) - C(10) - C(12)	110.6(5)
W(1) - C(13) - C(14)	122.2(4)	C(13) - C(14) - C(15)	127.5(5)
C(14) - C(15) - C(16)	123.1(5)	C(14) - C(15) - C(22)	118.7(5)
C(16) - C(15) - C(22)	118.3(4)	C(15) - C(16) - C(17)	121.3(5)
C(15) - C(16) - C(21)	121.8(5)	C(17) - C(16) - C(21)	116.9(5)
C(16) - C(17) - C(18)	121.9(5)	C(17) - C(18) - C(19)	119.5(5)
C(18) - C(19) - C(20)	119.9(5)	C(19) - C(20) - C(21)	120.9(6)
C(16) - C(21) - C(20)	120.8(5)	C(15) - C(22) - C(23)	121.2(5)
C(15) - C(22) - C(27)	121.3(5)	C(23) - C(22) - C(27)	117.6(6)
C(22) - C(23) - C(24)	121.3(5)	C(23) - C(24) - C(25)	120.5(6)
C(24) - C(25) - C(26)	119.1(7)	C(25) - C(26) - C(27)	120.9(6)
C(22) - C(27) - C(26)	120.5(5)	O(1) - C(31) - C(32)	109.0(5)
O(1) - C(31) - C(33)	105.4(4)	C(32) - C(31) - C(33)	110.3(5)

Table C-4 (cont'd). Interatomic Angles (Deg.) with Esd's

O(1) - C(31) - C(34)	112.9(5)	C(32) - C(31) - C(34)	109.7(4)
C(33) - C(31) - C(34)	109.5(6)	F(1) - C(32) - F(2)	105.7(5)
F(1) - C(32) - F(3)	106.1(4)	F(2) - C(32) - F(3)	105.8(6)
F(1) - C(32) - C(31)	114.3(6)	F(2) - C(32) - C(31)	113.2(4)
F(3) - C(32) - C(31)	111.2(5)	F(4) - C(33) - F(5)	107.3(5)
F(4) - C(33) - F(6)	106.8(6)	F(5) - C(33) - F(6)	106.8(4)
F(4) - C(33) - C(31)	112.4(4)	F(5) - C(33) - C(31)	113.7(6)
F(6) - C(33) - C(31)	109.6(5)	O(2) - C(35) - C(36)	106.8(4)
O(2) - C(35) - C(37)	108.3(4)	C(36) - C(35) - C(37)	109.3(4)
O(2) - C(35) - C(38)	114.7(4)	C(36) - C(35) - C(38)	108.5(5)
C(37) - C(35) - C(38)	109.2(5)	F(7) - C(36) - F(8)	106.5(4)
F(7) - C(36) - F(9)	105.9(4)	F(8) - C(36) - F(9)	106.5(4)
F(7) - C(36) - C(35)	111.3(4)	F(8) - C(36) - C(35)	113.3(4)
F(9) - C(36) - C(35)	112.8(5)	F(10) - C(37) - F(11)	106.7(4)
F(10) - C(37) - F(12)	106.1(5)	F(11) - C(37) - F(12)	106.3(4)
F(10) - C(37) - C(35)	110.4(4)	F(11) - C(37) - C(35)	113.6(5)
F(12) - C(37) - C(35)	113.2(4)		

Table C-5. Anisotropic Displacement Coefficients ($\mathring{A}^2$ x 10^4)^a

	U_{11}	U_{22}	U_{33}	U_{12}	U_{13}	U_{23}
W(1)	181(1)	142(1)	179(1)	-64(1)	-34(1)	-21(1)
P(1)	221(7)	209(6)	231(7)	-51(6)	-17(6)	-33(5)
O(1)	276(20)	199(17)	310(20)	-91(15)	51(16)	-14(15)
O(2)	239(18)	141(16)	259(19)	-62(14)	19(15)	-27(14)
O(3)	401(23)	355(21)	230(20)	-107(18)	8(17)	-58(17)
O(4)	374(22)	183(18)	326(21)	17(16)	-5(17)	-62(16)
O(5)	265(20)	461(23)	364(23)	-105(18)	10(17)	-133(19)
N(1)	162(20)	141(19)	202(21)	-36(17)	-37(17)	-13(16)
F(1)	764(28)	377(20)	537(24)	-147(20)	-61(21)	226(18)
F(2)	1272(41)	512(24)	411(23)	-91(26)	-210(24)	-117(19)
F(3)	472(24)	837(30)	578(26)	-237(22)	-169(20)	299(22)
F(4)	629(25)	363(20)	811(29)	-308(19)	235(22)	33(19)
F(5)	734(28)	479(22)	917(32)	-273(21)	542(25)	-268(22)
F(6)	398(22)	657(26)	991(35)	-300(21)	-101(23)	165(24)
F(7)	350(19)	572(22)	404(20)	-64(17)	-133(16)	-132(17)
F(8)	308(18)	386(19)	519(22)	8(15)	59(16)	-67(16)
F(9)	404(20)	188(16)	644(24)	-62(14)	-90(17)	100(15)
F(10)	730(27)	510(22)	283(19)	151(20)	-168(18)	-55(17)
F(11)	496(21)	534(21)	392(20)	-183(18)	162(17)	-225(17)
F(12)	638(24)	581(22)	343(19)	-408(20)	6(17)	-138(16)
C(1)	155(24)	133(22)	191(25)	-14(19)	-20(20)	-67(19)
C(2)	229(26)	176(24)	225(27)	-69(21)	-8(21)	-42(20)
C(3)	370(33)	201(26)	290(31)	-125(25)	-13(25)	-14(23)
C(4)	379(33)	266(28)	367(33)	-175(26)	-49(26)	-111(25)
C(5)	369(33)	311(30)	244(30)	-90(25)	-106(25)	-99(24)
C(6)	208(26)	193(25)	276(28)	-16(21)	-31(22)	-70(21)
C(7)	301(30)	178(26)	267(29)	-130(23)	-21(23)	-27(22)
C(8)	446(42)	450(40)	358(40)	-20(33)	-152(35)	-52(31)
C(9)	482(42)	581(44)	282(36)	-258(38)	3(30)	-53(31)
C(10)	284(31)	306(29)	268(30)	-112(26)	-60(24)	-35(23)
C(11)	710(55)	480(42)	272(35)	-207(42)	12(35)	-40(30)

Table C-5 (cont'd). Anisotropic Displacement Coefficients (Å^2 x 10^4)[a]

	U_{11}	U_{22}	U_{33}	U_{12}	U_{13}	U_{23}
C(12)	535(47)	330(36)	478(46)	-73(34)	-40(37)	90(32)
C(13)	261(28)	182(25)	216(27)	-56(22)	-38(22)	-36(21)
C(14)	284(29)	215(27)	289(29)	-133(23)	1(23)	-94(23)
C(15)	216(26)	234(26)	216(27)	-77(22)	-23(22)	-44(21)
C(16)	177(26)	247(25)	280(28)	-65(21)	-51(21)	-58(22)
C(17)	254(29)	299(30)	263(30)	-79(24)	-67(23)	-70(25)
C(18)	291(31)	360(32)	264(32)	-82(25)	-78(25)	28(25)
C(19)	325(33)	279(31)	487(39)	-85(26)	-114(28)	36(28)
C(20)	399(35)	245(29)	431(37)	-29(26)	-139(28)	-128(27)
C(21)	331(32)	284(29)	221(31)	-58(24)	-92(25)	-18(24)
C(22)	311(29)	277(27)	201(27)	-144(24)	-9(22)	-56(21)
C(23)	319(31)	377(33)	224(29)	-158(28)	-12(24)	-39(24)
C(24)	352(36)	598(42)	282(32)	-298(33)	-27(28)	-26(29)
C(25)	627(45)	540(41)	339(35)	-396(37)	-68(32)	-117(30)
C(26)	694(49)	353(35)	489(41)	-243(35)	-32(36)	-210(30)
C(27)	398(36)	337(32)	405(35)	-131(28)	-56(29)	-121(27)
C(28)	894(68)	427(43)	311(39)	-195(45)	43(39)	-18(32)
C(29)	750(64)	275(36)	559(52)	129(39)	111(47)	-99(34)
C(30)	227(32)	409(37)	415(38)	-84(29)	-30(29)	-116(32)
C(31)	257(28)	161(24)	349(30)	-122(22)	79(23)	-7(21)
C(32)	531(41)	319(32)	346(34)	-166(29)	-4(29)	36(27)
C(33)	409(36)	317(32)	567(42)	-205(29)	127(33)	-31(30)
C(34)	501(44)	273(32)	390(38)	-159(31)	97(35)	-95(28)
C(35)	239(27)	144(23)	309(29)	-51(21)	74(23)	-55(21)
C(36)	246(29)	243(27)	326(31)	-65(23)	3(24)	-82(23)
C(37)	336(32)	297(29)	270(30)	-69(26)	58(25)	-68(24)
C(38)	464(39)	219(30)	446(39)	-155(29)	164(34)	-85(28)

[a] The anisotropic displacement exponent takes the form: $-2\pi^2(h^2a^{*2}U_{11} + \ldots + 2hka^*b^*U_{12})$.

Table C-6. H-Atom Coordinates (x10^4) and Isotropic Displacement Coefficients (Å^2 x 10^4)

	x	y	z	U
H(3)	4252(48)	6607(44)	2573(23)	106(118)
H(4)	4925(52)	6441(46)	3683(25)	219(131)
H(5)	4870(60)	4752(52)	4395(30)	396(164)
H(7)	2744(49)	4761(45)	1834(23)	113(122)
H(8A)	1246(64)	6641(54)	1302(33)	430(170)
H(8B)	899(74)	6574(61)	2011(34)	500(220)
H(8C)	1822(75)	7362(71)	1797(36)	678(228)
H(9A)	4985(89)	4661(76)	1544(40)	837(270)
H(9B)	4499(69)	6092(63)	1467(32)	530(194)
H(9C)	3798(66)	5492(56)	985(34)	486(182)
H(10)	3025(52)	2769(42)	4166(23)	107(121)
H(11A)	4336(80)	3325(67)	5133(37)	637(250)
H(11B)	2562(77)	3909(65)	4967(33)	576(203)
H(11C)	3445(63)	2517(58)	5329(31)	438(169)
H(12A)	5896(67)	1995(56)	4324(30)	384(187)
H(12B)	5204(91)	1606(79)	3774(48)	969(308)
H(12C)	5098(81)	1121(74)	4475(39)	725(250)
H(13)	558(54)	4061(50)	1758(26)	272(140)
H(14)	-89(52)	1859(48)	1771(24)	195(130)
H(17)	-1441(65)	4364(57)	-103(31)	422(182)
H(18)	-2050(52)	6464(45)	-607(27)	202(130)
H(19)	-2475(63)	7991(58)	81(30)	453(174)
H(20)	-2460(64)	7418(57)	1267(31)	478(176)
H(21)	-1848(55)	5340(47)	1636(28)	223(145)
H(23)	-3731(56)	3762(50)	494(26)	254(145)
H(24)	-4702(64)	2666(53)	-20(29)	350(165)
H(25)	-3517(73)	462(64)	-71(35)	657(215)
H(26)	-1136(74)	-437(67)	392(35)	651(216)
H(27)	-4(69)	771(57)	894(31)	513(184)
H(28A)	-54(100)	3626(86)	5081(49)	1098(336)

Table C-6 (cont'd). H-Atom Coordinates (x10^4) and Isotropic Displacement Coefficients ($Å^2$ x 10^4)

	x	y	z	U
H(28B)	-1294(92)	3612(74)	4642(40)	826(281)
H(28C)	326(106)	2527(95)	4690(49)	1125(376)
H(29A)	-1319(93)	7147(87)	2958(47)	1037(313)
H(29B)	-1060(108)	6477(95)	3738(56)	1299(406)
H(29C)	-2194(86)	6450(74)	3354(40)	654(290)
H(30A)	-1903(58)	2838(50)	2700(26)	258(139)
H(30B)	-2867(73)	4191(67)	2615(36)	581(218)
H(30C)	-3352(88)	3418(72)	3083(39)	789(263)
H(34A)	702(62)	-645(52)	2601(30)	356(162)
H(34B)	2194(67)	-1064(55)	2827(30)	343(187)
H(34C)	1481(78)	-1854(71)	3212(37)	769(236)
H(38A)	4196(66)	2394(59)	1695(30)	449(172)
H(38B)	5346(55)	1813(48)	2336(28)	222(146)
H(38C)	5730(54)	1475(44)	1616(25)	194(126)

D. X-ray Diffraction Study of $W[CH{=}CH\text{-}C(O)\text{-}OCH_2CH_2CH_2Cl]Cl(N\text{-}2,6\text{-}C_6H_3\text{-}Me_2)(PEt_2Ph)_2$

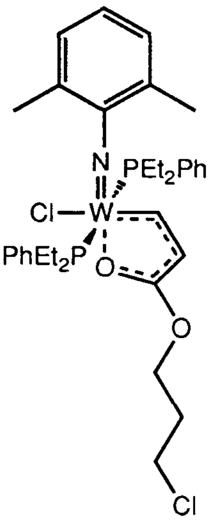

(See Chapter 2, Figure 4 for the ORTEP plot.)

Table D-1. Experimental Data for the X-ray Diffraction Study of $W[CH{=}CH\text{-}C(O)\text{-}OCH_2CH_2CH_2Cl]Cl(N\text{-}2,6\text{-}C_6H_3\text{-}Me_2)(PEt_2Ph)_2$

Formula: $C_{34}H_{47}NO_2P_2Cl_2W$	Fw: 818.4
Temperature (K): 158	Crystal System: Triclinic
Space Group: $P\bar{1}$	Z = 2
$\underline{a}$ = 10.301(2) Å	α = 93.752(16)°
$\underline{b}$ = 12.981(3) Å	β = 104.624(14) °
$\underline{c}$ = 13.903(3) Å	γ = 100.901(15)°
$\underline{V}$ = 1753.9(6) Å^3	D_{calcd}, Mg/m^3 = 1.55
Radiation: MoKα (λ = 0.710730 Å)	Diffractometer: Siemens P3(R3m/V Syst.)
Data Collected: $+h$, $\pm k$, $\pm l$	Monochromator: Highly oriented graphite
Scan Range: 1.20° plus Kα-separation	Scan Type: θ-2θ
2θ Range: 4.0 to 50.0°	Scan Speed: 3.5 deg min^{-1} (in ω)
Absorption Correction: Semi-empirical (ψ-scan method)	μ(MoKα), mm^{-1} = 3.637 Reflections Collected: 6596
No. of Variables: 379	Reflections with $\lvert F_0\rvert > 2.0\sigma(\lvert F_0\rvert)$: 5920
Goodness of Fit: 1.37	R_F = 3.0%, R_{wF} = 3.7%

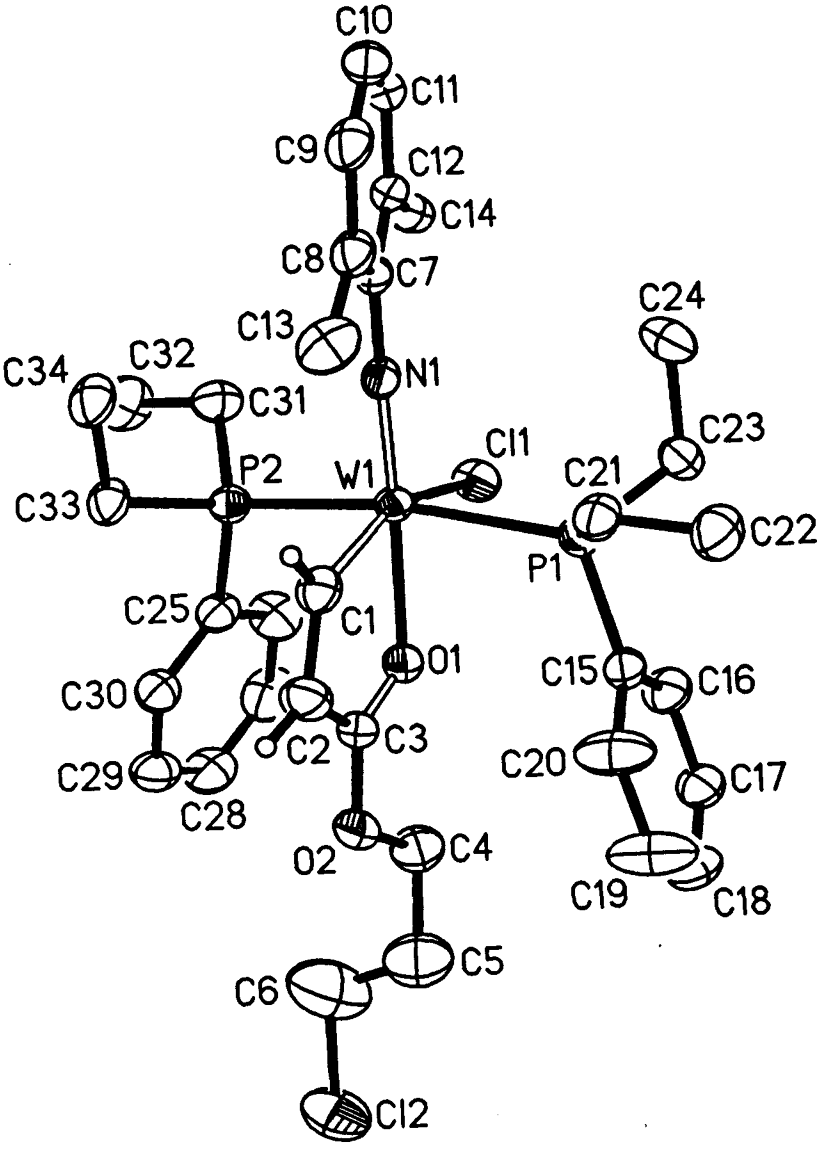

Figure D-1. ORTEP plot of $\overline{\mathrm{W[CH{=}CH{-}C(O}}\mathrm{){-}OCH_2CH_2CH_2Cl]Cl(N{-}2{,}6{-}C_6H_3{-}Me_2)(PEt_2Ph)_2}$ (second view). Thermal ellipsoids are drawn at the 50% probability level.

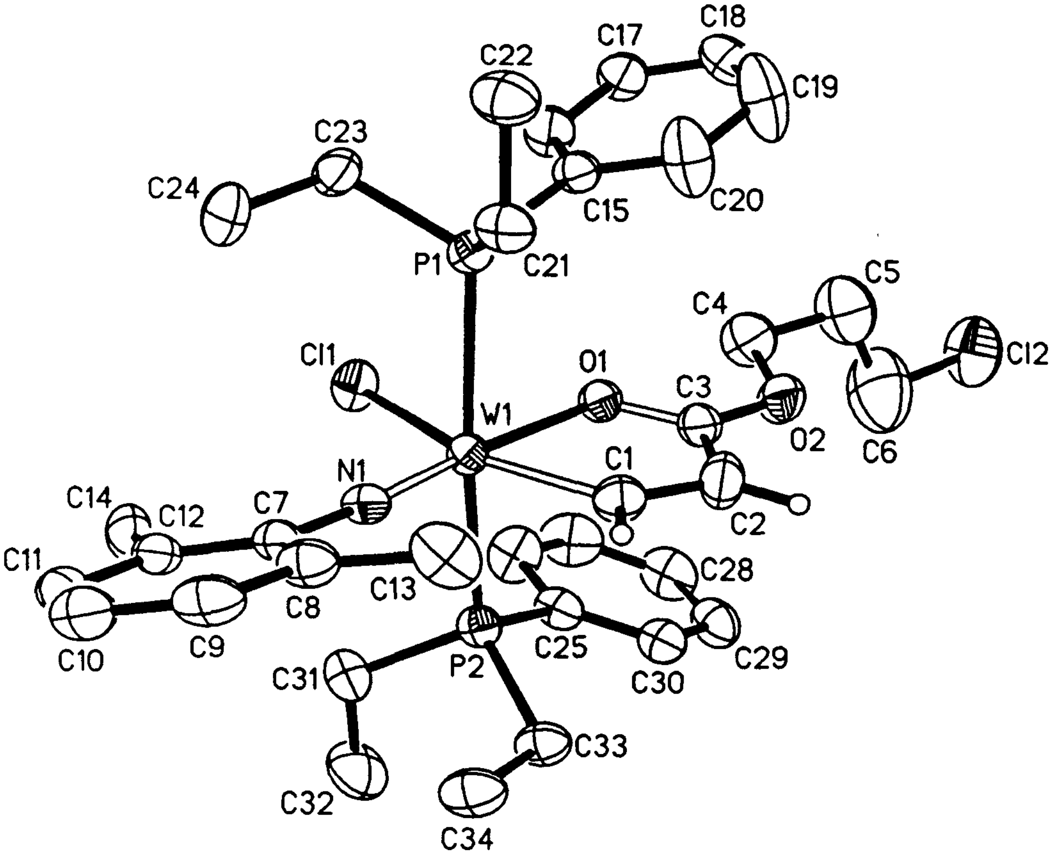

Figure D-2. ORTEP plot of W[CH=CH-C(O)-OCH$_2$CH$_2$CH$_2$Cl]Cl(N-2,6-C$_6$H$_3$-Me$_2$)(PEt$_2$Ph)$_2$ (third view). Thermal ellipsoids are drawn at the 50% probability level.

Table D-2. Atomic Coordinates (x 10^4) and Equivalent Isotropic Displacement Coefficients (Å^2 x 10^4)^a

	x	y	z	U(eq)
W(1)	806(1)	2672(1)	2709(1)	244(1)
Cl(1)	-522(1)	4101(1)	2580(1)	354(4)
Cl(2)	-2442(2)	1509(1)	-3823(1)	712(6)
P(1)	2767(1)	4077(1)	2570(1)	285(3)
P(2)	-1467(1)	1429(1)	2477(1)	283(3)
O(1)	151(3)	2611(2)	1075(2)	295(10)
O(2)	70(4)	1744(3)	-415(2)	434(12)
N(1)	1465(3)	2598(3)	3999(3)	268(11)
C(1)	1502(5)	1461(3)	2153(3)	357(16)
C(2)	1175(5)	1179(4)	1119(3)	428(18)
C(3)	456(5)	1862(3)	596(3)	337(15)
C(4)	-541(6)	2557(4)	-867(4)	485(19)
C(5)	-774(7)	2380(6)	-1994(5)	674(26)
C(6)	-1987(9)	1596(8)	-2464(6)	1028(41)
C(7)	1999(4)	2586(3)	5023(3)	283(13)
C(8)	3097(5)	2080(3)	5375(3)	349(15)
C(9)	3635(5)	2116(4)	6407(4)	417(17)
C(10)	3119(5)	2623(4)	7072(3)	468(18)
C(11)	2043(5)	3108(3)	6725(3)	414(17)
C(12)	1458(5)	3108(3)	5707(3)	331(15)
C(13)	3642(5)	1474(4)	4668(4)	456(19)
C(14)	297(5)	3657(4)	5364(3)	406(17)
C(15)	2713(4)	4342(3)	1290(3)	309(14)
C(16)	1969(5)	5058(4)	846(3)	393(17)
C(17)	1890(5)	5272(4)	-122(3)	404(17)
C(18)	2568(5)	4763(4)	-675(3)	426(17)
C(19)	3295(7)	4050(6)	-262(4)	681(28)
C(20)	3345(6)	3819(5)	712(4)	575(23)
C(21)	4444(4)	3744(4)	3061(3)	351(15)
C(22)	5700(5)	4566(4)	3042(4)	457(18)
C(23)	2920(5)	5396(3)	3198(3)	380(16)

Table D-2 (cont'd). Atomic Coordinates (x 10^4) and Equivalent Isotropic Displacement Coefficients (Å^2 x 10^4)[a]

	x	y	z	U(eq)
C(24)	3149(5)	5425(4)	4335(3)	453(18)
C(25)	-2614(4)	1327(3)	1217(3)	324(14)
C(26)	-3292(5)	2150(4)	953(4)	452(18)
C(27)	-4127(5)	2100(5)	-10(4)	524(20)
C(28)	-4292(5)	1252(4)	-720(4)	474(18)
C(29)	-3611(5)	467(4)	-470(3)	430(17)
C(30)	-2755(4)	497(4)	503(3)	353(15)
C(31)	-2494(5)	1766(4)	3308(3)	408(17)
C(32)	-3874(6)	1015(5)	3162(5)	593(23)
C(33)	-1354(5)	65(3)	2657(3)	357(15)
C(34)	-629(5)	-56(4)	3730(3)	441(17)

[a] Equivalent isotropic U defined as one third of the trace of the orthogonalized U_{ij} tensor.

Table D-3. Interatomic Distances (Å) with Esd's

W(1) - Cl(1)	2.495(1)	W(1) - P(1)	2.509(1)
W(1) - P(2)	2.512(1)	W(1) - O(1)	2.191(3)
W(1) - N(1)	1.766(3)	W(1) - C(1)	2.032(5)
Cl(2) - C(6)	1.819(8)	P(1) - C(15)	1.824(5)
P(1) - C(21)	1.833(5)	P(1) - C(23)	1.830(5)
P(2) - C(25)	1.829(4)	P(1) - C(31)	1.836(6)
P(2) - C(33)	1.826(5)	O(1) - C(3)	1.275(6)
O(2) - C(3)	1.350(5)	O(2) - C(4)	1.430(7)
N(1) - C(7)	1.393(5)	C(1) - C(2)	1.398(6)
C(2) - C(3)	1.388(7)	C(4) - C(5)	1.519(8)
C(5) - C(6)	1.430(10)	C(7) - C(8)	1.412(6)
C(7) - C(12)	1.414(7)	C(8) - C(9)	1.396(6)
C(8) - C(13)	1.498(8)	C(9) - C(10)	1.369(8)
C(10) - C(11)	1.375(8)	C(11) - C(12)	1.392(6)
C(12) - C(14)	1.499(7)	C(15) - C(16)	1.392(7)
C(15) - C(20)	1.375(8)	C(16) - C(17)	1.378(7)
C(17) - C(18)	1.376(8)	C(18) - C(19)	1.364(9)
C(19) - C(20)	1.397(8)	C(21) - C(22)	1.520(6)
C(23) - C(24)	1.536(7)	C(25) - C(26)	1.402(7)
C(25) - C(30)	1.377(6)	C(26) - C(27)	1.386(7)
C(27) - C(28)	1.385(8)	C(28) - C(29)	1.358(8)
C(29) - C(30)	1.409(6)	C(31) - C(32)	1.521(7)
C(33) - C(34)	1.523(6)		

Table D-4. Interatomic Angles (Deg.) with Esd's

Cl(1) - W(1) - P(1)	85.5(1)	Cl(1) - W(1) - P(2)	85.7(1)
P(1) - W(1) - P(2)	166.1(1)	Cl(1) - W(1) - O(1)	81.0(1)
P(1) - W(1) - O(1)	83.9(1)	P(2) - W(1) - O(1)	84.2(1)
Cl(1) - W(1) - N(1)	106.6(1)	P(1) - W(1) - N(1)	95.7(1)
P(2) - W(1) - N(1)	97.1(1)	O(1) - W(1) - N(1)	172.4(1)
Cl(1) - W(1) - C(1)	154.5(1)	P(1) - W(1) - C(1)	94.7(1)
P(2) - W(1) - C(1)	88.7(1)	O(1) - W(1) - C(1)	73.8(1)
N(1) - W(1) - C(1)	98.8(2)		
W(1) - P(1) - C(15)	114.1(1)	W(1) - P(1) - C(21)	112.9(2)
C(15) - P(1) - C(21)	104.8(2)	W(1) - P(1) - C(23)	116.4(2)
C(15) - P(1) - C(23)	102.2(2)	C(21) - P(1) - C(23)	105.2(2)
W(1) - P(2) - C(25)	113.1(1)	W(1) - P(2) - C(31)	115.7(1)
C(25) - P(2) - C(31)	104.2(2)	W(1) - P(2) - C(33)	114.5(2)
C(25) - P(2) - C(33)	104.0(2)	C(31) - P(2) - C(33)	104.0(2)
W(1) - O(1) - C(3)	114.9(3)	C(3) - O(2) - C(4)	115.7(4)
W(1) - N(1) - C(7)	177.6(3)	W(1) - C(1) - C(2)	120.0(4)
C(1) - C(2) - C(3)	111.5(5)	O(1) - C(3) - O(2)	119.4(4)
O(1) - C(3) - C(2)	119.6(4)	O(2) - C(3) - C(2)	121.0(4)
O(2) - C(4) - C(5)	109.5(5)	C(4) - C(5) - C(6)	111.8(6)
Cl(2) - C(6) - C(5)	113.0(6)	N(1) - C(7) - C(8)	120.2(4)
N(1) - C(7) - C(12)	119.5(4)	C(8) - C(7) - C(12)	120.3(4)
C(7) - C(8) - C(9)	118.5(5)	C(7) - C(8) - C(13)	121.4(4)
C(9) - C(8) - C(13)	120.1(4)	C(8) - C(9) - C(10)	121.4(5)
C(9) - C(10) - C(11)	119.8(4)	C(10) - C(11) - C(12)	121.9(5)
C(7) - C(12) - C(11)	118.1(4)	C(7) - C(12) - C(14)	122.0(4)
C(11) - C(12) - C(14)	120.0(5)	P(1) - C(15) - C(16)	120.5(4)
P(1) - C(15) - C(20)	122.1(4)	C(16) - C(15) - C(20)	117.4(4)
C(15) - C(16) - C(17)	122.4(5)	C(16) - C(17) - C(18)	119.1(5)
C(17) - C(18) - C(19)	119.8(5)	C(18) - C(19) - C(20)	120.7(6)
C(15) - C(20) - C(19)	120.5(6)	P(1) - C(21) - C(22)	116.7(3)
P(1) - C(23) - C(24)	113.3(3)	P(2) - C(25) - C(26)	119.2(3)
P(2) - C(25) - C(30)	121.5(4)	C(26) - C(25) - C(30)	119.2(4)

Table D-4 (cont'd). Interatomic Angles (Deg.) with Esd's

C(25) - C(26) - C(27)	119.8(5)	C(26) - C(27) - C(28)	120.8(5)
C(27) - C(28) - C(29)	119.3(4)	C(28) - C(29) - C(30)	121.0(5)
C(25) - C(30) - C(29)	119.8(5)	P(2) - C(31) - C(32)	115.5(4)
P(2) - C(33) - C(34)	112.8(3)		

Table D-5. Anisotropic Displacement Coefficients (Å^2 x 10^4)^a

	U_{11}	U_{22}	U_{33}	U_{12}	U_{13}	U_{23}
W(1)	279(1)	243(1)	198(1)	64(1)	35(1)	44(1)
Cl(1)	422(6)	336(6)	306(5)	168(5)	36(4)	52(4)
Cl(2)	763(10)	860(11)	382(7)	177(9)	-45(7)	-74(7)
P(1)	331(6)	257(5)	234(5)	38(4)	33(4)	44(4)
P(2)	286(5)	304(6)	242(5)	61(4)	35(4)	50(4)
O(1)	342(16)	280(15)	237(14)	39(12)	52(12)	34(11)
O(2)	634(22)	354(17)	262(16)	22(16)	99(15)	-9(13)
N(1)	252(17)	258(17)	270(17)	28(14)	41(14)	59(14)
C(1)	445(26)	300(23)	354(24)	125(20)	110(20)	106(18)
C(2)	634(32)	361(25)	341(24)	177(23)	176(23)	19(19)
C(3)	431(25)	318(23)	217(20)	-16(19)	85(18)	8(17)
C(4)	580(32)	515(31)	3317(25)	103(25)	39(23)	98(22)
C(5)	706(41)	839(46)	496(34)	262(36)	116(30)	112(31)
C(6)	1021(63)	1284(77)	663(48)	208(56)	120(44)	-181(48)
C(7)	292(21)	276(21)	225(19)	-17(17)	22(16)	54(16)
C(8)	337(23)	331(23)	325(23)	19(18)	15(19)	106(18)
C(9)	388(25)	383(25)	392(26)	11(20)	-35(21)	175(20)
C(10)	551(31)	428(28)	257(22)	-70(24)	-78(22)	94(20)
C(11)	571(30)	304(24)	279(23)	-74(21)	87(21)	17(18)
C(12)	394(24)	290(22)	257(21)	-43(18)	77(18)	48(17)
C(13)	392(26)	595(32)	446(27)	220(24)	110(22)	206(24)
C(14)	509(28)	399(26)	287(22)	90(22)	89(21)	-22(19)
C(15)	336(22)	308(22)	250(20)	25(18)	49(17)	53(16)
C(16)	524(29)	349(24)	338(24)	153(21)	112(21)	115(19)
C(17)	566(30)	351(25)	303(23)	118(22)	101(21)	102(19)
C(18)	402(25)	602(31)	283(23)	114(23)	80(20)	139(21)
C(19)	826(43)	1099(53)	319(27)	634(42)	190(28)	125(29)
C(20)	756(39)	812(41)	309(25)	533(34)	130(25)	139(25)
C(21)	315(22)	399(25)	294(22)	29(19)	19(18)	106(18)
C(22)	359(26)	527(31)	419(27)	-9(22)	49(21)	111(22)
C(23)	490(27)	297(23)	303(23)	31(20)	63(20)	6(18)

Table D-5 (cont'd). Anisotropic Displacement Coefficients ($Å^2$ x 10^4)[a]

	U_{11}	U_{22}	U_{33}	U_{12}	U_{13}	U_{23}
C(24)	516(29)	450(28)	333(25)	106(23)	31(22)	-64(21)
C(25)	256(21)	410(25)	265(21)	20(18)	26(17)	77(18)
C(26)	392(26)	506(30)	418(27)	175(23)	-25(21)	65(22)
C(27)	426(29)	618(35)	496(31)	167(25)	-15(24)	223(26)
C(28)	355(26)	657(35)	313(24)	46(24)	-53(20)	110(23)
C(29)	392(26)	550(31)	298(23)	26(23)	69(20)	15(21)
C(30)	302(22)	404(25)	313(22)	34(19)	41(18)	49(19)
C(31)	415(26)	493(29)	337(24)	108(22)	137(21)	31(20)
C(32)	453(30)	721(40)	640(36)	35(28)	282(28)	59(30)
C(33)	365(24)	322(23)	347(23)	47(19)	31(19)	110(18)
C(34)	451(27)	392(26)	397(26)	34(22)	-20(22)	168(21)

[a] The anisotropic displacement exponent takes the form: $-2\pi^2(h^2a^{*2}U_{11} + \ldots + 2hka^*b^*U_{12})$.

Table D-6. H-Atom Coordinates (x10^4) and Isotropic Displacement Coefficients (Å^2 x 10^4)

	x	y	z	U
H(1A)	2056	1082	2601	800
H(2A)	1419	587	811	800
H(4A)	41	3237	-601	800
H(4B)	-1407	2535	-720	800
H(5A)	7	2164	-2135	800
H(5B)	-862	3028	-2273	800
H(6A)	-1841	923	-2266	800
H(6B)	-2737	1755	-2232	800
H(9A)	4388	1780	6654	800
H(10A)	3504	2638	7779	800
H(11A)	1681	3459	7196	800
H(13A)	4380	1185	5041	800
H(13B)	2919	910	4278	800
H(13C)	3972	1937	4230	800
H(14A)	84	3965	5936	800
H(14B)	555	4203	4971	800
H(14C)	-494	3154	4965	800
H(16A)	1500	5415	1233	800
H(17A)	1367	5768	-410	800
H(18A)	2540	4915	-1345	800
H(19A)	3763	3692	-650	800
H(20A)	3831	3297	986	800
H(21A)	4458	3101	1685	800
H(21B)	4528	3606	3742	800
H(22A)	6521	4317	3315	800
H(22B)	5647	4697	2363	800
H(22C)	5718	5209	3433	800
H(23A)	2096	5641	2922	800
H(23B)	3672	5873	3067	800
H(24A)	3220	6131	4630	800

Table D-6 (cont'd). H-Atom Coordinates (x10^4) and Isotropic Displacement Coefficients (Å^2 x 10^4)

	x	y	z	U
H(24B)	2390	4960	4470	800
H(24C)	3982	5194	4617	800
H(26A)	-3184	2739	1441	800
H(27A)	-4598	2661	-188	800
H(28A)	-4878	1222	-1383	800
H(29A)	-3716	-118	-963	800
H(30A)	-2266	-55	673	800
H(31A)	-2656	2460	3210	800
H(31B)	-1966	1792	3988	800
H(32A)	-4340	1250	3623	800
H(32B)	-4424	996	2488	800
H(32C)	-3725	320	3277	800
H(33A)	-861	-181	2221	800
H(33B)	-2263	-371	2477	800
H(34A)	-588	-781	3795	800
H(34B)	285	370	3908	800
H(34C)	-1130	179	4167	800

E. X-ray Diffraction Study of W(=CHC_6H_4-*p*-Me)Cl_2(NPh)($PMePh_2$)$_2$

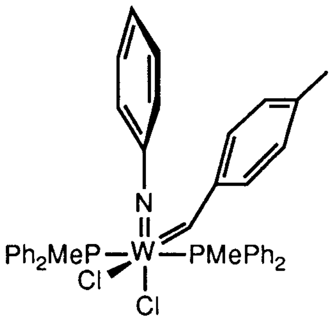

(See Chapter 3, Figure 3 for the ORTEP plot.)

Table E-1. Experimental Data for the X-ray Diffraction Study of W(=CHC_6H_4-*p*-Me)Cl_2(NPh)($PMePh_2$)$_2$

Formula: $C_{40}H_{39}NP_2Cl_2W$
Temperature (K): 168
Space Group: $P\bar{1}$
$\underline{a} = 9.6139(12)$ Å
$\underline{b} = 11.0269(14)$ Å
$\underline{c} = 17.559(2)$ Å
D_{calcd}, Mg/m^3 = 1.556
Radiation: MoKα ($\bar{\lambda} = 0.710730$ Å)
Data Collected: $+h$, $\pm k$, $\pm l$
Scan Range: 1.20° plus Kα-separation
2θ Range: 4.0 to 50.0°
Absorption Correction:
Semi-empirical (ψ-scan method)
No. of Variables: 415
Goodness of Fit: 1.08

Fw: 850.4
Crystal System: Triclinic
Z = 2
$\alpha = 92.665(11)°$
$\beta = 102.399(10)°$
$\gamma = 90.705(10)°$
$\underline{V} = 1815.6(4)$ Å^3
Diffractometer: Siemens P3 (R3m/V System)
Monochromator: Highly oriented graphite
Scan Type: θ-2θ
Scan Speed: 3.0 deg min^{-1} (in ω)
μ(MoKα), mm^{-1} = 3.51
Reflections Collected: 8664
Reflections with $|F_o| > 3.0\sigma(|F_o|)$: 7811
$R_F = 3.0\%$, $R_{wF} = 4.1\%$

Table E-2. Atomic Coordinates (x 10^4) and Equivalent Isotropic Displacement Coefficients (Å^2 x 10^4)[a]

	x	y	z	U(eq)
W(1)	3976(1)	1766(1)	2691(1)	177(1)
Cl(1)	6013(1)	1796(1)	3898(1)	301(3)
Cl(2)	5096(1)	-111(1)	2284(1)	284(3)
P(1)	5839(1)	2750(1)	2069(1)	220(2)
P(2)	2778(1)	218(1)	3380(1)	198(2)
N(1)	3275(3)	3048(3)	3087(2)	209(8)
C(1)	2603(4)	1583(3)	1677(2)	252(10)
C(2)	1392(4)	2237(3)	1240(2)	267(11)
C(3)	661(5)	1762(5)	516(3)	467(15)
C(4)	-476(5)	2351(6)	65(3)	522(17)
C(5)	-914(4)	3463(5)	321(3)	409(14)
C(6)	-194(4)	3942(4)	1048(3)	382(13)
C(7)	929(4)	3351(3)	1503(2)	314(11)
C(8)	-2113(5)	4137(6)	-168(3)	562(19)
C(9)	2882(4)	3997(3)	3538(2)	222(9)
C(10)	3916(4)	4843(3)	3926(2)	297(11)
C(11)	3533(5)	5749(4)	4418(2)	377(13)
C(12)	2146(5)	5807(4)	4523(2)	410(14)
C(13)	1133(5)	4987(4)	4128(3)	401(14)
C(14)	1471(4)	4070(3)	3634(2)	307(11)
C(15)	5467(4)	2547(4)	1005(2)	304(12)
C(16)	4539(5)	3294(5)	534(3)	466(16)
C(17)	4174(5)	3068(6)	-274.(3)	540(18)
C(18)	4712(7)	2100(5)	-614(3)	543(19)
C(19)	5638(8)	1378(5)	-154(3)	700(26)
C(20)	6028(7)	1576(4)	648(3)	556(20)
C(21)	6016(4)	4379(3)	2279(2)	228(10)
C(22)	7337(4)	4937(3)	2604(2)	311(12)
C(23)	7440(5)	6163(4)	2794(3)	383(13)
C(24)	6252(5)	6874(4)	2650(3)	398(14)
C(25)	4921(5)	6340(4)	2328(3)	366(13)

Table E-2 (cont'd). Atomic Coordinates (x 10^4) and Equivalent Isotropic Displacement Coefficients (Å^2 x 10^4)[a]

	x	y	z	U(eq)
C(26)	4814(4)	5092(3)	2154(2)	291(11)
C(27)	7622(4)	2171(3)	2389(3)	346(13)
C(28)	1474(4)	-794(3)	2751(2)	241(10)
C(29)	365(4)	-311(4)	2201(2)	316(12)
C(30)	-626(4)	-1063(4)	1711(3)	387(13)
C(31)	-497(5)	-2310(5)	1736(3)	475(16)
C(32)	605(6)	-2802(4)	2264(3)	496(17)
C(33)	1577(4)	-2053(3)	2777(3)	335(12)
C(34)	1868(4)	940(3)	4086(2)	240(10)
C(35)	2738(4)	1653(4)	4693(2)	315(12)
C(36)	2148(5)	2223(4)	5269(2)	402(14)
C(37)	693(5)	2083(4)	5242(2)	402(14)
C(38)	-159(5)	1403(4)	4632(3)	417(15)
C(39)	425(4)	829(4)	4060(2)	320(12)
C(40)	4019(4)	-777(3)	3972(2)	283(11)

[a] Equivalent isotropic U defined as one third of the trace of the orthogonalized U_{ij} tensor.

Table E-3. Interatomic Distances (Å) with Esd's

W(1) - Cl(1)	2.556(1)	W(1) - Cl(2)	2.490(1)
W(1) - P(1)	2.546(1)	W(1) - P(2)	2.538(1)
W(1) - N(1)	1.752(3)	W(1) - C(1)	1.975(3)
P(1) - C(15)	1.829(4)	P(1) - C(21)	1.814(3)
P(1) - C(27)	1.818(4)	P(2) - C(28)	1.815(3)
P(2) - C(34)	1.825(4)	P(2) - C(40)	1.821(4)
N(1) - C(9)	1.387(5)	C(1) - C(2)	1.467(5)
C(2) - C(3)	1.389(5)	C(2) - C(7)	1.404(6)
C(3) - C(4)	1.392(7)	C(4) - C(5)	1.388(8)
C(5) - C(6)	1.391(6)	C(5) - C(8)	1.508(7)
C(6) - C(7)	1.387(5)	C(9) - C(10)	1.397(5)
C(9) - C(14)	1.405(5)	C(10) - C(11)	1.395(6)
C(11) - C(12)	1.386(7)	C(12) - C(13)	1.370(6)
C(13) - C(14)	1.389(6)	C(15) - C(16)	1.387(6)
C(15) - C(20)	1.387(7)	C(16) - C(17)	1.396(6)
C(17) - C(18)	1.360(8)	C(18) - C(19)	1.359(8)
C(19) - C(20)	1.384(7)	C(21) - C(22)	1.398(5)
C(21) - C(26)	1.390(5)	C(22) - C(23)	1.375(6)
C(23) - C(24)	1.378(7)	C(24) - C(25)	1.394(6)
C(25) - C(26)	1.394(5)	C(28) - C(29)	1.404(5)
C(28) - C(33)	1.395(5)	C(29) - C(30)	1.379(5)
C(30) - C(31)	1.384(7)	C(31) - C(32)	1.385(7)
C(32) - C(33)	1.385(6)	C(34) - C(35)	1.406(5)
C(34) - C(39)	1.382(5)	C(35) - C(36)	1.392(6)
C(36) - C(37)	1.395(7)	C(37) - C(38)	1.384(6)
C(38) - C(39)	1.383(6)		

Table E-4. Interatomic Angles (Deg.) with Esd's

Cl(1) - W(1) - Cl(2)	84.7(1)	Cl(1) - W(1) - P(1)	83.4(1)
Cl(2) - W(1) - P(1)	81.4(1)	Cl(1) - W(1) - P(2)	85.8(1)
Cl(2) - W(1) - P(2)	80.7(1)	P(1) - W(1) - P(2)	159.8(1)
Cl(1) - W(1) - N(1)	89.5(1)	Cl(2) - W(1) - N(1)	173.5(10
P(1) - W(1) - N(1)	100.9(1)	P(2) - W(1) - N(1)	96.1(1)
Cl(1) - W(1) - C(1)	170.8(1)	Cl(2) - W(1) - C(1)	86.9(1)
P(1) - W(1) - C(1)	91.8(1)	P(2) - W(1) - C(1)	96.3(1)
N(1) - W(1) - C(1)	99.1(1)		
W(1) - P(1) - C(15)	113.9(1)	W(1) - P(1) - C(21)	112.7(1)
C(15) - P(1) - C(21)	105.5(2)	W(1) - P(1) - C(27)	114.0(2)
C(15) - P(1) - C(27)	104.5(2)	C(21) - P(1) - C(27)	105.4(2)
W(1) - P(2) - C(28)	115.7(1)	W(1) - P(2) - C(34)	111.9(1)
C(28) - P(2) - C(34)	106.3(2)	W(1) - P(2) - C(40)	113.7(1)
C(28) - P(2) - C(40)	105.1(2)	C(34) - P(2) - C(40)	103.0(2)
W(1) - N(1) - C(9)	168.8(2)	W(1) - C(1) - C(2)	138.1(3)
C(1) - C(2) - C(3)	119.6(4)	C(1) - C(2) - C(7)	123.7(3)
C(3) - C(2) - C(7)	116.7(4)	C(2) - C(3) - C(4)	122.4(5)
C(3) - C(4) - C(5)	120.6(4)	C(4) - C(5) - C(6)	117.4(4)
C(4) - C(5) - C(8)	121.7(4)	C(6) - C(5) - C(8)	121.0(4)
C(5) - C(6) - C(7)	122.1(4)	C(2) - C(7) - C(6)	120.7(3)
N(1) - C(9) - C(10)	119.4(3)	N(1) - C(9) - C(14)	120.2(3)
C(10) - C(9) - C(14)	120.3(3)	C(9) - C(10) - C(11)	119.1(4)
C(10) - C(11) - C(12)	120.5(4)	C(11) - C(12) - C(13)	120.0(4)
C(12) - C(13) - C(14)	121.3(4)	C(9) - C(14) - C(13)	118.8(3)
P(1) - C(15) - C(16)	121.4(3)	P(1) - C(15) - C(20)	120.4(3)
C(16) - C(15) - C(20)	118.1(4)	C(15) - C(16) - C(17)	120.8(5)
C(16) - C(17) - C(18)	120.5(5)	C(17) - C(18) - C(19)	118.7(5)
C(18) - C(19) - C(20)	122.4(6)	C(15) - C(20) - C(19)	119.5(5)
P(1) - C(21) - C(22)	121.4(3)	P(1) - C(21) - C(26)	120.0(3)
C(22) - C(21) - C(26)	118.4(3)	C(21) - C(22) - C(23)	120.6(4)

Table E-4 (cont'd). Interatomic Angles (Deg.) with Esd's

C(22) - C(23) - C(24)	120.9(4)	C(23) - C(24) - C(25)	119.7(4)
C(24) - C(25) - C(26)	119.3(4)	C(21) - C(26) - C(25)	121.0(4)
P(2) - C(28) - C(29)	119.8(3)	P(2) - C(28) - C(33)	121.5(3)
C(29) - C(28) - C(33)	118.7(3)	C(28) - C(29) - C(30)	120.7(4)
C(29) - C(30) - C(31)	119.8(4)	C(30) - C(31) - C(32)	120.2(4)
C(31) - C(32) - C(33)	120.3(4)	C(28) - C(33) - C(32)	120.2(4)
P(2) - C(34) - C(35)	115.6(3)	P(2) - C(34) - C(39)	124.8(3)
C(35) - C(34) - C(39)	119.5(4)	C(34) - C(35) - C(36)	119.9(4)
C(35) - C(36) - C(37)	119.8(4)	C(36) - C(37) - C(38)	119.7(4)
C(37) - C(38) - C(39)	120.6(4)	C(34) - C(39) - C(38)	120.3(3)

Table E-5. Anisotropic Displacement Coefficients (Å^2 x 10^4)^a

	U_{11}	U_{22}	U_{33}	U_{12}	U_{13}	U_{23}
W(1)	191(1)	178(1)	149(1)	24(1)	15(1)	-19(1)
Cl(1)	238(4)	390(5)	233(4)	53(3)	-35(3)	-19(3)
Cl(2)	382(5)	211(4)	277(4)	89(3)	114(3)	-14(3)
P(1)	210(4)	220(4)	235(4)	32(3)	61(3)	-18(3)
P(2)	219(4)	210(4)	159(4)	32(3)	24(3)	10(3)
N(1)	198(12)	231(14)	190(13)	27(11)	26(10)	14(11)
C(1)	261(16)	290(18)	194(16)	-23(14)	27(13)	10(13)
C(2)	229(16)	348(19)	218(17)	-17(14)	31(13)	45(14)
C(3)	374(22)	687(32)	259(21)	118(21)	-90(17)	-108(20)
C(4)	338(22)	913(40)	257(22)	111(24)	-58(17)	-13(23)
C(5)	227(17)	631(29)	348(22)	-10(18)	-33(16)	241(21)
C(6)	316(19)	317(20)	465(25)	2(16)	-44(18)	134(18)
C(7)	308(18)	281(18)	306(20)	-1(15)	-43(15)	54(15)
C(8)	294(21)	805(38)	564(31)	10(22)	-37(20)	394(29)
C(9)	271(16)	204(15)	171(15)	47(13)	9(13)	-13(12)
C(10)	375(19)	233(17)	249(18)	29(15)	-1(15)	-20(14)
C(11)	524(25)	274(19)	265(20)	72(17)	-53(18)	-52(15)
C(12)	603(27)	369(22)	232(19)	259(20)	33(18)	-39(16)
C(13)	415(22)	423(24)	394(23)	216(19)	143(19)	11(18)
C(14)	316(18)	305(19)	299(19)	89(15)	65(15)	-32(15)
C(15)	370(19)	330(19)	247(18)	-117(16)	167(16)	-71(15)
C(16)	384(22)	693(32)	275(21)	108(22)	-5(17)	-115(21)
C(17)	445(25)	876(41)	252(22)	-6(26)	-7(19)	-73(23)
C(18)	907(40)	491(28)	252(22)	-286(28)	214(24)	-88(20)
C(19)	1425(63)	345(26)	443(30)	44(32)	474(36)	-99(22)
C(20)	1106(46)	318(22)	347(24)	156(26)	373(28)	47(18)
C(21)	288(17)	211(16)	188(16)	12(13)	60(13)	-14(12)
C(22)	326(19)	251(18)	333(20)	6(15)	32(15)	-35(15)
C(23)	487(24)	316(21)	319(22)	-87(18)	51(18)	-72(16)
C(24)	684(30)	244(19)	288(21)	21(19)	151(20)	8(15)

Table E-5 (cont'd). Anisotropic Displacement Coefficients ($Å^2$ x 10^4)[a]

	U_{11}	U_{22}	U_{33}	U_{12}	U_{13}	U_{23}
C(25)	513(24)	271(19)	339(21)	122(17)	127(18)	74(16)
C(26)	334(18)	288(18)	261(18)	72(15)	73(15)	51(14)
C(27)	223(17)	261(18)	554(26)	47(14)	84(17)	22(17)
C(28)	248(16)	254(17)	217(17)	-40(13)	51(13)	-10(13)
C(29)	308(18)	361(20)	257(19)	-19(15)	10(15)	31(15)
C(30)	310(19)	486(25)	322(21)	-55(18)	-25(16)	20(18)
C(31)	400(23)	460(26)	503(28)	-189(20)	-16(20)	-47(21)
C(32)	515(27)	297(22)	630(33)	-111(20)	44(24)	-31(21)
C(33)	338(19)	267(19)	385(22)	-10(15)	48(17)	3(16)
C(34)	265(16)	270(17)	184(16)	75(13)	36(13)	42(13)
C(35)	307(18)	421(22)	205(17)	100(16)	34(14)	-46(15)
C(36)	428(23)	517(26)	236(19)	173(20)	16(17)	-49(18)
C(37)	431(22)	522(26)	275(20)	223(20)	116(17)	5(18)
C(38)	339(21)	549(27)	389(24)	194(19)	114(18)	67(20)
C(39)	313(18)	421(22)	236(18)	95(16)	68(15)	47(16)
C(40)	313(18)	274(18)	243(18)	93(14)	7(14)	44(14)

[a] The anisotropic displacement exponent takes the form: $-2\pi^2(h^2a^{*2}U_{11} + \ldots + 2hka^*b^*U_{12})$.

Table E-6. H-Atom Coordinates (x 10^4) and Isotropic Displacement Coefficients ($Å^2$ x 10^4)

	x	y	z	U
H(1A)	2784	866	1386	800
H(3A)	951	998	324	800
H(4A)	-968	1986	-428	800
H(6A)	-488	4706	1239	800
H(7A)	1394	3704	2005	800
H(8A)	-2290	3812	-698	800
H(8B)	-1859	4984	-150	800
H(8C)	-2960	4058	34	800
H(10A)	4880	4793	3860	800
H(11A)	4233	6343	4679	800
H(12A)	1900	6422	4873	800
H(13A)	170	5044	4194	800
H(14A)	761	3491	3362	800
H(16A)	4146	3972	771	800
H(17A)	3547	3607	-591	800
H(18A)	4436	1933	-1168	800
H(19A)	6024	700	-396	800
H(20A)	6688	1053	958	800
H(22A)	8179	4458	2701	800
H(23A)	8351	6533	3025	800
H(24A)	6336	7733	2773	800
H(25A)	4090	6831	2224	800
H(26A)	3894	4721	1944	800
H(27A)	7912	2427	2930	800
H(27B)	8257	2503	2094	800
H(27C)	7614	1302	2324	800
H(29A)	295	554	2169	800
H(30A)	-1398	-723	1349	800
H(31A)	-1169	-2835	1383	800
H(32A)	686	-3667	2286	800
H(33A)	2334	-2400	3144	800

Table E-6 (cont'd). H-Atom Coordinates (x 10^4) and Isotropic Displacement Coefficients ($Å^2$ x 10^4)

	x	y	z	U
H(35A)	3737	1755	4707	800
H(36A)	2736	2705	5688	800
H(37A)	288	2457	5647	800
H(38A)	-1164	1332	4608	800
H(39A)	-173	352	3642	800
H(40A)	3538	-1212	4305	800
H(40B)	4787	-306	4295	800
H(40C)	4387	-1340	3635	800

F. X-ray Diffraction Study of $W(=CHC_6H_4\text{-}o\text{-}OMe)(N\text{-}2,6\text{-}C_6H_3\text{-}Me_2)[OCMe(CF_3)_2]_2(THF)$

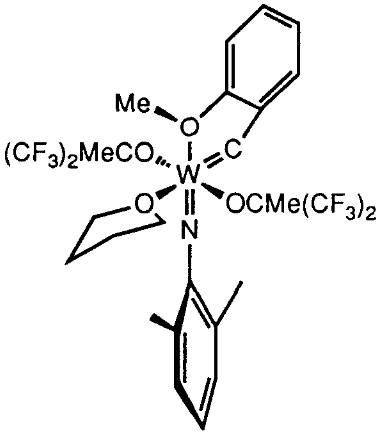

(See Chapter 3, Figure 4 for the ORTEP plot.)

Table F-1. Experimental Data for the X-ray Diffraction Study of $W(=CHC_6H_4\text{-}o\text{-}OMe)(N\text{-}2,6\text{-}C_6H_3\text{-}Me_2)[OCMe(CF_3)_2]_2(THF)$

Formula: $C_{28}H_{31}NO_4F_{12}W$	Fw: 857.4
Temperature (K): 173	Crystal System: Monoclinic
Space Group: $P2_1/c$	Z = 4
a = 12.606(3) Å	V = 3108.0(13) $Å^3$
b = 12.981(3) Å	β = 91.85(2)°
c = 18.998(5) Å	D_{calcd}, Mg/m^3 = 1.830
Radiation: MoKα (λ = 0.710730 Å)	Diffractometer: Nicolet P3
Data Collected: $+h$, $+k$, $\pm l$	Monochromator: Highly oriented graphite
Scan Range: 1.20° plus Kα-separation	Scan Type: θ-2θ
2θ Range: 4.0 to 50.0°	Scan Speed: 3.0 deg min^{-1} (in ω)
Reflections Collected: 6054	μ(MoKα), mm^{-1} = 3.90
No. of Variables: 415	Reflections with $\lvert F_0 \rvert > 0$: 5269
Goodness of Fit: 1.39	R_F = 3.8%, R_{wF} = 4.4%

Table F-2. Atomic Coordinates (x 10^4) and Equivalent Isotropic Displacement Coefficients (Å^2 x 10^4)[a]

	x	y	z	U(eq)
W(1)	2489.6(.1)	1575.3(.1)	1961.6(.1)	182.9(.7)
C(1)	4022(4)	1477(3)	1899(3)	224(15)
C(3)	5674(4)	2045(4)	1274(3)	318(17)
C(4)	6117(4)	2482(4)	688(3)	344(18)
C(5)	5469(5)	2781(5)	119(3)	371(19)
C(6)	4376(4)	2641(4)	132(3)	307(17)
C(7)	3955(4)	2229(4)	728(3)	240(15)
C(8)	2208(5)	1998(5)	180(3)	340(18)
C(9)	2165(4)	829(4)	3503(3)	226(15)
C(10)	2987(4)	411(4)	3936(3)	268(16)
C(11)	2758(4)	105(4)	4616(3)	276(16)
C(12)	1750(5)	210(4)	4869(3)	329(17)
C(13)	948(5)	654(4)	4445(3)	307(17)
C(14)	1136(4)	961(4)	3759(3)	260(16)
C(15)	4096(4)	315(5)	3678(3)	347(18)
C(16)	273(4)	1447(4)	3303(3)	352(19)
C(17)	2953(4)	3866(4)	2458(3)	241(15)
C(18)	2354(5)	4082(5)	3126(3)	431(22)
C(19)	2897(5)	4820(4)	1972(3)	314(17)
C(20)	4119(5)	3643(5)	2663(4)	404(20)
C(21)	2337(4)	-626(4)	1242(3)	296(17)
C(22)	1532(5)	-1039(5)	687(3)	405(21)
C(23)	2309(6)	-1325(4)	1897(4)	467(24)
C(24)	3433(5)	-648(5)	942(4)	555(26)
C(25)	-23(4)	1262(4)	1390(3)	300(17)
C(26)	-1041(4)	1884(4)	1445(3)	352(18)
C(27)	-723(5)	2919(4)	1153(3)	361(19)
C(28)	388(4)	3067(4)	1469(3)	321(17)
F(1)	2377(4)	3265(3)	3551(2)	641(17)
F(2)	2774(3)	4867(3)	3512(2)	531(13)
F(3)	1335(3)	4313(3)	3012(2)	617(15)

Table F-2 (cont'd). Atomic Coordinates (x 10^4) and Equivalent Isotropic Displacement Coefficients ($Å^2$ x 10^4)[a]

	x	y	z	U(eq)
F(4)	1938(3)	5103(2)	1790(2)	475(12)
F(5)	3409(3)	5637(3)	2255(2)	505(13)
F(6)	3390(3)	4590(3)	1371(2)	508(13)
F(7)	552(3)	-1120(3)	910(2)	555(14)
F(8)	1473(4)	-406(3)	133(2)	632(16)
F(9)	1799(3)	-1969(3)	432(2)	554(14)
F(10)	3086(4)	-1080(3)	2356(2)	742(18)
F(11)	2416(4)	-2309(3)	1748(3)	858(21)
F(12)	1404(5)	-1231(4)	2238(3)	780(19)
N(1)	2360(3)	1134(3)	2818(2)	237(13)
O(1)	2872(3)	2084(3)	812(2)	267(11)
O(2)	2402(3)	3096(3)	2102(2)	231(10)
O(3)	1972(3)	345(3)	1422(2)	265(11)
O(4)	823(3)	2018(3)	1546(2)	235(10)

[a] Equivalent isotropic U defined as one third of the trace of the orthogonalized U_{ij} tensor.

Table F-3. Interatomic Distances (Å) with Esd's

W(1) - C(1)	1.943(5)	W(1) - N(1)	1.737(4)
W(1) - O(1)	2.346(3)	W(1) - O(2)	1.995(4)
W(1) - O(3)	1.995(3)	W(1) - O(4)	2.294(3)
C(1) - C(2)	1.436(7)	C(2) - C(3)	1.407(7)
C(2) - C(7)	1.405(7)	C(3) - C(4)	1.383(8)
C(4) - C(5)	1.389(8)	C(5) - C(6)	1.391(8)
C(6) - C(7)	1.374(7)	C(7) - O(1)	1.393(6)
C(8) - O(1)	1.446(6)		
C(9) - C(10)	1.411(7)	C(9) - C(14)	1.410(7)
C(9) - N(1)	1.391(6)	C(10) - C(11)	1.391(7)
C(10) - C(15)	1.502(8)	C(11) - C(12)	1.380(8)
C(12) - C(13)	1.396(8)	C(13) - C(14)	1.390(7)
C(14) - C(16)	1.507(8)		
C(17) - C(18)	1.523(8)	C(17) - C(19)	1.545(7)
C(17) - C(20)	1.535(8)	C(17) - O(2)	1.382(6)
C(18) - F(1)	1.333(8)	C(18) - F(2)	1.353(8)
C(18) - F(3)	1.330(8)	C(19) - F(4)	1.299(7)
C(19) - F(5)	1.345(6)	C(19) - F(6)	1.352(7)
C(21) - C(22)	1.536(8)	C(21) - C(23)	1.542(9)
C(21) - C(24)	1.512(9)	C(21) - O(3)	1.389(6)
C(22) - F(7)	1.323(8)	C(22) - F(8)	1.336(7)
C(22) - F(9)	1.347(7)	C(23) - F(10)	1.328(9)
C(23) - F(11)	1.316(7)	C(23) - F(12)	1.336(10)
C(25) - C(26)	1.523(8)	C(25) - O(4)	1.473(6)
C(26) - C(27)	1.513(8)	C(27) - C(28)	1.518(8)
C(28) - O(4)	1.474(6)		

Table F-4. Interatomic Angles (Deg.) with Esd's

C(1) - W(1) - N(1)	99.2(2)	C(1) - W(1) - O(1)	74.2(2)
N(1) - W(1) - O(1)	173.0(2)	C(1) - W(1) - O(2)	97.6(2)
N(1) - W(1) - O(2)	101.2(2)	O(1) - W(1) - O(2)	82.0(1)
C(1) - W(1) - O(3)	103.0(2)	N(1) - W(1) - O(3)	100.2(2)
O(1) - W(1) - O(3)	79.7(1)	O(2) - W(1) - O(3)	147.3(1)
C(1) - W(1) - O(4)	153.7(2)	N(1) - W(1) - O(4)	107.0(2)
O(1) - W(1) - O(4)	79.8(1)	O(2) - W(1) - O(4)	75.2(1)
O(3) - W(1) - O(4)	75.1(1)	W(1) - N(1) - C(9)	174.6(4)
W(1) - O(1) - C(7)	112.1(3)	W(1) - O(1) - C(8)	128.4(3)
W(1) - O(2) - C(17)	138.8(3)	W(1) - O(3) - C(21)	138.4(3)
W(1) - O(4) - C(25)	123.5(3)	W(1) - O(4) - C(28)	126.9(3)
W(1) - C(1) - C(2)	121.9(4)		
C(1) - C(2) - C(3)	126.6(5)	C(1) - C(2) - C(7)	117.4(5)
C(3) - C(2) - C(7)	116.0(5)	C(2) - C(3) - C(4)	121.6(5)
C(3) - C(4) - C(5)	120.0(5)	C(4) - C(5) - C(6)	120.5(5)
C(5) - C(6) - C(7)	118.3(5)	C(2) - C(7) - C(6)	123.6(5)
C(2) - C(7) - O(1)	112.8(4)	C(6) - C(7) - O(1)	123.6(4)
C(7) - O(1) - C(8)	117.2(4)		
C(10) - C(9) - C(14)	120.8(4)	C(10) - C(9) - N(1)	120.5(5)
C(14) - C(9) - N(1)	118.7(4)	C(9) - C(10) - C(11)	118.7(5)
C(9) - C(10) - C(15)	121.0(5)	C(11) - C(10) - C(15)	120.3(5)
C(10) - C(11) - C(12)	121.1(5)	C(11) - C(12) - C(13)	119.8(5)
C(12) - C(13) - C(14)	121.1(5)	C(9) - C(14) - C(13)	118.4(5)
C(9) - C(14) - C(16)	120.5(5)	C(13) - C(14) - C(16)	121.1(5)
C(18) - C(17) - C(19)	109.7(5)	C(18) - C(17) - C(20)	108.7(5)
C(19) - C(17) - C(20)	109.1(4)	C(18) - C(17) - O(2)	106.6(4)
C(19) - C(17) - O(2)	105.9(4)	C(20) - C(17) - O(2)	116.7(4)
C(17) - C(18) - F(1)	110.9(5)	C(17) - C(18) - F(2)	113.2(5)
F(1) - C(18) - F(2)	105.7(5)	C(17) - C(18) - F(3)	114.2(5)
F(1) - C(18) - F(3)	106.2(5)	F(2) - C(18) - F(3)	106.1(5)
C(17) - C(19) - F(4)	114.2(5)	C(17) - C(19) - F(5)	112.3(4)

Table F-4 (cont'd). Interatomic Angles (Deg.) with Esd's

F(4) - C(19) - F(5)	108.3(4)	C(17) - C(19) - F(6)	108.4(4)
F(4) - C(19) - F(6)	106.7(5)	F(5) - C(19) - F(6)	106.5(5)
C(22) - C(21) - C(23)	108.5(5)	C(22) - C(21) - C(24)	109.0(5)
C(23) - C(21) - C(24)	109.7(5)	C(22) - C(21) - O(3)	105.6(4)
C(23) - C(21) - O(3)	108.6(5)	C(24) - C(21) - O(3)	115.1(5)
C(21) - C(22) - F(7)	114.3(5)	C(21) - C(22) - F(8)	110.2(5)
F(7) - C(22) - F(8)	105.8(5)	C(21) - C(22) - F(9)	113.1(5)
F(7) - C(22) - F(9)	106.9(5)	F(8) - C(22) - F(9)	106.0(5)
C(21) - C(23) - F(10)	110.7(5)	C(21) - C(23) - F(11)	113.1(6)
F(10) - C(23) - F(11)	107.2(6)	C(21) - C(23) - F(12)	112.3(5)
F(10) - C(23) - F(12)	106.5(6)	F(11) - C(23) - F(12)	106.8(6)
C(26) - C(25) - O(4)	103.9(4)	C(25) - C(26) - C(27)	102.2(4)
C(26) - C(27) - C(28)	102.7(5)	C(27) - C(28) - O(4)	104.9(4)
C(25) - O(4) - C(28)	109.3(4)		

Table F-5. Anisotropic Displacement Coefficients (Å^2 x 10^4)^a

	U_{11}	U_{22}	U_{33}	U_{23}	U_{13}	U_{12}
W(1)	190(1)	183(1)	174(1)	-6(1)	-33(1)	7(1)
C(1)	259(27)	235(26)	179(24)	-70(20)	13(20)	-9(20)
C(2)	248(27)	212(24)	275(27)	24(21)	-9(21)	53(21)
C(3)	240(28)	349(30)	367(31)	41(26)	31(24)	45(23)
C(4)	247(29)	396(32)	391(33)	0(26)	73(25)	38(24)
C(5)	353(33)	349(32)	419(34)	17(27)	101(27)	65(26)
C(6)	357(32)	297(28)	267(28)	-23(23)	11(24)	55(24)
C(7)	246(27)	246(25)	227(26)	-15(21)	-4(21)	6(21)
C(8)	391(33)	426(33)	196(26)	12(24)	-109(24)	-8(26)
C(9)	309(28)	194(24)	172(24)	9(20)	-20(21)	-28(21)
C(10)	289(28)	289(27)	223(26)	-33(22)	-47(21)	-11(23)
C(11)	399(31)	236(26)	191(25)	41(21)	-20(22)	-16(22)
C(12)	426(33)	335(30)	225(27)	21(24)	-6(24)	-8(26)
C(13)	348(31)	272(28)	304(29)	-6(22)	62(24)	-64(23)
C(14)	218(27)	285(27)	274(27)	-40(22)	-39(21)	-39(22)
C(15)	287(29)	441(33)	308(29)	29(27)	-57(23)	43(26)
C(16)	223(29)	456(35)	375(33)	69(26)	9(24)	21(24)
C(17)	262(28)	243(26)	215(26)	-31(21)	-33(21)	1(21)
C(18)	500(41)	434(36)	361(35)	-132(29)	28(30)	-124(30)
C(19)	379(31)	193(26)	363(32)	18(24)	-71(25)	-93(24)
C(20)	292(32)	392(33)	517(39)	-110(29)	-155(28)	0(26)
C(21)	324(30)	192(25)	366(31)	-85(23)	-79(24)	8(22)
C(22)	494(40)	331(32)	383(35)	-120(28)	-93(29)	21(28)
C(23)	741(51)	81(25)	562(44)	35(25)	-254(39)	10(27)
C(24)	377(38)	459(39)	829(55)	-301(38)	8(36)	40(30)
C(25)	186(27)	319(28)	388(32)	-49(24)	-117(23)	-42(22)
C(26)	245(29)	301(29)	503(37)	4(27)	-94(26)	29(23)
C(27)	316(31)	286(29)	474(36)	-1(27)	-114(26)	11(24)
C(28)	326(31)	205(25)	423(34)	7(24)	-115(25)	30(23)
F(1)	1177(40)	485(24)	266(20)	-2(17)	77(22)	-207(23)

Table F-5 (cont'd). Anisotropic Displacement Coefficients ($Å^2 \times 10^4$)[a]

	U_{11}	U_{22}	U_{33}	U_{23}	U_{13}	U_{12}
F(2)	725(27)	434(21)	434(21)	-226(18)	8(19)	-107(19)
F(3)	444(24)	715(28)	705(29)	-266(22)	209(20)	-46(20)
F(4)	478(22)	299(18)	635(24)	77(17)	-179(18)	12(16)
F(5)	664(26)	282(18)	556(23)	-8(16)	-194(19)	-165(17)
F(6)	641(25)	506(22)	380(20)	54(17)	79(18)	-158(19)
F(7)	390(22)	493(22)	776(29)	-243(21)	-95(20)	-78(18)
F(8)	1013(35)	503(23)	364(21)	-47(18)	-262(21)	-127(22)
F(9)	659(26)	381(20)	614(25)	-314(19)	-79(20)	30(19)
F(10)	1133(40)	435(23)	624(28)	43(21)	-508(27)	108(24)
F(11)	1464(50)	154(18)	920(35)	-50(20)	-517(33)	125(23)
F(12)	1044(40)	714(30)	589(29)	235(24)	144(27)	-194(28)
N(1)	218(22)	201(21)	288(23)	-28(18)	-34(18)	21(17)
O(1)	251(19)	347(20)	199(18)	12(16)	-48(15)	-1(16)
O(2)	214(18)	201(17)	273(19)	-40(15)	-73(15)	-2(14)
O(3)	271(19)	219(18)	301(19)	-41(16)	-48(15)	38(15)
O(4)	225(18)	170(16)	302(19)	26(15)	-97(15)	0(14)

[a] The anisotropic displacement exponent takes the form: $-2\pi^2(h^2a^{*2}U_{11} + \ldots + 2hka^*b^*U_{12})$.

Table F-6. H-Atom Coordinates (x10^4) and Isotropic Displacement Coefficients (Å^2 x 10^4)

	x	y	z	U
H(1A)	4425	1134	2267	800
H(3A)	6127	1834	1664	800
H(4A)	6870	2585	676	800
H(5A)	5778	3082	-288	800
H(6A)	3926	2829	-264	800
H(8A)	2582	2277	-209	800
H(8B)	2049	1286	91	800
H(8C)	1560	2373	234	800
H(11A)	3313	-182	4914	800
H(12A)	1600	-22	5335	800
H(13A)	255	746	4630	800
H(15A)	4547	15	4040	800
H(15B)	4089	-118	3268	800
H(15C)	4361	984	3558	800
H(16A)	-373	1478	3556	800
H(16B)	481	2131	3174	800
H(16C)	163	1039	2886	800
H(20A)	4161	3060	2973	800
H(20B)	4496	3496	2243	800
H(20C)	4430	4233	2894	800
H(24A)	3438	-215	533	800
H(24B)	3940	-395	1288	800
H(24C)	3618	-1339	813	800
H(25A)	39	975	927	800
H(25B)	6	714	1729	800
H(26A)	-1252	1939	1924	800
H(26B)	-1609	1580	1167	800
H(27A)	-1192	3452	1303	800
H(27B)	-720	2909	648	800
H(28A)	366	3399	1920	800
H(28B)	810	3476	1164	800

G. X-ray Diffraction Study of $W(=CHC_6H_4\text{-}o\text{-}OMe)[N\text{-}2,6\text{-}C_6H_3\text{-}(i\text{-}Pr)_2][OCMe(CF_3)_2]_2$

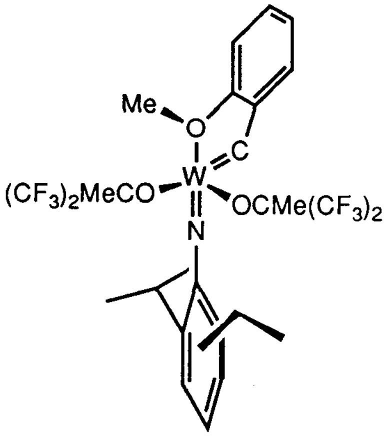

(See Chapter 3, Figure 5 for the ORTEP plot.)

Table G-1. Experimental Data for the X-ray Diffraction Study of $W(=CHC_6H_4\text{-}o\text{-}OMe)[N\text{-}2,6\text{-}C_6H_3\text{-}(i\text{-}Pr)_2][OCMe(CF_3)_2]_2$

Formula: $C_{28}H_{31}NO_3F_{12}W$	Fw: 841.4
Temperature (K): 183	Crystal System: Monoclinic
Space Group: $P2_1/c$	$Z = 4$
$\underline{a}$ = 14.341(2) Å	$\underline{V}$ = 3100.1(6) Å^3
$\underline{b}$ = 9.736(1) Å	β = 92.21(1)°
$\underline{c}$ = 22.217(3) Å	D_{calcd}, Mg/m^3 = 1.803
Radiation: MoKα (λ = 0.710730 Å)	Diffractometer: Syntex $P2_1$
Data Collected: $+h, +k, \pm l$	Monochromator: Highly oriented graphite
Scan Range: 1.20° plus Kα-separation	Scan Type: θ-2θ
2θ Range: 4.0 to 50.0°	Scan Speed: 3.0 deg min^{-1} (in ω)
Reflections Collected: 6092	μ(MoKα), mm^{-1} = 3.91
No. of Variables: 530	Reflections with $\lvert F_o \rvert > 0$: 5195
Goodness of Fit: 1.00	$R_F = 3.4\%$, $R_{wF} = 4.1\%$

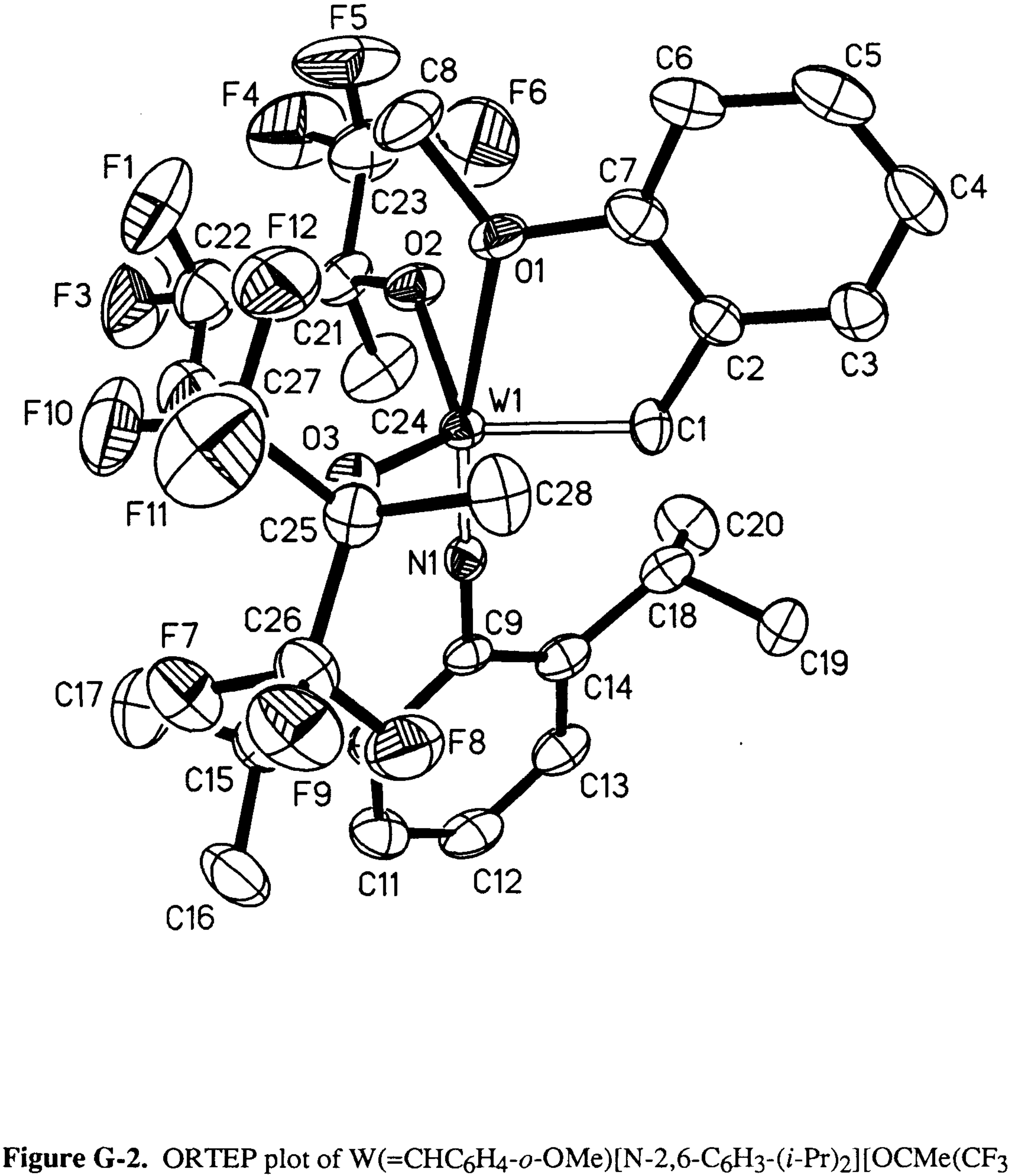

Figure G-2. ORTEP plot of $W(=CHC_6H_4\text{-}o\text{-}OMe)[N\text{-}2,6\text{-}C_6H_3\text{-}(i\text{-}Pr)_2][OCMe(CF_3)_2]_2$ (second view). Thermal ellipsoids are drawn at the 50% probability level.

Table G-2. Atomic Coordinates (x 10^4) and Equivalent Isotropic Displacement Coefficients ($\mathring{A}^2$ x 10^4)[a]

	x	y	z	U(eq)
W(1)	2318.6(.1)	1182.4(.2)	1293.2(.1)	203(1)
C(1)	1074(3)	1902(5)	1395(2)	256(14)
C(2)	884(3)	2955(5)	1841(2)	260(14)
C(3)	-1(4)	3501(6)	1941(2)	341(16)
C(4)	-100(5)	4521(6)	2373(3)	398(18)
C(5)	652(5)	4996(6)	2710(2)	429(19)
C(6)	1535(4)	4457(6)	2625(2)	377(17)
C(7)	1625(4)	3440(5)	2195(2)	327(15)
C(8)	3236(5)	2941(7)	2502(3)	458(21)
C(9)	1758(3)	-1118(4)	357(2)	235(13)
C(10)	2315(3)	-1346(5)	-138(2)	298(15)
C(11)	2054(4)	-2407(5)	-538(2)	372(17)
C(12)	1275(4)	-3187(6)	-450(3)	397(18)
C(13)	721(4)	-2926(5)	33(2)	355(16)
C(14)	949(3)	-1908(5)	453(2)	292(15)
C(15)	3195(4)	-545(6)	-246(3)	351(17)
C(16)	3220(5)	74(8)	-882(3)	528(23)
C(17)	4051(5)	-1434(8)	-134(4)	576(26)
C(18)	310(4)	-1639(5)	964(2)	313(15)
C(19)	-544(4)	-854(7)	726(3)	392(18)
C(20)	39(5)	-2948(7)	1291(3)	472(21)
C(21)	3231(4)	-1053(5)	2111(3)	342(16)
C(22)	4227(5)	-906(7)	1897(3)	569(23)
C(23)	3250(5)	-1281(7)	2793(3)	572(24)
C(24)	2756(6)	-2261(7)	1792(4)	561(27)
C(25)	3144(3)	3785(5)	643(2)	311(15)
C(26)	3230(4)	3617(6)	-39(3)	379(17)
C(27)	4050(4)	4424(6)	916(3)	425(19)
C(28)	2305(5)	4675(6)	776(3)	394(20)
F(1)	4733(3)	-10(5)	2210(2)	816(18)
F(2)	4197(3)	-436(7)	1331(2)	937(21)

Table G-2 (cont'd). Atomic Coordinates (x 10^4) and Equivalent Isotropic Displacement Coefficients (Å^2 x 10^4)^a

	x	y	z	U(eq)
F(3)	4696(3)	-2074(5)	1907(2)	903(20)
F(4)	3747(4)	-2371(5)	2960(2)	905(19)
F(5)	3581(4)	-222(5)	3106(2)	866(19)
F(6)	2392(4)	-1509(7)	2972(2)	1110(25)
F(7)	3944(3)	2845(3)	-187(2)	513(12)
F(8)	2460(3)	3019(4)	-275(2)	551(13)
F(9)	3315(3)	4826(4)	-322(2)	605(13)
F(10)	4787(3)	3673(4)	862(2)	722(16)
F(11)	4208(3)	5659(4)	694(2)	809(18)
F(12)	3967(3)	4613(4)	1514(2)	608(13)
N(1)	2009(3)	-69(4)	763(2)	224(11)
O(1)	2469(2)	2847(3)	2058(1)	311(11)
O(2)	2784(3)	204(3)	2010(2)	325(11)
O(3)	3100(2)	2445(3)	878(1)	269(10)

^{a}Equivalent isotropic U defined as one third of the trace of the orthogonalized U_{ij} tensor.

Table G-3. Interatomic Distances (Å) with Esd's

W(1) - O(1)	2.352(3)	W(1) - O(2)	1.952(3)
W(1) - O(3)	1.923(3)	W(1) - N(1)	1.741(4)
W(1) - C(1)	1.939(5)		
C(1) - C(2)	1.459(7)	C(2) - C(3)	1.401(7)
C(2) - C(7)	1.381(7)	C(3) - C(4)	1.392(8)
C(4) - C(5)	1.370(9)	C(5) - C(6)	1.391(9)
C(6) - C(7)	1.386(7)	C(7) - O(1)	1.385(6)
C(8) - O(1)	1.452(7)		
C(9) - C(10)	1.400(7)	C(9) - C(14)	1.415(7)
C(9) - N(1)	1.401(6)	C(10) - C(11)	1.404(7)
C(10) - C(15)	1.511(7)	C(11) - C(12)	1.371(8)
C(12) - C(13)	1.384(8)	C(13) - C(14)	1.391(7)
C(14) - C(18)	1.508(7)	C(15) - C(16)	1.538(9)
C(15) - C(17)	1.515(9)	C(18) - C(19)	1.522(8)
C(18) - C(20)	1.525(8)		
C(21) - C(22)	1.528(9)	C(21) - C(23)	1.532(9)
C(21) - C(24)	1.521(9)	C(21) - O(2)	1.395(6)
C(22) - F(1)	1.317(8)	C(22) - F(2)	1.337(8)
C(22) - F(3)	1.322(8)	C(23) - F(4)	1.324(8)
C(23) - F(5)	1.322(8)	C(23) - F(6)	1.326(9)
C(25) - C(26)	1.534(8)	C(25) - C(27)	1.543(8)
C(25) - C(28)	1.521(8)	C(25) - O(3)	1.408(6)
C(26) - F(7)	1.322(7)	C(26) - F(8)	1.337(7)
C(26) - F(9)	1.343(6)	C(27) - F(10)	1.295(7)
C(27) - F(11)	1.322(7)	C(27) - F(12)	1.351(7)

Table G-4. Interatomic Angles (Deg.) with Esd's

O(1) - W(1) - O(2)	74.2(1)	O(1) - W(1) - O(3)	82.4(1)
O(2) - W(1) - O(3)	121.1(1)	O(1) - W(1) - N(1)	170.2(1)
O(2) - W(1) - N(1)	106.4(2)	O(3) - W(1) - N(1)	105.1(2)
O(1) - W(1) - C(1)	74.1(2)	O(2) - W(1) - C(1)	111.7(2)
O(3) - W(1) - C(1)	112.4(2)	N(1) - W(1) - C(1)	96.9(2)
W(1) - O(1) - C(7)	112.9(3)	W(1) - O(1) - C(8)	125.5(3)
W(1) - O(2) - C(21)	134.3(3)	W(1) - O(3) - C(25)	143.6(3)
W(1) - N(1) - C(9)	177.4(3)	W(1) - C(1) - C(2)	122.0(3)
C(1) - C(2) - C(3)	124.7(4)	C(1) - C(2) - C(7)	117.8(4)
C(3) - C(2) - C(7)	117.5(4)	C(2) - C(3) - C(4)	119.9(5)
C(3) - C(4) - C(5)	121.2(6)	C(4) - C(5) - C(6)	120.1(5)
C(5) - C(6) - C(7)	118.2(5)	O(1) - C(7) - C(2)	113.1(4)
O(1) - C(7) - C(6)	123.6(5)	C(2) - C(7) - C(6)	123.2(5)
C(7) - O(1) - C(8)	118.1(4)		
N(1) - C(9) - C(10)	118.7(4)	N(1) - C(9) - C(14)	119.5(4)
C(10) - C(9) - C(14)	121.9(4)	C(9)- C(10) - C(11)	117.8(5)
C(9) - C(10) - C(15)	123.3(4)	C(11) - C(10) - C(15)	118.9(5)
C(10) - C(11) - C(12)	121.1(5)	C(11) - C(12) - C(13)	120.2(5)
C(12) - C(13) - C(14)	121.6(5)	C(9) - C(14) - C(13)	117.3(5)
C(9) - C(14) - C(18)	123.0(4)	C(13) - C(14) - C(18)	119.6(5)
C(10) - C(15) - C(16)	113.5(5)	C(10) - C(15) - C(17)	110.8(5)
C(16) - C(15) - C(17)	109.1(6)	C(14) - C(18) - C(19)	109.3(4)
C(14) - C(18) - C(20)	112.8(5)	C(19) - C(18) - C(20)	111.6(5)
O(2) - C(21) - C(22)	107.3(4)	O(2) - C(21) - C(23)	106.0(4)
C(22)- C(21) - C(23)	109.9(5)	O(2) - C(21) - C(24)	114.1(5)
C(22) - C(21) - C(24)	109.6(5)	C(23) - C(21) - C(24)	109.8(5)
C(21) - C(22) - F(1)	113.6(6)	C(21) - C(22) - F(2)	109.1(5)
F(1) - C(22) - F(2)	105.5(6)	C(21) - C(22) - F(3)	113.3(6)
F(1) - C(22) - F(3)	106.9(5)	F(2) - C(22) - F(3)	108.0(6)
C(21) - C(23) - F(4)	112.5(5)	C(21) - C(23) - F(5)	113.6(5)

Table G-4 (cont'd). Interatomic Angles (Deg.) with Esd's

F(4) - C(23) - F(5)	107.4(6)	C(21) - C(23) - F(6)	109.9(5)
F(4) - C(23) - F(6)	106.1(6)	F(5) - C(23) - F(6)	107.0(6)
O(3) - C(25) - C(26)	105.8(4)	O(3) - C(25) - C(27)	106.1(4)
C(26) - C(25) - C(27)	109.4(4)	O(3) - C(25) - C(28)	114.2(4)
C(26) - C(25) - C(28)	110.3(5)	C(27) - C(25) - C(28)	110.8(4)
C(25) - C(26) - F(7)	113.5(4)	C(25) - C(26) - F(8)	109.7(4)
F(7) - C(26) - F(8)	106.9(4)	C(25) - C(26) - F(9)	112.4(4)
F(7) - C(26) - F(9)	107.3(5)	F(8) - C(26) - F(9)	106.7(4)
C(25) - C(27) - F(10)	114.5(5)	C(25) - C(27) - F(11)	112.0(5)
F(10) - C(27) - F(11)	109.0(5)	C(25) - C(27) - F(12)	109.6(5)
F(10) - C(27) - F(12)	105.8(5)	F(11)- C(27) - F(12)	105.4(5)

Table G-5. Anisotropic Displacement Coefficients (Å^2 x 10^4)[a]

	U_{11}	U_{22}	U_{33}	U_{23}	U_{13}	U_{12}
W(1)	218(1)	191(1)	198(1)	-8(1)	-12(1)	6(1)
C(1)	174(22)	259(24)	338(26)	-13(20)	49(20)	-26(19)
C(2)	307(26)	248(23)	230(23)	17(18)	55(20)	-7(20)
C(3)	369(29)	363(27)	295(27)	67(23)	66(23)	23(24)
C(4)	503(36)	320(28)	382(30)	33(23)	171(26)	163(26)
C(5)	714(43)	275(27)	308(28)	-71(23)	128(28)	9(27)
C(6)	549(36)	331(28)	252(26)	-61(22)	27(25)	-4(26)
C(7)	412(29)	290(24)	281(26)	19(21)	51(22)	34(22)
C(8)	403(35)	428(35)	526(39)	-170(30)	-195(29)	21(28)
C(9)	282(24)	202(22)	214(22)	-5(17)	-71(18)	66(18)
C(10)	332(26)	302(25)	258(24)	-20(20)	-13(20)	74(21)
C(11)	466(34)	321(27)	331(28)	-78(22)	33(25)	53(24)
C(12)	498(34)	303(28)	376(30)	-125(24)	-153(26)	22(25)
C(13)	375(29)	291(25)	388(29)	-25(22)	-118(23)	-29(23)
C(14)	348(27)	216(23)	304(26)	34(19)	-90(21)	24(20)
C(15)	359(29)	345(29)	351(29)	-98(24)	48(23)	74(23)
C(16)	557(41)	665(43)	374(33)	-21(31)	195(30)	-54(36)
C(17)	441(39)	524(40)	764(55)	7(40)	21(36)	102(32)
C(18)	324(27)	301(26)	307(27)	44(21)	-62(22)	-21(22)
C(19)	293(29)	457(33)	422(33)	-5(28)	-40(25)	30(25)
C(20)	550(40)	381(32)	491(38)	72(28)	112(33)	-62(30)
C(21)	344(28)	272(26)	401(29)	54(21)	-106(22)	49(21)
C(22)	476(38)	637(42)	591(42)	83(34)	-22(32)	150(33)
C(23)	632(43)	622(43)	453(36)	196(33)	-100(32)	95(34)
C(24)	666(53)	285(32)	713(53)	17(31)	-206(42)	46(31)
C(25)	301(26)	278(26)	355(27)	84(20)	25(21)	-7(20)
C(26)	397(30)	369(28)	378(29)	35(23)	87(24)	-5(25)
C(27)	419(32)	298(27)	564(36)	-48(25)	85(27)	-80(24)
C(28)	387(34)	240(28)	561(42)	85(27)	106(29)	49(25)
F(1)	408(22)	797(29)	1222(38)	13(27)	-247(24)	-108(21)

Table G-5 (cont'd). Anisotropic Displacement Coefficients ($Å^2$ x 10^4)[a]

	U_{11}	U_{22}	U_{33}	U_{23}	U_{13}	U_{12}
F(2)	540(25)	1664(50)	619(28)	319(31)	169(21)	133(30)
F(3)	559(26)	888(33)	1248(41)	-123(29)	-143(26)	418(24)
F(4)	1212(41)	770(30)	709(29)	360(24)	-276(27)	265(29)
F(5)	1329(44)	844(32)	398(22)	-48(21)	-303(24)	222(30)
F(6)	875(38)	1778(57)	689(32)	588(35)	182(28)	37(38)
F(7)	584(22)	502(20)	464(19)	9(16)	166(17)	63(17)
F(8)	522(22)	708(24)	417(19)	10(17)	-70(16)	-92(18)
F(9)	815(27)	472(20)	540(22)	223(17)	159(19)	29(19)
F(10)	308(19)	807(28)	1047(34)	-291(24)	-30(20)	51(19)
F(11)	841(31)	477(22)	1103(36)	192(23)	-54(27)	-384(22)
F(12)	606(23)	620(23)	594(23)	-160(19)	-36(18)	-182(19)
N(1)	206(19)	226(19)	239(19)	15(15)	7(15)	55(15)
O(1)	298(19)	355(19)	274(18)	-78(15)	-74(15)	-11(15)
O(2)	394(20)	289(18)	285(18)	10(14)	-81(15)	69(15)
O(3)	274(18)	203(15)	329(18)	33(13)	10(14)	20(13)

[a] The anisotropic displacement exponent takes the form: $-2\pi^2(h^2a^{*2}U_{11} + \ldots + 2hka^*b^*U_{12})$.

Table G-6. H-Atom Coordinates (x10^4) and Isotropic Displacement Coefficients (Å^2 x 10^4)

	x	y	z	U
H(1)	559(33)	1590(47)	1175(20)	16(11)
H(3)	-471(35)	3211(49)	1702(22)	21(12)
H(4)	-680(46)	4756(65)	2410(28)	55(19)
H(5)	675(40)	5750(62)	2982(26)	41(15)
H(6)	2084(41)	4709(60)	2862(25)	45(17)
H(8A)	3388(40)	3868(57)	2515(26)	38(16)
H(8B)	3779(41)	2430(58)	2316(24)	41(15)
H(8C)	3053(47)	2431(72)	2842(31)	60(21)
H(11)	2525(38)	-2615(54)	-811(24)	35(15)
H(12)	1093(37)	-3807(49)	-721(24)	28(14)
H(13)	153(40)	-3535(55)	63(25)	37(15)
H(15)	3232(36)	78(53)	-9(23)	27(14)
H(16A)	2592(55)	648(79)	-1007(33)	75(22)
H(16B)	3830(49)	587(69)	-909(28)	57(18)
H(16C)	3252(43)	-577(70)	-1195(29)	51(17)
H(17A)	4093(34)	-1737(49)	242(24)	19(13)
H(17B)	4036(53)	-2251(85)	-406(33)	81(25)
H(17C)	4663(61)	-896(80)	-219(37)	90(27)
H(18)	619(38)	-1148(47)	1259(25)	29(14)
H(19A)	-875(43)	-1428(60)	386(29)	51(17)
H(19B)	-932(39)	-693(56)	1020(25)	33(14)
H(19C)	-412(32)	28(51)	585(21)	17(12)
H(20A)	-332(54)	-2767(79)	1601(34)	78(25)
H(20B)	525(52)	-3479(74)	1417(32)	63(22)
H(20C)	-426(50)	-3498(69)	994(32)	64(20)
H(24A)	2808(40)	-2231(58)	1348(28)	42(16)
H(24B)	2191(51)	-2188(74)	1907(31)	61(24)
H(24C)	2922(48)	-3111(81)	1962(31)	69(21)
H(28A)	2369(36)	5512(60)	599(23)	29(13)
H(28B)	2247(39)	4757(65)	1168(30)	45(18)
H(28C)	1856(43)	4265(64)	665(26)	36(17)